



IGNACIO VILLALÓN FORNÉS

**THE IMPROVEMENT OF
THE MAIN PROPERTIES
OF PHOSPHOGYPSUM
BINDING MATERIAL BY
USING THE CASTING AND
THE PRESS-FORMING
PROCESSING METHODS**

DOCTORAL DISSERTATION

K a u n a s
2 0 2 1

KAUNAS UNIVERSITY OF TECHNOLOGY

IGNACIO VILLALÓN FORNÉS

THE IMPROVEMENT OF THE MAIN
PROPERTIES OF PHOSPHOGYPSUM
BINDING MATERIAL BY USING THE
CASTING AND THE PRESS-FORMING
PROCESSING METHODS

Doctoral dissertation
Technological Sciences, Civil Engineering (T 002)

Kaunas, 2021

This doctoral dissertation was prepared at Kaunas University of Technology, Faculty of Civil Engineering and Architecture, Department of Civil Engineering and Architecture Competence Centre during the period of 2017–2021.

Scientific Supervisor:

Prof. dr. Danutė VAIČIUKYNIENĖ (Kaunas University of Technology, Technological Sciences, Civil Engineering, T 002).

Edited by: Dr. Armandas Rumšas (Publishing House “Technologija”)

Dissertation Defence Board of Civil Engineering Science Field:

Prof. Dr. Žymantas RUDŽIONIS (Kaunas University of Technology, Technological Sciences, Civil Engineering, T 002) – **chairperson**;

Prof. Dr. Mindaugas DAUKŠYS (Kaunas University of Technology, Technological Sciences, Civil Engineering, T 002);

Prof. Dr. Rimvydas KAMINSKAS (Kaunas University of Technology, Technological Sciences, Civil Engineering, T 002);

Prof. Dr. Pavel KRIVENKO (Kyiv National University of Construction and Architecture (KNUCA), Ukraine, Technological Sciences, Materials Engineering, T 008);

Dr. Ina PUNDIENĖ (Vilnius Tech, Technological Sciences, Materials Engineering, T 008).

The official defence of the dissertation will be held at 10 a.m. on the 7th of January, 2022, at the public meeting of Dissertation Defence Board of Civil Engineering Science Field in the Dissertation Defence Hall at Kaunas University of Technology.

Address: K. Donelaičio 73-403, LT-44249 Kaunas, Lithuania.

Tel. no. (+370) 37 300 042; fax. (+370) 37 324 144; e-mail doktorantura@ktu.lt.

This doctoral dissertation was sent out on 7 December, 2021.

The doctoral dissertation is available on the internet at <http://ktu.edu> and at the library of Kaunas University of Technology (K. Donelaičio 20, LT-44239 Kaunas, Lithuania).

© I. Villalón Fornés, 2021

KAUNO TECHNOLOGIJOS UNIVERSITETAS

IGNACIO VILLALÓN FORNÉS

FOSFOGIPSO RIŠAMOSIOS MEDŽIAGOS
PAGRINDINIŲ SAVYBIŲ PAGERINIMAS
NAUDOJANT LIEJIMO BEI PRESAVIMO
FORMAVIMO METODUS

Daktaro disertacija
Technologijos mokslai, statybos inžinerija (T 002)

Kaunas, 2021

Disertacija rengta 2017–2021 metais Kauno technologijos universiteto Statybos ir architektūros fakultete, Statybos ir architektūros kompetencijų centre.

Mokslinis vadovas:

prof. dr. Danutė VAIČIUKYNIENĖ (Kauno technologijos universitetas, technologijos mokslai, statybos inžinerija, T 002).

Redagavo: Violeta Meiliūnaitė (Leidykla „Technologija“)

Statybos inžinerijos mokslo krypties disertacijos gynimo taryba:

prof. dr. Žymantas RUDŽIONIS (Kauno technologijos universitetas, technologijos mokslai, statybos inžinerija, T 002) – **pirmininkas**;

prof. dr. Mindaugas DAUKŠYS (Kauno technologijos universitetas, technologijos mokslai, statybos inžinerija, T 002);

prof. dr. Rimvydas KAMINSKAS (Kauno technologijos universitetas, technologijos mokslai, statybos inžinerija, T 002);

prof. dr. Pavel KRIVENKO (Kijevo nacionalinis statybos ir architektūros universitetas (KNUCA), Ukraina, technologijos mokslai, medžiagų inžinerija, T 008);

dr. Ina PUNDIENĖ (Vilnius Tech, technologijos mokslai, medžiagų inžinerija, T 008).

Disertacija bus ginama viešame statybos inžinerijos mokslo krypties disertacijos gynimo tarybos posėdyje 2022 m. sausio 7 d. 10 val. Kauno technologijos universiteto Disertacijų gynimo salėje.

Adresas: K. Donelaičio g. 73-403, 44249 Kaunas, Lietuva.

Tel. (370) 37 300 042; faks. (370) 37 324 144; el. paštas doktorantura@ktu.lt..

Disertacija išsiųsta 2021 m. gruodžio 7 d.

Su disertacija galima susipažinti internetinėje svetainėje <http://ktu.edu> ir Kauno technologijos universiteto bibliotekoje (K. Donelaičio g. 20, 44239 Kaunas).

© I. Villalón Fornés, 2021

TABLE OF CONTENTS

LIST OF TABLES	10
LIST OF FIGURES	10
INTRODUCTION	14
1. LITERATURE REVIEW	18
1.1. The production of orthophosphoric acid during which the problematic by-product phosphogypsum is obtained	18
1.2. Composition of PG	20
1.2.1. Presence of ²²⁶ Ra and of other radionuclides in PG	20
1.2.2. Presence of phosphate and fluoride compounds in PG	21
1.2.3. Presence of trace heavy metals and rare earth elements in PG.....	21
1.3. The environmental problem of the PG deposits and the necessity of PG recycling	22
1.4. Application of PG in agriculture, soil stabilisation and road base construction	24
1.4.1. Application of PG in agriculture	24
1.4.2. Application of PG in soil stabilisation and road base construction	25
1.5. Application of PG in the field of building materials	28
1.5.1. Issue of PG toxicity and necessity of its purification in order to make it suitable for building materials	29
1.5.2. The usage of PG as an additive to cement in building materials.....	35
1.5.3. Improvement of the mechanical strength of PG to make it suitable for load-bearing building products.....	35
1.5.4. Improvement of the waterproofing properties of PG building products	40
1.5.5. Thermal and acoustic insulation properties of gypsum and PG building products	44
1.6. Conclusions	47
2. EXPERIMENTAL METHODS AND MATERIALS	48
2.1. Experimental methods	48
2.1.1. Microstructural analysis	48
2.1.2. Chemical and mineral composition analysis	48
2.1.3. Colorimetric analysis.....	48
2.1.4. Investigation of the physical properties.....	49
2.1.5. Thermal and acoustic analysis methods	49
2.1.6. Testing methods for the mechanical properties of PG specimens.....	50
2.1.7. Radiological assessment.....	51
2.2. Employed materials	52
2.2.1. Three types of HH-PG from different origins	52
2.2.2. Waste of synthetic zeolite (ZW).....	59
2.2.3. Waste metallurgical sludge (MS)	61
2.2.4. Wood fibre (WF and NF)	64

2.2.5. Hydrated lime	66
2.3. Summary of the properties of materials	66
3. RESULTS AND DISCUSSION.....	68
3.1. Comparative investigation of the aptness of PGs from different origins to be used as binding materials in structural building products	70
3.1.1. Experimental procedures	70
3.1.2. Experimental results	75
3.1.3. Partial conclusions.....	86
3.2. Investigation of press-forming processing to produce structural PG products	87
3.2.1. Experimental procedures	88
3.2.2. Experimental results	90
3.2.3. Partial conclusions.....	96
3.3. Adsorption of acidic-soluble impurities of PG by zeolitic waste additive (ZW)	98
3.3.1. Experimental procedures	98
3.3.2. Experimental results	99
3.3.3. Partial conclusions.....	105
3.4. Improvement of water-resistance of PG specimens by adding waste metallurgical sludge (MS)	106
3.4.1. Experimental procedures	107
3.4.2. Experimental results	108
3.4.3. Partial conclusions.....	115
3.5. Improvement of the thermal and acoustic insulation of load bearing PG specimens by including waste wood fibre additive (WF)	117
3.5.1. Experimental procedures	117
3.5.2. Experimental results	119
3.5.3. Partial conclusions.....	125
4. MAIN RESULTS AND CONCLUSIONS.....	127
SANTRAUKA	130
Įvadas.....	130
1. Medžiagos ir tyrimo metodai.....	132
1.1. Eksperimentinių tyrimų metodai	132
1.2. Pradinės medžiagos	133
2. Tyrimo rezultatai ir jų aptarimas	140
2.1. Skirtingos kilmės PG rišamosios medžiagos naudojimo konstrukciniuose produktuose tinkamumo vertinimas	140
2.2. PG bandinių mechaninių savybių gerinimas taikant presavimo formavimo metodą	144
2.3. PG tirpių bei rūgščių P_2O_5 bei F^- junginių mažinimas, naudojant ceolito atliekas (ZW) priedą.....	147
2.4. PG bandinių vandens atsparumo padidinimas pridedant metalurgijos šlamo atliekas (MS) priedą.....	149

2.5. PG gaminių termoizoliacinių savybių gerinimas naudojant medžio atliekas (WF) priedą	152
3. Pagrindiniai rezultatai bei išvados.....	154
REFERENCES	157
CURRICULUM VITAE	173
LIST OF PUBLICATIONS ON THE TOPIC OF THE DISSERTATION	174
ACKNOWLEDGEMENTS	175

DESIGNATIONS

Symbols and Abbreviations

Materials:

BFS – blast furnace slag
CSA – calcium sulfoaluminate clinker
DH – dihydrate (DH-PG – dihydrate phosphogypsum)
FA – fly ash
FGD – flue gas desulphurization gypsum
FCC – fluid catalytic cracking
HH – hemihydrate (HH-PG – hemihydrate phosphogypsum)
MS – waste metallurgical sludge
NF – natural wood fibre
NORM – naturally occurring radioactive material
PC – Portland cement
PG – phosphogypsum
REE – rare earth element
WF – waste wood fibre
ZW – zeolitic waste

Organisations

FIPR – Florida Institute of Phosphate Research
IAEA – International Atomic Energy Agency
TFI – The Fertilizer Institute
US EPA – United States Environmental Protection Agency
WHO – World Health Organisation

Parameters:

CS – compressive strength
 CS_{150} – compressive strength of standard 150x150x150 mm cubic or 150x150 mm cylindrical specimens
 FS – flexural strength
 LOI – loss on ignition
 I – radionuclide activity concentration index
 PPF – press-forming pressure
 ScF – scale factor of the compressive strength
 SF – softening factor
 SPL – sound pressure level
 n_0 – value of the control specimen
 n_{opt} – value of the optimal specimen
 n_{rec} – value of the recommended specimen
 r – correlation coefficient
 w/s – water/solid weight ratio employed to produce the initial paste
 λ – thermal conductivity

ρ – density of the hardened specimens

Experimental methods

EDS – energy-dispersive X-ray spectroscopy

SEM – scanning electron microscopy

XRD – X-ray diffraction analysis

XRF – X-ray fluorescence analysis

Concepts

Acidic-soluble impurities –soluble P_2O_5 and F^- impurities which are frequent in the composition of PG and which are highly undesirable since they weaken the strength of the PG specimens and, at the same time, damage the environment.

Green specimens – the specimens which, in the middle of the manufacturing process, present the final geometry, but have not undergone yet the curing process and, therefore, exhibit null mechanical strength.

Hardened specimens – the specimens which have been cured for a certain period of time and, therefore, are composed mainly of DH-PG crystals and exhibit good values of mechanical strength.

Phosphogypsum – the main by-product of the production process of phosphate fertilisers. It is composed of hydrated $CaSO_4$ crystals and, to a lesser extent, of impurities (phosphate, fluoride, radionuclides, trace heavy metals and trace REE).

Radionuclide activity concentration – the content of radioactive isotopes (known as radionuclides) in a certain material. The calculation of the radionuclide activity concentration in building materials is based on the content of three radionuclides: ^{226}Ra , ^{232}Th and ^{40}K .

The wet process – the main chemical process employed to produce orthophosphoric acid and, as a by-product, PG. The process consists of the digestion of phosphate ore by concentrated sulphuric acid.

LIST OF TABLES

Table 1. Typical and maximum values of radionuclide concentration of different common building materials and industrial by-products, including PG, in the EU countries [64]

Table 2. Description and properties of the different humid HH-PGs

Table 3. XRF composition of commercial gypsum and investigated PGs (wt%)

Table 4. XRF composition of the ZW (wt%)

Table 5. The XRF chemical composition of MS (wt%)

Table 6. Summary table of the properties of investigated materials

Table 7. Composition, processing and analysis methods of different groups of specimens of the 1st stage of investigation

Table 8. *ScF* values for the *CS* of specimens of different sizes, calculated from the results of Fig. 26. The values marked in bold come from Lithuanian Standard LST 1974 [147]

Table 9. Values of the activity concentrations of main radionuclides (Bq/kg) and of *I* index for different employed materials

Table 10. Quantitative crystal composition of PG specimens (by XRD Rietveld refinement)

Table 11. Comparative impact of different additives on soluble P₂O₅ content of PG specimens

Table 12. Summary table of the results of the investigation on the influence of MS additive on the properties of PG specimens: soluble phosphate content, *LOI*, *CS*₁₅₀ and *SF*

Table 13. Composition of the different employed pastes, including different amounts of WF (or NF) and ZW additives

Table 14. Mechanical, thermal and acoustic properties of the recommended composition of specimens with WF additive

LIST OF FIGURES

Fig. 1. View of the manufactured humid PG powder in a chemical plant of phosphate fertilisers, straight after the wet process

Fig. 2. View of a field next to Kėdainiai (Lithuania) with a PG stack in the background

Fig. 3. Schematic view of the ‘two step hydration process’ as proposed by Zhou *et al.* [94]

Fig. 4. Images of different press-forms (with the respective PG specimens produced with each one) (a), the press-forming process (b) and the *CS* test (c), by using *ToniTechnik* 2020.0600/132/02 computerised press

Fig. 5. Hot-drying of the HH-PG powder (a) and view of the different HH materials (b)

Fig. 6. XRD patterns of different PGs and natural gypsum

- Fig. 7.** SEM images of crystal conglomerates of different HH powders: natural gypsum (a), I-type PG (b), II-type PG (c), III-type PG (d). Scale: x200 (index '1', and x1500 (index '2'))
- Fig. 8.** Particle size distribution of initial HH materials: natural gypsum (a), I-type PG (b), II-type PG (c), III-type PG (d)
- Fig. 9.** SEM images (marked with index '1') and EDS distribution of phosphorus (index '2', green dots) and fluorine (index '3', red dots) on the crystals of different types of HH powders: natural gypsum (a), I-type PG (b), II-type PG (c), III-type PG (d). Scale: x1000
- Fig. 10.** XRD pattern of ZW based on faujasite mineral
- Fig. 11.** SEM images of ZW. Scale: x200 (a) and x3000 (b)
- Fig. 12.** Particle size distribution of ZW
- Fig. 13.** Macroscopic view of MS modifier
- Fig. 14.** SEM image of MS particles, at scales x200 (a) and x900 (b)
- Fig. 15.** Particle size distribution of MS
- Fig. 16.** XRD pattern of MS
- Fig. 17.** Macroscopic view of wood fibre (the ruler is given for scaling)
- Fig. 18.** SEM images of NF (a) and WF (b), at scales x50 (index '1'), x500 (index '2') and x1000 (index '3')
- Fig. 19.** Results of sieve analysis of both NF and WF
- Fig. 20.** Schematic view of the 5 stages of investigation
- Fig. 21.** Graphical explanation of the 1st stage of investigation
- Fig. 22.** View of the different specimens (dimensions given in mm) produced through casting (cubic specimens) or press-forming (cylindrical specimens) to investigate the influence of the size of the specimens on *CS* values
- Fig. 23.** Flowchart of experimental processes of 1st stage of the study
- Fig. 24.** Results of pH analyses of the initial materials (a) and of hardened PG specimens of D group, including different amounts of Ca(OH)₂ (b)
- Fig. 25.** Hydration temperature analyses of A group pastes of natural gypsum and different PG types (a) and of D group pastes with different Ca(OH)₂ contents (b) during the early stages of hydration
- Fig. 26.** Influence of the scale of specimens on the ρ (a) and the *CS* (b) of hardened specimens of group C produced with III-type PG
- Fig. 27.** Results of *LOI* (a), ρ (b) and *CS*₁₅₀ (c) of A group specimens created with different materials, after different curing durations
- Fig. 28.** Influence of *CS*₁₅₀ of different specimens on the processing type: either casting (A group) or press-forming under 15 MPa pressure (B group)
- Fig. 29.** Views of microstructures of hardened specimens produced through casting with different materials: natural gypsum (a), I-type PG (b), II-type PG (c), III-type PG (d). Scale: x2000
- Fig. 30.** Views of the microstructure of specimens of group B produced through press-forming: I-type PG (a), III-type PG (b). Scale: x2000
- Fig. 31.** Graphical explanation of the 2nd stage of investigation
- Fig. 32.** Flowchart of the experimental processes of the 2nd stage of study

Fig. 33. Neutralisation of soluble acidic impurities: pH values (a) and soluble phosphate and fluoride contents (b), depending on the included Ca(OH)_2 amounts

Fig. 34. Cause-effect relations between the investigated properties of the specimens

Fig. 35. Influence of *PF*P on ρ of the hardened specimens cured without immersion (a) and with immersion (b), produced with different *w/s* ratios

Fig. 36. Influence of the *w/s* ratio on *LOI* of hardened specimens cured without immersion (a) and with immersion (b) and processed under different *PF*Ps

Fig. 37. Dependences of the CS_{150} of representative specimens: on the *PF*P of specimens produced with *w/s* = 0.15 (a) and on the *w/s* ratio of specimens processed under a *PF*P of 25 MPa (b)

Fig. 38. Linear correlation between ρ and CS (a) and between *LOI* and CS (b) with the correspondent correlation coefficients *r* and their interpretation (underlined)

Fig. 39. Microscopic images of PG specimens manufactured under *PF*Ps of 10 MPa (a) and 25 MPa (b) (both cured with immersion); scale: x1000

Fig. 40. Graphical explanation of the 3rd stage of investigation

Fig. 41. Flowchart of the experimental processes of the 3rd stage of study

Fig. 42. Results of pH (left vertical axis) and soluble P_2O_5 content (right vertical axis) in PG specimens with different amounts of ZW additive

Fig. 43. XRD crystal composition of the specimens produced with different amounts of ZW additive

Fig. 44. Dependence of ρ (a) and CS_{150} (b) of the specimens on ZW content and *PF*P

Fig. 45. SEM microscopic images of specimens with different amounts of ZW additive: 0 wt% (a), 2.5 wt% (b) and 10 wt% (c and d); scale x2000 (the scale of image d is x1500)

Fig. 46. Graphical explanation of the 4th stage of investigation

Fig. 47. Flowchart of the experimental processes of the 4th stage of study

Fig. 48. Investigation of neutralisation of soluble P_2O_5 content in PG specimens by different amounts of MS additive (see pH values in the left vertical axis, and soluble P_2O_5 content in the right vertical axis)

Fig. 49. Investigation of the hydration temperature of pastes with different amounts of MS (a) and *LOI* of specimens after curing (b)

Fig. 50. XRD patterns of specimens produced with different contents of MS modifier

Fig. 51. CS values of dry specimens ($CS_{150(dry)}$) and of specimens after immersion of either 30 days ($CS_{150(30)}$) or 90 days ($CS_{150(90)}$), manufactured either with different MS amounts (columns marked with percentages) or with the pozzolanic recipe: 75% PG, 20% PC and 5% FA (columns marked with 'PC&FA')

Fig. 52. SF values of the specimens after immersion of either 30 days (SF_{30}) or 90 days (SF_{90}), manufactured either with different MS amounts (columns marked with percentages) or with the pozzolanic recipe: 75% PG, 20% PC and 5% FA (columns marked with 'PC&FA')

Fig. 53. Microscopic images of representative specimens: dry specimens with 0.0 wt% (a) and 0.4 wt% (b) of MS, and similar specimens after immersion of 90 days (c and d, for the respective amounts of MS)

- Fig. 54.** Graphical explanation of the 5th stage of investigation
- Fig. 55.** Images of steps for the paste preparation: preparing separate components in the required amounts (1), blending (2) and casting (3)
- Fig. 56.** Images of the manufactured specimens for different tests: 2 cm-sided cubes for *CS* test (a), the 4x4x16 cm prisms for *FS* test (already tested) (b) and 30x30x5 cm panels for measurements of λ (c)
- Fig. 57.** Flowchart of experimental processes of the 5th stage of the study
- Fig. 58.** XRD patterns of PG specimens with different fibre contents and types
- Fig. 59.** Dependence of ρ (a) and CS_{150} (b) values of specimens on their content and type of fibre, and on their content of ZW additive
- Fig. 60.** Results of ρ (a) and the mechanical properties (b) of PG specimens with different amounts of WF
- Fig. 61.** Microscopic images of PG specimens with wood fibre, enhanced by x100 (a) and x500 (b)
- Fig. 62.** Dependence of λ on the content of WF in PG specimens
- Fig. 63.** Dependence of the sound pressure level (*SPL*) of natural noise on the amount of WF in PG screen (a) and the *SPL* frequency spectrum (noise filtered with standard frequency octaves) of PG screens with different WF contents (b)

INTRODUCTION

Phosphogypsum (PG) is the main by-product manufactured during the production of phosphate fertilisers which are essential and irreplaceable resources for the entire agriculture industry all around the world [1, 2]. As a side-effect of this agricultural necessity, humungous amounts of PG are produced globally. In fact, the predicted global production for the end of the current decade is 200–250 million tonnes [1]. However, a major part of this by-product is not recycled, but rather stored in huge stockpiles or poured into water bodies, which constitutes an important threat for the surrounding ecosystems since various hazardous impurities, such as ^{226}Ra radionuclide and its progeny, soluble-acidic P_2O_5 and F^- compounds and potentially toxic trace heavy metals are typically found in the composition of PG.

The only solution seems to involve the recycling of PG in other applications, mainly agriculture, soil stabilisation, road base construction and building materials [1]. The fact that PG presents excellent binding properties (like natural gypsum) makes it an especially palatable material for the field of building materials. Besides, there is another important aspect to consider. The main binding material employed in the construction industry for a long time has been Portland cement (PC) whose production presents serious ecological problems derived from the high CO_2 emissions of its manufacturing process. Therefore, nowadays, an important ‘crusade’ against PC is taking place by looking for alternative green binders. In this context, gypsum-based binding materials are being widely investigated. The application of PG in building products would, in this manner, carry a double ecological win: the reduction of the ecological risks of PG stacks and its condition of a ‘green binding material’.

However, the interesting potential of PG as a binding material is restrained by several obstacles. First, numerous limitations have been imposed due to the environmental and health risks carried by the above mentioned impurities of PG composition, especially the radionuclides. Second, it is of importance that gypsum-based binding materials are not hydraulic (in contrast to PC) and, therefore, are not waterproof; they exhibit weakening of their mechanical strength in the case of exposure to humid conditions. That implies that the usage of gypsum-based products is essentially limited to the dry conditions of indoor applications. Therefore, the scientific community is searching for ways of mitigating the drawbacks of PG so that it could be employed in a safe manner in building products. To do so, not only the above mentioned impurity content must be reduced, but also the physical-mechanical and the waterproofing properties of PG specimens must be improved so that PG products become a competitive solution in the industrial-commercial sector building materials.

Despite the numerous investigations on the topic, the rates of utilisation of PG in building materials remain insignificant, whereas the growth of PG stockpiles even accelerates. The main problem of the majority of the performed investigations in this area seems to be the way in which they are performed. Usually, the improvement of various properties of PG is addressed separately, but that is not an efficacious approach since the applicability of PG depends, at the same time, on several factors

(radiological protectivity, soluble P_2O_5 and F^- impurity content, physical-mechanical properties, water-resistance). Hence, a comprehensive study on the different above listed aspects is required. In this context, the current investigation is performed.

The main goal of the current work involves improving the main properties of PG to make it a suitable binding material for building products by processing specimens through the casting and the press-forming methods and through the addition of various industrial waste modifiers.

The tasks of the investigation

1. To study the radioactivity levels of PG from different origins (either from igneous or sedimentary phosphate rock) and to evaluate the radiological aptness of each type to be used in building products.
2. To reduce the presence of harmful acidic-soluble P_2O_5 and F^- compounds by including different modifiers, which would allow a broader application of PG products.
3. To enhance the mechanical strength of PG specimens, especially by applying the method of press-forming, while also considering the influences of the microstructure of the initial hemihydrate phosphogypsum (HH-PG) and of the included additives.
4. To improve the water-resistance properties of PG specimens by modifying the composition of PG mixtures.
5. To produce PG specimens with better thermal and acoustic insulation properties.

Scientific novelty

- The influences of the nature, the microstructure and the processing method of the PG on the radioactivity level and on the physical and mechanical aptness of PG specimens have been determined.
- The press-forming method has been proposed as an effective way to improve the mechanical strength of PG specimens.
- The effects of $Ca(OH)_2$, zeolitic waste (ZW), metallurgical sludge (MS) and waste wood fibre (WF) additives on the physical, mechanical and chemical properties of the PG binding material have been defined.

Methods of the research

First, the initial materials have been characterised by the pertinent analyses. Their microstructure has been studied through SEM microscopy, and their chemical and crystal composition by EDS, XRF and XRD analyses. The radionuclide activity concentration has been evaluated through gamma spectroscopy, whereas the particle size distribution has been studied through the laser method in the dry suspension mode.

Second, the properties of PG pastes and specimens have been investigated by employing various methods. The hydration process of the pastes has been monitored through hydration temperature analysis, whereas the hydration degree of the hardened specimens has been defined by *LOI* measurements. The mechanical properties of the specimens have been investigated by the mechanical strength tests

indicated by the European Standard EN 13279-2 [3]. The water-resistance properties of PG specimens have been evaluated on the grounds of the softening factor (*SF*). The SEM characterisation of the microstructure of the specimens has been performed to support the results of the mechanical strength and the results of water resistance. The reduction of the soluble-acidic phosphate and fluoride impurities in PG specimens has been evaluated through both pH and colorimetry measurements of aqueous solutions. Finally, the thermal insulation properties have been investigated by taking the ready state hot-box approach.

Practical relevance

- The good physical and mechanical properties of PG specimens including high mechanical strength, a satisfactory degree of hydration and improved thermal insulation properties offer new possibilities to the utilisation of PG as a/the binding material for structural building products, such as load-bearing bricks or blocks.
- The enhanced waterproofing properties of PG specimens increase the application range of PG building products.
- The investigations on the radioactivity and on the reduction of the acidic-soluble impurities give valuable information about the protectivity and safety of the employed PG.
- The utilisation of PG in building products is bound to reduce the negative environmental impact of the useless and humungous PG stockpiles.

The main statements of the doctoral dissertation are the following:

1. The microstructure of HH-PG determines the hydration degree and mechanical strength of PG specimens.
2. The specimens processed under press-forming exhibit 1.6–2.1 times higher mechanical strength than those produced through casting.
3. The addition of a certain content of a ZW additive reduces up to 7.5 times the harmful soluble P_2O_5 impurity content.
4. The addition of a waste MS additive improves by 2 times the water-resistance of PG specimens.

Approval of the results of the study

The results of the performed investigations have been published in 4 research articles of scientific journals included in the *Clarivate Analytics Web of Science* database (with the citation index) and belonging to Q1 and Q2 quartiles. Some of the results have been made public in 3 international conferences: *GreenChem-18* (Madrid, Spain), the 19th *ICMB* (Brno, Czech Republic) and the 2nd *Vitrogeowastes* (Baeza, Spain).

Structure and scope of the work

The dissertation is composed of an introduction and 4 numbered chapters (which include the literature review, the methodology, the main results of the investigation and the conclusions). Additionally, the summary in the Lithuanian

language, the list of references, the author's CV and the list of publications on the topic of the dissertation along with the acknowledgements are provided. The dissertation is comprised of 176 pages, and it contains 14 tables, 63 figures and 157 sources in the list of references.

1. LITERATURE REVIEW

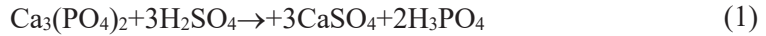
1.1. The production of orthophosphoric acid during which the problematic by-product phosphogypsum is obtained

Orthophosphoric acid (H_3PO_4) is the main feedstock employed to produce synthetic phosphate fertilisers, essentially granular and liquid ammonium phosphate fertilisers [2]. H_3PO_4 is usually expressed as P_2O_5 , which is the main compound conforming the material. The phosphate industry producing this material is of critical importance at the global scale, since there are no substitutes for phosphorus in agriculture [2]. In this way, each year, more than 30 million tonnes of orthophosphoric acid are manufactured worldwide [1]

Phosphate minerals are the prime materials from which phosphate synthetic fertilisers are produced. Thus, the global mine production of phosphate rock is humungous (in 2019, it was estimated to be $240 \cdot 10^6$ t), with the main manufacturing countries being China, Morocco and Western Sahara, the United States and Russia [2]. Phosphate ores contain mainly calcium and phosphorus, and their deposits differ according to their nature: sedimentary, igneous, metamorphic, biogenic, and the deposits caused by weathering [1]. Most of the deposits are sedimentary, while only 4% are igneous [4]. The content of impurities and organic materials tends to be lower in the igneous phosphate ores than in the sedimentary ones. One or more phosphate minerals are contained in the composition of the ores, with apatite representing the main mineral group also including fluorapatite, hydroxyapatite, carbonate-hydroxyapatite and francolite minerals. The general chemical formula of the apatite minerals is $\text{Ca}_{10}(\text{PO}_4, \pm \text{CO}_3, \pm \text{OH})_6(\text{OH}, \text{F}, \text{Cl})_2$ [1].

The processing methods of phosphate rocks into P_2O_5 and other products is comprehensively described by the International Atomic Energy Agency (IAEA) [1]. Worldwide, approximately 85% of all the extracted phosphate ores are processed into orthophosphoric acid (P_2O_5) through the so-called ‘wet process’ which involves the digestion of the phosphate rock by concentrated sulphuric acid [5]. To a lesser extent, the wet process based on hydrochloric acid is used to obtain high purity P_2O_5 . There are other processing methods for the phosphate rock, such as the digestion by nitric acid (to produce nitrophosphate fertilisers), the ‘thermal process’ (to produce elemental phosphorus), and the direct application as a fertiliser. Most of the produced orthophosphoric acid through the ‘wet process’ is further processed to manufacture fertilisers, whereas a small part is employed for animal feed and other products.

Hence, orthophosphoric acid is mainly produced through the ‘wet process’ which involves the so-called ‘acid attack’ under concentrated sulphuric acid. The basic chemical reaction is presented in Eq. (1) (IAEA [1]). As observed, together with P_2O_5 , important amounts of a by-product called phosphogypsum (PG) are also produced (see Fig. 1). PG is composed of CaSO_4 crystals as the natural gypsum, but with the addition of radionuclides and harmful contaminants of environmental concern.



There is a wide variety of different ‘wet processes’ employed to manufacture orthophosphoric acid. Focusing on the nature of the produced PG, the various methods differ on the level of hydration of the precipitated PG crystals which can be either dihydrate (DH) ($\text{CaSO}_4 \cdot 2\text{H}_2\text{O}$) or hemihydrate (HH) ($\text{CaSO}_4 \cdot 0.5\text{H}_2\text{O}$) and on the purity of the precipitated PG: according to the method, different amounts of residual P_2O_5 are present in the composition of PG. The different techniques are classified in two main groups: the ‘weak acid’ and the ‘strong acid’ methods.

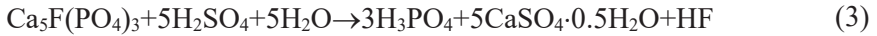


Fig. 1. View of the manufactured humid PG powder in a chemical plant of phosphate fertilisers, straight after the wet process

- a) The ‘weak acid’ methods. The produced orthophosphoric acid contains a relatively low amount of P_2O_5 (20–32%). The most popular method of this kind is called the ‘dihydrate method’, in which, the produced PG crystals are of the DH form ($\text{CaSO}_4 \cdot 2\text{H}_2\text{O}$). To this category, we also assign the ‘hemihydrate recrystallisation method’ which produces DH-PG crystals with a residual P_2O_5 content of 2.5% and the ‘dihydrate-hemihydrate method’ in which the produced PG crystals are of the HH form, with a very low amount (1%) of residual P_2O_5 .
- b) The ‘strong acid’ methods. The produced orthophosphoric acid contains a higher amount of P_2O_5 (in relation to that obtained by the ‘weak acid’ methods), in the range of 36–52%. The main employed method of this group is known as the ‘hemihydrate method’ where the produced PG crystals are of the HH form, with 8% of P_2O_5 contaminant, which conforms a considerable amount. The other method belonging to this group is called the ‘hemidihydrate method’ which produces DH-PG crystals after the recrystallization of the initially precipitated HH-PG crystals.

The chemical process of the digestion of fluorapatite where DH-PG crystals are produced is described by Tayibi *et al.* [6] in Eq. (2). Meanwhile, the chemical

reaction where HH-PG crystals precipitate is given by Vaičiukynienė *et al.* [7] in Eq. (3).



HH-PG is a binding material which can be used in building products, whereas DH-PG does not exhibit binding properties. During the ‘wet process’, the rates of production of the by-product PG are enormous and much higher (by 4–6 times) than the manufactured amounts of P_2O_5 . In fact, the outcomes of processing 1 t of phosphate rock are 1.46 t of PG and 0.24–0.36 t of P_2O_5 [1]. Thus, this ‘side effect’ of the phosphate fertilisers’ industry cannot be ignored. According to IAEA [1], the global production of PG is constantly increasing, with the prediction for the year 2030 being between 200–250·10⁶ t. However, even though the production of this by-product is enormous and disproportionate, only about 15% of it is recycled into useful applications [8], while the rest is directly stored in huge stockpiles or water bodies which are continually growing.

1.2. Composition of PG

PG is mainly composed of hydrated CaSO_4 crystals (up to 92% of its content), but with additional impurities which come from the raw material [9] and the processing process. The phosphate ores from which PG is manufactured, aside from calcium, also contain important amounts of P_2O_5 (4–40%), fluorine (from less than 1% to more than 4%), and trace heavy metals and radionuclides [1]. As a consequence, all these compounds (further referred to as ‘impurities’ or ‘contaminants’) will be present to a greater or lesser extent in PG. These contaminants not only produce negative environmental problems in the surrounding areas of PG stockpiles, but also limit the recycling of PG (in construction products, agriculture, etc.) due to its potential risks for the environment and for human health. Hence, as mentioned, the main typical contaminants which are present in the composition of PG are radionuclides from the ^{238}U decay chain (especially, ^{226}Ra), soluble phosphate and fluoride compounds and heavy metals.

1.2.1. Presence of ^{226}Ra and of other radionuclides in PG

Phosphate rocks are naturally radioactive, especially due to the presence of uranium (^{238}U), thorium (^{232}Th) and their decay products (^{230}Th , ^{226}Ra , ^{210}Pb , ^{210}Po), which in the phosphate ore are in equilibrium [10]. This equilibrium is broken with the digestion of the phosphate rock by sulphuric acid during the ‘wet process’, and radionuclides undergo a selection process which was extensively studied by Mazzili *et al.* [10], Szajerski [11] and Bolívar *et al.* [12]. After investigating the radionuclide presence in phosphate rock as well as in PG, Mazzili *et al.* [10] concluded that, during the ‘wet process’, about 90% of ^{226}Ra , 80% of ^{232}Th plus ^{230}Th , 100% of Pb and 78% of Po precipitate to PG. On the other hand, according to Bolívar *et al.* [12], most of ^{238}U precipitates in P_2O_5 .

In this way, noticeable amounts of ^{226}Ra , and also uranium and other uranium decay particles are typically included in the composition of PG [1, 9, 13]. Thus, PG is classified as a Naturally Occurring Radioactive Material (NORM) [1, 14] and there are restrictions to its usage. The activity concentration of ^{226}Ra and its progeny in PG derived from sedimentary phosphate ores tend to be 200–3000 Bq/kg, while that of PG from igneous phosphate ores is usually lower, specifically, between 10 and 700 Bq/kg [1].

1.2.2. Presence of phosphate and fluoride compounds in PG

Phosphate (P_2O_5) and fluoride (F^-) compounds are typically present in PG [1, 8, 15, 16, 17, 18, 19]. As mentioned in Section 1.1, depending on the kind of the employed ‘wet process’, a higher or lesser amount of residual P_2O_5 will remain in PG. In fact, the P_2O_5 content can vary in a wide range, between 0.05% and 8% [1]. Meanwhile, the presence of fluoride depends on the original raw material (see Eq. (2) and Eq. (3)) and typically goes from 0.1 to 1.8% [1]. According to Kaziliūnas *et al.* [16], these phosphate and fluoride impurities are present in various forms:

- a) in the surface of calcium sulphate crystals forming acidic water-soluble compounds (H_3PO_4 , $\text{Ca}(\text{H}_2\text{PO}_4)_2 \cdot \text{H}_2\text{O}$, H_2SiF_6);
- b) substituted in the crystal lattice of CaSO_4 (effectively, solid solutions of $\text{CaHPO}_4 \cdot 2\text{H}_2\text{O}$, SrSO_4 , Na_2SiF_6);
- c) forming non-soluble compounds, such as apatite and quartz.

The harmful impurities are acidic water-soluble ones since they can dissolve and escape from the material through leaching water. The dissolved phosphate in high concentrations can cause eutrophication of rivers and lakes. Meanwhile, the dissolved fluoride in drinking water in concentrations higher than 1.5 mg/L can cause dental skeletal fluorosis [20]. The same happens after a repeated ingestion of plants with elevated levels of fluoride [1]. Besides, by evaporation, the dissolved fluoride may escape in the form of toxic gases, such as HF, H_2SiF_6 and SiF_4 which are dangerous for human health [16, 21]. Water-soluble phosphate and fluoride impurities also produce weakening in the mechanical properties of PG [16, 17].

1.2.3. Presence of trace heavy metals and rare earth elements in PG

According to Pérez-López *et al.* [22], during H_3PO_4 production through the ‘wet process’, between 2 and 12% of each trace element present in the phosphate rock is transferred to PG. Among those trace elements, PG typically contains small amounts of heavy metals: arsenic, barium, cadmium, chromium, lead, mercury, selenium and silver [6, 23]. These heavy metals, especially Cd, are considered potentially toxic elements and should be regarded with caution. The presence of Cd in air, water or food can trigger cancer and other diseases in organ systems [24].

On the other hand, some of these heavy metals, especially of the group of rare earth elements (REE) present in PG, are valuable resources for other industries. The REE are a group of 17 elements (the 15 lanthanides and 2 other elements, i.e., scandium and yttrium) with similar chemical properties. In recent times, these REE have gained unique importance in the industry of high-tech products: hybrid cars,

wind turbines, compact fluorescence lights, flat screen television, mobile phones, disc drives and defence technologies [25]. Hence, the interest on these materials, together with their price and demand, has been increasing [26, 27]. This situation has led for the REE to be classified as ‘critical’ in some countries (EU, USA and Japan) due to the risks of supply shortage and to the higher impact that such a shortage would produce to the economy [28]. In this context, alternative ways of extraction and recycling of REE must be found. The REE contained in PG makes it a valuable resource, from which these compounds can be recovered [29, 30].

The presence of heavy metals in PG produced from igneous phosphate rock is usually lower than PG from sedimentary rocks, whereas the REE content tends to be higher [1].

1.3. The environmental problem of the PG deposits and the necessity of PG recycling

The constant production of PG all over the world, the rapid growth of PG stacks, and the lack of alternatives and effective ways to recycle this material leads to a global ecological problem. PG stacks cause chemical and radiological contamination of the surrounding areas: exposure to toxic HF gas, soil and ground water contamination with radionuclides, acidity or mobile anions, among others [31]. Moreover, these deposits occupy large areas which could be employed with more useful purposes (parks, buildings, recreation, etc.). A view of a PG stockpile in Lithuania is given in Fig. 2.



Fig. 2. View of a field next to Kėdainiai (Lithuania) with a PG stack in the background

The radiological influence which PG deposits make on the surrounding environments and urban areas has been widely investigated. Al Attar *et al.* [32] studied the radiological influence that a Syrian PG stack makes to the surrounding air, ground water, soil and plants and concluded that for, the first three cases, radioactivity was below the limit values, and what regards radioactivity

concentration on plants, it varies in terms of the plant species. The researcher suggested that the Syrian PG could be used for agriculture or soil stabilisation.

In Southwest Spain, there is an important PG stack where PG is produced from Moroccan sedimentary phosphate ores. The stack is located between the urban area of Huelva City and the estuary of the River Tinto which flows into the Atlantic Ocean. Therefore, PG poses important environmental risks for the ecosystems of the estuary and, what is even more important, major health risks for the inhabitants of Huelva. Thus, these risks have been widely investigated and evaluated by numerous studies. Bolívar *et al.* [12] measured the gamma emission inhalation rates 1 m above the surface of the Huelva PG stack and depicted values 6 times higher than those typically found above common soil. However, Dueñas *et al.* [33] reported that the calculated external γ -radiation dose received by the workers of the Huelva PG piles was 0.293 mSv/year, far below the agreed dose limit for workers at 20 mSv/year [34], while the reported annual dose for the public was found to be 0.35 mSv/year, which is below the recommended annual dose limit of 1 mSv/year [34], thereby concluding that, from the radiological point of view, the PG stack does not carry any risk for health. Another important aspect to consider is the presence of fluoride compounds in PG. Toxic HF gas is released from PG stockpiles thus causing serious problems in the vicinity. Therefore, Torres-Sánchez *et al.* [21] investigated the contamination of the air by HF gas in the surroundings of the Huelva PG stacks and determined that the highest emission of HF was related to a brine situated in the stack territory, from which most of the HF evaporates, especially in summer. The study concluded that this HF emission to the air can be one of the main causes of the high incidence of asthmatic symptoms observed in the city of Huelva. Pérez-López *et al.* [22] studied the potential risks of contamination of the estuarine zone in the case of a hypothetical collapse of the PG stack with regard to the mobility of the toxic trace elements contained in PG (heavy metals and uranium), thereby evaluating three environmental scenarios: water leaching, exposure to oxidising, and reducing conditions. The investigation gives an idea of the extreme contamination potential of the PG stack to the estuarine zone and to agricultural soils due to the above listed scenarios. Cánovas *et al.* [35] also explored the Huelva PG stack. They investigated the mobility and fluxes of the REE, including Y and Sc, under weathering conditions. Despite the observed low mobility, it was depicted that around 104 kg/year of REE and 40 kg/year of Y and Sc are released to the estuary, thereby damaging the environment. Therefore, the authors suggested that the development of methods to extract these valuable materials from the PG stack should be encouraged, and that would reduce their harmful impact on the ecosystems of the estuary.

Therefore, the environmental problem produced by the storage of PG in the above mentioned stockpiles should be faced and dealt with. The best way to do it would be to find effective applications to recycle PG. However, the contaminants contained in the PG composition (especially the radionuclides) are targeted by national and international restrictions or even prohibitions to the usage of this material. For instance, in June 1992, in the US, the Environmental Protection Agency (US EPA) [36] banned the utilisation of PG other than agriculture in the United States due to the radioactivity risks for health carried by this material. Besides, all

PG exceeding 370 Bq/kg radioactivity was prohibited for all uses. Therefore, from that point on, in the US, most of the investigations related to the use of PG in road bases or construction materials have been virtually frozen. However, in April 2020, The Fertilizer Institute (TFI) presented a petition [37] with the purpose to remove the EPA prohibition. The TFI request was based on comprehensive studies which proved that the usage of PG in road construction is protective with human health because the radioactivity exposure levels are far below the EPA established radiation safety limits (3 for 10000) below those of the natural exposure levels. Besides, economic analysis presented in the Appendix 6 of the document strongly encourages the utilisation of PG by predicting that the reusing of PG would comport important cost savings related to the management of PG stacks between \$37 and \$160 million for the analysed period (2020–2042). Hence, 28 years after the prohibition, in October 2020, EPA approved again the use of PG for road construction [38], therefore, investigations in this field are expected to be retaken.

As a result of the above mentioned and similar regulatory obstacles, the stockpiles continue growing. The situation generates a real vicious circle of a difficult solution. Although it is true that PG has been applied with relative success in such areas as agriculture, back-fill and road base construction, and building materials [1], still, the relatively small amounts of recycled PG have not led to a significant reduction of the PG storage problem. Due to the above mentioned reasons, the interest of the scientific community in the applicability of the PG is increasing with each year [39] across a wide range of fields.

1.4. Application of PG in agriculture, soil stabilisation and road base construction

The main fields of the application of PG are agriculture, soil stabilisation, road base construction and building materials [1]. The three initial ones are explained in this section, whereas the application in building materials shall be described in Section 1.5. Other important fields in which PG is utilised are the recovery of sulphur [40], marine applications (to create artificial oyster cultches and reefs [41, 42, 43]), and landfill [44].

1.4.1. Application of PG in agriculture

PG can be employed in agriculture as a fertiliser or as a conditioner for agricultural soil. According to Alcordo and Rechcigl [45], gypsum and PG are potential bulk carriers for micronutrients and low-analysis micronutrients. PG is a good source of S and Ca for crops, and a good material to amend the agricultural soil in multiple situations, as listed by Rutherford *et al.* [31]:

- a) for highly weathered soils with a relatively low amount of exchange capacity or a low amount of extractable nutrients;
- b) for soil with high sodicity in dense subsoil horizons and for soil with various levels of sodicity with a tendency towards dispersion and crusting;
- c) for acid soils with important amounts of aluminium;
- d) for calcareous soils.

However, the environmental concerns caused by the presence of radionuclides, heavy metals, REE and other contaminants have been investigated by various researchers. Papastefanou *et al.* [46] investigated the radioactivity levels of soil tilled with PG in Greece and of rice samples originating from those fields. An increase of the radioactivity levels in both soil and rice was observed. The achieved levels did not constitute a risk for health, but ^{226}Ra activity in the employed PG should be constantly monitored to keep the agricultural products safe from the radiological perspective.

Abril *et al.* [47] investigated the activity concentration of radionuclides in non-reclaimed soil, reclaimed soil without PG amendment, and reclaimed soil with PG amendment and observed a non-significant effect of PG amendments in comparison to the reclaimed non-amended plots. Besides, the researchers discovered that the cadmium concentrations in tomatoes grown from PG amended soils were substantially higher than those found in tomatoes from the market survey. A very strong correlation between ^{226}Ra of the soil and the cadmium concentration of tomatoes was depicted.

1.4.2. Application of PG in soil stabilisation and road base construction

There is abundant research regarding the utilisation of PG in road base structures. The PG can be employed in two ways:

1. for base soil stabilisation: PG is blended with base soil aggregates to improve their engineering properties;
2. as the road base layer: PG is employed to create a rigid and strong layer with engineering properties like those of the other materials in use. The PG layer is also a good way to seal the soil from hazardous materials which may be present in the road surface.

The PG usage for the road base is a desirable solution since it helps to recycle the PG of the stockpiles in considerable amounts, and also because of the economic aspect: PG is a cheap alternative to other typical road base materials, especially when these materials are not found in the nearby areas.

In the United States, the availability of PG is enormous. Therefore, in the decade of the 1980s, PG was regarded as a valuable material. There was abundant research on the utilisation of PG to improve road bases. The results were, in general, positive and promising. Extensive investigation was performed at the Florida Institute of Phosphate Research (FIPR) by Chang *et al.* [48]. The study was intended to describe the complex aspects of the application of PG in road construction, and the experiment comprehended a wide range of stages: laboratory tests, analysis of experimental road sections, environmental investigation, and economic analysis. The laboratory tests revealed that HH-PG is a better construction material for roads than DH due to its performance under wet conditions, especially when mixed with sand at a ratio of 2/1 (HH-PG/sand). Besides, the experimental roads delivered satisfactory mechanical and deflection performance. What regards the economic aspect, the construction of the experimental road turned out to be 5 times cheaper than the conventional roads. The assessment of the environmental impact of the PG experimental roads revealed that their gamma radiation levels were higher than

before the construction of the road, but within the normal levels for backgrounds, and that ^{222}Rn levels determined in the air and water, and ^{226}Ra found in the soil surrounding the roads did not reveal any significant changes before and after the completion of the roads. Besides, several ground water monitoring wells were installed along the road, and, in some of them, significant upward trends of SO_4 were observed, but still within the allowed concentration limits for drinking water. Hence, no particular risks for health were identified. Therefore, the study revealed the enormous potential of using PG as a construction material for road bases.

In another study sponsored by FIPR, Figueroa *et al.* [49] also investigated the usage of both DH and HH-PG in the secondary road-base construction and obtained similar satisfactory results with respect to the *CS* properties in dry and soaked conditions. HH-PG was water-resistant, while DH-PG was not. Thus, a small amount (1–2%) of cutback asphalt RC-70 was added to DH-PG as a waterproof admixture with the objective to improve its behaviour in humid conditions. Although the *CS* was lower after developing soaked conditions, the specimens remained bonded together, showing in this way the effectiveness of the waterproofing additive.

Gregory *et al.* [50] investigated the usage of PG in the road base construction by stabilising it with various amounts of Portland cement (PC) and fly ash (FA). The employed PG was produced in Texas. Two types of PG, with $\text{pH}=3$ and $\text{pH}=5$, respectively, were employed. It was found that the stabiliser content, the pH of PG, and the dry density of the mixture exert major influence on the *CS* of the stabilised mixtures. The PG with a more acidic pH did not produce strong enough specimens to be employed in road bases. Otherwise, the less acidic PG, when mixed with 30% of FA and 10% of PC, met the requirements.

Taha *et al.* [51], also representing the US, investigated the suitability of employing cement-stabilised PG in the road base construction. For this purpose, 8 different types of cement were used due to the influence of tricalcium aluminate (C_3Al) which is differently present in various cements regarding *CS* and the expansive characteristics of PG blends. The cement-stabilised PG was mixed with sand. The unconfined *CS* of dry-cured and water-immersed specimens was tested. It was noticed that, during the water immersion test of the different specimens produced with different types of cements, the *CS* of some of them decreased, whereas the *CS* of the remaining samples increased. Moreover, expansion analysis, freeze-thaw testing and wet-dry testing was performed. It was concluded that the cement-stabilised PG mixtures constitute a good material to be employed in road bases and subbases. However, the type of the cement determines the properties of these mixtures, and it should be chosen carefully. This impact was attributed to the reaction between C_3Al , contained in the cement, and the sulphates contained in the PG which can trigger the formation of ettringite and thaumate crystals and may cause eventual cracking of the pavement.

Regardless of the generally positive results as obtained by the American researchers, in 1992, the usage of PG in road base constructions was banned in the US [36], only to be allowed again 28 years later [38]. Therefore, during this period, investigation dealing with the usage of PG in road construction continued in other countries.

Paige-Green and Gerber [52] performed a study of the usage of PG in South African roads. PG was employed as a substitute for the traditional road layerwork materials, and also as a base-soil stabiliser. Experimental road sections were built in two sites: Edenvale and Tembisa. Six months after the construction, the deflections in the PG stabilised roads were found to be higher than the normal deflections expected from a control base. However, the unconfined CS varied from 0.4 to 1.8 MPa, while in the control gravel stabilised base it varied from 0.21 to 0.39 MPa. After 19 months, a second monitoring observation was carried out. The strength of the PG stabilised bases was found to have increased with time, between 86 and 121%, while in the control gravel stabilised bases, it increased only between 30 and 50%. Therefore, the study showed that, after that period, the employed materials were performing effectively and that the PG stabilisation of road bases is a cost-effective solution in comparison to the usage of the conventional materials.

Degirmenci *et al.* [53] studied the stabilisation of soil by using PG with cement and FA in Turkey. The mixture decreased the plasticity index, which is a highly positive factor, and increased the CS of stabilised soil in comparison to the score of unstabilised soil. Cement had a higher effect in increasing the CS than FA. In the authors' opinion, the utilisation of waste materials, such as PG and FA, instead of the conventional and more expensive ones as PC constitutes significant contribution for the economy of Turkey, as well as an effective solution for the contamination problem.

Folek *et al.* [54] performed an interesting investigation in Poland, where the climate is colder and more aggressive than in the previously considered places. The researchers produced a three-component mixture: PG, FA and a road binder, in proportions 60/40/8. FA neutralised the acidity of PG, whereas the road binder enhanced the strength of the mixture. The mixture was used for one of the layers of an experimental 30 m² parking lot. The pavement consisted of several layers, the main of which was a PG-based layer separated from the following ones by a waterproofing membrane. The CS results from some mixtures created and cured in the laboratory (1.3 MPa) were similar to those of the specimens cut from the experimental parking lot (1.7 MPa). The resistance of the PG layer to the freeze-thaw cycles proper of the Polish winter season was satisfactory, and, in fact, the strength of the specimens taken from the parking lot after the winter not only did not decrease, but they actually increased by 3 times. Field tests were also performed on a separate part of the parking lot. The geotechnical and CS test indicated that the three-component (PG, FA and binder) mixtures are suitable to be used in the upper layers of a road loaded with light traffic, whereas PG-FA mixtures without a binder are suitable for the construction of the lower layers or of road embankments because they meet the requirements for road embankment materials below the frost penetration zone. The achieved radioactivity levels observed in the mixtures and specimens were below the allowed thresholds. The only environmental hazard is the elevated presence of sulphates in the effluent water from the parking lot, which was remarkably higher than the limit.

Sarkka [55] described a project which took place in the cold climate conditions of Finland, in the region of Kemira. PG was employed to stabilise the road base and

also as a sealing material (specifically to protect ground water from leaching). The renovation of two old roads was performed by using PG mixtures. In the first road, PG and gravel mixtures were used as the structural material. In the second road, the focus was directed towards the sealing effect of the PG layer. The results showed that the leaching effect must be improved because PG did not show adequate impermeability. The stabilisation of the old roads showed that the strength development and the bearing capacity were better than the reference roads.

Therefore, most of the performed research concludes that PG is suitable to be employed in road-base construction. However, the main constraints to this application, according to IAEA [1], involve three aspects:

1. economic obstacles [56]: PG is a cheap material to be used in road base construction as long as the construction site is located not farther than 150 or 200 km from the PG source [57];
2. cultural obstacles: the manufacturers of roads are more inclined to continue using the conventional materials such as sand and gravel, instead of starting to use an innovative solution, such as PG;
3. regulatory obstacles: the presence of harmful contaminants in PG, especially radionuclides, suggests that PG has to overcome the regulations and prohibitions of some countries, such as the above mentioned no-longer valid prohibition in the USA.

1.5. Application of PG in the field of building materials

PG is regarded as a valuable resource in the field of building materials, especially due to its potential as a binding material. Therefore, there is abundant research focused on improving the properties of PG so that to convert it into a suitable material for building products. Rashad [8] made an extensive review of the utilisation of PG in this field, according to which, the main areas of research are related to mechanical strength (30.56%), setting time (13.89%), purification (18.52%), water absorption and permeability (10.19%), while the less popular topics are workability, unit weight, and expansion behaviour. Other comprehensive reviews on PG utilisation in the field of building materials have been carried out by Dvorkin *et al.* [58], Saadaoui *et al.* [5], Bandgar *et al.* [59].

PG can be employed in building products as a substitute of natural gypsum. Kovler and Somin [9] compared both materials, thus reviewing the pros and cons of each one of them. At a first glance, it appears that, from the economic point of view, the utilisation of a residual material as PG would be preferable to natural gypsum which should be extracted in mines. However, the drying and purification processes that PG undergoes so that to become suitable for building products may be not so economic. Besides, radioactivity and the presence of heavy metals in its composition (especially Cd) restrict its utilisation. In countries where there is no natural gypsum, such as Japan or the Netherlands, or where it is available at faraway distances (e.g., in France), the utilisation of PG as a substitute of natural gypsum can be a good solution. It could be used as plasters, flooring slabs, blocks, wallboards, sheeting and gypsum form plastering machines [9].

1.5.1. Issue of PG toxicity and necessity of its purification in order to make it suitable for building materials

As previously mentioned, the main problem limiting the utilisation of PG is the hazardous compounds present in its composition: radionuclides, soluble phosphate and fluoride compounds, and trace elements, especially heavy metals. These contaminants are a potential risk for the environment and for human health. Thus, in order to ensure safe usage of PG in building products, it should be purified. There are three main ways to purify PG from harmful contaminants [9]:

1. to use clean phosphate rock to produce PG (free from radium and heavy metals);
2. to use a clean production process;
3. to purify the obtained PG.

According to Kovler and Somin [9], the purification of PG during the production process of phosphoric acid only reduces the content of the residual P_2O_5 contaminant whose purification depends on the employed production method, as described in Section 1.1. Meanwhile, the concentration of radium and heavy metals is scarcely reduced (if reduced at all) by any production process.

Radioactivity of PG regarding its application in building materials

Radioactivity is the most important obstacle when it comes to the application of PG in building materials. The main issue is the emanation of ^{222}Rn [60, 61], a poisonous gas of the decay of ^{226}Ra . Radon gas is usually emanated by soils or rocks, and, through soil gas infiltration, it tends to concentrate in enclosed spaces, such as mines or houses [62]. Other sources of this gas are building materials and water extracted from wells. According to the World Health Organisation (WHO) [62], the inhalation of ^{222}Rn produces tens of thousands of deaths of lung cancer each year globally. In fact, the cases of lung cancer which can be attributed to indoor exposure to radon ranges between 3 and 14%. Therefore, the presence of radon in building materials must be monitored and restricted. In fact, the prohibition of PG usage in the USA (see Section 1.3) was only related to radioactivity. In the European Union, the guidelines to limit the presence of ^{222}Rn in building materials are provided in the Council Directive 2013/59/Euratom [63]. This directive determines that each Member State should establish a reference level of indoor ^{222}Rn concentration, in all cases lower than 300 Bq/m^3 . In order to ensure the accomplishment of this requirement, the document sets the gamma dose limit emitted by building materials of 1 mSv/year . When the gamma dose does not surpass this limit, the presence of ^{226}Ra radionuclide in building materials will be small enough to make it unlikely that ^{222}Rn emanation would surpass the level of 300 Bq/m^3 .

In order to identify building materials of concern, the above mentioned directive recommends using the activity concentration index I which indicates the equivalent concentration of ^{226}Ra , while also taking into account the concentration of ^{232}Th and ^{40}K radionuclides. Thus, index I is calculated as presented in Eq. (4).

$$I = \frac{C_{Ra-226}}{300 \text{ Bq} \cdot \text{kg}^{-1}} + \frac{C_{Th-232}}{200 \text{ Bq} \cdot \text{kg}^{-1}} + \frac{C_{K-40}}{3000 \text{ Bq} \cdot \text{kg}^{-1}} \leq 1.0 \quad (4)$$

where C_{Ra-226} , C_{Th-232} and C_{K-40} are the activity concentrations of radium, thorium and potassium in a building material. Index I is applied for the final building material which is employed in construction, and not to its separate components. The European Council's document indicates that the $I \leq 1.0$ limit can be used as a useful tool to identify the materials which can cause the reference ^{222}Rn level to be exceeded. The $I \leq 1.0$ limit was based on an experiment performed in a closed room with dimensions of 4.0x5.0x2.8 m, made entirely of concrete (with a density of 2350 kg/m³ and a thickness of 200 mm) which was without any doors or windows [64]. However, the real situations may strongly differ from those of the experiment, so that, in the case that index I exceeds 1.0, the gamma dose can be calculated more precisely by considering the density and the thickness of the material, the amounts in which it is intended to be used (in bulk amounts or for superficial uses) and the type of the building. Besides, when the building material is employed in lesser amounts (ceilings, tiles, boards), the more liberal limit $I \leq 6.0$ is recommended [64].

As explained in Section 1.2.1, the radionuclide concentration in PG mostly depends on the nature of the original phosphate rock [9, 14]. For instance, apatite rocks are of igneous origin, while phosphorite ores are sedimentary, hence, PG obtained from apatite ores is expected to exhibit a lower radioactivity level than PG obtained from phosphorite ores. Hence, PG obtained in different countries may present a wide range of radioactivity levels. Kovacs *et al.* [65] presented a list of the radioactivity levels of 31 countries located worldwide. The majority of the countries presented ^{226}Ra contents between 100 and 700 Bq/kg, with respective I values being between 0.7 and 2. However, there are important exceptions. The maximum radioactivity level was observed in PG from Morocco, with ^{226}Ra content of 1420 Bq/kg (the I value was not given, but only the contribution of ^{226}Ra gave a value of 4.7) and in the United Kingdom where PG exhibited ^{226}Ra concentration of 1020 Bq/kg and an index value of $I = 3.6$. On the other hand, PG produced in Sri Lanka contained as low ^{226}Ra radionuclide content as 35 Bq/kg, but still relatively high ^{40}K concentration of 585 kg/m³, thus, the index was derived as $I = 0.7$. For comparison purposes, the mean radium concentration values found in different specimens of normal European gypsum and in the European common soil are 15 and 36 Bq/kg, respectively, and their mean I values are 0.13 and 0.45, respectively [66]. Besides, the typical and maximum levels of radioactivity of different materials used in building products, as well as those of industrial by-products, including PG, are given in document RP-112 [64], as represented in Table 1. The provided values are useful to compare and understand that the radioactivity of PG is by far higher than that of the 'normal' building products.

Table 1. Typical and maximum values of radionuclide concentration of different common building materials and industrial by-products, including PG, in the EU countries [64]

Material	Typical activity concentration (Bq/kg)			Maximum activity concentration (Bq/kg)		
	²²⁶ Ra	²³² Th	⁴⁰ K	²²⁶ Ra	²³² Th	⁴⁰ K
Most common building materials (may include by-products)						
Concrete	40	30	400	240	190	1600
Aerated and light weight concrete	60	40	430	2600	190	1600
Clay (red) bricks	50	50	670	200	200	2000
Sand-lime bricks	10	10	330	25	30	700
Natural building stones	60	60	640	500	310	4000
Natural gypsum	10	10	80	70	100	200
Most common industrial by-products used in building materials						
PG	390	20	60	1100	160	300
Blast furnace slag	270	70	240	2100	340	1000
Coal fly ash	180	100	650	1100	300	1500

Hence, in most cases, most of the PG types surpass the recommended radioactivity level of $I \leq 1.0$. However, in some cases, the utilisation of PG in building products is not dangerous. Campos *et al.* [13] analysed the radon exhalation of bricks and plates made of Brazilian PG and concluded that the utilisation of PG in building materials is a safe practice from the radiological point of view. During an investigation performed in Brazil in several stages [67, 68, 69], some researchers created an experimental house and covered the walls with PG boards and a PG ceiling. The depicted ²²²Rn gas concentration in the air of different rooms reached 120 Bq/m³, far below the established limit of 300 Bq/m³. The value of I for the employed PG was 1.8, but it was not a problem since PG was only employed for superficial purposes. The study concluded that the use of PG for wall boards and ceilings in dwellings is a radiologically safe practice.

Kovler and Somin [9] realised the problem of the difficult purification of PG from radioactive compounds. According to them, there exist some methods of removing ²²⁶Ra which are based on the recrystallisation of CaSO₄ in either nitric acid or sulphuric acid while further adding Ba-ions. However, these methods are not economically feasible. Therefore, Kovler and Somin performed a series of preliminary investigations which delivered promising results [70, 71, 72, 73, 74, 75] where an alternative purification approach was adopted. The results of these studies were further described and explained by the authors in a further review paper [9]. Radioactive compounds are present in the form of insoluble radium sulphates which is the main impurity, aside from other metal salts. The proposed method involves a topochemical reaction at a temperature of 140–350 °C where a small amount of a special reagent is added to the polluted grey PG. This reaction results in readily soluble radioactive salts and other metal salts which can be easily removed by means of solution in the reactor, while washing and filtering. In this way, the equivalent

radium content in PG was reduced by 25 times (from 450 to 19 Bq/kg), and, in some cases, even by 40 times, the content of harmful phosphate and fluoride was also reduced; it decreased by 20 and 5 times, correspondingly. Thus, by this method, the grey contaminated PG was processed into a white and clean material which could be used as a gypsum binder. This technology would be economically feasible if the industrial installations for the production of gypsum binder were built near the phosphate plant.

Romero-Hermida *et al.* [76] performed two different procedures to treat PG. The first one is based on the application of NaOH. The second procedure is based on the reaction with a residual liquid of the aluminium industry. Plain PG exhibited a radioactivity level of $I = 2.0$. The obtained by-products from the treatment with soda (putty lime and solid CaCO_3) presented I values of 2.4 and 2.7. Meanwhile, the obtained by-products from the second treatment were katoite and calcite; they exhibited I values of 1.5 and 1.4. Therefore, all the obtained materials are classified as NORM, but they can still be used in surface products because of $I \leq 6$. Moreover, a mortar was produced with the lime putty of the 1st procedure with a lime/sand ratio of 1/3 and a water/lime ratio of 0.5 (calculated by weight). The depicted I index for this mortar was 0.8, and this indicates that it is not a NORM; hence it can be used without restrictions when producing building materials.

Gascó *et al.* [77] studied the radiological risks of using PG as a modifier to cement. The concentration of the main radionuclides (^{226}Ra , ^{210}Pb and ^{210}Po) in a type of cement with a PG modifier decreased by 5 to 10 times in comparison to their concentrations depicted in plain PG. Hence, the presence of these radionuclides decreased proportionally to the used amount of PG. The behaviour of ^{232}Th and ^{40}K radionuclides was different: the concentration of ^{232}Th in the modified cement remained the same (with respect to that of plain PG), whereas the concentration of ^{40}K even increased by 50 times. This happened because ^{232}Th and, especially, ^{40}K are present in high concentrations in the sand mixed to produce the cement. Even so, the radioactivity levels of this PG modified cement fulfilled the regulations of the EU countries and, therefore, it is proposed as an effective way to utilise PG in building products.

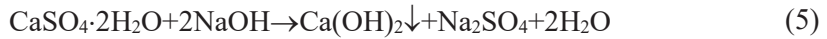
Content of soluble acidic P_2O_5 and F^- impurities in PG regarding its utilisation in building materials

As described in Section 1.2.2, significant contents of P_2O_5 and F^- impurities are contained in PG, among which, the soluble compounds are the problematic ones since they damage the environment, cause health concerns and even weaken the mechanical properties of the material. Therefore, numerous studies on the neutralisation and removing of these acidic soluble impurities have been performed.

Singh [17] determined the influence of P_2O_5 and F^- impurities on the microstructure properties of natural gypsum plaster. The author imitated the impurities of PG by adding 0.5–1.5% soluble reagents H_3PO_4 , $\text{Ca}(\text{H}_2\text{PO}_4)_2 \cdot \text{H}_2\text{O}$ and NaF to a plaster of natural gypsum. The microstructure of the gypsum crystals changed from needle shapes to prismatic, rhombic and lath shapes. This microstructure retarded the normal set time and considerably reduced the CS of the

pastes. Some sparingly soluble phosphate and fluoride reagents were also employed, but their effects on the properties of the plaster were not as determinant as those of the soluble ones. Hence, the performed investigation confirmed the negative effects of acidic impurities on the properties of PG.

Cárdenas-Escudero *et al.* [78] investigated treatment of PG which would help to mitigate two environmental problems at the same time: the management of a by-product (PG), and the harmful emissions of greenhouse gases. PG was dissolved in an alkali soda solution (NaOH), thereby producing portlandite (Ca(OH)₂) in the solid state and Na₂SO₄ dissolved in water (see Eq. (5)). Then, the carbonization process through which the produced portlandite evolved into calcite (CaCO₃) (see Eq. (6)) was analysed, ultimately revealing that all the Ca content of portlandite was carbonated, and so indicating the efficacy of this process when seeking to reduce greenhouse gases. In summary, PG as a by-product was used as a calcium source to produce CO₂ sequestration, thereby helping to fight the climate change. Besides, most of the harmful impurities which are present in PG, such as P, F and hazardous heavy metals, precipitated in portlandite and, subsequently, in the final calcite, whereas the sodium sulphate solution was free of those impurities. Thereby, the immobilisation of these hazardous components in calcite resulted to be an efficacious mechanism to mitigate the issue of their transferring to the liquid state, thus avoiding further risks for the environment and for human health.



Romero-Hermida *et al.* [79] processed PG in the same way (see Eq. (5)) to obtain lime putty (portlandite) and compared its rheological properties to those of commercial lime powder and aged lime putty. The obtained lime putty from PG treatment, aside from exhibiting the same environmental advantages as described by Cárdenas-Escudero *et al.* [78], also presented appropriate behaviour in terms of the rheological properties (i.e., linear viscoelasticity and viscous flow behaviour), which makes it a suitable substitute for the commercial limes used in composite materials in the building industry.

Kaziliūnas *et al.* [16] neutralised soluble P₂O₅ and F⁻ by applying lime suspension under autoclave (hydrothermal) conditions. In this way, the acidic impurities were transferred into non-soluble compounds: Ca₅(PO₄)₃OH·mH₂O, Ca₃(PO₄)₂·nH₂O, CaF₂, CaSiF₆. The increased content of alkali compounds in the recycling water did not damage the properties of the material nor did that hinder the neutralisation process. Neutralised PG can be used to produce gypsum-based binding materials.

Leškevičienė *et al.* [80] studied the recovery of DH-PG of a Lithuanian stockpile (formed prior to 1997) into the α-HH form by applying lime suspension and isothermal hot-drying at 130 °C temperature. The analysed DH-PG of the stockpiles contained a low content of fluoride and phosphate impurities due to the long-term effect of the rainwater washing. Therefore, the material was proven to have a good perspective of getting converted into α-HH and ending up being utilised

as a binding material. In the same study, the authors also analysed the potential of HH-PG which is directly taken from the production lines of the same Lithuanian factory. The acidic soluble impurities of this HH-PG were neutralised by applying lime suspension at $> 50\text{ }^{\circ}\text{C}$. The dry specimens produced with this neutralised material reached $CS = 28.0\text{ MPa}$. It must be noted that the proposed processing does not require any washing.

Singh [18] investigated the way to make PG a suitable material to manufacture cement and gypsum plaster by treating PG with an aqueous citric solution. This processing transferred soluble P_2O_5 and F^- impurities to water removable aluminates, citrates and ferrates. After such a treatment, PG met the conditions to be used in the intended applications.

Ennaciri *et al.* [15] proposed a method of purifying P_2O_5 and F^- impurities from PG which involved sieving PG with a $200\text{ }\mu\text{m}$ filter (since the larger particles are richer in impurities than the smaller ones) and the subsequent application of sulphuric acid at $60\text{ }^{\circ}\text{C}$ for 2 h. The application of 20% of sulphuric acid was sufficient to create PG suitable to be used as plaster. In order to create an apt PG for the industry of cement, a higher concentration of sulphuric acid (50%) is necessary. Aliedeh and Jarrah [19] developed a multivariable 2^4 factorial methodology to investigate the purification of the PG by adding either sulphuric or nitric acid solutions and by cleaning the material through washing/leaching P_2O_5 . The investigated variables were the particle size, the acid concentration, the loading, and the number of washings. The results of the treatment stressed the importance of the number of washings. The optimum treatment with sulphuric acid was obtained with a loading of $0.15\text{ g PG} / 1\text{ g solution}$ and with three washings. Meanwhile, the optimum parameters for the treatment with nitric acid resulted from a loading of $0.4\text{ g PG} / 1\text{ g solution}$ and 3 washings.

Nizevičienė *et al.* [81] treated PG under the application of ultrasound and by including a fluid catalytic cracking (FCC) additive from the petrochemical industry in which synthetic zeolite is the predominant compound. This zeolite was employed as a sorbent to neutralise the acidic soluble P_2O_5 and F^- compounds. The mechanical properties of the PG specimens increased by 4 times when the zeolite was added in amounts between 0.5 and 10 wt%, and ultrasound treatment was applied. Besides, the zeolite additive effectively neutralised the acidic impurities and regulated the hydration and the setting times of the PG paste. In a later study [14] the researchers performed a similar investigation, but modified the time of ultrasound treatment during the mixing of the paste (either 0.5 or 2 min). In this case, the pastes processed with 5% zeolite additive and 2 min of sonication treatment exhibited 35% higher CS than the pastes produced without either zeolite or ultrasound. Besides, radiological assessment of the employed PG was performed.

The effectivity of the FCC additive was also confirmed by Li *et al.* [82] who investigated the adsorption of phosphate impurities in wastewater (not in PG) by adding FCC analyst containing lanthanum. Phosphate was adsorbed in LaPO_4 and KH_2PO_4 compounds, and the adsorption rates exceeded the 99% value.

1.5.2. The usage of PG as an additive to cement in building materials

In a similar way to natural HH gypsum, PG can be employed as an additive to cement. Several examples on this topic are given further. Islam *et al.* [83] studied the effect of a PG additive on the properties of PC. The employed PG was either processed by washing and drying, or not processed at all. The analysed properties were the setting time, the flow and the *CS* of the prepared pastes for the explored mortar and concrete specimens. In general, the performance of washed PG was better than that of a non-processed sample. The addition of 5–10% of PG to cement clinker produced satisfactory results. Altun and Sert [84] studied the effect of weathered PG from the stockpiles on the setting time and the mechanical properties of the PC. The phosphate and fluoride impurities determined the retarding effect of PG on the setting time of PC. The highest 28-day *CS* was obtained by adding 3 wt% of PG. Hence, as a set retarder of PC, PG additive is a good alternative to natural gypsum.

1.5.3. Improvement of the mechanical strength of PG to make it suitable for load-bearing building products

PG can be utilised not only as an additive, but also as the main binding material in load-bearing building products. This solution is more desirable for both the producers of fertilisers and PG recyclers since PG is utilised in higher amounts. The suitability of PG in structural building products depends, to an important extent, on the physical and mechanical properties exhibited by the manufactured PG products. Those properties mainly depend on the nature of the HH-PG crystals (their microstructure and chemical composition) and on the processing methods.

Influence of the microstructure and chemical composition of hemihydrate PG (HH-PG) on the mechanical properties of load-bearing building products

The effect of the chemical composition and the microstructure of HH-PG crystals on the physical-mechanical properties of the hardened specimens has been considered by many researchers. The microstructure and composition of HH-PG mainly depends on the nature of the phosphate ore (its origin, composition, microstructure) and on the specific parameters of the ‘wet process’ (temperature, mineral – H₂SO₄ ratio). Several examples are further described.

Leškevičienė *et al.* [85] performed investigation on the influence of the mineralogical composition and the crystal microstructure of PG on the main physical and mechanical properties of DH specimens.

Valančius *et al.* [86] studied the influence of the technological parameters of the ‘wet process’ on the microstructure and properties of the produced α -type HH-PG crystals. For this purpose, a laboratory imitation of apatite digestion by sulphuric acid was performed. It was determined that the optimum properties of the material are obtained when the wet process takes place for 8 h at 97 °C temperature and with an apatite – sulphuric acid ratio of 1.03. After grinding dry HH-PG, the *CS* of the produced specimens reached 27 MPa. The appropriate processing method produced a well-defined HH microstructure with regularly oriented HH crystals with needle shapes. This adequate crystalline microstructure determined the fast hydration process and the excellent physical and mechanical properties.

Duan *et al.* [87] investigated the combined effect of both the modifiers organic acid salt ions (RCOO^-) and Al^{3+} on the microstructure and physical-mechanical properties of α – HH-PG crystals. When employed separately, the RCOO^- modifier retarded the hydration of HH and improved the productivity, whereas the Al^{3+} modifier restrained HH crystals from growing longitudinally, thus producing short hexagonal prisms. However, the combined effect of both, employed in amounts of 0.06% each, produced superposition of the effects of both modifiers, therefore the resulting HH crystals exhibited smaller length/diameter ratios and more regular shapes. The well-defined crystal geometry determined the high values of the mechanical properties: a flexural strength (*FS*) of 6.7 MPa and a *CS* of 25.65 MPa.

Kybartienė *et al.* [88] performed comparative analysis of the physical-mechanical properties of two PG types produced from igneous apatite ores from different mines: Kovdor and Kirov. The material from Kovdor presented a lower content of P_2O_5 (and a correspondingly higher pH value) than the PG from Kirov, and that determined, to an important extent, the physical and mechanical properties: the specimens from Kovdor PG hydrated faster (full hydration in 1 d) and reached a *CS* value of 7 MPa, whereas the Kirov PG specimens exhibited slow hydration (full hydration in 105 d.) and a *CS* of 1.5 MPa. Moreover, the hydration kinetics of both HH-PG types were analysed by the thermal method, and the heat quantity produced during the dehydration process was determined.

Influence of the processing method on the mechanical properties of PG load-bearing building products

Hence, it becomes clear that the properties of the phosphate ore and the parameters of the ‘wet process’ determine the microstructural properties of HH-PG and, indirectly, the physical and mechanical properties of DH-PG specimens. However, the physical and mechanical properties can also be improved by further processing the HH-PG paste by suitable methods. For this purpose, a wide variety of processes has been investigated: autoclaving, addition of fibre, treatment by a constant magnetic field, press-forming, and many others. Some of them are considered in this section.

Zieliński [89] studied the effect of a constant magnetic field of 1 T induction on the properties of composites made of industrial wastes. Most of the composites included important amounts of PG. The magnetic field was either applied to the produced specimens or to the mixing water. Ten different types of specimens were produced by mixing several materials: PC, gypsum, quartz sand, PG, FA and $\text{Ca}(\text{OH})_2$, which were eventually blended with water to produce pastes. The composites with the best results were those specimens made of gypsum / PG / $\text{Ca}(\text{OH})_2$ / H_2O (proportions by weight of 1.4/1.4/0.14/2, respectively) and of PC / PG / $\text{Ca}(\text{OH})_2$ / FA / H_2O (3/1.4/0.14/1.5/2.5). The *FS* of the composites increased by 30% (from 2.35 to 3.07 MPa) and 150% (from 2.39 to 6.11 MPa) for the first and second composites, respectively. Magnetic treatment also enhanced the *CS* values of the second composite by 110% (from 7.09 to 14.98 MPa). The *CS* values of the first composite decreased by 2% (from 5.73 to 5.60 MPa). The author offered an interesting explanation for these tendencies: magnetic treatment of

the mixing water enhanced the strength of the hydrogen bounds, thereby ordering the structure of the liquid. This fact changed the hydration dynamics of the pastes. Aside of the mechanical characteristics, the influence of the magnetic treatment on other properties was also investigated: specifically, absorbability, frost resistance, and brittleness.

Degirmenci [90] studied the potential of cement-free binders produced from industrial wastes to be employed in the construction industry by modifying the type of the employed PG (either HH or DH), and the recipe of the composite. The employed materials were FA, PG and $\text{Ca}(\text{OH})_2$. Six paste types were produced by mixing the materials in different proportions: the FA content went from 90 to 40%, whereas the PG content went from 0 to 50%, respectively. The $\text{Ca}(\text{OH})_2$ content was 10% in all cases. As mentioned above, PG was applied either in the raw form (DH) or calcined at 150 °C for 2 h (HH). The addition of DH-PG decreased the *CS* of the specimens, whereas HH-PG enhanced it to reach a maximum value of 13.76 MPa when the HH-PG content was 50%. Moreover, the water absorption of the specimens produced with HH-PG was 20% lower than that of the specimens produced with DH-PG. It was also determined that the specimens with PG developed important undesirable volumetric changes in contact with water. That is a problem because it would restrict all the uses of PG composite binders therefore ultimately limiting them to dry indoor conditions. The author commented that the curing of the specimens in steam conditions is a possible solution to this issue because it improves the hydration of calcium sulphate crystals and considerably reduces the further volumetric changes produced by additional hydration.

Hua *et al.* [91] performed an investigation on the influence of the addition of fibre on the mechanical properties and frost resistance of binding materials made of PG, blast-furnace slag (BFS) and $\text{Ca}(\text{OH})_2$, with proportions of 60/40/4 (by weight), respectively. Three different types of fibre were employed: mineral, glass and polypropylene. Each type of fibre was added in four different proportions, with respect to the dry mixture: 0.00%, 0.35%, 0.70% and 1.00% (by volume). The addition of fibre (especially polypropylene) significantly improved the water resistance and the freeze-thaw resistance of the specimens. The mechanical properties (the *FS*) of the specimens were improved by the addition of fibre, but did not depend on the type of the fibre. Besides, the anti-impact grade of the specimens with polypropylene fibre was excellent, much better than that of the other types. In general, polypropylene fibre dispersed more easily in the mixture and presented a much better bond with the crystal matrix than the other types of fibre. Considering jointly the outcomes of the study, it can be stated that the general performance of polypropylene fibre was the best one.

Yang *et al.* [92] employed autoclaving as a suitable method to manufacture load-bearing wall bricks. Bricks were produced by mixing PG, FA, lime and sand in different proportions: 35–50% of PG, 13–18% of FA, 5–15% of lime, and 26–40% of sand. Three types of PG were employed: raw PG, autoclaved PG under low steam pressure (0.12 MPa pressure and 120 °C temperature) and autoclaved PG under high steam pressure (0.8 MPa pressure and 180 °C temperature). Bricks were manufactured by press-forming different pastes under 20 MPa pressure and by

further autoclaving under 0.8 MPa steam pressure for 4 h. After testing the specimens, the influences of the different parameters became clearer. First, the higher amount of $\text{Ca}(\text{OH})_2$ remarkably enhanced the mechanical properties of the specimens due to higher activation of the hydration reactions between different materials. Moreover, the processing of PG under low pressure changed its crystalline phase to HH which hydrates better than the anhydrite produced by autoclaving PG under high pressure. Finally, a further increase of the content of PG resulted in a decrease of the mechanical strength of the specimens. In summary, the mechanical properties of the produced specimens yielded a better result with a higher content of lime, a lower content of PG, and achieved pre-processing of PG under low pressure.

Another important method is press-forming. As described previously in this section, Yang *et al.* [92] employed press-forming to produce green bricks, which were eventually treated by autoclaving. Usually, in order to manufacture gypsum specimens, the typical water/solid (w/s) ratio ranges between 0.4 and 0.6. However, the processing by press-forming allows a much lower w/s ratio, that of about 0.2. Otherwise, leaching would occur during the press-forming, thereby damaging the microstructure of the specimens by producing undesirable pores and subsequently weakening the mechanical performance of PG specimens. However, the lower content of water carries an important drawback: the manufactured specimens will present a low hydration degree. If a PG product is poorly hydrated, a further contact with moisture will produce an undesirable volume change which will cause cracking, deformations, or even failure of the building elements in which it is employed. Therefore, the authors who investigate the processing of PG by press-forming have to face the hydration problem. Several interesting studies on this issue were carried out by Zhou *et al.*; they are described below.

In their first investigation, Zhou *et al.* [93] studied the treatment of PG paste by press-forming and the hydration-recrystallisation method intended to produce non-fired bricks. The employed materials were PG (from 65 to 85 wt%), $\text{Ca}(\text{OH})_2$ (from 1.3 to 1.7wt%), PC (4 wt% in all cases) and river sand (from 29.7 to 9.3 wt%). After blending with water, the green specimens were manufactured by press-forming under press-forming pressure (PPF) of 20–40 MPa, with a further wet curing intended to promote the reaction of PC. Then, the specimens were hot-dried at 180 °C for 2 h in order to change the crystalline phase of the bricks from DH to HH. Subsequently, the HH specimens were submerged in water, where second hydration happens, and the specimens' crystalline phase turned again into DH. In this way, the observed microstructure of the specimens changed into a regular, dense and interlock matrix of DH crystals with enhanced final mechanical properties. The optimal composition of the pastes was found to be 75 wt% PG, 19.5 wt% river sand, 4.0 wt% PC and 1.5 wt% $\text{Ca}(\text{OH})_2$, with which, the manufactured bricks exhibited high mechanical strength: $CS = 21.8$ MPa and $FS = 5.2$ MPa. The hydration-recrystallisation method was found to be an effective processing way of PG to produce structural building products.

However, the authors (Zhou *et al.*) determined that the main methods used to manufacture PG bricks suffer from some shortages: the indispensable use of cement, press-forming under elevated pressures, and the high energy consumption by the

autoclaving process. In order to overcome these drawbacks, Zhou *et al.* proposed a creative ‘two step hydration process’, thus also including press-forming [94]. According to this novel method, first of all, DH-PG was mixed with a small amount of hydrated lime to neutralise the acidic impurities. The mixture was hot-dried at 180 °C to convert the DH crystalline phase into HH. Then, a certain amount of river sand was mixed in, and, once the dry mixture was prepared, the paste was produced by adding water. The *w/s* ratio in all cases was 0.22. Then, the press-forming of the specimens was carried out under a varying *PPF* between 4 and 20 MPa. The press-formed green specimens were naturally air-cured for 1 day (the first step of hydration). Eventually, the specimens were immersed in water for 30 min in order to allow non-HH crystals to crystallise, thereby forming a more compact crystal lattice (the second step of hydration). After the immersion, the specimens were naturally cured for 1–28 days. To make the process more understandable, a schematic view has been included (see Fig. 3). Hence, the composition of the specimens was completely cement-free, and the optimum recipe was found to be 75 wt% PG, 23.47 wt% river sand and 1.53 wt% Ca(OH)₂. The immersion of the specimens corrected the hydration shortage of the press-forming processing, thus causing a much denser and more interlocked DH crystal matrix and enhancing the mechanical properties of the specimens. The *CS* and the *CS* after 15 freeze-thaw cycles were 29 MPa and 23 MPa when the press-forming was carried out with the relatively low pressure of 10 MPa. Higher *CS* values were obtained by press-forming the specimens under more elevated pressures. However, higher pressures require more energy, i.e., they are less cost-effective. Considering jointly the mechanical properties and the economical aspect of the process, the authors recommend the application of *PPF* = 10 MPa.

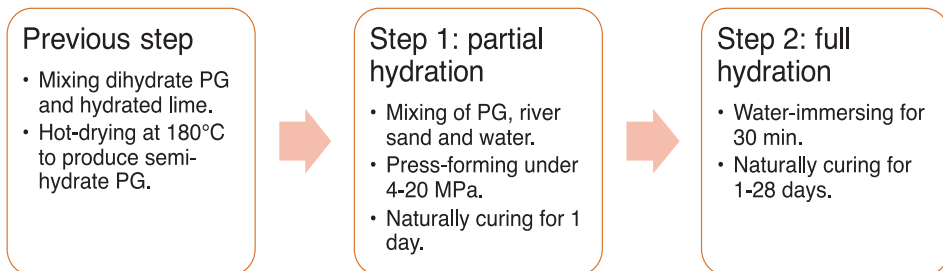


Fig. 3. Schematic view of the ‘two step hydration process’ as proposed by Zhou *et al.* [94]

In a third study, Zhou *et al.* [95] proposed a method to create PG tiles through the application of intermittent pressing hydration. The sole raw material employed to produce tiles was HH-PG. A certain amount of water was added to granulate HH-PG. Then, the material was press-formed, immersed in water and pressed under intermittent *PPF*. The optimal processing parameters were found to be: *w/s* ratio of 0.35, *PPF* of 20 MPa, pressure application frequency of 1 time each 2 min, and the number of repetitions equalling to 24. The application of the intermittent method with the above mentioned parameters produced hardened tiles with a *FS* of

18.9 MPa, which is a very high value. Hence, the intermittent pressing method is a highly efficacious way to utilise PG in the form of strong tiles.

There are other studies discussing the processing of PG through press-forming, mostly from China [96, 97, 98, 99, 100]. As it can be observed from the previous descriptions, the application of press-forming is a very promising method to utilise PG in strong structural building products. However, the studies on this topic are rather scarce, and extensive further research is still needed.

1.5.4. Improvement of the waterproofing properties of PG building products

It is widely known that CaSO_4 is not a hydraulic binder, such as PC. The good performance in moisture conditions exhibited by PC makes it the ideal material to be used in a wide variety of ways in the building industry, and even for applications in underground or submarine conditions. Meanwhile, DH CaSO_4 crystals are not characterised by especially good water-resistance properties. In fact, these crystals dissolve in water. Therefore, in the case of contact with water, the mechanical properties of gypsum products get remarkably reduced. This fact limits the usage of gypsum products mainly to indoor conditions. Hence, the described situation helps us to understand why PC-based concrete is the second most consumed material in the planet (water is the first), whereas gypsum is far behind. However, the production of PC bears serious environmental concerns due to the high amounts of CO_2 emitted during the burning of the clinker, which increases the warehouse effect in the atmosphere. Therefore, the creation of alternative ‘green cements’ is one of the first priorities for the researchers in the field of building materials. In this context, the creation of a gypsum-based binding material with good water-resistance properties is one of the most realistic possibilities to solve the ecological problem. Besides, if the employed material is PG, instead of natural gypsum, the ecological win becomes double.

Addition of polymers and organic additives to PG pastes

There are a number of different approaches to creating a water-resistant gypsum or PG [101]. One of the most popular ways is the application of polymers or other organic additives. For instance, Li *et al.* [102] studied the effect of a water-proof additive on the growth of gypsum crystals and on the final water-resistance properties of gypsum specimens. The additives were composed of organic emulsion, emulsified by polyvinyl alcohol, stearic acid and saline water-proofing admixture. The water-proofing additive restrained the growth of crystals longitudinally. Under these conditions, the organic emulsion turned the crystals from needle-shaped to coarse stick geometries, while the saline water-proofing additive produced short pole geometries. As a result of these microstructural changes, the water absorption of the specimens was reduced, and the *CS* was enhanced. Singh and Garg [103] created a polymerised compound made with PG anhydrite plaster. The employed anhydrite PG (phosphoanhydrite) was ground, and mixed with suitable chemical activators. Eventually, the material was mixed with 2–3% monomer methyl methacrylate (MMA), with a proper catalyst, and the other materials to be used were as follows: red mud or FA, metallic oxide pigments and chopped glass fibre and quartz sand.

After the blending of the paste, floor tiles were manufactured by moulding (with vibration), cured in steam conditions, dried, ground and polished. During the hydration of the phosphoanhydrite, the MMA monomer got polymerised into polymethyl methacrylate which filled the voids of the crystal lattice and increased the mechanical properties, as well as the durability of the tiles against water. Hence, the manufactured tiles were proven to be suitable for flooring. Zhang *et al.* [104] improved the water-resistance properties of the gypsum products by combining methyl silicon aldoxide, PC and manganese slag powder. The optimal composition was 66.7 wt% gypsum, 8.3 wt% PC, 25 wt% manganese slag powder and 0.083 wt% methyl silicon aldoxide. In this way, the softening coefficient (after immersion in water) was improved to 0.76. Moreover, numerous patents for the creation of water-proof gypsum through polymerisation were obtained: by incorporating polyvinyl alcohol and wax-asphalt emulsion [105], by adding either oxidised paraffin emulsion or a mixture composed of paraffin emulsion and polymer emulsion [106], by adding an aqueous solution of asphalt and wax, and, to a lesser extent, polyvinyl alcohol and a borate compound [107], by incorporating siloxane [108, 109], by adding an aqueous emulsion including paraffinic hydrocarbon, polyvinyl alcohol and montan wax [110], among others.

Addition of pozzolans and PC or BFS to PG pastes

Another popular way to increase the water resistance of gypsum (or PG) is the addition of PC or slag together with aluminosilicate materials in active forms, usually known as pozzolans. Pozzolanic materials do not have binding properties until they are activated by alkaline PC or slag. Pozzolanic materials can be natural or synthetic. Among the synthetic ones, there are several waste materials of the pozzolanic nature: FA, silica fume, BFS, zeolitic waste (ZW), etc. The addition of these alkali-activated pozzolan materials to gypsum reduces voids and improves water resistance.

Magallanes-Rivera *et al.* [111] created composites made of gypsum and 10–25 wt% of BFS and a pozzolanic material, either silica fume or FA. In all cases, 10% of PC related to the weight of BFS + pozzolans was added as a chemical activator. During the first 24 h, HH gypsum hydrated completely. During the further 7–90 days, the chemical activation of the pozzolans took place. The formation of C-S-H was assumed, and ettringite was detected in the later stages of hardening. The CS of the different specimens increased from 65% to 175%, and water absorption decreased by as much as 1.67 times with respect to the control specimens. Being so, both the mechanical properties and the water resistance performance of gypsum specimens were remarkably improved.

Singh and Garg [112] created various composite binders with a HH-PG content between 65–70 wt% and a pozzolan additive. In each case, a different pozzolan was included: FA, BFS, or red mud. In all cases, a certain amount of PC and of a chemical retarder were also added to the mixture. Some of the specimens were produced with processed HH-PG (by washing and wet sieving, which removed the acidic and organic impurities), while others were manufactured with unprocessed materials. The specimens were immersed in water for 28 days, and in this way their water-resistance was checked. The control specimens (made of plain plaster) presented

poor water-resistance since leaching of the crystal lattice was observed. The composite binders exhibited much better water-resistance. During the immersion period, the water absorption increased, but without leaching of the matrix. The water-resistance performance was attributed to the formation of cementitious compounds, such as ettringite ($C_3A \cdot 3CaSO_4 \cdot 32H_2O$) and tobermorite (C-S-H). Besides, the specimens composed of HH-PG and BFS presented the highest *CS* values: 35 MPa after 28 days of curing (the control specimens exhibited *CS* = 14 MPa).

Huang *et al.* [113] studied the hardening, the degree of hydration, and the mechanism of PG-BFS based binding materials. To do so, the mixtures were prepared by mixing 45 wt% PG, 48 wt% BFS, 7 wt% cement clinker and 1 wt% chemical activator (relative to the binder). The properties of the composite binding materials were compared to those of PC of grade 32.5. The *CS* and *FS* and softening factor values of mortars produced with the composite binding material reached 45MPa, 6.5 MPa and 0.87, correspondingly, which are very similar values to those of the mortars made with 32.5 PC binder. These properties can be explained by the microstructural analysis of the composite material which revealed that needle-shaped ettringite crystals, board-like gypsum crystals and portlandite crystals intertwined with each other, thereby forming a very dense crystal matrix. Besides, these crystals were covered and wrapped by C-S-H gels, resulting in an even more compact matrix.

Camarini and De Milito [114] studied the performance of the durability and the mechanical properties of wall renderings created by mixing β -type HH gypsum (75 wt%) and BFS-PC (25 wt%). Control specimens were also created by using 100 wt% of HH gypsum. Wall renderings were analysed after 3 years of exposure to either indoor or outdoor conditions. The results clarified that, during the outdoor exposure period, the *CS* of the renderings made of the composite material not only did not decrease, but even slightly increased, presenting, after 3 years, similar *CS* values to those of the control specimens exposed to indoor conditions (~5 MPa). On the other hand, during the same period, the *CS* of the control renderings exposed to outdoor conditions decreased by 3 times. As in the previous case, microscopic analysis helped to explain the mechanisms of this performance. The crystal matrix of the composite binding material was found to be very compact, and a fine C-S-H layer coated the gypsum crystals, thus preventing them from dissolving in water.

Pang *et al.* [115] investigated the microstructure, the mechanical properties and the water-resistance of specimens made of flue gas desulphurisation gypsum (FGD) and ground granulated BFS, and an alkaline chemical activator, either $Ca(OH)_2$ or $CaCl_2$. The *CS* of the specimens cured under normal conditions improved with the addition of BFS up to 60 wt%. Besides, the finer were the BFS particles, the higher were the *CS* values. The effect of the activator, the water resistance and the freeze-thaw resistance were analysed with specimens produced with 45 wt% FGD and 50 wt% BFS. The $CaCl_2$ activator produced stronger specimens than $Ca(OH)_2$. Meanwhile, if considering the water resistance, the *CS* of the specimens significantly increased during the period of 7 to 28 days of immersion, and then remained constant. The enhanced water resistance owes to the low porosity and a dense crystal matrix. The microstructural analysis revealed that porosity was

reduced by the development of rod-like ettringite crystals formed during the curing in steam conditions. On the other hand, the freeze-thaw resistance of the specimens was poor, 14.2 MPa after 30 cycles, i.e., inferior to the value exhibited by a plain FGD binding material after 200 cycles (34.6 MPa).

Kuryatnyk *et al.* [116] studied the valorisation of two different types of Tunisian PG as hydraulic binders. For this purpose, the produced pastes were created by adding 70 wt% of PG and 30 wt% of calcium sulfoaluminate (CSA) clinker. The CSA clinker differs from the ordinary PC clinker in terms of its relatively high sulphate content. During the hydration of CSA cements, the main produced product is ettringite [117]. The produced mortars were cured in air or water conditions. The mortars produced with the first PG type presented the same mechanical properties, independently of the curing conditions. In this case, the precipitation of delayed ettringite short crystals was depicted in the pores of the specimens. These crystals closed the pores and enhanced the water-resistance of the material. On the other hand, the specimens produced with the second type of PG cracked and completely lost the *CS* after 30 d of curing under water. In this case, the humid environment led to the precipitation of massive ettringite crystals into the specimens' pores, thereby causing the above mentioned deterioration. Hence, PG-CSA cement was found to be a good hydraulic binder as long as the precipitation of massive ettringite is avoided.

Addition of waste metallurgical modifiers to PG pastes

An alternative approach to enhancing the water resistance of the hydrated CaSO_4 crystal matrix involves the addition of fine metallurgical modifiers. These additives foster the formation of scarcely soluble coatings around DH crystals, thereby protecting them from the effect of water. Investigations in this field have been mostly performed by scientists from Russia, and the results they obtained are highly promising.

Tokarev *et al.* [118] studied the influence of an ultrafine aluminous mixture (metallurgical wastes with Al_2O_3) as an additive intended to modify the properties of anhydrite binders. The addition of 3–4 wt% aluminous material activated the hydration of anhydrite in such a way that the DH crystal matrix of the produced specimens ended up being extremely compact. The mechanical strength of the specimens increased by 100%, in comparison to that of the specimens without the additive. Moreover, the additive created an amorphous coating around DH crystals, which protected them from the effects of water. In a similar way, Sokolova *et al.* [119] employed bog iron, principally composed of iron oxide, which improved the softening factor of the gypsum matrix, and enhanced the *CS* of the specimens by 10%.

Yakovlev *et al.* [120] included a metallurgical waste (flue) dust (produced in the steel manufacturing industry) as an additive to either anhydrite or gypsum binders and studied the mechanical and water-resistance properties of the produced specimens. The exhibited properties of the specimens including the additive were compared with those of the control specimens produced with plain anhydrite or plain HH binders, respectively. The optimal flue dust content with the anhydrite binder was 1 wt%, which enhanced the *CS* of the specimens by 40% (thus reaching 8 MPa)

and improved their water resistance (given by the softening coefficient). The optimal additive content for the gypsum binder was 1.5 wt%, with which the *CS* was enhanced by 30% (12 MPa), which slightly improved the water resistance. Analysis of the microstructure of the specimens helped to understand more deeply the improved properties. The microstructural analysis of the specimens made of plain anhydrite revealed a chaotic, irregular and porous matrix with crystals of different shapes and geometries. The addition of the metallurgical additive produced a denser matrix of smaller crystals, which was the reason of the better exhibited durability properties. With respect to the gypsum formations, it was observed that when plain HH was employed, the microstructure of the hydrated specimens was very porous and consisted of lamellar and prismatic crystals distributed in random directions thus leaving numerous pores and voids in between the crystals. When the additive was included, the predominant crystals were the prismatic ones, and block structures were also present. Moreover, according to the authors, it is likely that the addition of metallurgical dust encouraged the formation of amorphous coatings around the gypsum crystals and so improved even more the water-resistance of the gypsum crystal matrix.

Pervyshin *et al.* [121] studied the effect of man-made modifiers based on metallurgical dust and carbon nanotubes on the microstructure and properties of gypsum compositions. The optimal concentration of metallurgical dust and carbon nanotubes were 0.2 wt% and 0.005 wt%, respectively, i.e., very small amounts. The addition of both modifiers produced a synergistic effect and improved the values of *FS* and *CS* by 70.5% and 138.3%, respectively, after 7 days of hydration. The water resistance improvement was remarkably superior in the produced compositions: the control samples made of plain gypsum exhibited a softening factor of 0.4, while that of the modified samples was 0.85. The microstructure of the specimens was profoundly improved by the modifiers. The carbon nanotubes acted as crystallisation centres of the gypsum crystals, and the hydration products from metallurgical dust created an amorphous phase based on calcium and aluminium hydrosilicates which formed block aggregates among the gypsum crystals, thereby enhancing the mechanical properties and restraining the harmful effect of water.

Hence, numerous ways to improve the water-resistance properties of gypsum or PG specimens have been reviewed. All of them have in common the application of different additives (polymers, pozzolans, metallic dust) which, through mechanisms of filling the voids among gypsum crystals or by creating an amorphous coating around them, protect gypsum (or PG) specimens from the dissolving effect of water.

1.5.5. Thermal and acoustic insulation properties of gypsum and PG building products

When it comes to the utilisation of PG in building materials, mechanical strength and water-resistance are not the only important parameters to be considered. The possible applications of PG in blocks or panels for walls determine the importance of the thermal and acoustic aspects. There are numerous ways of improving the thermal and acoustic insulation properties of gypsum-based products

which share the common challenge of doing so while maintaining sufficient mechanical strength. Several examples are reviewed further in this thesis.

Some authors improved the insulation properties of gypsum specimens by adding foaming agents. Arroyo *et al.* [122] improved the thermal and acoustic insulation properties of gypsum plasters by including a water-based foam. This foam increased the porosity of the plaster by 35 percentage points (from 53% to 88%), thus reducing the thermal conductivity coefficient (λ) from 0.40 to 0.143 W/(m·K). Besides, the tested specimens also delivered satisfactory quality of acoustic absorption. However, the foam agent sharply reduced the *CS* value of the specimens. To avoid this softening, a certain amount of microsilica (SiO₂) was included. The additive enhanced the mechanical strength of the specimens by 199.10% without spalling their acoustic and thermal insulation properties. Yong *et al.* [123] included an H₂O₂ foaming agent to the PG mixture and studied its effect on the mechanical properties, thermal conductivity and pore suspension of the produced PG foam insulation materials. The optimal H₂O₂ content was found to be 4–5% with which the PG foam specimens presented low bulk density (≤ 500 kg/m³), low λ values (≤ 0.13 W/(m·K)) and sufficient *CS* values for partition walls (≥ 0.24 MPa). Vimmrová *et al.* [124] compared two alternative approaches towards producing a lightweight gypsum material with satisfactory load-bearing and thermal insulation performances. The first approach consisted in using a light-foam gypsum matrix with higher-density aggregates (microsilica, calcium carbonate and cement), whereas the second one was based on using a higher-density gypsum matrix with light aggregates (expanded perlite). In all cases, FGD gypsum was employed. The specimens that were produced by following the second approach were found to be more successful, especially those containing 5 wt% of perlite which exhibited satisfactory thermal insulation properties ($\lambda = 0.12$ W/(m·K)) and mechanical strength (*CS* = 2 MPa). Meanwhile, the specimens manufactured while following the first approach (with foamed gypsum), despite presenting satisfactory thermal insulation behaviour, still failed to exhibit sufficient mechanical strength.

A popular approach to improve the thermal and acoustic insulation properties is based on including various organic additives to the gypsum mixture. Binici *et al.* [125] studied the thermal and acoustic performance of bio-based composite materials made of cornstalk and gypsum. NaOH and aluminium dust additives were also included in order to increase the water resistance of the mixtures. Hence, the specimens were created by mixing 300 g of binders, (cement from 50 to 250 g and gypsum from 300 to 100 g, correspondingly), additives (NaOH – either 17 or 20 g, and aluminium dust – either 10 or 8 g, correspondingly), 200 g of corn stalk and 300 g of H₂O. The specimens containing the highest gypsum content and the lowest cement content exhibited the lowest thermal conductivity of $\lambda = 0.1$ W/(m·K). Besides, the specimens with a higher aluminium dust content exhibited better sound insulation properties than the remaining samples. Cherki *et al.* [126] analysed the thermal properties of composites made of granular cork and gypsum plaster. The study revealed that the λ values of the composite material were 3 times lower than those of plain gypsum plaster. Guna *et al.* [127] improved the properties of gypsum ceiling tiles by including a reinforcement made of organic materials: sheep wool and

coir fibre. The specimens were created with 70 wt% gypsum and 30 wt% fibre, while modifying the ratio between coir and wool. This natural reinforcement enhanced the strength of the specimens (which went up to 90% higher). The fibre increased the λ of the tiles with respect to plain gypsum. However, it was determined that the λ value of the tiles increased with higher wool contents. On the other hand, the coir fibre presented a better acoustic insulation behaviour than the wool. Sair *et al.* [128] studied the performance of eco-friendly gypsum composites and their suitability to be used in building materials. The composites were produced by including an organic additive to the gypsum mixture. The organic additive consisted of cork fibre and paper waste which were combined in the mixtures in various proportions reaching up to 60 wt% of the gypsum mixture. The specimens with a higher content of cork fibre had the best thermal insulation performance ($\lambda = 0.07 \text{ W}/(\text{m}\cdot\text{K})$), thus reducing the λ value by 3.6 times with respect to the plain plaster specimens. The sound insulation tendencies were found to be improved in a similar way. On the other hand, the mechanical properties of the specimens were found to be satisfactory when higher amounts of paper waste (and, correspondingly, lesser amounts of cork fibre) were employed. Hence, the authors recommend the addition of 30 wt% of cork fibre and 30 wt% of paper waste as a ‘compromise’ solution to achieve, at the same time, satisfactory thermal and acoustic insulation performance and sufficient load-bearing properties.

The improvement of the thermal and acoustic insulation properties of gypsum-based products can be also achieved by means of including various additives, such as polymers and inorganic materials. Cao *et al.* [129] enhanced the *CS* value of the thermal insulation gypsum thus exhibiting a low density by reinforcing it with superplasticisers (40 wt% vitrified microsphere, 0–0.5 wt% sulfonated naphthalene formaldehyde and polycarboxylate). The authors determined that the optimal sulfonated naphthalene formaldehyde and polycarboxylate contents of 0.2 and 0.5 wt% enhanced the *CS* values of the thermal insulation gypsum by 96.8% and 87.1%, respectively. Gencil *et al.* [130] created a new gypsum composite material containing diatomite and polypropylene fibre. Diatomite, a material which is present in fossilised microscopic plants, was included in amounts up to 20 wt%, and the polypropylene fibre of up to 1% was used. The addition of diatomite increased the porosity of the specimens, and, at the same time, reduced their λ , whereas the polypropylene fibre improved their mechanical properties. Li *et al.* [131] evaluated the thermal insulation performance of the casted-in-situ PG composite walls. The main employed binding material was PG, but certain amounts of FA and $\text{Ca}(\text{OH})_2$ were also included to improve water resistance. Small amounts of SC protein retarder and melamine superplasticiser were also included. Finally, vitrified microspheres were included in order to improve the thermal insulation properties. The optimal composition consisted of 70 wt% PG, 22.5 wt% FA, 7.5 wt% $\text{Ca}(\text{OH})_2$, 0.2 wt% SC protein retarder, 0.7 wt% melamine superplasticiser and 20 v% vitrified microsphere. When focusing on the thermal insulation behaviour, the λ coefficient of the composites was reduced from 0.248 to 0.163 $\text{W}/(\text{m}\cdot\text{K})$ when 20 v% vitrified microsphere additive was included, although it produced a negative effect on the *CS* values.

Hence, there are numerous and different methods to improve the thermal and acoustic insulation properties of PG-based building products which would increase the applicability of this material in a significant way.

1.6. Conclusions

The concerns about the ecological problem carried by PG are of global scale since the continually increasing PG stacks seriously damage the surrounding environment (see Section 1.3). An important part of the solution lies in PG utilisation in the field of building materials. Numerous methods have been developed to improve the physical and mechanical properties of PG products and to reduce the amount of harmful phosphate and fluoride impurities of its composition. Some of these methods have been reviewed in Section 1.5. In this perspective, the aim of the current study is to investigate the suitability of PG to be employed in structural building products by analysing the influence of the microstructure, the chemical composition, the inclusion of additives (ZW, MS, Ca(OH)_2 , WF) and the method of processing (casting or press-forming) regarding their physical and mechanical properties while also considering the mitigation of the risks for health and environment (especially, radioactivity and the content of soluble P_2O_5 and F⁻ compounds). The investigated physical and mechanical properties are the hydration degree, the *CS* and *FS*, the thermal and acoustic insulation behaviour, and the water resistance.

2. EXPERIMENTAL METHODS AND MATERIALS

2.1. Experimental methods

During the performed investigations, various types of analyses were performed which were related to the microstructure, chemical composition, physical properties, mechanical properties, thermal and acoustic properties, and the radioactivity level of the initial materials and the manufactured specimens. The various employed methods are systematically reviewed further in the thesis.

2.1.1. Microstructural analysis

The microstructures of the initial HH powder, DH-PG specimens and the additives were investigated by *Scanning Electron Microscopy* (SEM). The employed device was the SEM microscope *Hitachi S-3400N Type II* [132]. The resolution of images (of secondary electrons in high vacuum) is ≥ 3 nm with 30 kV and ≥ 10 nm with 3 kV. In different studies, several acceleration voltages were applied: 3, 5, 10 and 15 kV. In some cases, together with the SEM analysis, Energy-dispersive X-ray Spectroscopy (EDS) chemical composition was determined with a *Bruker Quad 5040* EDS detector (123 eV).

2.1.2. Chemical and mineral composition analysis

The chemical element composition of the different materials (HH-PG, ZW, MS) was determined by *X-ray Fluorescence* (XRF) analysis. The employed device was a *Bruker X-ray S8 Tiger WD* which featured a rhodium (Rh) tube. The employed anode voltage was up to 60 kV, and the electric current was up to 130 mA. The powder samples of the different materials were analysed in a helium atmosphere. The results were depicted by using the *SPECTRA Plus QUANT EXPRESS* method.

The mineral composition and the crystal phases of the materials and the specimens were depicted with the *X-ray Diffraction* (XRD) method. The XRD patterns of the different materials were analysed with an X-ray diffractometer *DRON-6* with *Bragg-Brentano* geometry. Radiation of Ni-filtered CuK_α and a graphite monochromator were employed. The voltage was 30 kV, and the emission current was 20 mA. The individual phases and reflections were identified with the *Oxford Cryosystems Crystallographica Search-Match* software by using the references of the database *PDF-2* [133]. Alternatively, the software *Panalytical HighScore+ 3* was also employed. The quantifications of the powder diffraction data were analysed by Rietveld whole-profile refinements by employing the *General Structure Analysis System* software [134].

2.1.3. Colorimetric analysis

The presence of acidic water-soluble P_2O_5 content in the PG was analysed with a *Hanna HI713 Checker HC*® – *Phosphate LR* (low range) colorimeter [135] featuring a measurement range between 0.00 and 2.50 ppm, a resolution of 0.01 ppm and an accuracy of ± 0.04 ppm. The presence of soluble fluoride compounds in PG was depicted with a similar device, a *Hanna HI729 Checker HC*® – *Fluoride LR* (low range) colorimeter [136] with a measuring range between 0.00 and 2.00 ppm,

a resolution of 0.01 ppm and an accuracy of ± 0.04 ppm. The measurement procedure was performed according to the Lithuanian Standard TS-21-154-86 by preparing the specimens in the following way: a gypsum saturated and filtered solution was firstly prepared. Then, 2 g of the analysed PG powder were included in ~ 300 mL of the solution which was shaken for 30 min to allow the phosphate and fluoride soluble compounds to be transferred from PG to water. Eventually, more of the initial gypsum-saturated solution was added in order to complete the total volume of 500 mL. In order to remove PG powder, the solution was filtered with a mechanical filter. In this way, soluble phosphate and fluoride content measurements could be performed after applying the respective reagents for each device.

2.1.4. Investigation of the physical properties

The hydration degree of the PG specimens (either HH or DH) was depicted by the *loss on ignition* method (*LOI*). The method involves calcining the specimens at a sufficient temperature (≥ 400 °C) with the objective to remove the bound water molecules of the HH ($\text{CaSO}_4 \cdot 0.5\text{H}_2\text{O}$) or DH ($\text{CaSO}_4 \cdot 2\text{H}_2\text{O}$) crystals, thereby converting the entire material into anhydrite (CaSO_4) crystals. Being so, the *LOI* values define the relative difference between the initial (m_0) and final (m_1) mass of the specimens before and after the calcination process: $LOI = (m_1 - m_0) / m_0$. Hence, the *LOI* values reflect the relative amount of the bound water content in the gypsum molecules. In the performed experiments, the ground specimens, in amounts of ~ 4 g, were calcined at temperatures of 400 or 500 °C (depending on the experiment) for 1.5 h. The mass values were measured with an accuracy of ± 0.001 g. The theoretical *LOI* values for pure HH and pure DH gypsum are 6.2% and 21.85%, respectively [137].

The particle size distribution of the employed powder materials was depicted with a *Cilas 1090* laser particle size analyser [138]. The measurements were performed in the dry dispersion mode, and the measurement range was between 0.1 and 500 μm .

The pH values of the initial materials were depicted with a *AD8000 Professional Multi-Parameter pH-ORP-Conductivity-TDS-TEMP Bench Meter* [139]. The device features a measurement range between -2 and +16 pH, a resolution of 0.01 pH and an accuracy of ± 0.01 pH. Before performing the pH measurements, the device was calibrated in two or three points by using reference buffers of 4.00, 7.00 and 10.00 pH (in some cases, the third buffer was 9.21 pH). The measurements were carried out from aqueous solutions resulting from adding 2 g of the analysed powder to 20 mL of water.

2.1.5. Thermal and acoustic analysis methods

The hydration reaction of $\text{CaSO}_4 \cdot 0.5\text{H}_2\text{O}$ crystals is an exothermic process. Therefore, the initial stages of the hydration of HH-PG were monitored by measuring the hydration temperature. Immediately after forming the pastes, the hydration temperature was depicted by employing the semi-adiabatic method with the device *Pico Technology 8 – channel USB TC-08 Data Logger* and a *K* – type thermocouple

[140]. The measurement range was between -270 and +1820 °C, and the set measurement rate was each 30 s.

The thermal conductivity (λ) of the specimens was analysed with a heat-flow-meter, by employing the ready state hot-box approach, as recommended by Asadi *et al.* [141]. The measurements were performed with flat rectangular dry specimens of 30x30x5 cm geometry, according to the European Standard EN 12667 [142].

The acoustic insulation of the PG specimens was assessed by using a closed sound isolating case including a speaker on the one side and a microphone on the other side. The PG panel specimens (250x250x18 mm) were set between both above mentioned devices inside the isolating case. Hence, the PG panel is the only path for the sound waves to travel from the speaker to the microphone. The employed devices were a broadband speaker *Visaton BG17* and a sound amplifier *Vector Research VA – 1400*. The constant *sound pressure level (SPL)* was evaluated in two ways: by measuring the A-weighted *SPL* values and by measuring the frequency spectrum while using standard octave sound filters (31.5, 63, 125, 250, 500, 1000, 2000, 4000 and 8000 Hz).

2.1.6. Testing methods for the mechanical properties of PG specimens

The press-forming of the different PG specimens and the *CS* test were performed with a computerised press *ToniTechnik 2020.0600/132/02* [143] (see Fig. 4). The press-forming process was performed by applying a loading rate of 0.05 MPa/s or 0.6 MPa/s, till the load reached the required *PF*. The press-forming process was performed with metallic cylindrical forms of different sizes, with diameters of 26.4 mm, 80.0 mm and 100 mm. The same computerised press was employed to perform the *CS* test to the hardened specimens, during which, the loading rate was set either at 0.6, 0.7 or at 1.0 MPa/s (depending on the experiment), according to the European Standard EN 13279-2 [3], and the measuring rate was 0.02 s.

The test of *FS* was performed with the same apparatus as the *CS* test and the indications of Standard EN 13279-2 [3]. In this case, the specimens were prisms of 40x40x160 mm geometry which were supported on two rolls, separated by 100 mm. A concentrated load was applied at the middle of the pan, with a loading rate of 50 N/s, till fracture was achieved. The *FS* (MPa) was calculated according to Eq. (7).

$$FS = \frac{1.5 \cdot F \cdot l}{b^3} \quad (7)$$

where F (N) is the load at the fracture, l is the span length (100 mm), and b is the side of the square section of the prism (40 mm).

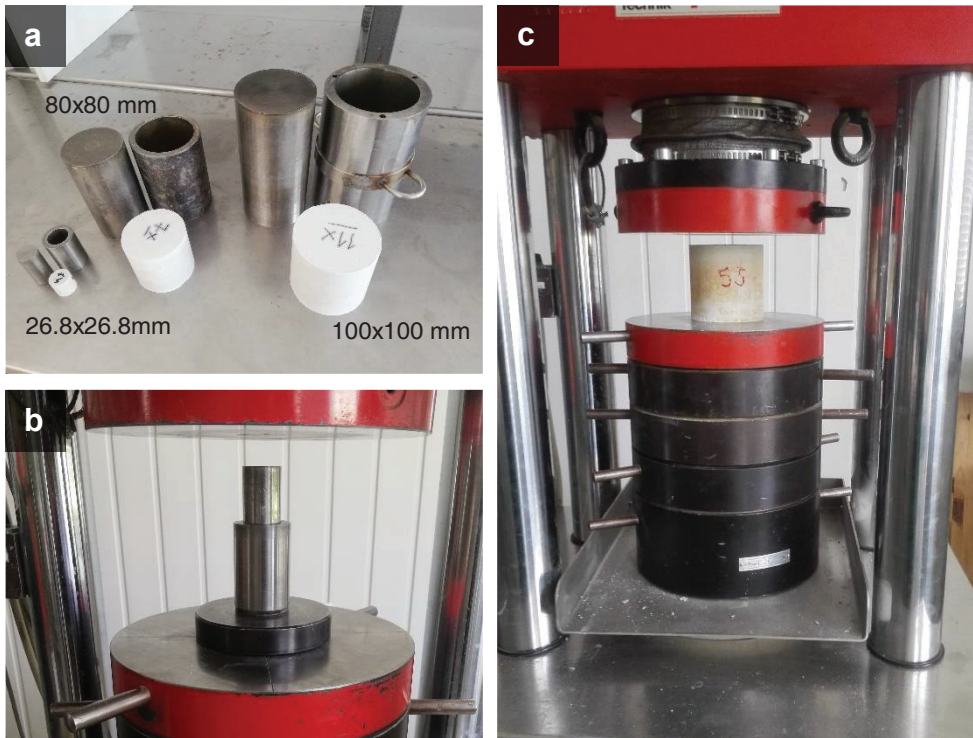


Fig. 4. Images of different press-forms (with the respective PG specimens produced with each one) (a), the press-forming process (b) and the CS test (c), by using *ToniTechnik* 2020.0600/132/02 computerised press

2.1.7. Radiological assessment

The activity concentration of radionuclides in the different HH-PG specimens was analysed through high resolution gamma spectrometry by using the *BEGe*, a *broad-energy*, semiconductor detector and the software *Canberra-Packard GENIE 2K v.3.4*, according to the internal procedure of the *Silesian Centre of Environmental Radioactivity* which is certified by the *Polish Accreditation Centre (PCA)*. For every investigated radionuclide, the minimum detectable activity (MDA) was below 1 Bq/kg. The expanded uncertainty was considered with a coverage coefficient of 2, which gives a degree of confidence of $\sim 95\%$.

The activity concentration of ^{226}Ra was assessed based on a 186 keV energy line. It was verified with the activity concentrations of its decay products ^{214}Bi and ^{214}Pb , based on, respectively, 609, 1120, 1765 keV, and 295, 352 keV energy lines. The activity concentration of ^{210}Pb was obtained directly with a 46 keV energy line. Due to the low energy level of this measurement, the results were modified by performing the pertinent corrections [144]. The ^{40}K activity concentration was assessed in a direct way at a 1461 keV energy line.

The fact that ^{232}Th is a pure alpha emitter makes it impossible for gamma spectroscopy to measure its activity concentration. Therefore, the activity

concentration of ^{232}Th was evaluated from its decay products ^{228}Ra and ^{228}Th . Each of these decay products was assessed in a specific way. On the one hand, the ^{228}Ra activity concentration is evaluated through its decay products ^{228}Ac (measured with an energy line of 911 keV), which is in equilibrium with ^{228}Ra in such conditions as those of the measured PG samples. On the other hand, the ^{228}Th activity concentration was calculated from the activity concentrations of its decay products ^{212}Pb and ^{208}Tl , depicted at energy lines of 239 and 583 keV, respectively. At the same time, correction for the activity concentration of ^{208}Tl was necessary due to the radioactive decay probability, which leads to the emission of this energy line. Besides, the relative proportions among ^{228}Ra and ^{228}Th give additional information regarding the actual presence of ^{232}Th in the sample.

If the activity concentration of a radionuclide is measured with more than one energy line, the result is calculated as a weighed mean of the different measurements, by applying a weighting factor equal to the reciprocal of the emission probability of each energy line.

2.2. Employed materials

During the different stages of the ongoing investigation, numerous materials were employed. In all the cases, the main binding material was HH-PG. Besides, different waste additives and modifiers were employed to improve the microstructural, physical and mechanical properties of the PG specimens and to make them suitable to be used as building products. These additives were the following:

- a) waste synthetic zeolite (ZW) included to reduce the acidic-soluble phosphate and fluoride impurities in PG;
- b) waste metallurgical sludge (MS) included to improve the water resistance of the PG specimens;
- c) waste wood fibre (WF) employed to improve the acoustic and thermal insulation properties of the PG specimens.

Besides, in some cases, small amounts of $\text{Ca}(\text{OH})_2$ additive were included to neutralise the acidic phosphate and fluoride impurities of PG. All the presently mentioned materials are described in the following subsections.

2.2.1. Three types of HH-PG from different origins

In the current study, the employed HH-PG was produced in a Lithuanian phosphate fertiliser chemical plant where the ‘wet process’ takes place by using input raw phosphate materials from several origins, mostly apatite rocks from Kirov or Kovdor mines (Russia), and phosphorite rocks from Morocco and South Africa (SA). It must be reminded that apatite rocks are of the igneous origin, while phosphorites are sedimentary. In Section 1.2, it was explained that the PG of igneous origin usually exhibits lower radioactivity (see Section 1.2.1), a lower content of trace heavy metals, and a higher content of REE (see Section 1.2.3) than the PG of sedimentary origin. In general, the content of impurities of the PG of igneous origin is lower than that of the PG of sedimentary origin. Being so, in the above mentioned factory, there are two production lines. In the first line, the input phosphate material

consists of a mixture of the different phosphate rocks. In the second line, the sole employed raw material is apatite from the Russian mine of Kovdor. Being so, three different PG types were taken from both production lines to be investigated in the current study, two of them (types I and II) from the first line, and the other type (type III) – from the second line.

Table 2. Description and properties of the different humid HH-PGs

Title of PG	Type I	Type II	Type III
Mines from which the phosphate rock is extracted	Kirov – Morocco	SA – Morocco	Kovdor
Proportions	81% Kirov 19% Morocco	50% SA 50% Morocco	100% Kovdor
Nature of phosphate rock	apatite (Kirov) phosphorite (Morocco)	phosphorite	apatite
Humidity	31.8%	22.0%	18.5%
Total P ₂ O ₅ content	0.86%	0.86%	1.13%
Soluble P ₂ O ₅ content	0.40%	0.43%	0.29%

The main properties of the different investigated HH-PG types are given in Table 2. Henceforth, the different PG types shall be referred according to the labelling given in Table 2 (PG of types I, II and III). It can be observed that PG types I and II have respective lower P₂O₅ total contents than PG III-type. However, as described in Sections 1.2.2 and 1.5.1, the harmful P₂O₅ compounds are the soluble ones whose content is two times lower in the III-type PG than in the other two types. Hence, from this point of view, the III-type PG is the cleanest material.

HH-PGs were produced through the wet process in the form of a humid powder. Further, this humid HH-PG was taken from the respective production line and immediately hot-dried at 100 °C for ~ 6 h (see Fig. 5a), so that the moisture was completely removed. Otherwise, HH crystals would hydrate and evolve into DH compounds which do not exhibit binding properties. Once HH-PG had become completely dry, it was stored hermetically till its usage. A view of the different dry powder HH materials is given in Fig. 5b. The appearance of each one seems to be related to its igneous or sedimentary origin: the III-type PG (produced entirely from igneous rocks) is the whitest, whereas the II-type PG (manufactured entirely from sedimentary rocks) is denoted by a greyish or even brownish tone. Meanwhile, the colour of the I-type PG (with both igneous and sedimentary origins) is intermediate. Besides, for comparative purposes, a natural commercial HH gypsum *Knauf Baugips* was investigated together with the different PG types (further referred to as the *natural* material).

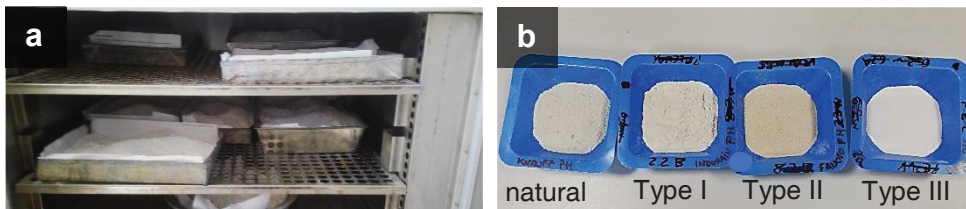


Fig. 5. Hot-drying of the HH-PG powder (a) and view of the different HH materials (b)

The chemical composition of the different materials is presented in Table 3. Aside from the specific components of CaSO_4 , the main depicted impurities are SiO_2 , P_2O_5 and SrO and F . The content of SiO_2 compounds is higher in the natural gypsum than in PG, whereas the opposite tendency happens regarding the P_2O_5 and CeO_2 compounds. It can be noticed that the phosphate content in the different PG types of Table 3 are 10–30 percentage points lower than those of Table 2. This happens because, in Table 2, the measurements were performed with wet HH-PG, whereas in the XRF analysis, the moisture had already been removed. Besides, Table 3 reveals the important fluorine content in the I and II types of PG (those of the sedimentary nature), whereas in the III-type PG and in the natural gypsum, this element was not determined at all. The high content of soluble P_2O_5 and F^- compounds in the different HH-PG powders determined the strong acidity of the materials in comparison to the almost neutral pH of the natural gypsum (see the pH values in Fig. 24a). The amounts of Al_2O_3 , MgO , Fe_2O_3 and K_2O were remarkably higher in the natural gypsum than in PG. Meanwhile, certain trace contents of REE (Ce, Nd, La and Y) were depicted only in the different PG materials, and not in the natural gypsum. As expected, the overall REE content is higher in the type I PG (of the entirely sedimentary nature) than in the other samples. Besides, none of the heavy metals classified by EPA as potentially toxic elements (As, Ba, Cd, Cr, Pb, Hg, Se and Ag, see Section 1.2.3) were traced in any of the materials.

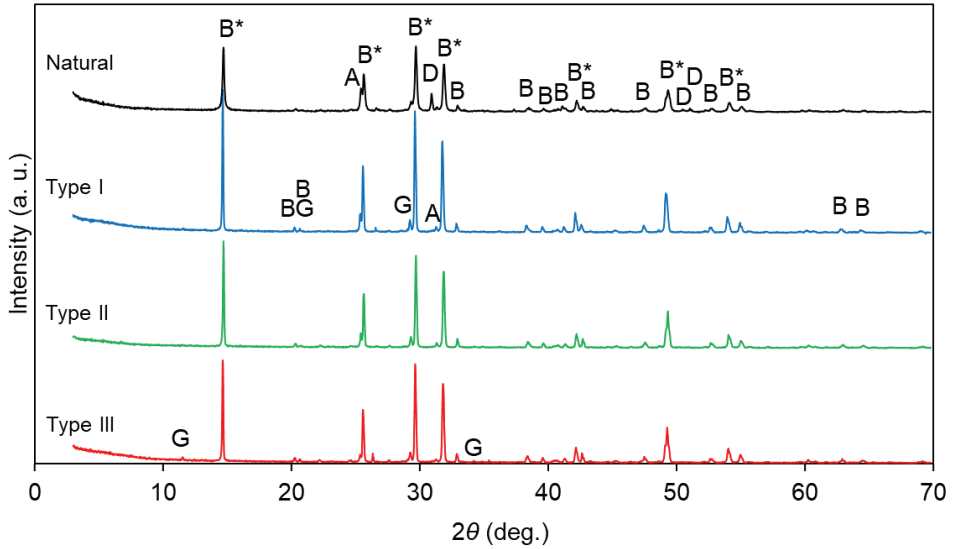
Table 3. XRF composition of commercial gypsum and investigated PGs (wt%)

Comp.	Natural	Type I	Type II	Type III	Comp.	Natural	Type I	Type II	Type III
SO ₃	44.30	47.77	48.49	49.50	K ₂ O	0.77	0.07	0.05	0.04
CaO	38.23	38.42	39.32	38.78	ZrO ₂	0.003	-	-	0.005
SiO ₂	5.26	0.83	2.14	2.94	ZnO	-	-	-	0.004
P ₂ O ₅	0.29	1.15	1.08	1.30	TiO ₂	0.07	0.06	0.02	-
SrO	0.18	1.88	0.27	0.41	Y ₂ O ₃	-	0.03	0.03	-
CeO ₂	-	0.35	0.21	0.19	CuO	-	0.008	-	-
Al ₂ O ₃	1.77	0.20	0.09	0.16	Nb ₂ O ₅	-	0.002	0.002	-
MgO	3.17	0.11	0.11	0.15	MnO	0.008	-	-	-
Nd ₂ O ₃	-	0.08	0.10	0.07	F*	-	1.85	1.42	-
Fe ₂ O ₃	0.52	0.08	0.01	0.06	H ₂ O**	6.2	6.9	6.7	6.4
La ₂ O ₃	-	0.21	-	0.05	Total	100	100	100	100

*Note: F content is defined by EDS analysis

**Note: H₂O content is defined by the *LOI* method

The different materials were also investigated by XRD analysis which shows the crystal phase of CaSO₄. The XRD patterns are given in Fig. 6. The predominant peaks are those of HH gypsum crystals, but smaller peaks of DH gypsum and anhydrite were also determined. All the *LOI* values of the different materials given in Table 3 yielded between 6.0% and 7.0%, thereby confirming the predominant HH nature of the crystals, since the theoretical *LOI* of the HH crystal phase of gypsum is 6.2% (meanwhile, the theoretical *LOI* of the DH crystal phase is 21.85%). Moreover, in the content of the natural gypsum, a certain amount of a dolomite additive was found.



Explanation:

G – DH gypsum ($\text{CaSO}_4 \cdot 2\text{H}_2\text{O}$, ref. Code: 1-385)

B – HH gypsum ($\text{CaSO}_4 \cdot 0.5\text{H}_2\text{O}$, ref. Code: 33-310)

A – anhydrite (CaSO_4 , ref. Code: 83-437)

D – dolomite ($\text{CaMg}(\text{CO}_3)_2$, ref. Code: 36-426)

B* - the “B” peaks which cover smaller “A” peaks

Fig. 6. XRD patterns of different PGs and natural gypsum

The SEM images of HH CaSO_4 crystals of the different materials are given in Fig. 7. The differences between the crystals of the analysed materials are very notorious. The natural gypsum (see Fig. 7a) was processed through grinding, and that is reflected in the irregular shapes of the crystals which exhibit different sizes and geometries. Besides, the HH crystals of the natural gypsum are separated, so differing from the HH-PG crystals which are grouped among themselves thus forming bigger conglomerates. The crystals of the I-type HH-PG (see Fig. 7b) present lamellar and sharp geometries and can reach thicknesses of 5 μm and lengths of 15 μm . The crystals of the II-type HH-PG are similar to those of type I, but they exhibit thicker (even 10 μm) and rounder shapes. Finally, the II-type HH-PG crystals (see Fig. 7c) are much more massive than the previous ones, and their geometries are better defined: prismatic shapes with hexagonal cross-sections, and diameter/length ratios of, approximately, 1/2. The length of the crystals goes from 10 to 30 μm .

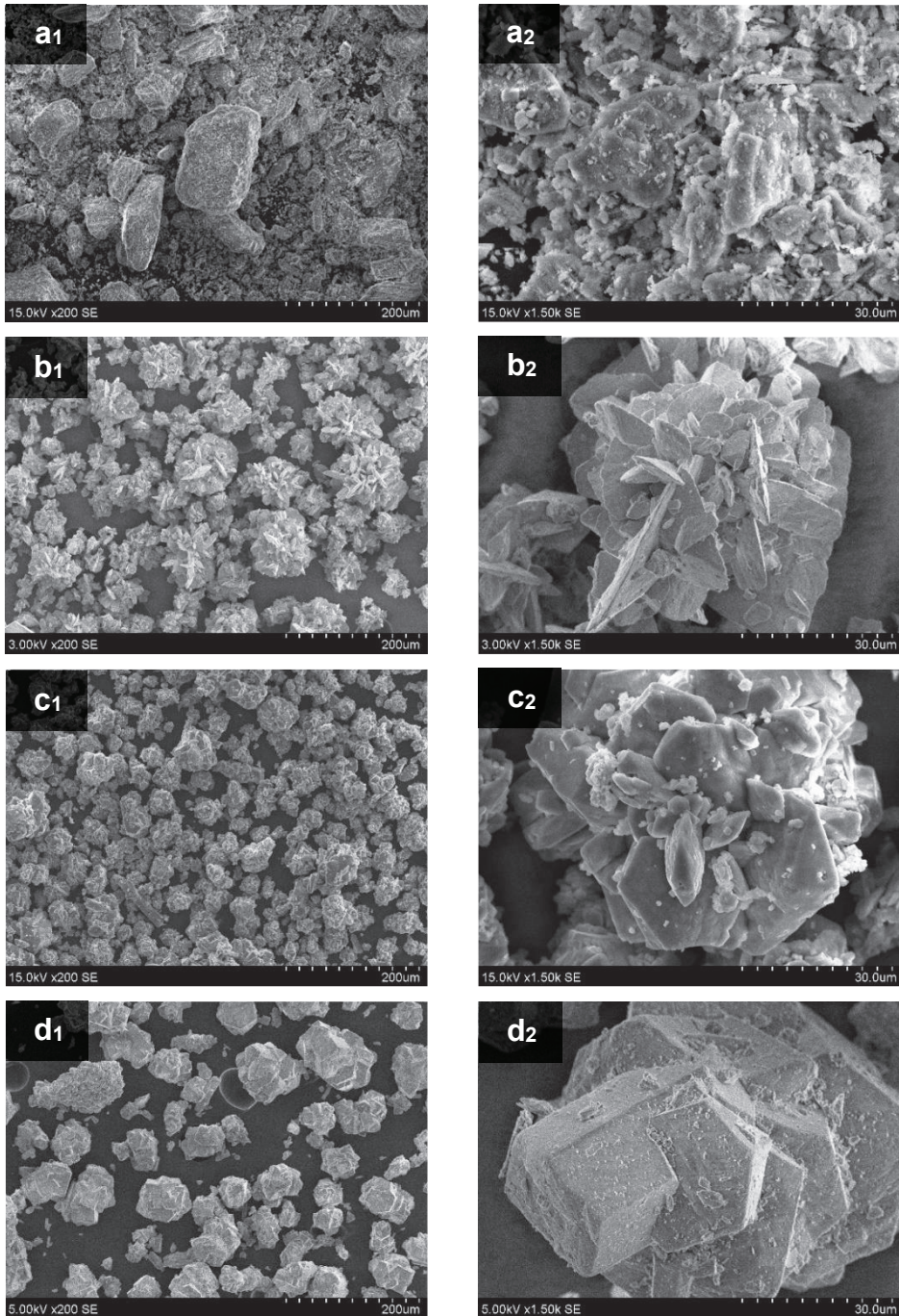


Fig. 7. SEM images of crystal conglomerates of different HH powders: natural gypsum (a), I-type PG (b), II-type PG (c), III-type PG (d). Scale: x200 (index '1', and x1500 (index '2')

The specific gravity of the natural gypsum is 2.47, which is a smaller value than those of the various PG types: 2.70, 2.74 and 2.67 for type I, type II and type III PG, respectively. The particle size distribution of each material is presented in Fig. 8. Among the analysed PG types, the largest conglomerates were those of type III, followed by type II and type I. Meanwhile, the particle distribution of the natural gypsum must be considered specifically, since, as noticed from Fig. 7 images, the crystals are separated, and they do not form conglomerates. In this case, and important share of the crystals falls within the interval of 30–100 μm , i.e., they are bigger than the crystals of any of the PG types.

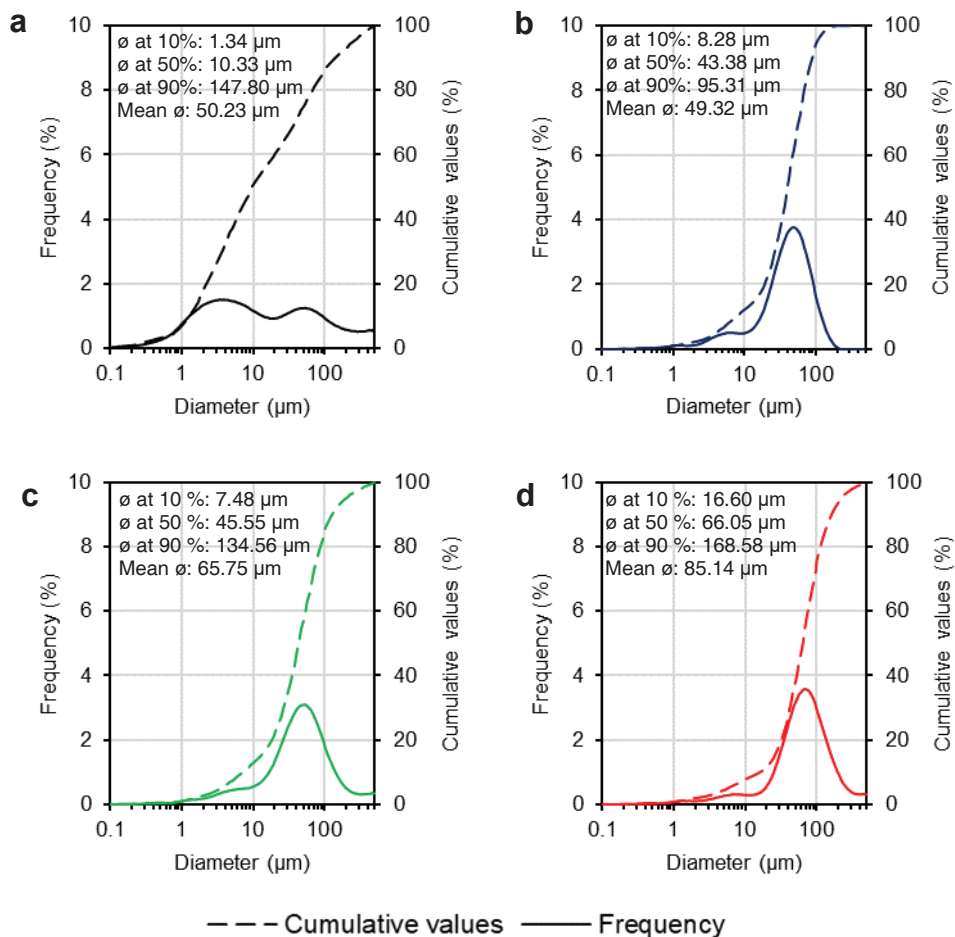


Fig. 8. Particle size distribution of initial HH materials: natural gypsum (a), I-type PG (b), II-type PG (c), III-type PG (d)

The distribution of phosphate and fluoride impurities on the calcium sulphate crystals was investigated by SEM-EDS analysis (see Fig. 9). As shown in Table 3, fluorine was not determined in the compositions of natural gypsum and in the PG of type III, whereas in type I and type II PG, it was detected in important amounts. The phosphate impurities were depicted in all the materials, but the content in the natural

gypsum was about 5 times lower than in the PG powders. Fig. 9 shows that both phosphate and fluoride impurities are evenly distributed on the surfaces of calcium sulphate crystals. These impurities reduce the mechanical properties of the eventually hardened PG specimens. However, the fact that the impurities are evenly distributed and do not form layers or conglomerates is positive, since the above mentioned weakening is expected to happen to a lesser extent.

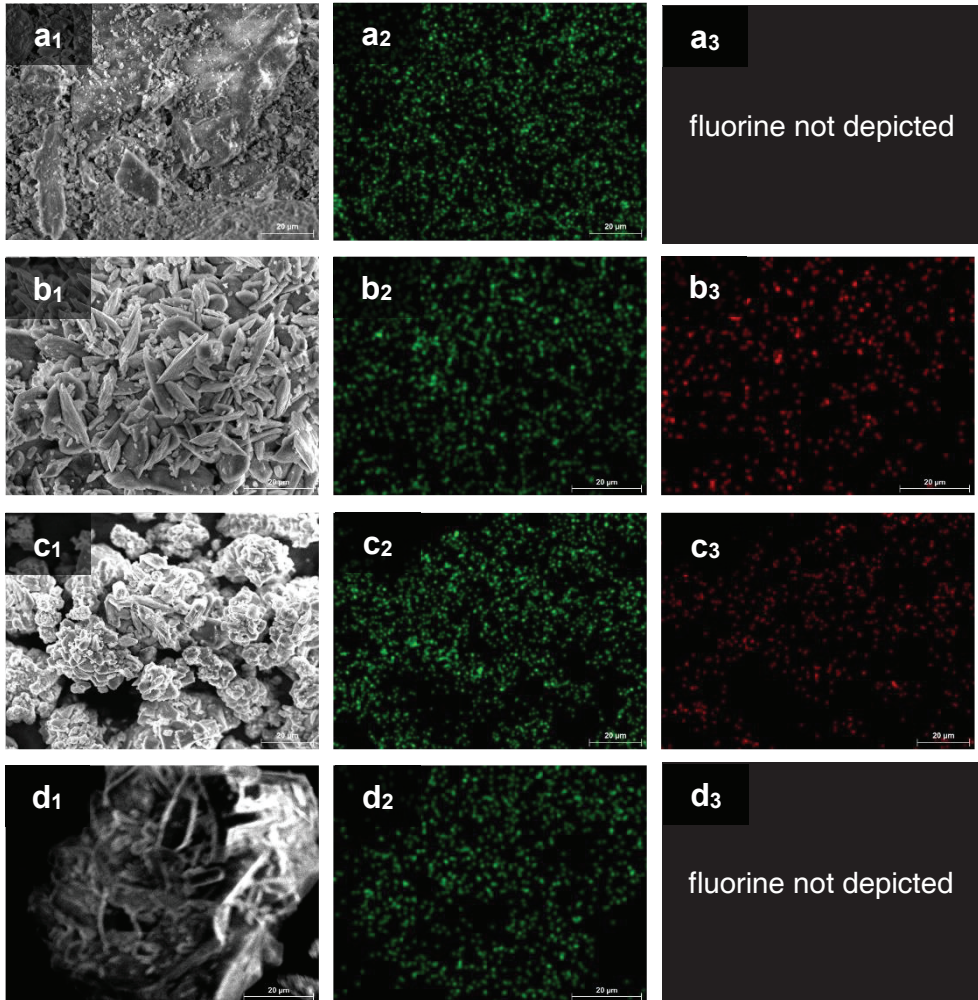


Fig. 9. SEM images (marked with index '1') and EDS distribution of phosphorus (index '2', green dots) and fluorine (index '3', red dots) on the crystals of different types of HH powders: natural gypsum (a), I-type PG (b), II-type PG (c), III-type PG (d). Scale: x1000

2.2.2. Waste of synthetic zeolite (ZW)

As explained in Section 1.5.1, zeolites are microporous materials of the aluminosilicate nature which are frequently employed in industrial processes as sorbents and catalysts. Zeolites can be either natural or synthetic. In the current

study, zeolitic waste (ZW) is employed as an additive to PG to adsorb the acidic soluble impurities in the specimens. The presently used ZW is a synthetic material which was employed in the process of fluid catalytic cracking of the petrochemical industry. During the process, zeolite was contaminated with oil, and thus it became a waste material.

Table 4. XRF composition of the ZW (wt%)

Al ₂ O ₃	SiO ₂	La ₂ O ₃	SO ₃	TiO ₂	Fe ₂ O ₃	MgO	Na ₂ O	CeO ₂	V ₂ O ₅	CaO	P ₂ O ₅
50.7	36.4	1.67	1.14	0.932	0.647	0.634	0.332	0.268	0.117	0.077	0.075
K ₂ O	WO ₃	ZrO ₂	NiO	Ga ₂ O ₃	PbO	CuO	ZnO	SrO	Nb ₂ O ₅	CoO	
0.042	0.017	0.013	0.011	0.005	0.005	0.004	0.004	0.003	0.002	0.002	

The chemical composition of ZW is given in Table 4. As observed, ZW is composed mainly of Al₂O₃ and SiO₂ compounds, which is appropriate to its aluminosilicate nature. Besides, a wide variety of other elements is also present in important amounts in the form of oxide compounds: REE (La and Ce), non-metals (S, P), transition metals (Ti, Fe and V), alkaline and alkaline-earth metals (Na, K, Mg and Ca), and small amounts of other trace elements.

ZW is an acidic material. The pH values of the zeolites which were used in similar studies belonged to the range of 4–4.52 [145, 146]. In the case of the investigated material, the depicted pH was 4.35.

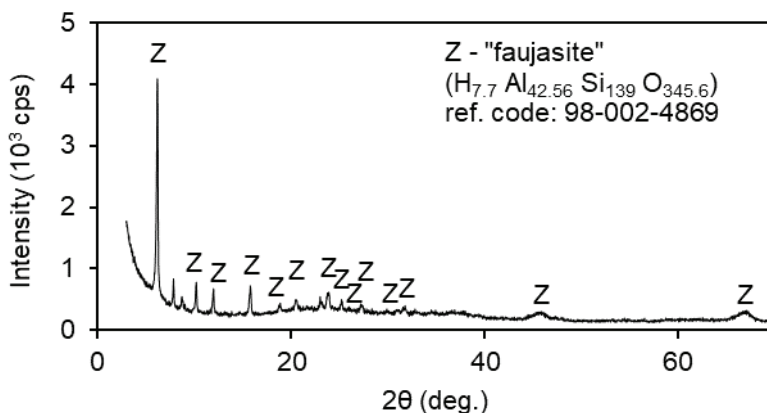


Fig. 10. XRD pattern of ZW based on faujasite mineral

The XRD pattern given in Fig. 10 shows that ZW is mainly composed of the faujasite mineral, thus confirming the aluminosilicate nature depicted by XRF analysis (see Table 4).

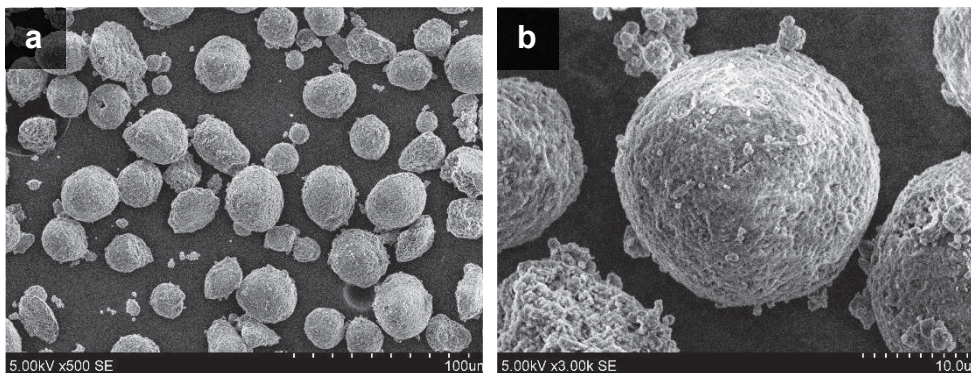


Fig. 11. SEM images of ZW. Scale: x200 (a) and x3000 (b)

The microstructure of ZW particles was investigated by SEM analysis (see Fig. 11). ZW particles show well-defined spherical geometries and microporous surfaces.

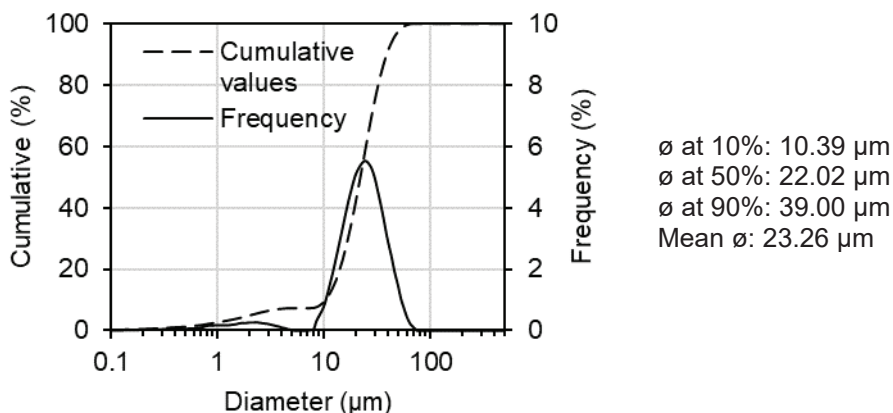


Fig. 12. Particle size distribution of ZW

The specific gravity of ZW particles is 2.33, i.e., it is slightly lower than those of PG powders. The analysis of the particle size distribution (see Fig. 12) reveals that the diameters of ZW particles mostly range from 10 to 40 μm , with the average value of 23.3 μm . The particle size values shown in Fig. 12 match accurately with the sizes of the particles observed in the images of Fig. 11.

2.2.3. Waste metallurgical sludge (MS)

Another additive employed in the current study was a waste product created in the ship building and repair yard *JSC Vakarų Metalgama* of Klaipėda (Lithuania), where metallic parts of ships are cut by CNC plasma in special water baths, and, consequently, metallurgical sludge (MS) is deposited at the bottom. Hence, in the presently mentioned yard, ca. 25 tonnes of MS are produced annually, which are eventually carried to the scrap for recycling. When this MS is extracted from the bath

and dried, its consistency is that of a fine black powder (Fig. 13). In an ongoing study, MS is intended to be employed as a modifier to improve the durability (more precisely, the water resistance) of the PG specimens.



Fig. 13. Macroscopic view of MS modifier

SEM analysis clarified that the MS particles are of various sizes and mostly of oval or spherical geometries (see Fig. 14).

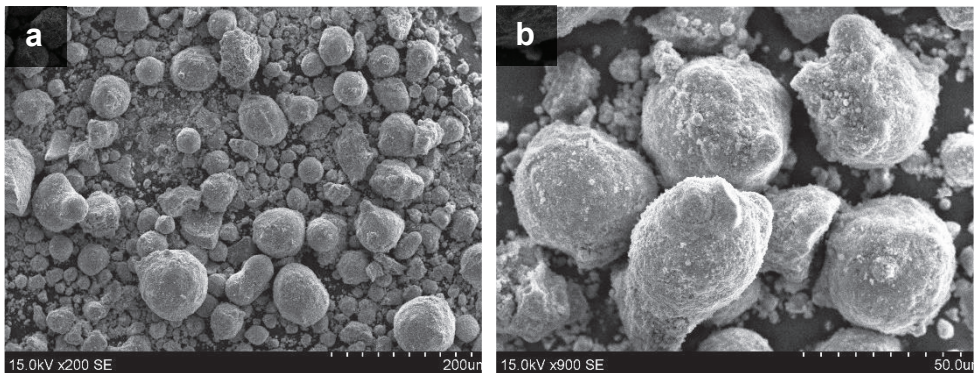


Fig. 14. SEM image of MS particles, at scales x200 (a) and x900 (b)

The specific gravity of the MS particles is 7.04, i.e., about 3 times heavier than that HH-PG particles. The particle size distribution presented in Fig. 15 confirms the observed variety of sizes, since the scatter of the diameters was found to be elevated. It can be observed that there are three diameter frequency peaks, distributed in an interesting way: at about 0.3 μm , 3 μm and 30 μm . Hence, each peak is about 10 times higher than the previous one. Of course, the clear predominant peak is that of 30 μm , and that determines the mean diameter value of 23 μm .

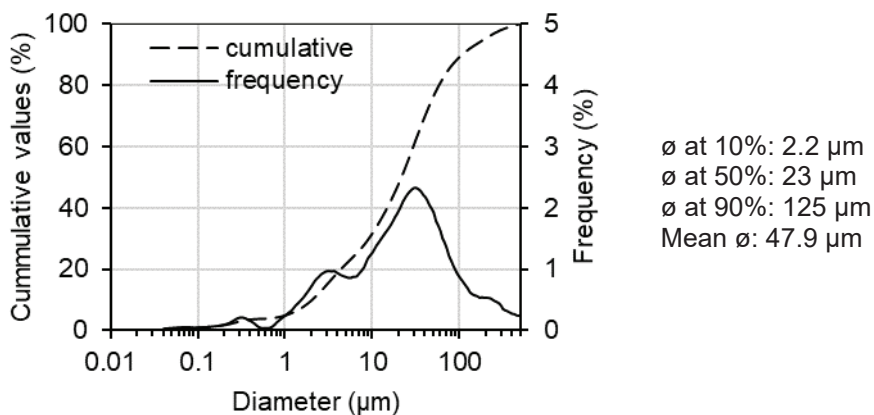


Fig. 15. Particle size distribution of MS

The metallic parts of ships (from which MS is produced) are made of structural carbon-manganese steel of S355 carbon-manganese grade. Thus, the elemental composition of MS is expected to be similar to that of this type of steel. The XRF chemical composition of MS is given in Table 5. The clearly predominant element is Fe, but there are also noticeable amounts of transition metals (Mn and Zn), non-metals (Si, P), and alkali-earth metals (Ca). Other trace elements, mostly some transition and post-transition metals (Al, Cr, Cu, Ni, Nb, V) and some REE (Gd, Eu), were determined in very low amounts. The C content does not appear in Table 5 since XRF analysis cannot trace it (in principle). However, S355 steel typically contains 0.16–0.18 wt% of carbon, thus a similar amount is expected to be present in MS.

Table 5. The XRF chemical composition of MS (wt%)

Fe	Mn	Si	Zn	Ca	P	Gd	Al	Cr	Eu	Cu
95.1	2.65	0.87	0.49	0.24	0.17	0.10	0.08	0.08	0.08	0.04
Ni	Nb	V	S							
0.02	0.02	0.02	0.02							

The depicted pH = 6.05 shows that MS powder is almost neutral, slightly acidic (see Fig. 48). The XRD pattern of MS (see Fig. 16) reveals the main compounds in which the chemical elements are combined. The main peaks are those of ferrite, but there are also other iron-based compounds, such as iron oxide, hematite and magnetite.

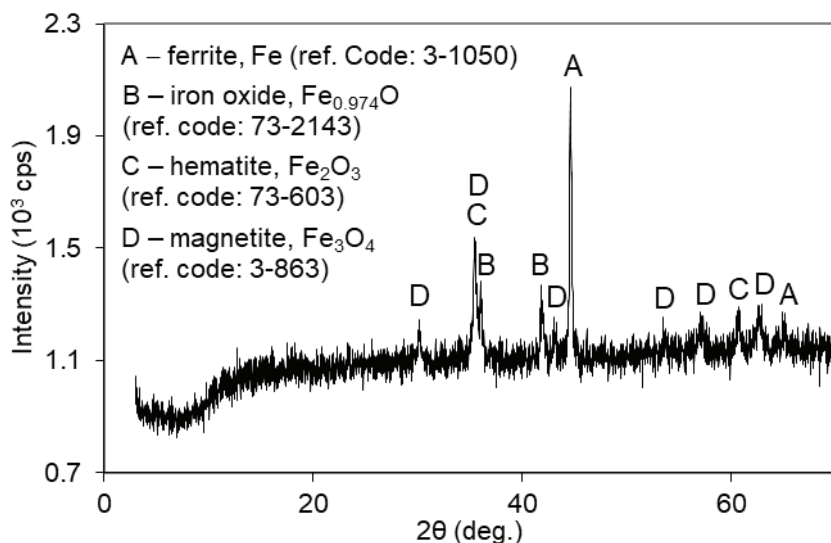


Fig. 16. XRD pattern of MS

2.2.4. Wood fibre (WF and NF)

Two types of wood fibre were employed in the current study: one directly manufactured from natural wood (further referred to as *NF*), and the other one processed from waste particle boards (further referred to as *WF*). Wood fibre is included in the PG mixture to improve the thermal and sound insulation properties of the hardened specimens. A macroscopic view of both types of fibre is given in Fig. 17.

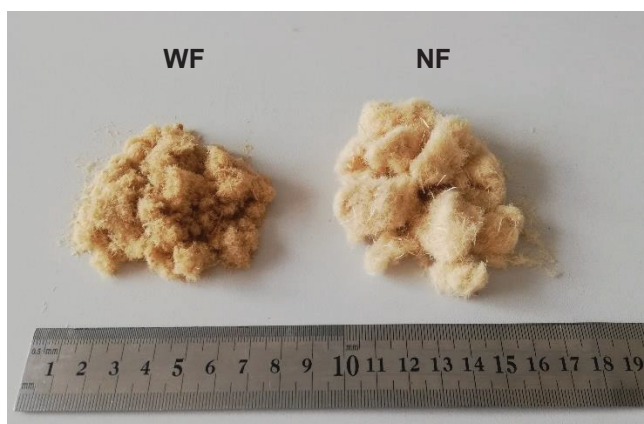


Fig. 17. Macroscopic view of wood fibre (the ruler is given for scaling)

Meanwhile, microscopic views of the different fibres are given in Fig. 18. Looking at the different images, it is difficult to distinguish one type of fibre from the other. There are no noticeable morphological differences in between the different

fibres. Their microstructures are, in fact, very similar. Besides, in both cases, the fibres seem to be partially covered with a varnish (or similar) coating.

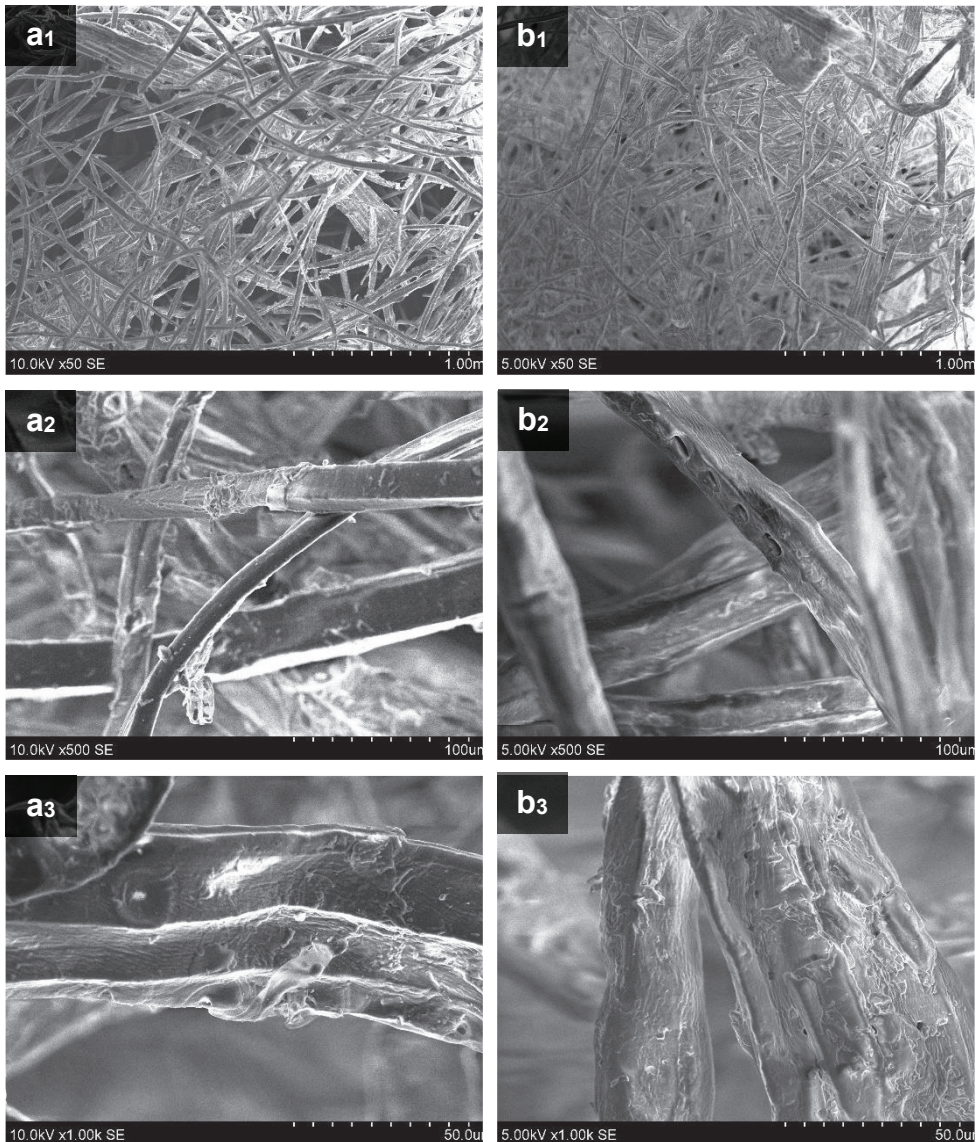


Fig. 18. SEM images of NF (a) and WF (b), at scales x50 (index '1'), x500 (index '2') and x1000 (index '3')

The size of the fibre was investigated through the sieve analysis whose results are given in Fig. 19. However, sieve analysis is not an accurate method to measure the diameter of a fibre since some fibres may not pass through the sieve due to their length or due to the fact that they are intertwined with other fibres. This method is more suitable for granular materials. Even so, the sieve analysis still gives useful comparative information regarding NF and WF by virtue of presenting the

approximate values of the sizes of each one. From the results exhibited in Fig. 19, it can be noticed that NF presents frequencies >5% in the sieves with meshes between 1 and 8 mm (included), whereas the waste fibre presented those frequencies with sieve meshes between 0.0 and 4 mm. Hence, NF is coarser than WF. Besides, in both cases, the fibres were mostly retained in the 2 mm sieve.

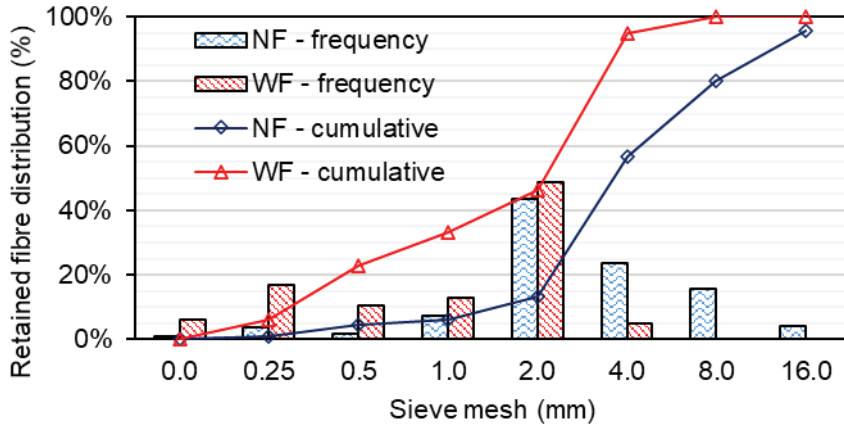


Fig. 19. Results of sieve analysis of both NF and WF

2.2.5. Hydrated lime

As explained in Section 1.5.1, $\text{Ca}(\text{OH})_2$ is a common method to neutralise the acidic-soluble P_2O_5 and F^- compound of PG due to its highly alkaline nature ($\text{pH} = 12.79$, see Fig. 24a). The specific gravity of $\text{Ca}(\text{OH})_2$ particles was determined to be 1.97, and the average diameter was $5.57 \mu\text{m}$ (which was not directly measured, but actually calculated from the exhibited Blaine specific surface of $12.9 \cdot 10^3 \text{ cm}^2/\text{g}$). In this way, $\text{Ca}(\text{OH})_2$ particles are smaller and lighter than those of HH-PG.

2.3. Summary of the properties of materials

A summary of the main properties of the different materials described in the current section is given in Table 6.

Table 6. Summary table of the properties of investigated materials

Material	pH	Mean particle size (μm)	Specific gravity	Microstructure	Colour
Natural HH gypsum	6.16	50.23	2.47	Separate crystals with irregular shapes	Grey
I-type HH-PG	2.88	49.32	2.70	Conglomerates of flat and sharp crystals	Grey
II-type HH-PG	2.87	65.75	2.74	Conglomerates of relatively flat and round-edged crystals	Bone
III-type HH-PG	3.63	85.14	2.67	Conglomerates of massive crystals with prismatic hexagonal geometries	White
ZW	4.35	23.26	2.33	Spherical particles	Bone
MS	6.05	47.9	7.04	Spherical and oval particles	Black
Ca(OH) ₂	12.79	5.57*	1.97	-	White
WF	-	2000 – 4000**	-	Long fibres	Dark brown
NF	-	2000 – 4000**	-	Long fibres	Light brown

***Note:** particle size of Ca(OH)₂ was not directly depicted, but calculated from the measured Blaine specific surface, by establishing comparison of the ratios between the measured Blaine specific surface and the mean particle size of other employed materials

****Note:** see the comments to the particle size of the fibre with respect to Fig. 19

3. RESULTS AND DISCUSSION

The aim of the current study is to analyse the aptness of PG to be employed as the main binding material in load-bearing building products, such as bricks or blocks. A thorough research has been performed to consider the different aspects to make this kind of usage possible. Hence, the ongoing investigation has been performed in 5 stages:

1. **Comparative investigation of the aptness of PGs from different origins to be used as binding materials in structural building products.** At this first stage, several PG types from different origins are analysed and compared with the objective to check the suitability of each one to be used as a binding material, while considering the acidic soluble impurity content, the hydration process, the physical-mechanical properties and the radionuclide activity concentration. Besides, the influence of the size of the specimens and of the processing method (casting vs. press-forming) on the ρ and the *CS* of the specimens is addressed.
2. **Investigation of the press-forming processing to produce structural PG products.** During this stage, the processing of press-forming specimens in pursuit of obtaining specimens with the optimal properties is investigated. The influences of the processing parameters such as *PFP*, *w/s* ratio, and the curing method (with or without immersion) on the ρ , the *LOI* and the *CS* of the specimens are assessed, and, in this way, the optimal processing parameters are identified.
3. **Adsorption of the acidic-soluble impurities of PG by zeolitic waste additive (ZW).** The efficiency of ZW additive in adsorbing the acidic soluble impurities of PG is investigated. Besides, the influence of this additive on the hydration and mechanical properties of PG specimens is evaluated.
4. **Improvement of the water-resistance of PG by adding waste metallurgical sludge (MS).** The problem of the softening of DH-PG crystals in water is addressed by including a small amount of MS in the composition of PG specimens. The effect of the MS additive on the neutralisation of soluble P_2O_5 , the hydration, the physical-mechanical properties and, of course, the softening (after a certain period of immersion in water) of PG specimens is thoroughly investigated.
5. **Improvement of the thermal and acoustic insulation of the load bearing PG specimens by including a waste wood fibre additive (WF).** The dependence of the thermal and acoustic insulation properties of the specimens on the WF content is investigated. Besides, the influence of the content and the type of the fibre (when comparing WF and NF) on the physical-mechanical properties of the specimens is studied. A certain amount of ZW was also included in the mixtures with the objective to adsorb acidic-soluble impurities.

It must be noted that the investigation tasks named in the 'Introduction' section do not necessarily coincide with each individual stage of the investigation. Some tasks are addressed in the same stage, whereas, in other cases, the same task is investigated across several stages. The stages of the investigation are summarised in Fig. 20. The results of each investigation stage are described in the following subsections.

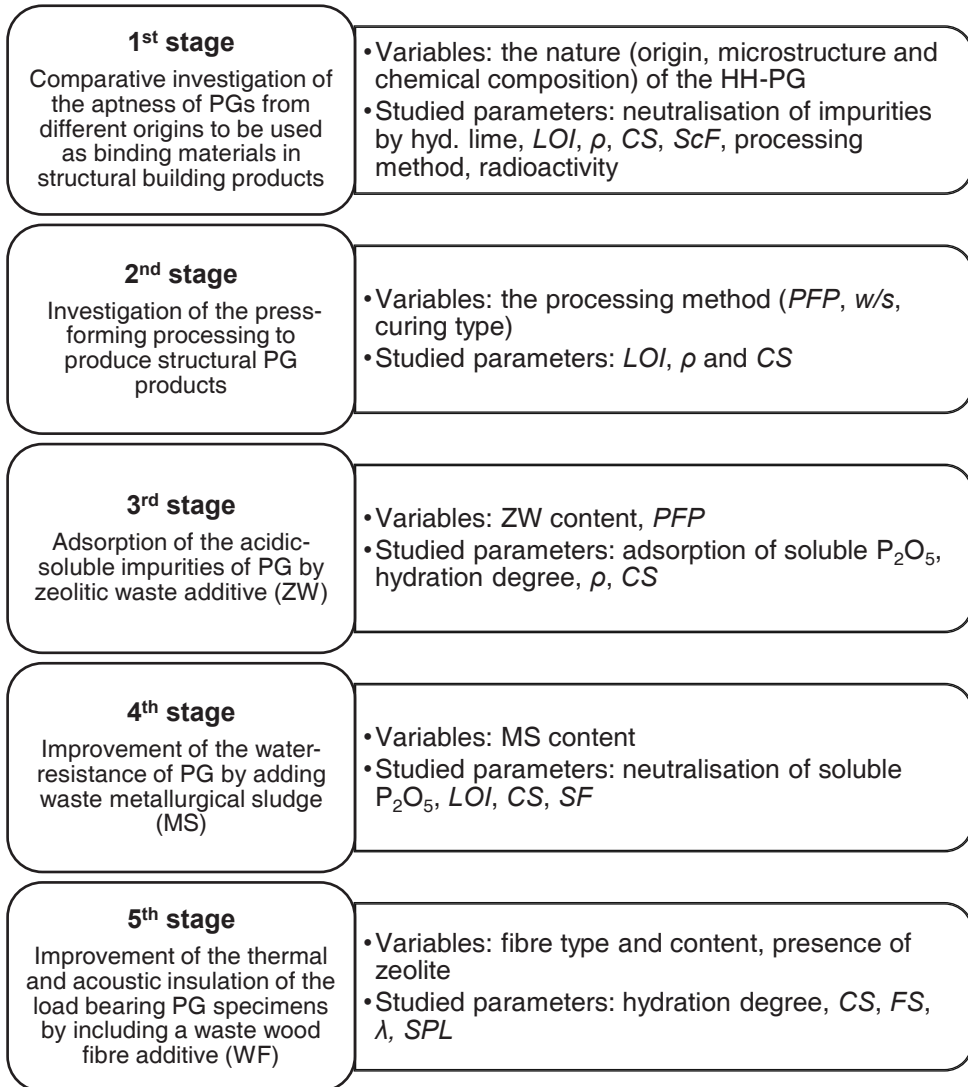


Fig. 20. Schematic view of the 5 stages of investigation

3.1. Comparative investigation of the aptness of PGs from different origins to be used as binding materials in structural building products

The 1st task of the investigation consists of the identification of the factors which determine the physical and mechanical properties of PG, and the evaluation whether the material is protective enough towards the ecosystem and the human health. With this purpose, DH-PG specimens were produced by using three types of PG from different origins which were already characterised in Section 2.2.1: the I-type PG (of igneous and sedimentary origin), the II-type PG (of sedimentary origin), and the III-type PG (from igneous origin). Besides, a commercial HH gypsum (referred to as 'natural') was also employed to produce the reference specimens. The aptness of each of the materials to be used in building products as the binding material was checked by considering the following parameters:

- the microstructure;
- the chemical composition (including the content of soluble P_2O_5 and F-impurities);
- the hydration, physical and mechanical properties (LOI , ρ and CS);
- the processing method: casting vs. press-forming;
- the radionuclide activity concentration.

The dependences among the different analysed parameters were investigated. The graphical explanation of the 1st investigation stage is given in Fig. 21.

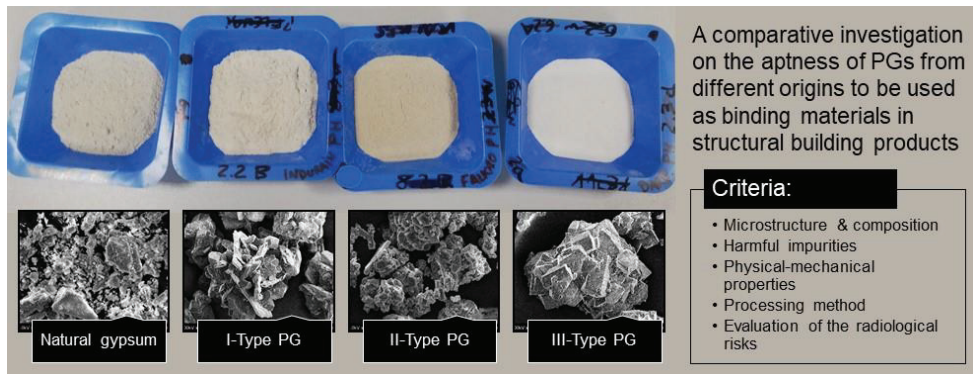


Fig. 21. Graphical explanation of the 1st stage of investigation

3.1.1. Experimental procedures

Four different groups of pastes and specimens were produced by attending to the composition of the mixtures, the processing method and the applied methods of analysis:

- group A: these specimens were employed to analyse and compare the dynamics of the hydration process and the mechanical properties of the DH specimens produced with the different HH materials;
- group B: these specimens were processed through the press-forming method, and their purpose was to investigate the impact of this type of processing on their mechanical properties;

- group C: the purpose of these specimens was to assess the effect of the specimen size on their *CS* values;
- group D: the main goal of these specimens was to investigate the efficiency of the $\text{Ca}(\text{OH})_2$ additive with regard to neutralising the acidic-soluble compounds of PG composition.

Detailed description of the different groups of specimens and their respective methods of analysis are given in Table 7.

Table 7. Composition, processing and analysis methods of different groups of specimens of the 1st stage of investigation

Group	Composition of dry mixture	w/s ratio	Method	Specimen geometry	Curing	Analysis method
A	Natural HH (100 wt%)	0.45	Casting	Cubic: 20mm-sided	Conditions: 100% humidity Duration: 2h, 1d., 3d., 7d., 14d., 28d.	- Hydration temperature - loss on ignition (LOI) - CS test - SEM
	I-Type HH-PG (100 wt%)	0.55				
	II-Type HH-PG (100 wt%)	0.40				
	III-Type HH-PG (100 wt%)	0.35				
B	Natural HH (100 wt%)	0.25	Press-forming	Cylindrical: 26.8x26.8mm	Conditions: 100% humidity Duration: 7d.	- CS test - SEM
	I-Type HH-PG (100 wt%)	0.25				
	II-Type HH-PG (100 wt%)	0.21				
	III-Type HH-PG (100 wt%)	0.20				
C	III-Type HH-PG (100 wt%)	0.35	Casting	Cubic: 20mm, 70mm and 100mm sided	Conditions: 100% humidity Duration: 7d.	- Scale factor (SF) - CS test
		0.20	Press-forming	Cylindrical: 26.8x26.8mm, 80x80mm, 100x100mm		
D	- All PG types (100-98.5 wt%) - Ca(OH) ₂ additive: 0.0-1.5 wt%	0.35, 0.45, 0.55	Casting	Pat-form specimens	Conditions: 100% humidity Duration: 7d.	- Hydration temperature - pH

The different specimens were produced via two alternative methods: casting (moulding) or press-forming. Firstly, the preparation of the A group specimens (by casting) is explained. The dry PG powder was blended with a certain content of water in order to produce the different cementitious pastes. In the case of each material, a different amount of water was added to produce pastes with the 'normal' consistency, according to the 'dispersal method' as described in European Standard EN 13279-2 [3]. Hence, the employed w/s ratios were 0.45, 0.55, 0.40 and 0.35 for the natural gypsum and the I-type, II-type and III-types of PG, respectively. Once the A group pastes had been mixed, they were poured in silicone moulds which were eventually vibrated to ensure satisfactory distribution of the paste, thereby avoiding undesirable air bubbles in the specimens. Hence, with each material, 27 specimens of 2 cm-sided cubes were produced. The casted specimens were then stored in a chamber with 100% moisture conditions in order to ensure the optimum hydration. The specimens of the different materials were distributed in 6 subgroups, of 4 or 5 units each, which were cured for different durations: 2 h, 1 d., 3 d., 7 d., 14 d., and 28 d. In this way, the long-term dynamics of the curing process could be investigated. Besides, during the casting process (after blending with water), the portions of the pastes which were not used for casting were immediately investigated by hydration temperature measurements, which reflects the short-term dynamics of the hydration process.

Meanwhile, the B group specimens were produced through press-forming. In this case, the pastes were blended by adding approximately half of the employed water to produce the casted specimens. A lower w/s ratio must be employed because, otherwise, leaching would happen during the stage of press-forming, consequently damaging the microstructure of the specimens (the flow of the escaping water would produce undesirable pores). Being so, the employed w/s ratios were 0.25, 0.25, 0.21, 0.20 for the natural gypsum and the I-type, II-type and III-type PGs, respectively. The precise ratios were selected in such a way that green specimens of ca. 2170 kg/m³ were produced immediately after the application of press-forming. It must be noted that the blending of natural HH with such a low amount of water was a technologically difficult process due to the cohesive behaviour of the material. Meanwhile, HH-PG pastes did not exhibit such a cohesive behaviour, and the water-blending process could be performed in a relatively smooth way. The press forming process was carried out by applying a *PF* of 15 MPa. The obtained specimens were cylindrical, with a height equal to the diameter of 26.8 mm. Eventually, the specimens were cured in 100% humidity conditions for 7 d.

In the same way, the specimens of the C group of various sizes (see Fig. 22) were manufactured via the casting and the press-forming methods.

Once the curing process had been completed, the specimens (of all groups) were dried at 40 °C temperature in order to remove entirely the free water content, i.e., the water which is not included in the molecules of DH gypsum (CaSO₄·2H₂O). The drying process was completed when the constant mass was achieved. Eventually, having measured the geometrical parameters and the mass of the dry specimens, the *CS* test was performed.

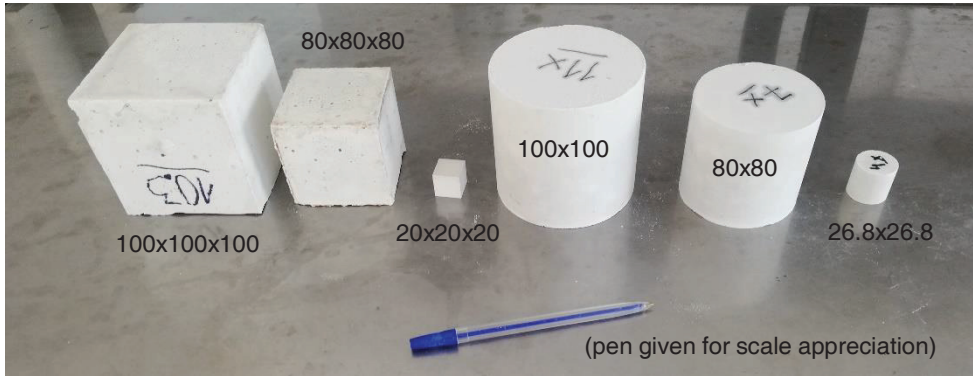


Fig. 22. View of the different specimens (dimensions given in mm) produced through casting (cubic specimens) or press-forming (cylindrical specimens) to investigate the influence of the size of the specimens on *CS* values

The microstructures of the crystal lattice of representative DH specimens of groups A and B were further investigated through EDS and XRD analyses, respectively.

The neutralisation of acidic soluble P_2O_5 and F^- impurities was studied from the D group specimens which were produced by including in the mixture different amounts of $Ca(OH)_2$. In this way, DH pats were created, and, after curing and drying, their aqueous solutions were investigated by employing the pH test.

Finally, the radiological assessment of the initial HH materials was performed by determining the activity concentration of the main radionuclides: ^{226}Ra , ^{232}Th , ^{40}K and ^{210}Pb , and by calculating the activity concentration index I (see Eq. (4)).

The schematic sequence of the described experimental procedures is given in Fig. 23.

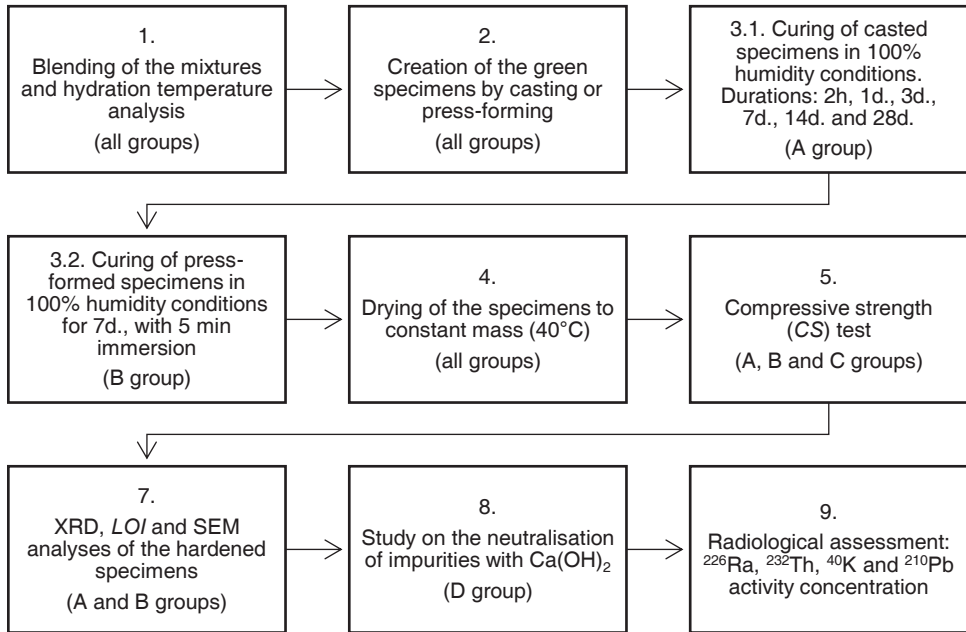


Fig. 23. Flowchart of experimental processes of 1st stage of the study

3.1.2. Experimental results

In order to check the suitability of the different PGs to be used as the binding material of structural building products, the main decisive aspects are further analysed and compared: the presence of acidic impurities (fluoride and phosphate) and their neutralisation, the physical and mechanical properties, and the radiological risks.

Neutralisation of soluble acidic impurities with $\text{Ca}(\text{OH})_2$

As mentioned in Section 1.2.2, PG typically contains important amounts of soluble P_2O_5 and F^- which cause environmental problems and reduce the mechanical properties of the binding material. The contents of P_2O_5 and fluorine in the different PG types (including the natural gypsum) are given in Table 3, and the differentiation between the soluble and non-soluble P_2O_5 content is presented in Table 2. According to the information given in both Table 2 and Table 3, the soluble P_2O_5 and F^- contents in type III PG is lower than in the types I and II PG, although it still remained substantially higher than the impurity content traced in the natural gypsum. It must be noted that the fluorine content given in Table 3 refers to the total content, and not only to F^- contained in soluble compounds (which are the harmful ones as this influences the acidic pH value). However, since F^- was not determined either in the natural gypsum or in the III-type PG, it becomes evident that the soluble F^- content in these materials is lower than that in the I and II types of PG. These tendencies of the soluble P_2O_5 and F^- contents are reflected in the results of the pH analyses given in Fig. 24a. The lower content of soluble P_2O_5 and F^- in the natural gypsum

determines an almost neutral pH, whereas PGs exhibit strong acidic values. In the same way, among the PGs, the III-type one exhibits the least acidic pH.

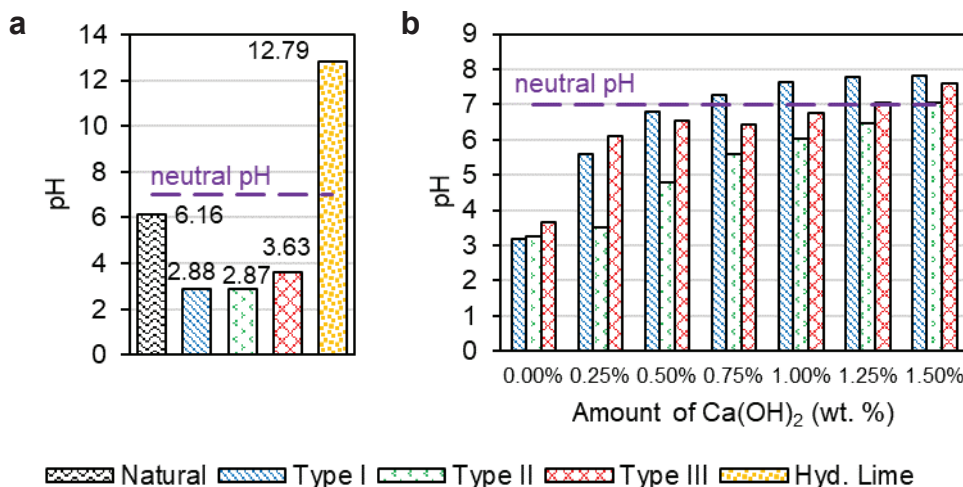


Fig. 24. Results of pH analyses of the initial materials (a) and of hardened PG specimens of D group, including different amounts of Ca(OH)₂ (b)

As mentioned in Section 1.5.1, soluble P₂O₅ and F⁻ impurities restrain the application of PG in building materials because of producing a negative impact on the environment, human health and the mechanical properties of PG products. The usual solution employed to reduce the content of these soluble impurities is the addition of a certain amount of hydrated lime which is strongly alkaline (see Fig. 24a). Ca(OH)₂ neutralises the acidic impurities by transferring them into non-soluble compounds, as explained by Kaziliūnas *et al.* [16] (see Section 1.5.1). Hence, different amounts of Ca(OH)₂ were added to the D group mixtures, and the results of the pH analysis performed with ground powder from the hardened specimens are presented in Fig. 24b, where different pH behaviours are observed. For instance, the PG of types I and III is more ‘sensitive’ to the addition of small amounts of Ca(OH)₂ than the PG of type II. The acidic impurities in PG get fully neutralised when the pH value surpasses 7, and that happens with Ca(OH)₂ contents of 0.75 wt%, 1.50 wt% and 1.25 wt% for type I, type II and type III PGs, respectively. Therefore, it can be stated that the addition of 1.50 wt% of Ca(OH)₂ is, in all cases, sufficient to fully neutralise the acidic soluble P₂O₅ and F⁻ impurities in PG, thereby avoiding their undesirable effects.

Influence of the PG nature, the processing method and the size of the specimens on the physical and mechanical properties of PG specimens

The hydration degree of hardened PG specimens is a crucial property. If CaSO₄ was not sufficiently hydrated, a further contact with moisture during the exploitation period would likely cause secondary hydration, consequently leading to undesirable volume changes. As a result, cracking, deformations or even failure would happen. Besides, the mechanical strength of gypsum depends, to an important extent, on the

quality of hydration. Hence, in order to use PG as the binding material of building products, it must be denoted by a satisfactory hydration degree.

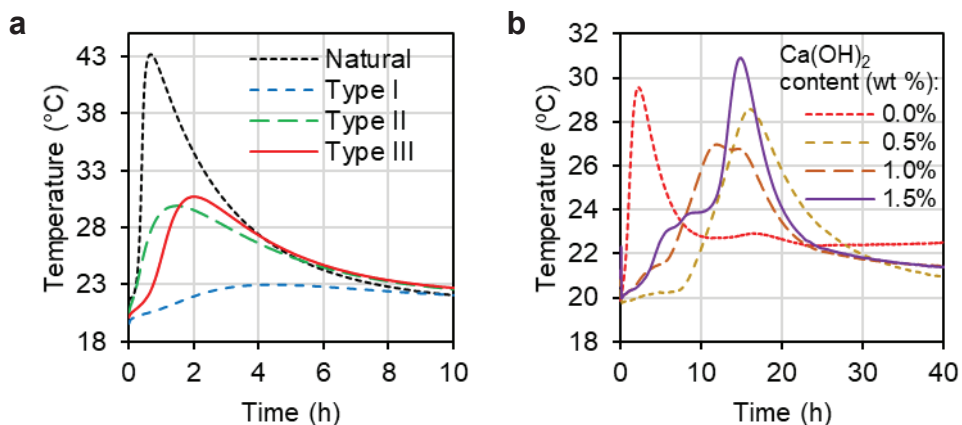


Fig. 25. Hydration temperature analyses of A group pastes of natural gypsum and different PG types (a) and of D group pastes with different Ca(OH)_2 contents (b) during the early stages of hydration

The hydration temperature analyses of the pastes of each type of PG and of the natural gypsum (belonging to group A) are given in Fig. 25a. It was observed that the hydration of the natural gypsum is the fastest one: the temperature peak ($43\text{ }^\circ\text{C}$) occurs at 30 min after the mixing. The hydration peak of the pastes of types II and III PG happen after 1 h 25 min (at $30\text{ }^\circ\text{C}$) and 2 h (at $31\text{ }^\circ\text{C}$), respectively. The hydration of the PG of type I is the slowest one: the peak is not clearly noticeable, but, if we take the most prominent value, it happens 4 h after blending, when reaching the temperature of $23\text{ }^\circ\text{C}$. These hydration differences could be produced by the soluble F^- and P_2O_5 (which hinder the hydration process) content or by the microstructure of PG crystals. The first seems to be the decisive factor explaining the faster hydration of the natural gypsum which contains much lower amounts of the above mentioned impurities than PG. However, the P_2O_5 and F^- impurities do not explain the slow hydration of the I-type PG, since the PGs of type I and II feature similar contents of these impurities (see Table 2 and Table 3) despite completely different early hydration rates (see Fig. 25a). Therefore, the clue factor which seems to determine the differences of the early hydration rates among the different PG types is the microstructure of HH crystals (see Fig. 7). The HH crystals of the I-type PG are flat and sharp in comparison to the more volumetric geometries of the PG crystals of types II and III. Being so, the flat geometries seem to be an obstacle for the water to approach the surfaces of the HH crystals, thus determining the slow hydration observed in Fig. 25a for the I-type PG.

Moreover, the influence of the hydrated lime content on the early rates of hydration is given in the hydration temperature analysis of Fig. 25b. In this case, the employed specimens belonged to group D. It can be clearly observed that Ca(OH)_2 acted as a retarder of the hydration process. When Ca(OH)_2 was included, the hydration peak occurred from 10 h to 20 h after the blending, i.e., much later than

the specimens without additive (2 h). There are no clear tendencies of the influence of the different Ca(OH)_2 contents on the hydration rates.

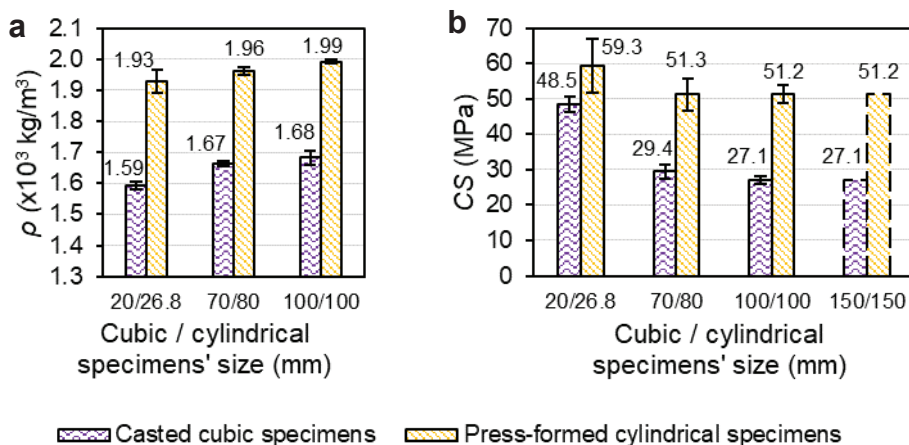


Fig. 26. Influence of the scale of specimens on the ρ (a) and the CS (b) of hardened specimens of group C produced with III-type PG

Before addressing the physical-mechanical properties of the specimens, it must be reconsidered that, at the current stage of the study, the manufactured specimens by casting (A group) are 2 cm-sided cubes, and the specimens processed through press-forming (B group) are 26.8x26.8 cm cylinders. These geometries are very small in comparison to the real life sizes of structural bricks or blocks in which PG is intended to be applied. Therefore, the exhibited CS values of the small specimens may differ from those of bigger specimens. Hence, a study of the influence of the scale of the specimens on their mechanical properties is still necessary. With this purpose, bigger specimens, corresponding to the C group, were produced (both by casting and press-forming, see Fig. 22). The ρ and CS results of the different specimens are presented in Fig. 26, and the values of the scale factor (ScF) are given in Table 8. All the specimens of this series were produced with the PG of type III. In Fig. 26, it can be noticed that for both the casted and the press-formed specimens, the ρ value increases with the bigger sizes of the specimens (see Fig. 26a). In addition, the ρ value of the press-formed specimens is ca. 1.2 times higher than that of the casted ones. Meanwhile, the tendencies of CS observed in Fig. 26b are different: the bigger are the specimens, the lower are the CS values. Considering the smallest specimens, the CS of the press-formed specimens (26.8x26.8 mm cylinders) surpassed by 1.2 times that of the casted specimens (20 mm-sided cubes). When bigger specimens were tested, the CS values of the press-formed specimens (cylinders of 80x80 mm and 100x100 mm) exceeded those of the casted specimens (70 cm-sided and 100 cm-sided cubes, respectively) by ca. 1.6 times. Hence, the effect of the specimen size on the CS of the cubic specimens manufactured through casting is higher than in the case of the press-formed cylindrical specimens, especially when their geometries are $\geq 70/80$ mm (see Fig. 26).

Table 8. *ScF* values for the *CS* of specimens of different sizes, calculated from the results of Fig. 26. The values marked in bold come from Lithuanian Standard LST 1974 [147]

Specimen type	Dimensions of cubes/cylinders (mm)		
	20 / 26.8	70 / 80	100 / 100
Casted cubic specimens	0.56	0.92	1.00
Press-formed cylindrical specimens	0.80	0.93	0.93

Since the aim of this study is to apply PG in structural building products, it is important to consider that the mechanical properties must be comparable to those of concrete. The European document EN 206-1 [148] establishes that the standard concrete specimens to perform the *CS* test are 150 mm-sided cubes or cylinders (CS_{150}). For the cases of testing smaller specimens, a *ScF* should be applied to the *CS* values in order to adjust them to the strength properties of the standard specimens. The *ScF* values of the different tested specimens are given in Table 8, and their calculation from the results of Fig. 26b is further explained. According to the Lithuanian additional requirements of the above mentioned standard [147], the *ScF* applied to the *CS* values of 100 mm-sided cubes is 1.00, whereas, for 100x100 mm cylinders, it is 0.93. Thus, these values are included in Table 8 in bold characters for the corresponding size of specimens. Since 150 mm-dimensioned specimens were not tested, the corresponding CS_{150} values were predicted by dividing the CS_{100} value by the respective *ScF* coefficients. In this way, the calculated results of CS_{150} are presented in Fig. 26b in columns with the dashed contours. Once the CS_{150} values have been obtained, the rest of the *ScFs* of Table 8 can be calculated ($ScF = CS_{150} / CS$). From the *ScF* results of Table 8, it can be noticed that the size of the casted specimens makes a greater effect on the *CS* values than the size of the press-formed ones. Henceforth, the strength values of the PG specimens shall be expressed in the normalised form (CS_{150}) so that the results obtained from specimens with different sizes could be easily compared.

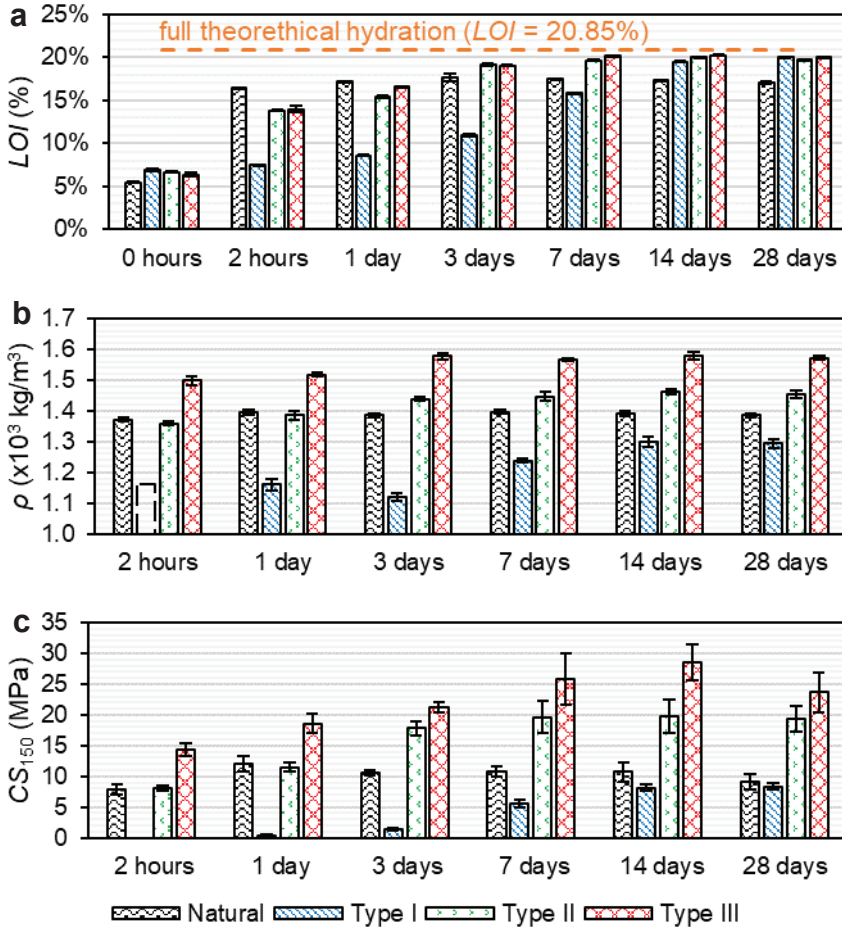


Fig. 27. Results of LOI (a), ρ (b) and CS_{150} (c) of A group specimens created with different materials, after different curing durations

Once the effect of the scale has been determined, the investigation of the physical-mechanical properties of the specimens can be addressed. The hydration temperature analysis (presented in Fig. 25) is an efficient method to describe the early stages (the first hours) of hydration. However, the hydration of DH-PG specimens not only takes place within the first few hours, but it continues for a longer period. As a means to monitor the long-term hydration behaviour of the different PG types (and that of the natural gypsum), the LOI method was employed. The results of LOI after different curing periods are given in Fig. 27a. The corresponding values of ρ and CS_{150} of the investigated specimens are given in Fig. 27b and Fig. 27c, respectively. The results presented in Fig. 27 belong to the A group specimens, i.e., 2-cm sided cubes produced through casting. Therefore, the $ScF = 0.56$ value was employed to calculate the CS_{150} values (see Table 8). It can be observed that the three parameters (LOI , ρ and CS_{150}) are closely related among themselves: the better is the hydration (LOI), the more compact is the crystal matrix, and the higher is the ρ value.

With a higher ρ , the specimens are expected to exhibit higher CS_{150} values. Therefore, in order to adequately determine the correlation among them, the results are provided in the same figure (Fig. 27), and the observed tendencies are further assessed. The natural gypsum hydrated very quickly. In 2 h, the LOI values achieved 16.42%, i.e., almost the maximum value. This value slightly increased during the first 3 days thereby ultimately reaching 17.7%, and then it stabilised. Similar tendencies were observed in the results of ρ and CS_{150} . The maximum $CS_{150} = 12$ MPa was achieved after 1 day of curing, and then, with longer curing periods, it slightly decreased due to gypsum softening in contact with moisture.

The PG of type I presented a prominently different hydration behaviour. The LOI values increased very slowly during the first 3 days of hydration. Between the 3rd and the 7th day, the LOI values considerably increased, and they ended up achieving an almost maximum value in 14 days, and then stabilised (the maximum LOI value was 20.00% after 28 curing days). The ρ and CS_{150} of the I-type PG specimens followed the behaviour of the LOI results, and the maximum achieved values were $\rho = 1300$ kg/m³ and $CS_{150} = 8$ MPa, after 14 curing days. It is interesting to consider that, even though the exhibited maximum LOI values of the I-type PG were higher than those presented by the natural gypsum, the ρ and the CS_{150} values were substantially lower. The ρ column of the specimens of the I-type PG after 2 h of curing is presented with a dashed contour due to the impossibility to measure their mass, since the green specimens were still not hardened at all, and, therefore, they could not be taken from the mould to perform the measurements.

The PGs of types II and III achieved satisfactory LOI between 3 and 7 curing days, i.e., their hydration happened more slowly than in the case of natural gypsum but much faster than in the case of the I-type PG. The maximum LOI values were 19.98% and 20.23% after 14 days for PG specimens of types II and III, respectively. Once again, the ρ and CS_{150} values corresponded closely to the observed LOI tendencies. The ρ and CS_{150} values of the specimens produced with these types of gypsum exhibited much higher values (especially those of type III PG) than those of the natural gypsum and of the I-type PG (which were the lowest). The maximum CS_{150} exhibited by type III PG was 29 MPa, i.e., it exceeded by 2.6 times the maximum values of the natural gypsum specimens. It must be taken into consideration that the natural gypsum is of β type, whereas PG belongs to the α category. Besides, the strength values exhibited by type III PG were comparable to those of concrete.

Hence, from the observations of the results presented by the different types of A group specimens in Fig. 27, some interesting conclusions arise. The correlation coefficient of the linear dependence between the ρ and the CS_{150} values (considering the results of all the specimens) is $r = 0.94$, i.e., a very strong correlation is detected (according to Taylor [149]). Hence, it can be stated that the ρ value strongly determines the CS value. On the other hand, the linear dependence between the LOI and the ρ values is lower (although still strong), i.e., $r = 0.72$. This fact suggests that LOI is not the only factor determining the ρ (and, subsequently, the CS_{150}) of the specimens. In fact, the nature and the microstructure of each of the employed materials also have a significant impact. Thus, very different ρ and CS_{150} values can

be observed between specimens of different materials, even though, in some cases, their *LOI* are fairly similar. Considering jointly the hydration and the mechanical performance of the specimens, it is clear that the best material to be employed in building products is the III-type PG, followed by the II-type PG. Meanwhile, the I-type PG suffers from poor mechanical properties and a slow hydration process, and therefore it is not appropriate for structural uses.

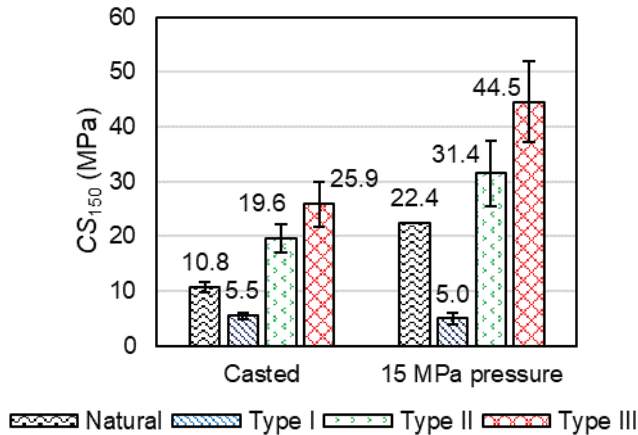


Fig. 28. Influence of CS_{150} of different specimens on the processing type: either casting (A group) or press-forming under 15 MPa pressure (B group)

As explained in Section 1.5.3, not only the nature of the employed material influences the mechanical performance of the manufactured specimens. The processing also makes an important contribution. In this case, the methods of casting and of press-forming (under a *PPF* of 15 MPa) were employed to produce the specimens of A and B groups, correspondingly. The *ScF* values of 0.56 and 0.8 were employed to calculate the values of CS_{150} for the respective specimens (see Table 8). A comparative graph of the mechanical properties of the specimens produced through the above mentioned processing methods is given in Fig. 28. In all cases, except for the I-type PG, the press-forming improved by 1.6–2.1 times the CS_{150} of the specimens with respect to the specimens produced through casting. The maximum CS_{150} value of the press-formed specimens was 44.5 MPa when the III-type PG was employed. In the case of PG of type I, the press-forming process did not help.

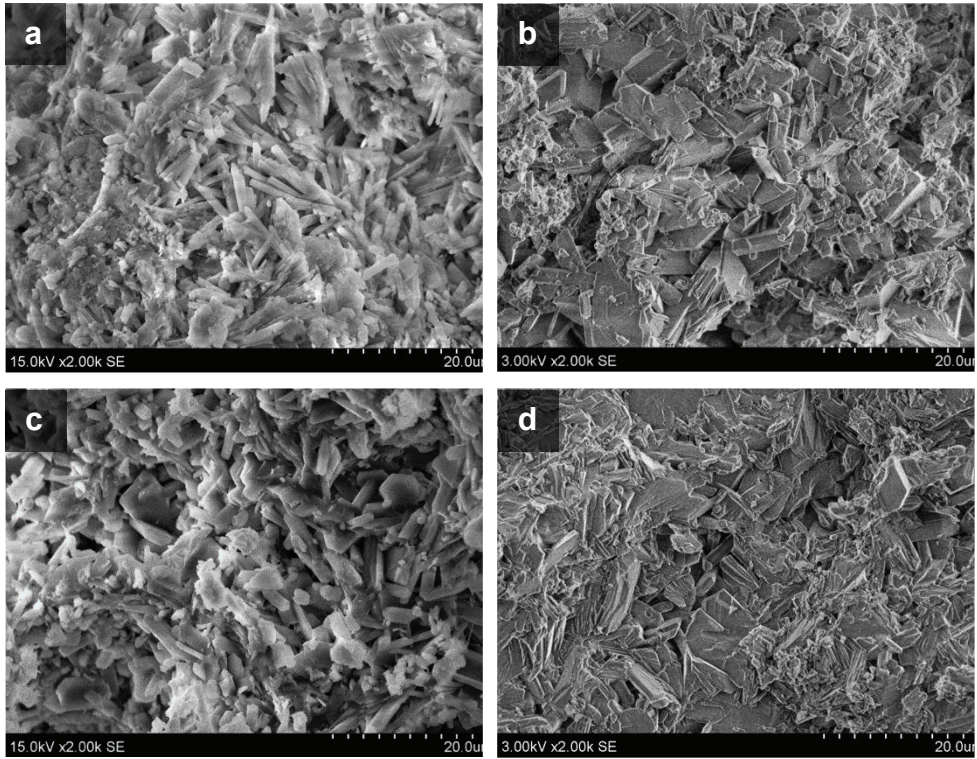


Fig. 29. Views of microstructures of hardened specimens produced through casting with different materials: natural gypsum (**a**), I-type PG (**b**), II-type PG (**c**), III-type PG (**d**).
Scale: x2000

The microscopic views of the different DH specimens produced by casting (belonging to A group) are given in Fig. 29. The natural gypsum DH crystals (see Fig. 29a) exhibit the typical geometry of the β gypsum crystals: needle-shaped thin crystals with hexagonal sections. Meanwhile, DH-PG crystals present the geometries of shorter and thicker hexagonal prisms, specific of the α type gypsum. Being so, type I and type II PG DH-crystal lattices (see Fig. 29b and Fig. 29c, respectively) are very porous, whereas the DH-crystal matrix of III-type PG is much more massive. That is the reason of the higher ρ and optimum CS of this type of PG.

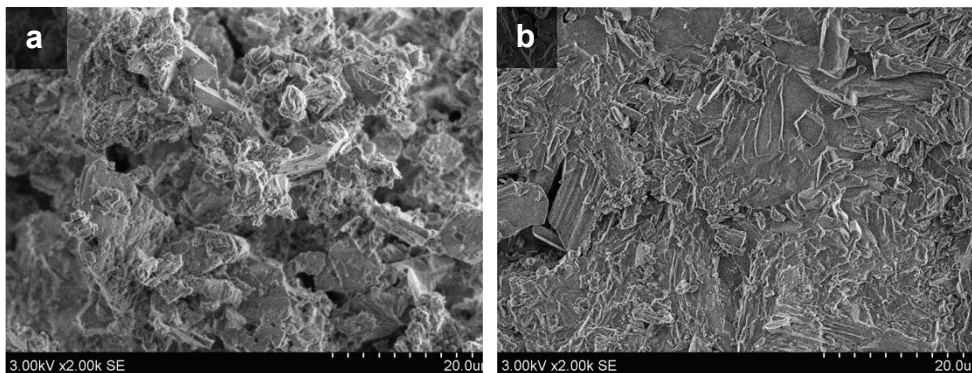


Fig. 30. Views of the microstructure of specimens of group B produced through press-forming: I-type PG (a), III-type PG (b). Scale: x2000

The microstructures of some representative press-formed specimens (of group B) are given in Fig. 30. For that purpose, the weakest specimens (of I-type PG, Fig. 30a) and the strongest specimen (of III-type PG, Fig. 30b) are presented. The crystal matrix of the press-formed specimen with I-type PG is very loose, with numerous pores and voids, even more than the casted specimens with the same material (see Fig. 29b). That explains the poor *CS* value exhibited by these types of specimens processed through press-forming (see Fig. 28). On the other hand, the crystal lattice of the III-type PG press-formed specimens (see Fig. 30b) presents a very dense and massive microstructure, even better than the one observed in Fig. 29d for casted specimens with the same type of PG. Hence, these observations strongly suggest that the improvement of the microstructure of the PG crystal lattice is the main cause of the better *CS* values obtained from the specimens processed through press-forming (see Fig. 28).

Radiological assessment of each PG type

Apart from the physical and mechanical properties, a major aspect which strongly determines the aptness of PG to be employed in building products is the radiological risk. As described in Section 1.2.1, numerous radionuclides (especially ^{226}Ra and its decay products) are typically present in the composition of PG. The reference limits of the radionuclide concentration in building materials and the radiological risks of PG are extensively described in Section 1.5.1. The radionuclide activity concentrations and the activity concentration index I of each material (the natural gypsum and PGs) are given in Table 9. It must be taken into consideration that the reference limit of $I \leq 1.0$ is given by the 2013/59/Euratom EU directive [63] as a useful tool to identify the building materials as either safe or risky from the radiological point of view (see Section 1.5.1). Index I is calculated from ^{226}Ra , ^{232}Th and ^{40}K radionuclide concentrations, according to Eq. (4). Since ^{232}Th cannot be measured directly by gamma spectroscopy [150], its value is computed from the activity concentrations of its progeny ^{228}Ra and ^{228}Th , as it is the usual practice suggested by the EU directive [63] and by the European Standard which, at the moment, is still being developed [151]. Besides, even though $I < 1.0$ is not met by a

certain material, it could still be used directly in building products if the gamma radiation dose for humans does not exceed the dose criterion 1 mSv/year [63]. Of course, in some cases, this type of evaluations based on the dose criterion constitutes a difficult task to perform, and that may hinder the application of those materials. However, in other cases, for instance, when the building material is employed in outdoor applications (for roads, bridges, etc.), or in superficial and small amounts (for tiles, boards, or similar), it is not difficult to prove that the dose criterion is satisfied.

The results of Table 9 reveal that, as expected, the radionuclide concentrations of the different PG types are much higher than those exhibited by the natural gypsum. Besides, the activity concentrations of the various PG types correlate with the nature of the phosphate rocks from which each specimen was processed (see Table 2). The III-type PG was processed completely from an igneous phosphate rock, and it produced a relatively low activity concentration ($I = 0.80$). On the other hand, the II-type PG is of the sedimentary origin, and that is reflected in the high radionuclide concentration values ($I = 2.74$). The PG of type I is of both igneous and sedimentary origin (mostly igneous), and the activity concentration is intermediate in comparison to the other PG types ($I = 0.93$). The PGs of types I and III present indexes $I < 1.0$. Hence, they could be considered as radiologically safe materials and, from this point of view, they can be employed without restrictions in building products. However, if the uncertainties are considered, their I values may surpass the reference limit, and a more precise radiological evaluation is required. The PG of type II presents the highest radionuclide concentrations, and its index I exceeds by almost 3 times the reference limit. This fact does not suggest that the material is banned from all uses in building products. In the appropriate proportions, it could constitute one ingredient of a final product which still meets the radiological requirements. For instance, a mixture of the natural gypsum and the II-type PG in weight proportions of 2:1 would satisfy the $I < 1.0$ limit. The II-type PG could be employed as the only material in application if the dose criterion 1 mSv/year is ensured.

Table 9. Values of the activity concentrations of main radionuclides (Bq/kg) and of I index for different employed materials

Material	^{226}Ra	^{228}Ra	^{228}Th	^{40}K	^{210}Pb	I
Natural gypsum	3.8 ± 0.3	3.2 ± 0.4	2.7 ± 0.6	128 ± 10	3.7 ± 1	0.07
I-type PG	200 ± 10	50.9 ± 2.6	47.4 ± 3.1	23.1 ± 6.3	237 ± 16	0.93
II-type PG	532 ± 50	191 ± 10	155 ± 10	25.3 ± 4.9	623 ± 22	2.74
III-type PG	49.1 ± 2.3	125 ± 10	116 ± 10	19.2 ± 3.5	38.4 ± 6.1	0.80

Hence, it can be stated that, when considering jointly the impurity neutralisation, the physical-mechanical properties and the radiological assessment of all the investigated PG types, the III-type PG is the most suitable one to be employed as a binding material of load-bearing building products. The other PG types present important drawbacks: the PG of type I exhibited slow hydration and poor physical and mechanical properties, whereas the radionuclide activity concentration in the PG of type II strongly exceeded the reference safety limit.

3.1.3. Partial conclusions

Comparative analysis of three PG types from different origins (for comparison purposes, the natural gypsum was also included) has been performed to evaluate the suitability of each PG to be used as a binding material in structural building elements. To do so, several aspects were considered: the content of soluble and acidic impurities, the physical and mechanical properties and the radiological risks. The best performing PG, from all points of view, appeared to be type III PG. Several conclusions arise from this first stage of the investigation:

1. **Neutralisation of P_2O_5 and F^- .** The content of soluble acidic P_2O_5 is higher in the case of Type I and Type II PGs than the PG of type III, which is the cleanest material. For all the PG types, an amount of 1.5 wt% $Ca(OH)_2$ additive is sufficient to completely neutralise soluble P_2O_5 and F^- into non-soluble compounds.
2. **Hydration process.** The natural gypsum hydrates much more quickly than PG. When comparing the PG types among themselves, the hydration of the I-type PG is much slower and less intensive than in the case of the other investigated materials. The determining factor seems to be the microstructure of HH crystals. The II-type and III-type PG crystals are more volumetric and, therefore, they hydrate more easily. Being so, the approximate durations of the hydration process are 2 h for the natural gypsum, 14 days for the I-type PG and 7 days for the PG of types II and III.
3. **Physical and mechanical properties.** The ρ value of the hardened specimens was influenced by *LOI*, the nature of the material (the microstructure of the crystal lattice), and the processing method (casting vs. press-forming). The CS_{150} values strongly correlated with the ρ values. The strongest specimens produced though casting were manufactured with the PG of type III, with a strength of $CS_{150} = 29$ MPa, i.e., 2.5 times stronger than the specimens produced with the natural gypsum. In general, the method of press-forming improved the *CS* of the specimens by 1.6–2.1 times, thereby reaching even as high a value of CS_{150} as 44.5 MPa.
4. **Radiological assessment.** The natural gypsum exhibited the lowest value of $I = 0.07$. The PG of types I and III presented I values of 0.93 and 0.80 which are below the reference limit of $I \leq 1.0$, hence, evidently, they can be applied in building materials without restrictions. The PG of type II presents the value $I = 2.74$, which exceed the reference limit. They could be used as an ingredient of a composite material (in the adequate proportions while ensuring that $I \leq 1.0$) or directly in applications where the human exposure to the gamma dose would not exceed 1 mSv/year as, for instance, in outdoor structures (bridges, roads, etc.) or in small amounts (tiles, boards, etc.).

3.2. Investigation of press-forming processing to produce structural PG products

In the 1st stage of the experiment, the dependences of the physical-mechanical properties of the specimens on numerous factors, such as the nature of the employed HH-PG (the microstructure and chemical composition), the size of the specimens (*ScF*) and the processing method (either casting or press-forming) were comprehensively analysed. Being so, the purpose of this 2nd stage involves focusing on the press-forming as a suitable processing method serving the objective to produce high performance PG specimens, while investigating the optimal processing parameters in our pursuit to manufacture the PG specimens with the best physical and mechanical properties. From the first approach towards the topic, as performed in the 1st stage of the experiment, the press-forming processing improved the *CS* values of the specimens by 1.6–2.1 times when the specimens were relatively small (26.8x26.8 mm cylinders, see Fig. 28), and by 2 times when they were bigger (80x80 mm and 100x100 mm cylinders, see Fig. 26), with respect to the specimens produced by casting. Therefore, at the current stage, cylindrical specimens of ‘bigger’ sizes (80x80 mm) were manufactured and tested.

However, the main drawback of the press-forming method is the fact that it allows a much lesser value of the *w/s* ratio than the casting method, since a higher *w/s* value would result in leaching during the press-forming and so would damage the microstructure of the specimen. This ‘shortage’ of water determines the lower *LOI* values of the press-formed specimens with respect to those of the casted ones. In order to ‘amend’ this issue, Zhou *et al.* [94] proposed curing the green specimens through the so-called ‘two-Step Hydration Process’, in which, green PG specimens were immersed in water for 30 min after the first day of curing. A more precise description of this method is given in Section 1.5.3 (see Fig. 3). At the current stage, for comparative purposes, some of the investigated specimens were cured according to this method (with immersion), while other specimens were not (i.e., immersion was not applied).

A simplified scheme of the investigations performed during this 2nd stage of the research is given in Fig. 31.

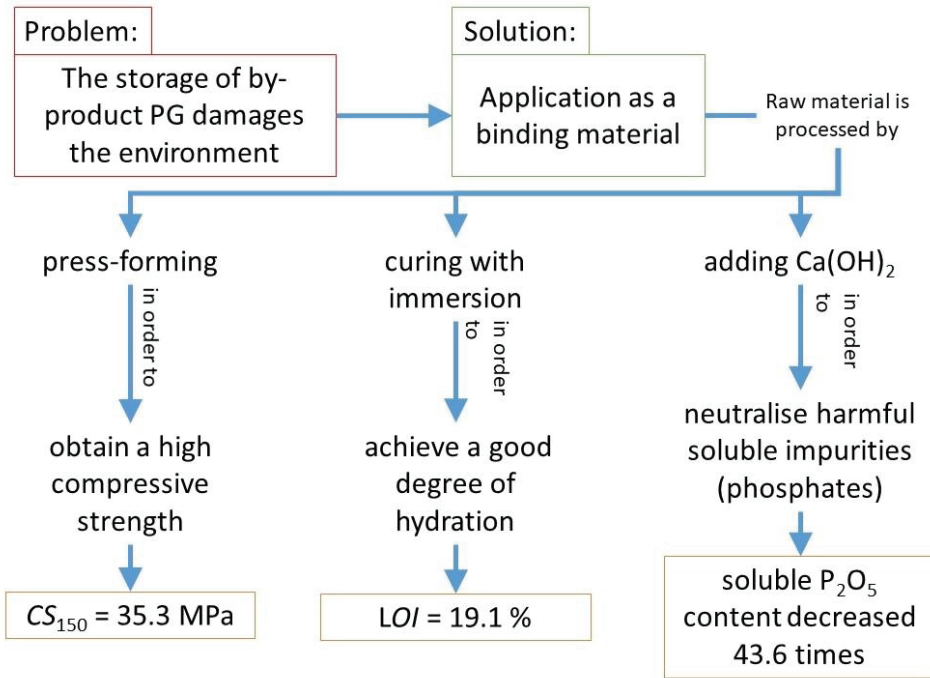


Fig. 31. Graphical explanation of the 2nd stage of investigation

3.2.1. Experimental procedures

For the current experiment, only one type of HH-PG was employed. This material was produced from phosphate rocks from SA (ca. 80 wt%) and from Kirov or Kovdor mines (ca. 20 wt%). Hence, the chemical composition and the microstructure are expected to be similar to the PG of type II, as described in Table 2 and Table 3, which is mostly produced from the raw material from SA. The PG of type II exhibited a high radionuclide activity concentration index $I = 2.74 > 1.0$ (see Table 9); therefore, its usage in building materials would be allowed only in a restricted way. However, at this stage, the matter of study is the press-forming processing method, so that the obtained results should also be valid for other radiologically protective PG types, such as the PG of type III, whose behaviour under press-forming is similar to that of the PG of type II (see Fig. 28).

First, the dry mixture was prepared by adding 1.5 wt% $\text{Ca}(\text{OH})_2$ to HH-PG. As depicted in the first stage of the experiment, such an amount of $\text{Ca}(\text{OH})_2$ is sufficient to neutralise the harmful soluble-acidic phosphate and fluoride impurities in the PG of type II (see Fig. 24b). Once the dry mixture had been prepared, the different pastes were blended by adding the required amounts of water. The theoretical w/s ratio to hydrate completely the HH gypsum powder is 0.17. However, the specific nature of PG, the included amount of hydrated lime, the press-forming process, and the curing conditions may cause modifications of this value. Hence, the pastes were produced with different w/s ratios: 0.07, 0.11, 0.15, 0.19, and 0.23. Subsequently, the press-

forming of the different pastes was performed. Several *PFPs* were employed: from 10 to 30 MPa, with an interval of 5 MPa. The used metallic press-form had a cylindrical geometry, with the internal dimensions of 80x80 mm (see Fig. 4), so that the produced green specimens would present the same geometry and size.

The produced green specimens immediately underwent the curing process. Two alternative curing methods were applied which are further referred to as ‘without immersion’ and ‘with immersion’.

- a) **Method without immersion.** This method follows the requirements of the Standard EN 13279-2 [3], according to which, the produced green specimens must be cured for 7 days under conditions of 60% humidity and 20 °C temperature. Since press-forming allows a low water content (with respect to the specimens produced by casting), this type of curing is expected to produce poorly hydrated specimens.
- b) **Method with immersion.** This method is employed to ‘correct’ the expected hydration shortage by following the ‘two-step hydration process’ as proposed by Zhou *et al.* [94]. After the press-forming, the green specimens are stored under the conditions described when defining the previous curing method. In this way, the first hydration of the gypsum crystals happens. However, 1 day after the start of the curing, the specimens are immersed in water for 45 min. This immersion produces a second stage of hydration of the PG crystals which had remained in the HH phase due to the lack of water. Therefore, better hydration of these specimens is expected. After the immersion, the specimens are stored again under EN 13279 – 2 Standard conditions till the 7 days of curing have been completed.

Once the curing had been completed, the hardened PG specimens were dried at 40 °C temperature till the constant mass was achieved. This process lasted approximately 10 days. Then, the *CS* test was performed. In addition, the *LOI* values of the different specimens were determined.

Finally, different amounts of Ca(OH)_2 additive were included to investigate the neutralisation of the water-soluble impurities of the press-formed specimens. To do so, the pH and the P_2O_5 and F^- contents were obtained. The sequence of the main experimental procedures is illustrated in Fig. 32.

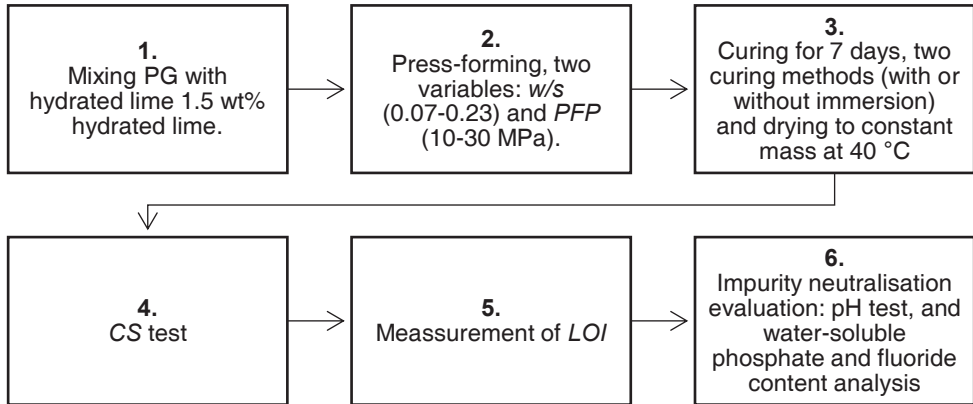


Fig. 32. Flowchart of the experimental processes of the 2nd stage of study

3.2.2. Experimental results

The suitability of the press-formed PG specimens as structural building products was checked by analysing the neutralisation of the acidic impurities, and the dependences of the physical and mechanical properties of the specimens on the processing parameters was determined.

Neutralisation of acidic soluble impurities with $\text{Ca}(\text{OH})_2$

First of all, the neutralisation of acidic soluble P_2O_5 and F^- impurities by the addition of $\text{Ca}(\text{OH})_2$ was checked. It must be clarified that, although in the 1st stage of the study, a similar investigation on the neutralisation of PG acidic impurities by $\text{Ca}(\text{OH})_2$ was performed (see Section 3.1.2), in the current case, an additional investigation was necessary because of the slightly different nature of the employed PG, so that the required amount of $\text{Ca}(\text{OH})_2$ additive may be adjusted. Hence, the pH dependence on the amount of the added $\text{Ca}(\text{OH})_2$ is given in Fig. 33a. It can be observed that the addition of 0.5 wt% of $\text{Ca}(\text{OH})_2$ reduced the acidity of PG, but it was still not sufficient to achieve neutral pH. When 1.5 wt% of $\text{Ca}(\text{OH})_2$ was included, an alkaline pH was determined, thus indicating the full neutralisation of the acidic P_2O_5 and F^- soluble compounds in PG.

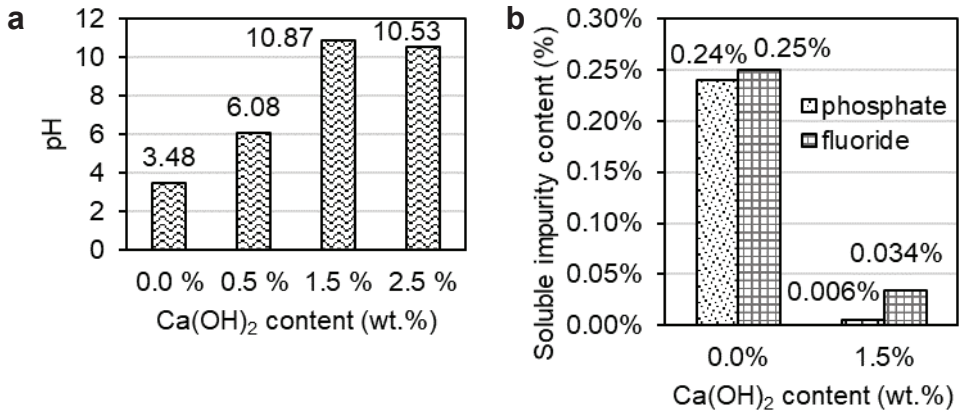


Fig. 33. Neutralisation of soluble acidic impurities: pH values (a) and soluble phosphate and fluoride contents (b), depending on the included Ca(OH)₂ amounts

Additionally, the soluble P₂O₅ and F⁻ contents in the PG specimens were measured, and the results are presented in Fig. 33b. The given results highlight even more the high efficiency of Ca(OH)₂ in neutralising the phosphate and fluoride compounds: when 1.5 wt% of Ca(OH)₂ was included, the soluble P₂O₅ and F⁻ contents were reduced by 40 and 7.4 times, respectively. Because of the obtained results, at this 2nd stage of the investigation, 1.5 wt% of Ca(OH)₂ was added in all the mixtures so that to produce the specimens for the remaining stages of the investigation.

Influence of the parameters of press-forming processing on the physical-mechanical properties of the specimens

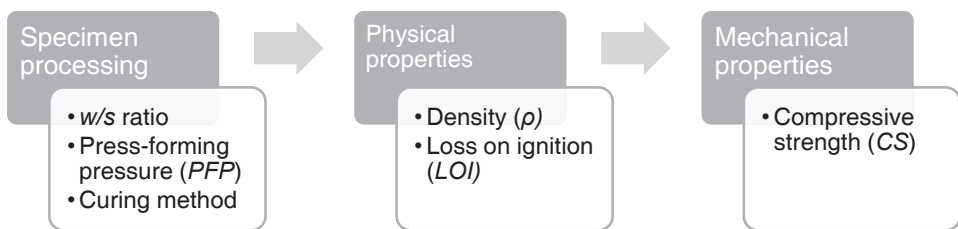


Fig. 34. Cause-effect relations between the investigated properties of the specimens

The optimal parameters of the processing method (*w/s* ratio, *PPF*, and the curing method) were investigated so that to produce specimens with high *LOI*, ρ and *CS* values, i.e., suitable to be employed in structural building products. A schematic view of the cause-effect dependences among these parameters is given in Fig. 34. The results are presented and discussed further in this thesis.

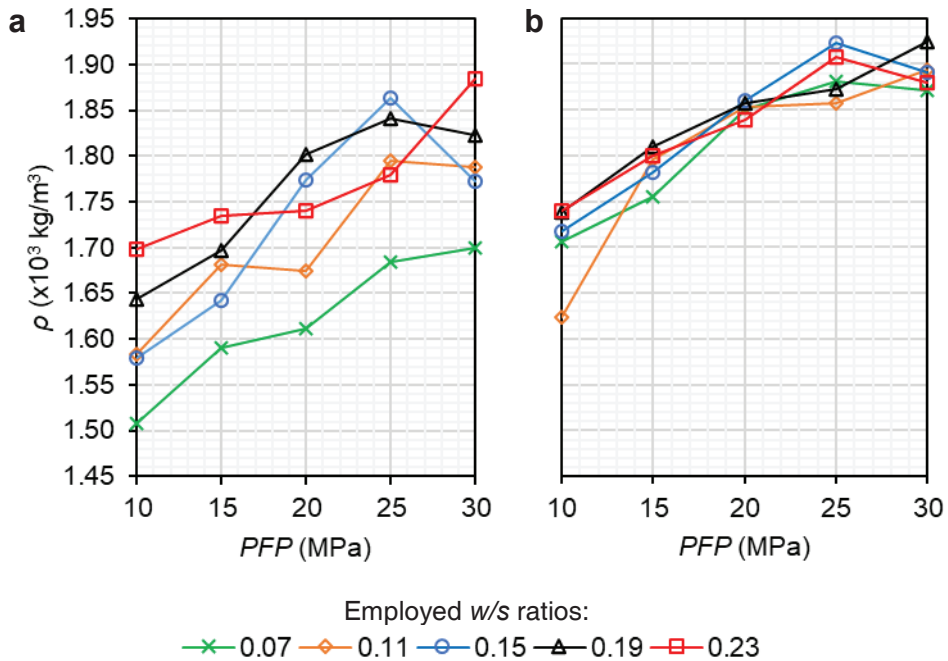


Fig. 35. Influence of $PF\!P$ on ρ of the hardened specimens cured without immersion (a) and with immersion (b), produced with different w/s ratios

First, the dependences of the ρ value of the specimens on the processing parameters, i.e., the applied $PF\!P$ (horizontal axes), the w/s ratio (tendency lines) and the curing method are given in Fig. 35. The results of the specimens cured without immersion are given in Fig. 35a, while those of the specimens cured with immersion are given in Fig. 35b. In both graphs of Fig. 35, when the $PF\!P$ values increase from 10 to 25 MPa, the ρ values correspondingly increase. The further increase of $PF\!P$ (30 MPa) generally do not improve the ρ value of the specimens, which mostly remain constant, or even decrease. This behaviour is attributed to the leaching observed when the pressure of 30 MPa is applied. If the $PF\!P$ value is excessively high, the water content would try to ‘escape’ from the material, thereby weakening the microstructure of the specimens. However, there are some exceptions where the 30 MPa pressure does improve the ρ value, especially in the case of the specimens with a w/s ratio of 0.23, processed without immersion.

The effect of the w/s ratio on the ρ of the specimens is extremely interesting and depends on the curing type. When no immersion is applied during curing (see Fig. 35a), the w/s ratio makes an important influence on the ρ value. While the w/s ratio increases from 0.07 to 0.19, the ρ value also increases. When $w/s = 0.23$ is employed, in most cases, the ρ values decrease, since the excess of water produces leaching during the press-forming. However, there are some exceptions, since the maximum $\rho = 1184 \text{ kg/m}^3$ is exhibited by specimens produced with $PF\!P = 30 \text{ MPa}$ and $w/s = 0.23$ (considering the specimens cured without immersion). When curing with immersion is applied (see Fig. 35b), prominently different tendencies are

observed: the differences between the various w/s lines almost disappear. In other words, the ρ values of the specimens become independent from their w/s ratio. The immersion process ‘corrects’ the water content differences between the specimens produced with different w/s ratios. By using this type of curing, the densest specimens are obtained ($\rho = 1924 \text{ kg/m}^3$), which are produced with $PPF = 30 \text{ MPa}$ and $w/s = 19$.

However, in both graphs of Fig. 35, it can be observed that the tendencies of the different w/s ratios are not very clear, and only general comments on the relation between ρ and the w/s can be given. When considering the general results, it seems that PPF is a more decisive factor than w/s in determining the ρ value of the specimens.

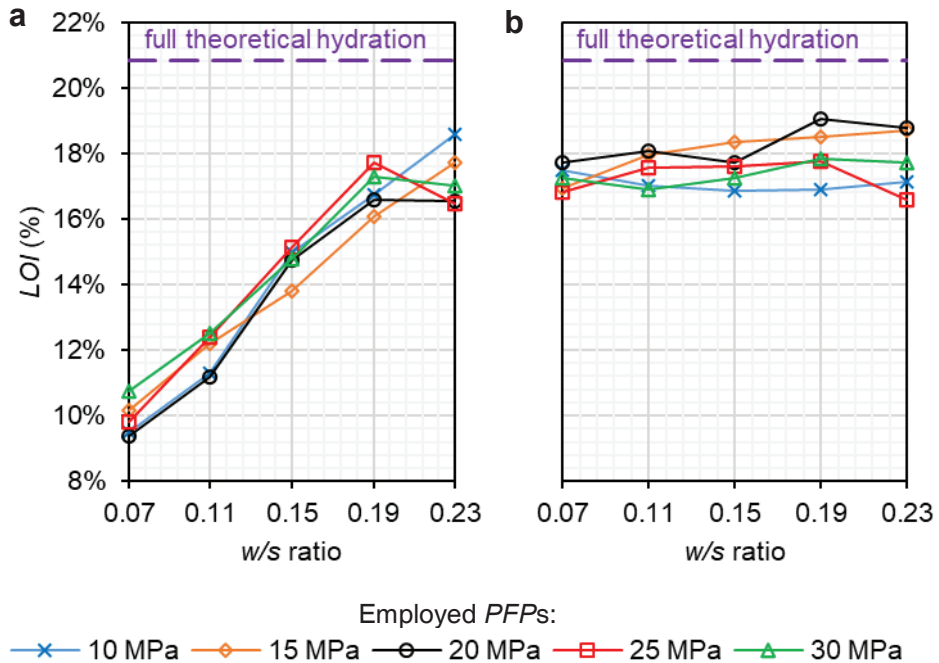


Fig. 36. Influence of the w/s ratio on LOI of hardened specimens cured without immersion (a) and with immersion (b) and processed under different $PPFs$

In the same way, the dependences of LOI on the processing parameters are presented in Fig. 36: the w/s ratios (horizontal axes), the PPF (tendency lines) and the curing method (graphs a or b). The influence of PPF on the LOI values is not very significant for both curing methods, since in both graphs the lines which indicate the different $PPFs$ are very similar to each other. The w/s ratio and the curing method are much more determinant. When curing without immersion is applied (see Fig. 36a), the LOI values correspondingly increase with higher w/s ratios, although, with w/s values, when exceeding 0.19, most of the LOI values stabilise. This behaviour was expected, since it is logical to predict that the higher water content in the mixture determines higher LOI values. However, when curing with immersion is applied (see Fig. 36b), the tendencies change, and LOI becomes independent from

the w/s ratio. The curing with immersion process efficaciously corrects the hydration shortage when low w/s ratios are applied. Hence, if the immersion process is applied, lower amounts of water can be included in the mixture. The maximum LOI was 19%, as depicted in the specimens produced with $w/s = 0.19\%$, $PPF = 20$ MPa, and the curing method ‘with immersion’.

From Fig. 35 and Fig. 36 graphs, the main dependences of the physical and hydration properties of the specimens on the processing parameters are identified: the ρ value of the specimens depend both on PPF and on the w/s ratio, whereas the LOI values mainly depend on the w/s ratio. If curing with immersion is applied, both the ρ and the LOI values become independent from the w/s ratio.

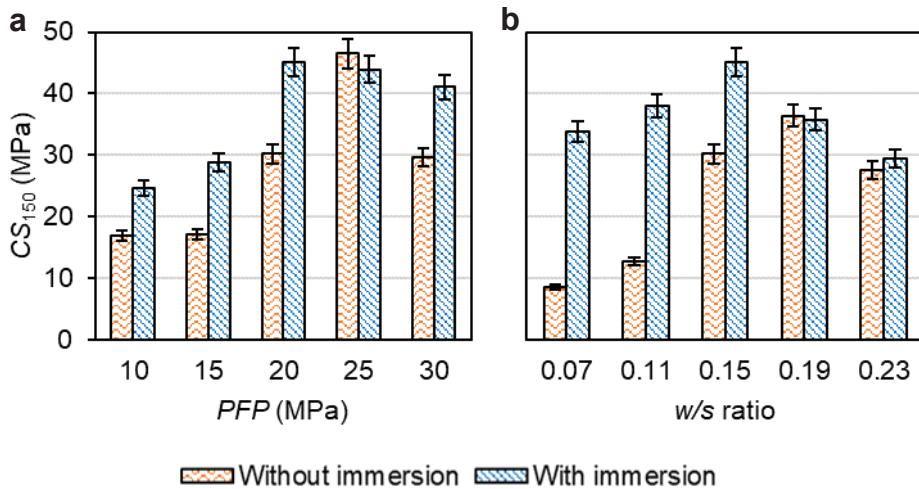


Fig. 37. Dependences of the CS_{150} of representative specimens: on the PPF of specimens produced with $w/s = 0.15$ (a) and on the w/s ratio of specimens processed under a PPF of 25 MPa (b)

The dependences of CS_{150} on the processing parameters are given in Fig. 37. It must be reminded that the CS_{150} values given in Fig. 37 (as well as in Fig. 38) correspond to the CS test performed with cylindrical 80x80 mm specimens which are not of the standard size. Thus, the standard CS_{150} values are calculated by multiplying the measured CS values by $ScF = 0.93$ (see Table 8). In Fig. 37, only the results of the representative specimens are presented. The dependence of CS_{150} on PPF (see Fig. 37a) is given from the specimens with a fixed w/s ratio of 0.15. Meanwhile, the dependence of CS_{150} on w/s (see Fig. 37b) is presented from the specimens produced under a PPF of 25 MPa. In Fig. 37a, it is shown that the enhancement of PPF produces higher CS_{150} values until reaching a certain optimal PPF value (25 MPa when the specimens were cured without immersion, and 20 MPa when the specimens were cured with immersion); the maximum CS_{150} values are obtained at 46.5 MPa. If this optimal value is exceeded, PPF damages the microstructure of the specimens, and the CS_{150} values start decreasing. With regard to the effect of the w/s ratio on CS_{150} (see Fig. 37b), it can be perceived that, with low w/s ratios, the specimens cured with immersion are stronger than those cured without immersion. However, when $w/s \geq 0.19$, CS_{150} becomes independent from the

curing method. Being so, the maximum CS_{150} value of 45.1 MPa (see Fig. 37b) is achieved when curing with immersion is applied to the specimens produced with $w/s = 0.15$. In the case of the specimens being produced without immersion, the optimal w/s was 0.19, which is the respective CS_{150} value of 36.5 MPa. A further increase of the water content produces a decrease of the CS values (due to leaching).

The tendencies observed in Fig. 37 reveal that, in general, the CS_{150} values of the specimens cured with immersion are higher than those cured without immersion, unless very precise parameters of w/s and PFp are employed ($PFp = 25$ MPa in Fig. 37a, and $w/s = 0.19$ in Fig. 37b); in this case, the CS_{150} values can be similar or even higher than those of the specimens cured with immersion. In this sense, curing with immersion allows wider ranges of the processing parameters while maintaining high CS_{150} values.

Considering jointly the hydration and the strength properties of the specimens, the recommended processing parameters are $w/s = 0.19$, $PFp = 20$ MPa and curing with immersion, with which the manufactured specimens exhibited high LOI values (19.1%) and a suitable CS_{150} value of 35.3 MPa which is comparable to the typical strength of cement.

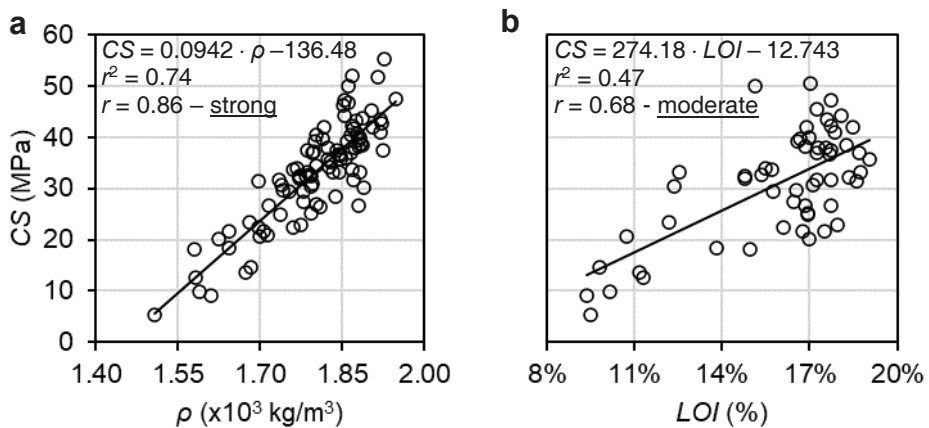


Fig. 38. Linear correlation between ρ and CS (a) and between LOI and CS (b) with the correspondent correlation coefficients r and their interpretation (underlined)

As expressed by the cause-effect relationships given in Fig. 34, the processing parameters determine the ρ and the LOI values of the specimens, which, at the same time, determine the CS . Hence, the dependences of CS on the processing parameters, as analysed in Fig. 37, are only indirect. Hence, the ‘direct’ CS dependences on the ρ and on the LOI values must be addressed, and, therefore, they are given in Fig. 38. In both cases, according to the least square method, the best fitting functions were identified to be the linear ones. The formulas of these linear approximations are given in the graph plot, together with the correlation coefficient r . According to the obtained r values, the correlation between the ρ and CS values (see Fig. 38a) is ‘strong’, while the dependence between the LOI and the CS values is ‘moderate’, as indicated by the interpretation of r explained by Taylor [149]. Being so, the ρ of the

specimens is more determinant than that of *LOI* regarding the *CS* values of the specimens.

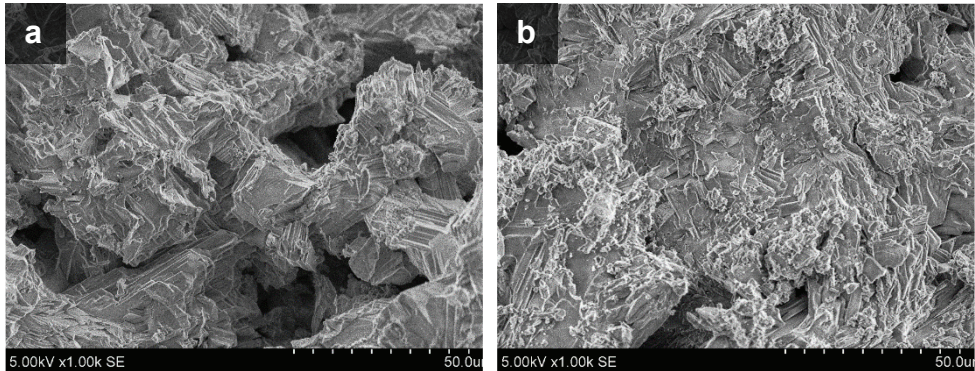


Fig. 39. Microscopic images of PG specimens manufactured under *PFPs* of 10 MPa (a) and 25 MPa (b) (both cured with immersion); scale: x1000

The microstructure of the PG specimens gives important clues to understand the effects of the different processing methods, since the important changes start at the microscopic level. The microstructures of the specimens produced under a *PFP* of 10 and 25 MPa are given in Fig. 39a and Fig. 39b, respectively. The specimen produced under the lower pressure presents a loose microstructure with numerous pores and caves, whereas the microstructure of the specimen produced under 25 MPa is denser and massive, hence, a higher *CS* value is expected. The press-forming process is an effective way to process the PG so that to produce strong and suitable structural building products.

3.2.3. Partial conclusions

At this 2nd stage, the optimal processing parameters to manufacture press-formed structural building products made of PG were investigated and identified. The main results are summarised as follows:

1. **Neutralisation of the acidic-soluble impurities.** As well as in the 1st stage of the investigation, the addition of 1.5 wt% of $\text{Ca}(\text{OH})_2$ to the HH-PG mixture was proven to be sufficient to effectively neutralise the acidic-soluble P_2O_5 and F^- impurities. The soluble P_2O_5 and F^- contents were reduced by 40 and 7.4 times, respectively.
2. **Hydration degree of the specimens.** The main drawback of the press-forming processing of PG is related with the low amount of *w/s* allowed in the mixtures. The results showed that the *LOI* values strongly depend on the *w/s* ratio of the mixtures. However, when immersion is applied during the curing period, the hydration ‘shortage’ is corrected, and the *LOI* of the specimens becomes independent from the *w/s* ratio. The maximum *LOI* value was 19.1%, as determined for the specimens produced with *w/s* = 0.19, *PFP* = 20 MPa and cured with immersion.
3. **Mechanical properties.** The *CS* of the specimens was proven to be mostly dependent on the ρ value (strong linear correlation), and, to a lesser extent, on the

LOI value (moderate correlation). In general, the ρ value of the specimens was improved by applying the *PF*P of 25 MPa. The strongest specimens, which exhibited a $CS_{150} = 46.5$ MPa, were obtained when *PF*P = 25 MPa and $w/s = 0.15$ was applied, and curing was without immersion. However, these specimens presented a poorly hydrated crystal phase ($LOI = 15.1\%$).

4. **Recommended processing parameters.** Considering jointly the hydration and the strength properties of the specimens, the recommended processing parameters are those described in conclusion No. 2 (with $w/s = 0.19$, *PF*P = 20 MPa and curing with immersion), which not only produced well hydrated specimens, but also with the suitable CS_{150} value of 35.3 MPa, which is comparable to the typical strength values of cement.

3.3. Adsorption of acidic-soluble impurities of PG by zeolitic waste additive (ZW)

Zeolites are microporous materials of aluminosilicate nature which are suitable to be employed as sorbents and catalysts in industrial processes. As explained in Section 1.5.1, these materials have been employed in some studies to adsorb the acidic soluble P_2O_5 and F^- compounds in PG, thereby mitigating their harmful effects. The adsorption mechanism through which zeolites adsorb phosphate compounds was explained by Sabadash *et al.* [152] whose study showed that this sorption takes place due to ion exchange and chemical sorption processes. Hence, the goal of the 3rd stage of the research is to investigate the effectivity of the ZW additive in reducing the acidic-soluble impurities in the PG specimens, and to investigate its influence on other properties of press-formed specimens, such as the hydration degree and CS.

To do so, specimens were produced by using the HH-PG of type III, which is extensively described in Section 2.2.1. This type of PG was selected since, according to the results of the 1st stage of the experiment (see Section 3.1), it was the best performing material from all points of view: it exhibited the lowest content of acidic impurities and of radioactivity, the best hydration process and the highest CS values. The employed ZW is synthetic waste from the petrochemical industry. Its microstructure, particle size and chemical composition are given in detail in Section 2.2.2. Graphical explanation of the 3rd stage of the investigation is given in Fig. 40.

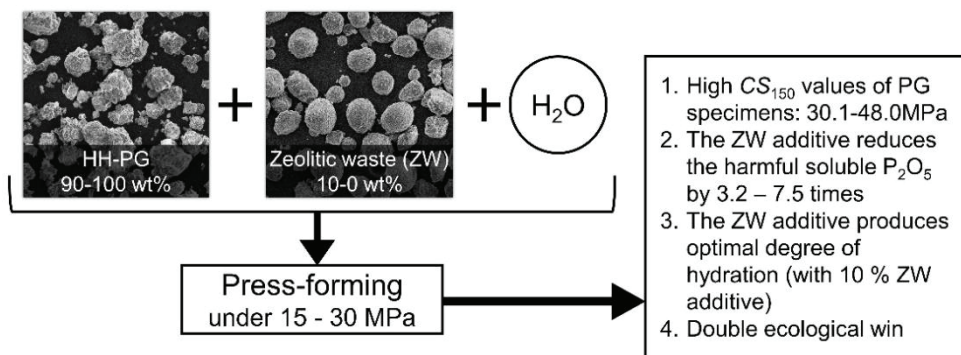


Fig. 40. Graphical explanation of the 3rd stage of investigation

3.3.1. Experimental procedures

The different dry mixtures were prepared by modifying the ZW content in HH-PG: 0.0 (control), 1.0, 2.5, 5.0, 7.5 and 10.0 wt%. Subsequently, water was included to produce the paste at a proportion of $w/s = 0.16$. Immediately after blending, the paste was press-formed by employing the smallest press-form (see Fig. 4), so that green cylindrical specimens of 26.8x26.8 mm dimensions were manufactured. Different PFPs were applied during the press-forming process: 15, 20, 25 and 30 MPa.

The green specimens were cured for 7 days by the method ‘with immersion’, as used in the 2nd stage of the investigation (as explained in Section 3.2.1). Since the specimens are smaller than those of the 2nd stage, the specimens were immersed in water for a shorter period of 5 min. Once the curing period had been completed, the specimens underwent drying at 40 °C till constant mass was achieved. Then, the CS test was performed.

Additional investigations were performed. The adsorption of the phosphate soluble impurities by ZW was analysed by measuring the pH value and the soluble P₂O₅ content in the PG specimens. The microstructure of the specimens was investigated through SEM microscopy, whereas the crystal phase (which indicates the quality of hydration) was determined by XRD spectroscopy. A simplified description of the experimental processes of the 3rd stage of the investigation is given in Fig. 41.

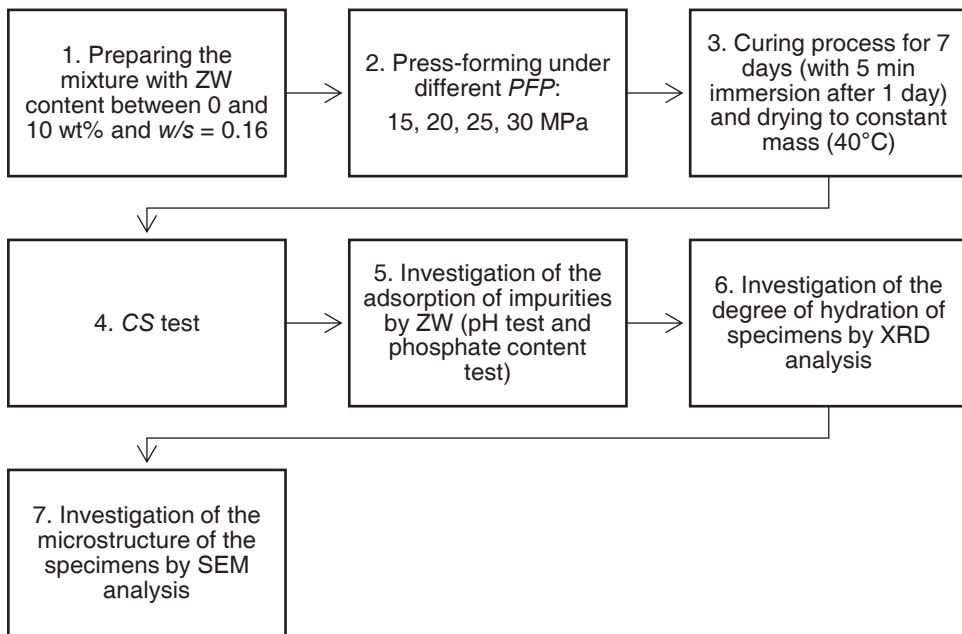


Fig. 41. Flowchart of the experimental processes of the 3rd stage of study

3.3.2. Experimental results

As mentioned above, the main goal of the 3rd stage is to investigate the effectivity of the adsorption of soluble acidic impurities and to study the influence of ZW on other properties of the press-formed PG specimens, such as the hydration degree, the ρ the CS values. Hence, the corresponding results are further presented and discussed.

Effectivity of adsorption of acidic-soluble impurities by ZW

The chemical composition of the III-type PG (see Table 2 and Table 3) reveals the presence of a certain content of soluble P_2O_5 , whereas F^- was not depicted. Therefore, the main compounds which cause the acidity in this type of PG are the soluble phosphate ones. In order to reduce the presence of these harmful compounds in PG, different amounts of ZW sorbent were included in the specimens. The results of pH and the soluble P_2O_5 content are given in Fig. 42.

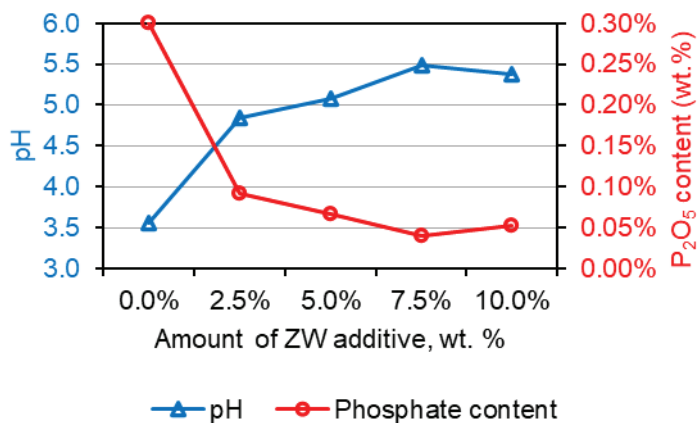


Fig. 42. Results of pH (left vertical axis) and soluble P_2O_5 content (right vertical axis) in PG specimens with different amounts of ZW additive

Before describing the pH results of Fig. 42, it must be pointed out that both initial materials are acidic: the pH values of the III-type PG and of ZW are 3.63 and 4.35, correspondingly (see Table 6). Therefore, the pH value of the PG specimens (including both materials) is likely to remain acidic. In Fig. 42, it can be observed that the pH values of the specimens gradually increase from 3.56 to 5.49 when the ZW content is enhanced from 0 to 7.5 wt%. With a higher than 7.5 wt% ZW content, the pH value does not change any more. The results of the soluble phosphate content closely correspond with the pH tendencies: with ZW content is in between 0 and 7.5 wt%, the soluble P_2O_5 content gradually decreases from 0.30 wt% to 0.04 wt%, and then it stabilises. Hence, the addition of ZW was proven to be an efficacious way to adsorb the harmful soluble P_2O_5 , thereby reducing its content in the PG by 3–7.5 times. It must be noted that the specimens produced with the ZW additive resulted in being less acidic than both initial materials.

Impact of ZW additive content on the degree of hydration of PG crystals

The crystal phase of the gypsum crystal of the specimens gives valuable information about their adequacy to be used in structural building products. If the specimens are well hydrated, it means that they are composed mainly of DH crystals ($CaSO_4 \cdot H_2O$), and that their crystal lattice is stronger and more compact. Besides, the problems of undesirable volume expansion due to additional hydration during

the exploitation period of the PG products would be avoided. For these reasons, the presence of HH or anhydrite crystals, which are a sign of insufficient hydration, is not desirable in hardened specimens. Therefore, the influence of ZW in the hydration quality of the specimens is further analysed.

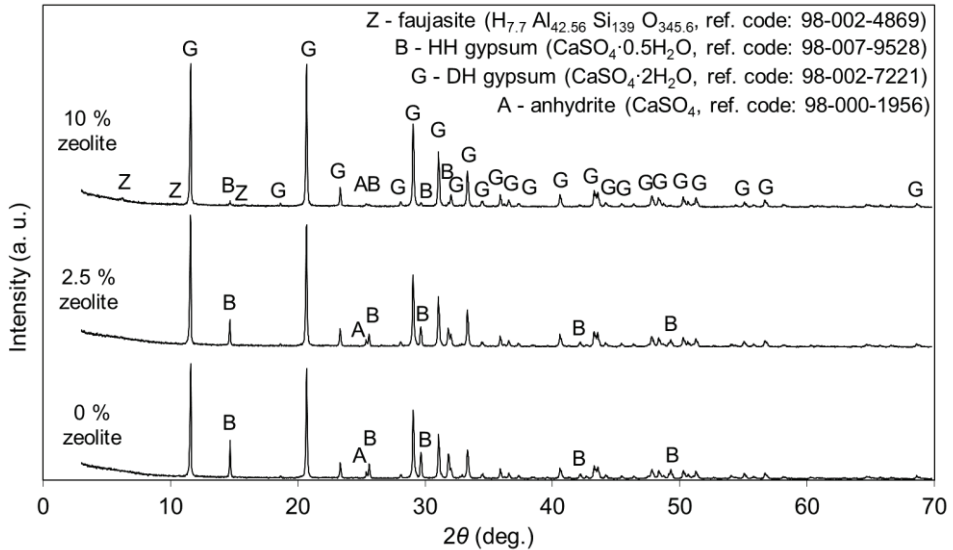


Fig. 43. XRD crystal composition of the specimens produced with different amounts of ZW additive

The crystal phases of the representative specimens including different amounts of the ZW additive were investigated by XRD analysis (see Fig. 43). The results reveal that, with higher contents of ZW (based on faujasite minerals), the HH and anhydrite peaks gradually decrease. In fact, these peaks almost disappear when the ZW content reaches 10 wt%. Thus, the ZW additive clearly improves the hydration of PG specimens.

Table 10. Quantitative crystal composition of PG specimens (by XRD Rietveld refinement)

Compound	Composition of PG specimens prepared with different amounts of ZW		
	0% ZW	2.5% ZW	10% ZW
DH gypsum	78.1%	83.6%	95.0%
HH gypsum	19.6%	14.2%	2.8%
Anhydrite	2.3%	2.2%	1.4%
Other compounds	-	-	0.8%

The quantitative analysis of the crystal phases was performed by the Rietveld refinement of the XRD patterns of Fig. 43, and the results are given in Table 10. The results demonstrate that the addition of the ZW additive strongly improves the hydration of the PG specimens. This improvement seems to be related to the porosity of ZW. During the blending of the mixtures and the immersion process, the ZW

particles absorb some water. Then, during the curing of the specimens, the gypsum crystals hydrate till the free water content has been employed. When the water has been fully consumed, no further hydration takes place. However, at this moment, ZW ‘gives back’ the absorbed water to the gypsum crystals, so that they could continue hydrating. In this way, ZW improves the hydration of the PG specimens. This mechanism of ‘giving back’ the water content was applied in other studies for other purposes such as, e.g., to maintain the microclimate in indoor spaces [153]. Nevertheless, the usage of this mechanism of zeolite to improve the hydration of gypsum crystals is novel. Moreover, the improvement of the hydration process by ZW may also be related to some extent to the adsorption of P_2O_5 impurities which hinder the crystallisation of the gypsum crystals.

Influence of the content of ZW additive and of PFP on the physical and mechanical properties of PG specimens

The ZW content makes a remarkable influence on the neutralisation of the acidic impurities and the hydration degree of the gypsum crystal matrix. Therefore, the ρ and CS values of the specimens are also affected.

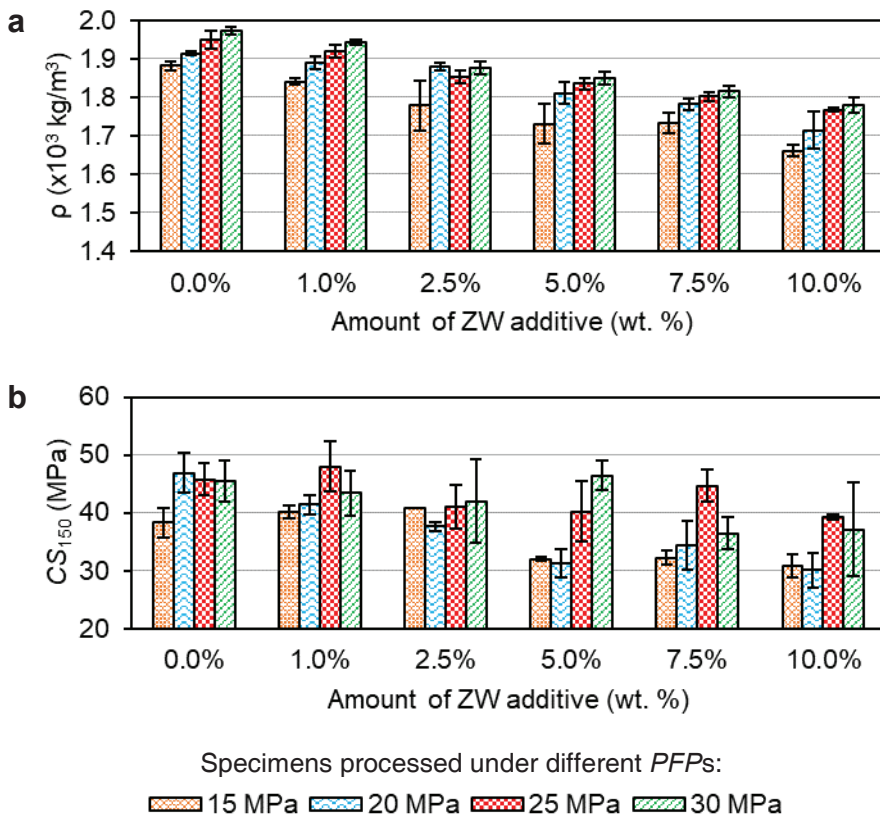


Fig. 44. Dependence of ρ (a) and CS_{150} (b) of the specimens on ZW content and PFP

Fig. 44 presents the influence of both the ZW content and *PPF* on the ρ (see Fig. 44a) and CS_{150} (see Fig. 44b) values of the press-formed PG specimens. It must be taken into consideration that the CS_{150} values given in Fig. 44 correspond to the *CS* test performed with cylindrical 26.8x26.8 mm specimens which are not of the standard size. Therefore, the CS_{150} values (as given in Fig. 44) were calculated by multiplying the measured values by $ScF = 0.80$ (see Table 8). The influences of the ZW content and *PPF* on ρ are clear and predictable: with a higher content of the ZW additive, which is a lighter material than PG (see their specific gravity values in Table 6), the ρ values of the specimens gradually decrease, while, with higher *PPF* pressures, ρ correspondingly increases. Meanwhile, the CS_{150} tendencies (see Fig. 44b) are more confusing. In general, the CS_{150} values of the specimens are closely related to the ρ tendencies: CS_{150} increases with a lower ZW content and with higher *PPFs*, ultimately reaching a maximum value of $CS_{150} = 48$ MPa. Despite these clear tendencies, it is observed that at, a higher ZW content, which differs depending on *PPF*, the CS_{150} values stop decreasing and even experience a peak. That peak happens at ZW contents of 5% (for the specimens processed under *PPF* = 30 MPa) and 7.5% (for the specimens with *PPFs* of 15, 20 and 25 MPa). This peak is very notorious for the specimens produced with *PPFs* of 25 and 30 MPa, with which, CS_{150} reaches values of 45 MPa and 46 MPa, respectively, while, for the rest, it is less noticeable. The explanation of this behaviour may be related to the fact that, as observed in Fig. 38, CS_{150} not only depends on ρ , but also on the hydration degree which is better in the specimens with a higher ZW content.

When considering comprehensively all the investigated properties, the recommended specimens are those manufactured with 7.5 wt% ZW additive and with *PPF* = 25 MPa, since they exhibit a high degree of hydration, satisfactory mechanical properties of $CS_{150} = 45$ MPa and a reduction of the soluble P_2O_5 content by 7.5 times.

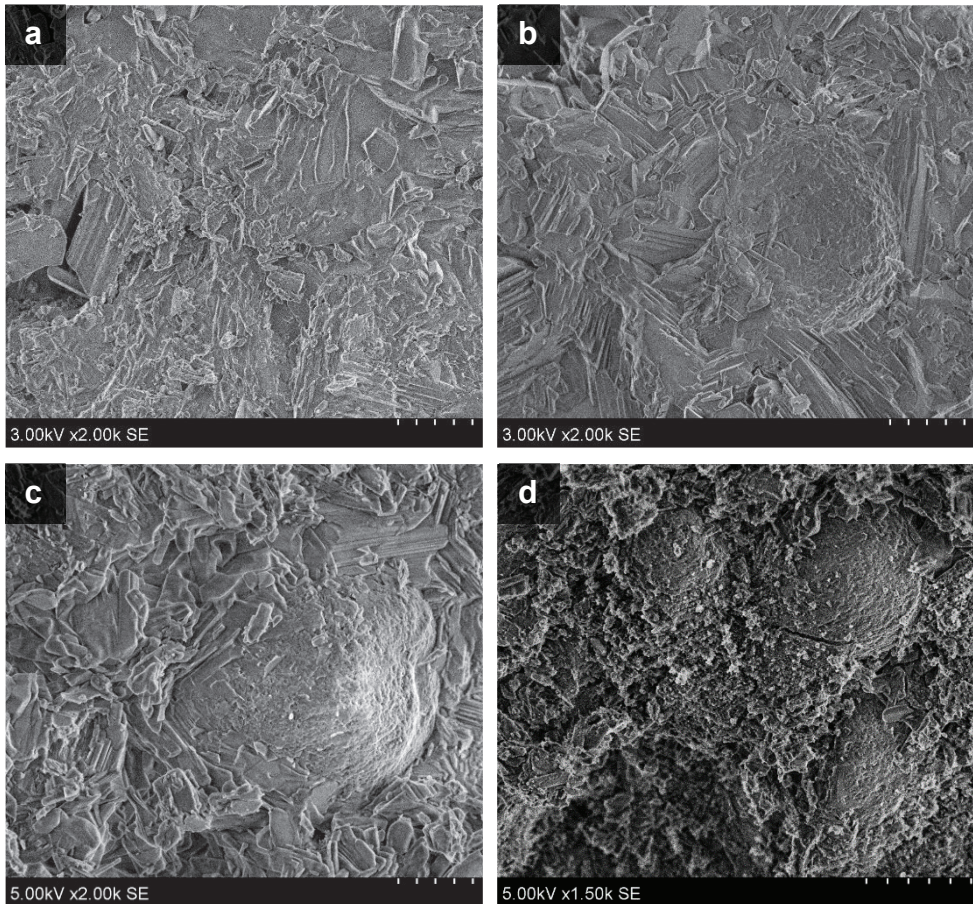


Fig. 45. SEM microscopic images of specimens with different amounts of ZW additive: 0 wt% (**a**), 2.5 wt% (**b**) and 10 wt% (**c** and **d**); scale x2000 (the scale of image **d** is x1500)

The microstructures of some of the investigated specimens are given in Fig. 45. The image of Fig. 45a corresponds to a specimen without the ZW additive and presents the densest and most compact DH crystal matrix, so that a high CS value is expected. The specimen presented in Fig. 45b contains a relatively small amount of ZW (2.5 wt%), and the observed ZW particle seems to be well-bound with the surrounding DH gypsum crystals. Hence, this specimen is expected to be strong. Finally, Fig. 45c and d present, at different scales, views of the microstructure of specimens with a higher ZW content (10 wt%). In this case, the ZW particles are close to each other, and the bond with the surrounding DH crystals seems to be weaker than in the previous case. These observations coincide with the CS_{150} results given in Fig. 44.

3.3.3. Partial conclusions

During the 3rd stage of the experiment, the ZW additive proved to be a suitable ‘teammate’ for HH-PG to create non-hazardous, well-hydrated and strong PG specimens. The conclusions of the investigation are further summarised.

1. **Adsorption of soluble phosphate impurities.** The ZW additive effectively reduced the amount of acidic soluble P_2O_5 compounds in the PG specimens. The addition of 2.5–7.5 wt% gradually reduced the presence of these impurities by 3–7.5 times, and, with further addition of ZW, the soluble P_2O_5 content remained stable.
2. **Improvement of the hydration of the specimens.** The XRD patterns revealed that the addition of ZW proportionally improved the hydration degree of the specimens. The maximum hydration degree was achieved when 10 wt% of ZW was added, with which, the specimens reached a DH crystal content of 95.0 wt%. The improvement of hydration is attributed to the ZW mechanism of ‘giving back’ the absorbed water content to the gypsum crystals and to the neutralisation of acidic-soluble compounds.
3. **Influence on the mechanical properties.** Since ZW is lighter than PG, the ρ value of the specimens was observed to be inversely proportional to the ZW content, and directly proportional to *PFPP*. In the 2nd stage of the investigation (see Section 3.2.3, conclusion No. 3), it was observed that the CS_{150} of the specimens mostly depended on ρ . In the 3rd stage, the CS_{150} tendencies also follow the ρ behaviour. However, at a certain ZW content (5 wt% or 7.5 wt%, depending on *PFPP*), a peak of CS_{150} values is observed. This is explained by the fact that the degree of hydration, and not only the ρ value, influences the CS of the specimens. Being so, the maximum CS_{150} of 48 MPa was exhibited by the specimens produced with a ZW content of 1.0 wt% and *PFPP* = 25 MPa. However, the degree of hydration of these specimens was poor.
4. **Recommended composition.** Considering jointly the reduction of the soluble P_2O_5 content, the hydration degree and CS_{150} , the specimens manufactured with the addition of 7.5 wt% of ZW and *PFPP* = 25 MPa are the best performing ones since they exhibit a satisfactory degree of hydration, a high mechanical strength of CS_{150} = 45 MPa, and a reduction of the soluble P_2O_5 content by 7.5 times (in comparison to the control specimens).
5. **Ecological aspect.** It must be noted that the ‘partnership’ among the waste ZW and FG is desirable not only because of the satisfactory physical and mechanical properties of the specimens, but also due to the fact that their entire composition is constituted of industrial waste products.

3.4. Improvement of water-resistance of PG specimens by adding waste metallurgical sludge (MS)

The main limitation of the gypsum-based binding materials stems from their low resistance to the effect of moisture. If a gypsum-based product gets in contact with water, it dissolves and loses to an important extent its mechanical strength. Since the purpose of the current research is to utilise PG as the binding material to produce PG load-bearing building products, the humidity-induced ‘softening’ is highly undesirable. The possibility to improve the water resistance of PG would allow its utilisation in outdoor conditions, thereby increasing its applicability. The different strategies employed to improve the water resistance of the gypsum-based products were described in Section 1.5.4, and there are mainly three of them: the addition of polymers and organic additives, the activation of pozzolanic additives, and the addition of metallic dust. The final strategy is the one adopted at the current stage of the research, where waste metallurgical sludge (MS), produced in the ship-repairing industry, is employed as a modifier of PG. This sludge is produced when the metallic parts of ships are cut by CNC plasma. A more extensive description of MS is given in Section 2.2.3. Hence, the novelty of the current research is the source of MS and the fact that it is utilised as a modifier of PG (and not of gypsum). In fact, in the 4th stage of the investigation, it was proven that MS and PG cooperate in a synergic way, since MS not only improves the water-resistance of the PG specimens, but also neutralises their acidic soluble P_2O_5 content.

A similar material of the same ship-repairing yard was employed by Grinys *et al.* [154] in concrete as a substitute of the fine aggregate. The metallurgical material enhanced the formation of C-S-H compounds, so that the concrete specimens exhibited higher ρ and CS values. Besides, there is abundant research on the usage of other types of waste sludge in the building materials, especially the sludge coming from drinking water treatment plants [155, 156]. However, in the ongoing investigation, MS comes from a different source, and its influence on the properties of PG is investigated. Besides, in order to evaluate the efficiency of this MS additive, some additional specimens with pozzolan additives were produced, which is the commonly employed solution to increase the water-resistance of gypsum (see Section 1.5.4). In this way, a comparison among the methods (either with MS or with pozzolans) could be established. The summarised graphical explanation of this investigation stage is given in Fig. 46.

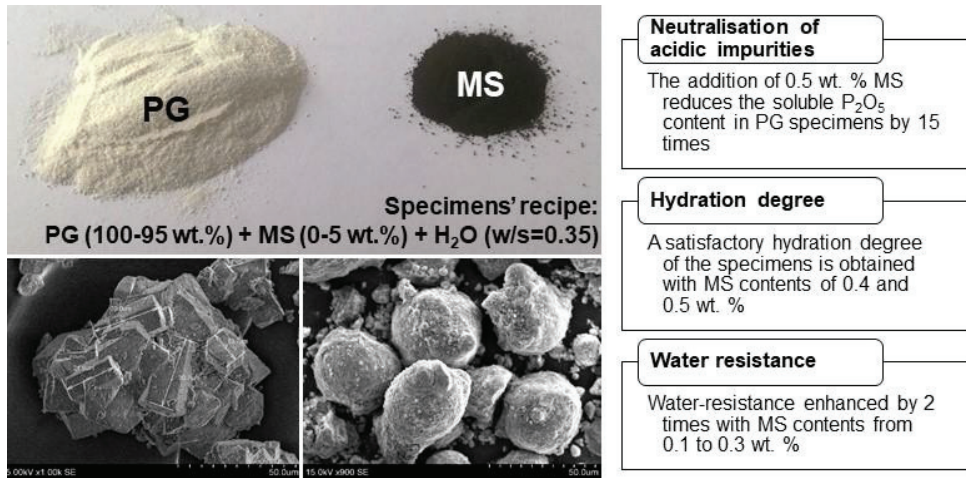


Fig. 46. Graphical explanation of the 4th stage of investigation

3.4.1. Experimental procedures

The HH-PG employed for this stage of the investigation is that of type III, since it is the best performing and less hazardous type of PG from all points of view. First, the different pastes were produced. HH-PG was mixed with different amounts of MS: 0.0 (control), 0.1, 0.2, 0.3, 0.4 and 0.5 wt%. Then, dry mixtures were blended with water ($w/s = 0.35$), and the different pastes were poured into different silicone moulds. Hence, 9 units of 20 mm-sided cubic specimens were casted with each paste. The specimens were cured for 14 days at room temperature and 100% humidity conditions so that to ensure optimum hydration. Besides, for comparison purposes, a group of specimens was produced with the pozzolanic recipe: 75% HH, 20% PC and 5% FA. These pozzolanic specimens were cured under the same conditions as the other specimens, but for 28 days (which is the time required to cure the PC). Once the curing period had expired, the specimens were dried at 40 °C temperature, till the constant mass value was achieved.

At this point, the *CS* test was performed with 3 dry specimens of each different mixture. The rest of the specimens were immersed in water. After 30 days of immersion, again, 3 specimens of each group were taken from water, and they underwent the *CS* test. Finally, the *CS* test was applied to the 3 remaining specimens of each group after 90 days of immersion.

Eventually, the microstructure of some representative specimens was analysed. Besides, the crystal phase of the specimens was investigated by conducting *LOI* and XRD analyses. Finally, the neutralisation of acidic-soluble phosphates was studied by measuring the pH value and the soluble P_2O_5 content. A graphical view of the sequence of the experimental procedures is given in Fig. 47.

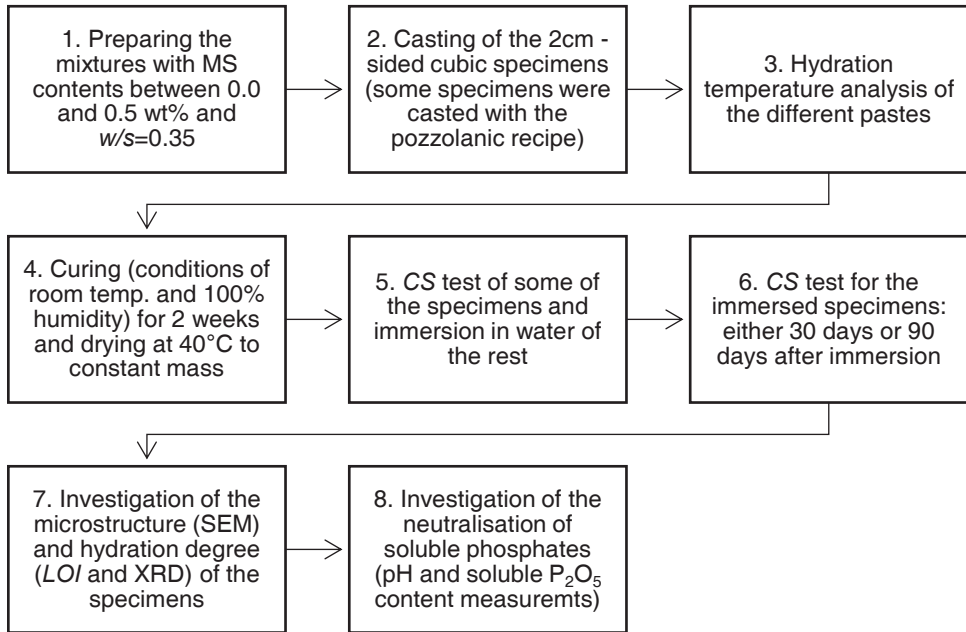


Fig. 47. Flowchart of the experimental processes of the 4th stage of study

3.4.2. Experimental results

MS is aimed to reduce the softening of the PG specimens in case of contact with moisture. Besides, the interesting side-effects that this modifier makes on the other properties of the PG specimens (neutralisation of acidic soluble impurities, hydration degree, ρ and CS_{150}) are addressed.

Effectivity of MS in neutralising acidic-soluble impurities

Since the main employed material during this stage is the III-type HH-PG, the only acidic-soluble impurity in its composition is P_2O_5 (according to Table 3, fluorine is not present). The iron oxide of MS composition (see Fig. 16) is expected to react with the soluble phosphate compounds, thereby producing scarcely soluble iron phosphate compounds. Some examples of these processes are given in Eqs. (8) and (9), as described by Vaičiukynienė *et al.* [7] and Sviklas *et al.* [157], respectively.



Therefore, the efficiency of neutralisation is further studied by performing the pH measurements and by analysing the soluble phosphate content. The corresponding results are given in Fig. 48.

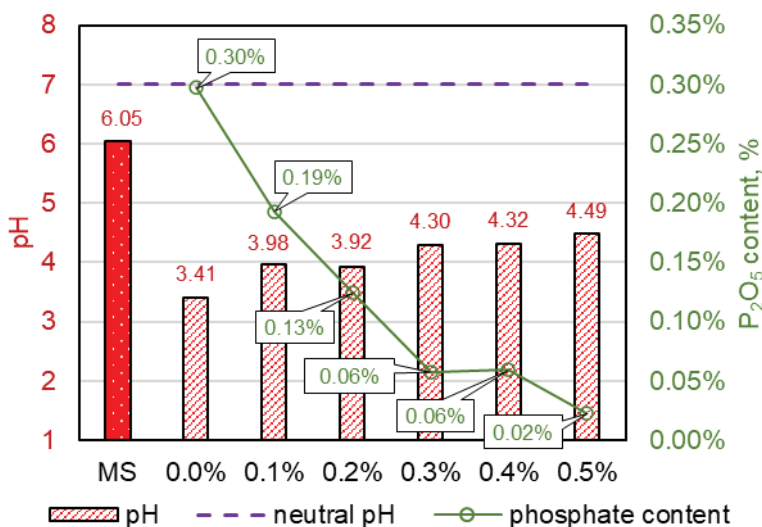


Fig. 48. Investigation of neutralisation of soluble P₂O₅ content in PG specimens by different amounts of MS additive (see pH values in the left vertical axis, and soluble P₂O₅ content in the right vertical axis)

The results of Fig. 48 reveal that the neutralisation of soluble phosphate compounds by MS is highly effective. Pure MS is a slightly acidic material (almost neutral), and its addition in small amounts to the strongly acidic HH-PG gradually increases the pH of the specimens from 3.41 to 4.49. Hence, the specimens' pH remains acidic. However, the changes regarding the soluble P₂O₅ content are more abrupt. There is a clear inversely proportional tendency between the included MS amount and the soluble P₂O₅ content: when the MS amount is enhanced from 0 to 0.5 wt%, the P₂O₅ content decreases from 0.3 wt% to 0.02 wt%, i.e., it was reduced by 15 times.

Table 11. Comparative impact of different additives on soluble P₂O₅ content of PG specimens

Additive	Additive amount (wt%)	Soluble P ₂ O ₅ reduction (times)	Ratio P ₂ O ₅ reduction / additive amount (times / wt%)	Reference
Ca(OH) ₂	1.5	40	26.6	Fig. 33
ZW	7.5	7.5	1.0	Fig. 42
MS	0.5	15	30.0	Fig. 48

The most striking aspect of these tendencies is the high impact of such a relatively small amount of MS on the soluble acidic phosphate content in the specimens. The comparative effect of the different additives during the whole investigation on the soluble P₂O₅ content is summarised in Table 11. It should be noted that the effect of MS (expressed as the ratio between the reduction of soluble phosphates and the included amount of the additive) is much higher than that of the

ZW additive and even slightly higher than that of $\text{Ca}(\text{OH})_2$. The effective neutralisation of the acidic impurities by MS also influences other properties of the PG specimens, such as the hydration process and the physical-mechanical properties of the specimens, which are considered in the following subsections.

Influence of MS modifier on the hydration of PG specimens

The hydration degree is an important property, on which, the suitability of the PG specimens to be employed in building products depends. The investigated hydration tendencies of the different PG specimens are presented in Fig. 49. The results of the hydration temperature analysis performed in the early hours after blending the pastes are presented in Fig. 49a. Meanwhile, the *LOI* values of the specimens cured for 2 weeks are given in Fig. 49b.

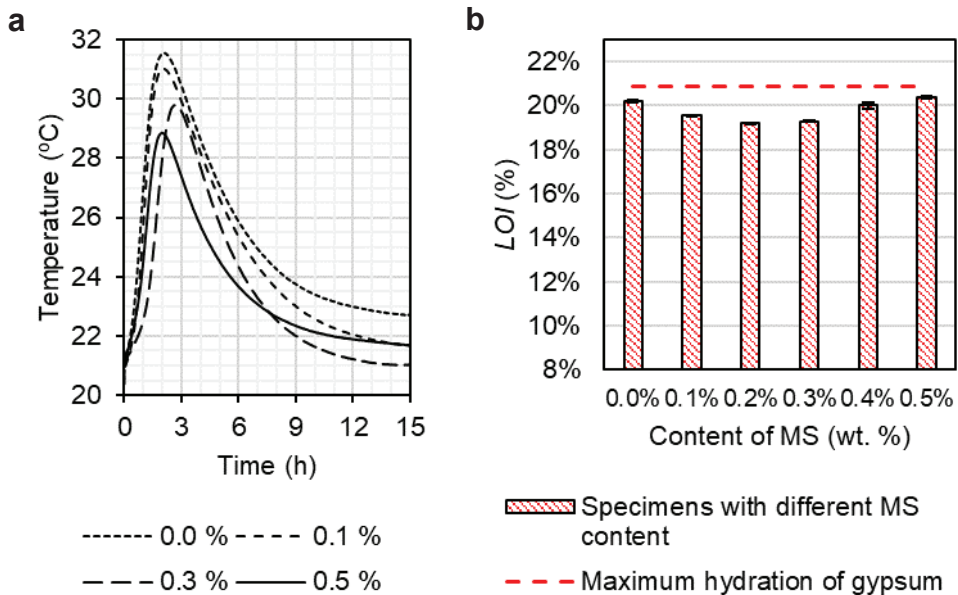


Fig. 49. Investigation of the hydration temperature of pastes with different amounts of MS (a) and *LOI* of specimens after curing (b)

The results of Fig. 49a reveal that MS hinders the early hydration process of the pastes, since the temperature peaks get lower when the included amount of MS is higher. This tendency is understandable since MS does not hydrate, and its presence requires a correspondingly lower amount of HH-PG, which is the binding material. Even so, MS does not act as a retarder for HH-PG hydration, and all the hydration peaks occur approximately at the same time, about 2–3 h after blending.

Fig. 49b presents the situation of the specimens once their hydration process has been completed. Although, for all the specimens, the *LOI* values are relatively satisfactory (>19%), the results reveal a slight decrease of the hydration rate when MS is included in amounts of 0.1–0.3 wt%, when the *LOI* values decrease to 19.20%, with respect to the control specimens (without MS) which exhibit *LOI* = 20.18%. However, when higher MS amounts are included (0.4 and 0.5 wt%), the *LOI* values

gradually increase and ultimately reach the excellent value of 20.37%, even becoming higher than that of the control specimens and approaching the maximum theoretical *LOI* value of DH gypsum (20.85 wt%). Hence, with higher amounts of MS, an excellent degree of hydration is achieved.

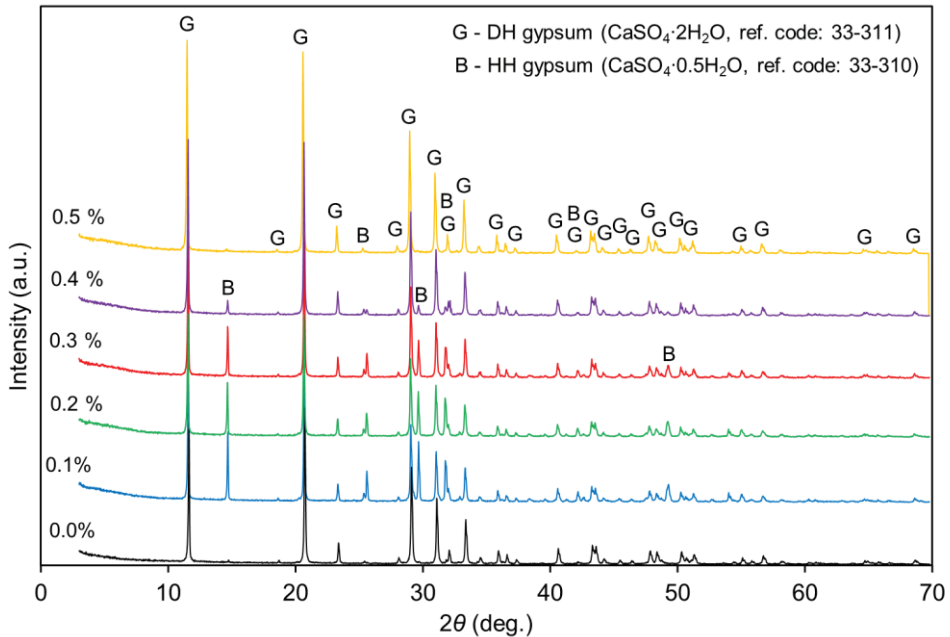


Fig. 50. XRD patterns of specimens produced with different contents of MS modifier

Moreover, a systematic study of the XRD patterns of PG specimens produced with different amounts of MS (see Fig. 50) confirms the tendencies observed from the *LOI* results (Fig. 49b). The control specimens exhibit a pattern with almost exclusively DH peaks. With MS contents of 0.1–0.3 wt%, the HH peaks become noticeable, thereby indicating poorer hydration. With higher MS contents (0.4 and 0.5 wt%), the HH peaks gradually disappear, thus indicating the excellent hydration degree of these specimens. However, the observed long-term hydration tendencies revealed in Fig. 49b and Fig. 50 (which perfectly match each other) do not coincide with the tendencies of the early hydration stages observed in Fig. 49a, where the higher MS content proportionally hindered the hydration process of HH-PG. This fact means that the first stages of hydration do not determine completely the final hydration degree of the specimens, and that a longer curing process (taking 2 weeks) can ‘fix’ the initial hydration shortage.

The high hydration degree exhibited by the specimens with 0.4 and 0.5 wt% of MS may be related to the neutralisation of soluble acidic phosphate impurities, as previously analysed (see Fig. 48). These impurities hinder the hydration process of HH-PG crystals. Therefore, their effective neutralisation by such amounts of MS seems to be the cause of the improved *LOI* values of the corresponding specimens.

Improvement of water-resistance of the specimens by MS additive

The described tendencies regarding the neutralisation of soluble phosphate impurities and the hydration behaviour may also influence the mechanical properties and the water-resistance of PG specimens which are further considered.

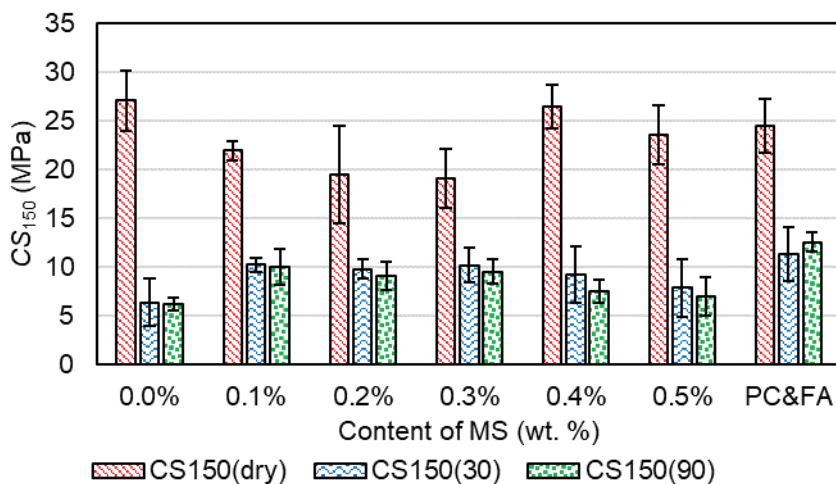


Fig. 51. CS_{150} values of dry specimens ($CS_{150(dry)}$) and of specimens after immersion of either 30 days ($CS_{150(30)}$) or 90 days ($CS_{150(90)}$), manufactured either with different MS amounts (columns marked with percentages) or with the pozzolanic recipe: 75% PG, 20% PC and 5% FA (columns marked with ‘PC&FA’)

The CS_{150} values of the dry specimens ($CS_{150(dry)}$) and of the specimens immersed for both 30 and 90 days ($CS_{150(30)}$ and $CS_{150(90)}$, respectively) are given in the column diagram of Fig. 51. Since the tested specimens are 2 cm-sided cubes, the standard CS_{150} values given in Fig. 51 are calculated by applying $ScF = 0.56$ (see Table 8) to the depicted CS values. The values of $CS_{150(dry)}$ follow the tendencies of the soluble phosphate content and LOI observed in Fig. 48 and Fig. 49b, respectively. The $CS_{150(dry)}$ value of the control specimens is 27.0 MPa, but the addition of 0.1–0.3 wt% of MS considerably reduces these values, thus reaching a minimum of 19.1 MPa. With the addition of 0.4 and 0.5 wt% of MS, the $CS_{150(dry)}$ values increase again, finally reaching (with 0.4 wt% MS) the value of 26.4 MPa.

When immersion is applied, a sharp decrease of the CS_{150} values is observed. The $CS_{150(30)}$ and $CS_{150(90)}$ values are far lower than the $CS_{150(dry)}$ ones. Besides, systematic analysis of $CS_{150(30)}$ and $CS_{150(90)}$ values shows that the immersed specimens follow the opposite strength tendencies than those of the dry specimens. The lowest values are those of the control specimens yielding $CS_{150(30)} = 6.4$ MPa. With small amounts of MS (from 0.1 to 0.3 wt%), the $CS_{150(30)}$ values increase to reach, approximately, 10.1 MPa. A further increase of MS (0.4 and 0.5 wt%) produces a gradual decrease of $CS_{150(30)}$. The values of $CS_{150(90)}$ are like those of $CS_{150(30)}$, but slightly smaller (by average, $CS_{150(90)} = 0.92 \cdot CS_{150(30)}$).

What regards the PC&FA specimens (produced with the ‘pozzolanic recipe’), they exhibit $CS_{150(dry)} = 24.5$ MPa, i.e., a slightly inferior value to the maximum

$CS_{150(dry)}$ obtained from the specimens with MS, but, at the same time, they present slightly superior $CS_{150(30)}$ and $CS_{150(90)}$ values (11.6 and 12.6 MPa, respectively) in comparison to those of the specimens with the MS modifier. Besides, in this case, the $CS_{150(90)}$ value of the specimens is higher than the $CS_{150(30)}$ value in contrast to the observed tendencies of the specimens with MS. This behaviour is explained by the pozzolanic activation process which takes place during immersion. In contact with water, PC activates FA, which acquires binding properties. In this way, the FA alkali-activation increases the CS values during the immersion period and explains the fact that $CS_{150(30)} < CS_{150(90)}$.

The water-resistance behaviour of the specimens can be described by the softening factor (SF) which is determined by the ratio between the CS values of the immersed and the dry specimens, as given in Eq. (10).

$$SF_{30 \text{ or } 90} = \frac{CS_{150(30 \text{ or } 90)}}{CS_{150(dry)}} \quad (10)$$

The different tendencies for SF values are presented in Fig. 52. When no MS is included (for control specimens), the water resistance is rather poor ($SF_{30} = 0.24$). However, with 0.1–0.3 wt% MS, the SF values are enhanced by 2 times, thus even reaching $SF_{30} = 0.53$ with 0.3 wt% MS content. This is a higher value than that of the PC&FA specimens. Besides, a further increase of MS produces a gradual decrease of SF . Again, the SF_{90} of the specimens with MS is always slightly smaller than the SF_{30} values, whereas, in the case of the PC&FA specimens, the opposite happens due to FA alkali-activation.

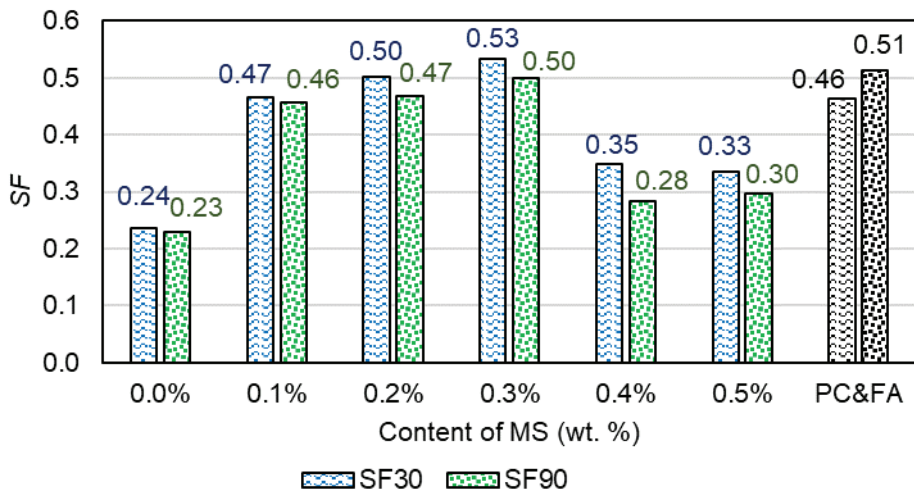


Fig. 52. SF values of the specimens after immersion of either 30 days (SF_{30}) or 90 days (SF_{90}), manufactured either with different MS amounts (columns marked with percentages) or with the pozzolanic recipe: 75% PG, 20% PC and 5% FA (columns marked with 'PC&FA')

As mentioned above, the observed water-resistance tendencies of the different specimens with the MS additive are essentially the opposite to the observed

tendencies of the soluble P_2O_5 content, LOI and $CS_{150(dry)}$. Hence, some inevitable questions arise: Which is the reason of this tendency? What is the decisive factor determining the water-resistance of the specimens? In other words, what is the mechanism of the water-resistance improving process?

In the study of Pervyshin *et al.* [121] the authors explained the improvement of the water-resistance of gypsum specimens when a metallurgical dust modifier was included. This modifier encouraged the formation of an amorphous phase of C-S-H which acted as a coating of the $CaSO_4 \cdot 2H_2O$ crystals and protected them from dissolving in water. A more extensive description of the investigation is given in Section 1.5.4. In order to check whether this mechanism also occurs in the current investigation, analysis of the microstructure of some representative dry and immersed specimens was conducted, and the corresponding SEM images are given in Fig. 53.

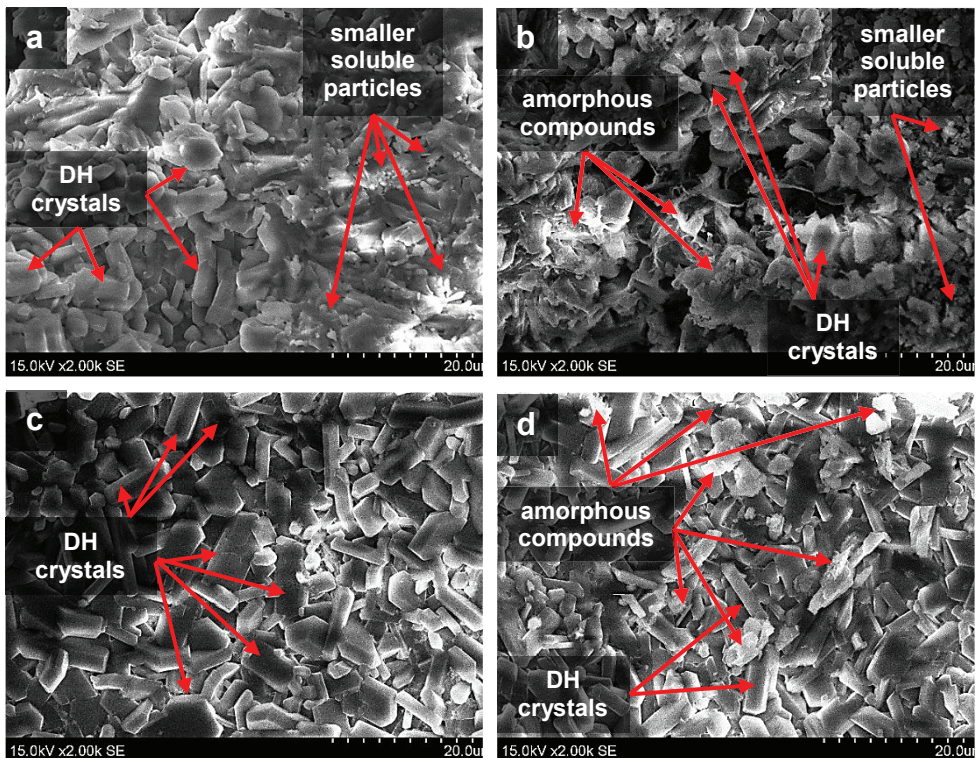


Fig. 53. Microscopic images of representative specimens: dry specimens with 0.0 wt% (a) and 0.4 wt% (b) of MS, and similar specimens after immersion of 90 days (c and d, for the respective amounts of MS)

The microstructures of the dry specimens without MS and with 0.4 wt% MS are given in Fig. 53a and b, respectively. In these images, DH crystals can be clearly depicted, together with numerous smaller particles. In Fig. 53b, some amorphous compounds can also be noticed. Meanwhile, the microstructures of the corresponding specimens after 90 days of immersion are given in Fig. 53c and d. In the case of the specimen without MS (see Fig. 53c), it can be seen that the smaller

compounds disappeared (probably dissolved in water), and only DH crystals remained. On the other hand, in the specimen with MS (see Fig. 53d), amorphous compounds are still observed. Hence, the formation of this C-S-H amorphous phase, as depicted by Pervyshin *et al.* [121] seems to be also the cause of the improvement of the water-resistance behaviour of the specimens which we observe in our research.

Table 12. Summary table of the results of the investigation on the influence of MS additive on the properties of PG specimens: soluble phosphate content, *LOI*, *CS*₁₅₀ and *SF*

Parameter	MS content in the optimal specimen	Value of the optimal specimen, n_{opt}	Value of the control specimen, n_0	n_{opt} / n_0
Soluble P ₂ O ₅ content	0.5 wt%	0.02%	0.30%	0.07
<i>LOI</i>	0.5 wt%	20.37%	20.18%	1.01
<i>CS</i> _{150(dry)}	0.4 wt%	26.4 MPa	27.0 MPa	0.98
<i>SF</i> ₃₀	0.3 wt%	0.53	0.24	2.20
<i>SF</i> ₉₀	0.3 wt%	0.50	0.23	2.17

The results of the 4th stage of the study are summarised in Table 12, in which, the optimum properties of the specimens (n_{opt}) with MS are compared with those of the control specimens (n_0) (without additive). In this way, the effect of MS on the soluble-acidic impurity neutralisation, the hydration degree, the mechanical strength and the water resistance of PG specimens can be perceived more clearly.

3.4.3. Partial conclusions

The addition of the waste MS modifier is not only a highly efficacious way to improve the water-resistance of PG specimens, but also to reduce their soluble P₂O₅ impurity content, to improve their degree of hydration and their mechanical strength, while also delivering a fully ecological solution.

1. **Neutralisation of soluble-acidic P₂O₅ and degree of hydration.** The addition of relatively small amounts of MS to PG specimens remarkably reduced the soluble P₂O₅ content: with 0.5 wt% MS, it decreased by 15 times. This is a higher impact than that of Ca(OH)₂ and of ZW as determined in the previous stages of the investigation. Besides, the neutralisation of these impurities produced an improvement of the *LOI* value of the specimens, especially with 0.4 and 0.5 wt% MS.
2. **Improvement of the water-resistance of specimens.** The addition of 0.1–0.3 wt% of MS improved the *SF* of the specimens by 2 times with respect to the control specimens. A further addition of MS (0.4 or 0.5 wt%) produced a decrease of *SF*.
3. **Simplicity and ecological aspect.** The *SF* values of the specimens produced with MS are comparable (and even slightly higher) to that of the PC&FA specimens (with pozzolanic activation), which is the usual way to enhance the water-resistance of gypsum. Besides, the required amount of MS is much smaller than

the additive amount in the PC&FA specimens, thereby indicating that the MS solution is simpler and requires less resources. Finally, it must be pointed out that the proposed solution is fully ecological, since only industrial by-products (PG and MS) constitute the manufactured specimens.

3.5. Improvement of the thermal and acoustic insulation of load bearing PG specimens by including waste wood fibre additive (WF)

So far, during the previous stages of our investigation, the protectivity of the material (radioactivity and neutralisation of soluble-acidic compounds), the processing methods (casting and press-forming), and the properties of the specimens (such as the microstructure, the degree of hydration, the *CS* value and water resistance) have been evaluated with the goal of determining the aptness of the PG binding material to be employed in load-bearing building materials. However, if PG products are intended to be employed as bricks or blocks for load-bearing walls, there are other properties which are also of great importance, especially the thermal and acoustic insulation, as described in Section 1.5.5. Being so, the goal of the current stage is to improve the thermal and acoustic insulation properties of the load-bearing PG specimens.

In order to increase the insulating properties of the specimens, a wood fibre obtained as a waste product from used particle walls (WF) was included. Moreover, for comparison purposes, some specimens were produced with a different fibre obtained from natural wood (NF). The detailed description and properties of both WF and NF are provided in Section 2.2.4. Aside from the effect of the fibre on the thermal and acoustic properties of the specimens, its influence on the hydration degree and the mechanical strength was evaluated.

Besides, certain amounts of the ZW additive were included in the specimens, since the soluble-acidic impurity content had to be reduced, in line with the task which ZW is able to perform efficiently, as concluded during the 3rd stage of the study (see Section 3.3). Being so, the joint effect of ZW and the wood fibre is investigated.

The summarised graphical explanation of this stage of investigation is given in Fig. 54.

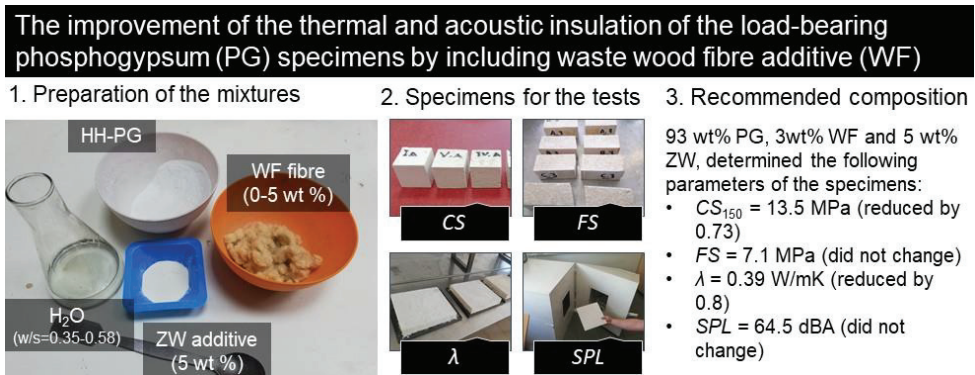


Fig. 54. Graphical explanation of the 5th stage of investigation

3.5.1. Experimental procedures

In a similar way to the previous stages of the investigation (3rd and 4th), the selected material for the experiments of the current 5th stage was the HH-PG of type

III whose properties are described in Section 2.2.1. Being so, four different types of pastes were prepared with different types and amounts of additives: either WF or NF fibre and with or without the ZW additive. The ingredients of the pastes of each group are described in Table 13.

Table 13. Composition of the different employed pastes, including different amounts of WF (or NF) and ZW additives

Group name	III-type HH-PG, wt%	Fibre, wt% (type of fibre)	ZW, wt%	w/s
Control 1	100	0	0	0.35
Control 2	95.0	0	5.0	0.35
Group 1	99.5–95.0	0.5–5.0 (WF)	0	0.37–0.58
Group 2	94.5–90.0	0.5–5.0 (WF)	5.0	0.37–0.58
Group 3	99.5–95.0	0.5–5.0 (NF)	0	0.37–0.67
Group 4	94.5–90.0	0.5–5.0 (NF)	5.0	0.37–0.67

As observed in Table 13, several mixtures were produced in each group by varying the fibre content: 0.5, 1, 2, 3, 4 and 5 wt%. Hence, each group contained 6 different mixtures. Besides, two control mixtures were manufactured without the fibre: the first one was made entirely of HH-PG, and the second group was with 5 wt% of ZW. In this way, 26 different pastes were created.

Once the dry mixtures had been created, they were blended with water. For each case, depending on the type and amount of the fibre, a ‘personalised’ w/s ratio was applied in order to produce a paste with normal consistency. The pastes with the NF additive required a higher w/s ratio than those with WF. The enhancement of the fibre content also required a corresponding increase of the w/s ratio.

After blending with water, the pastes were poured into silicone moulds for casting. In this way, 9 units of 20 mm-sided cubic specimens were produced with each paste. The preparation of the pastes and the casting process are illustrated in Fig. 55. Immediately after casting the pastes, they were cured for 7 days under conditions of 100% humidity at room temperature. Once the curing period had been completed, the specimens were dried to constant mass at 40 °C temperature. Eventually, the CS test was performed.

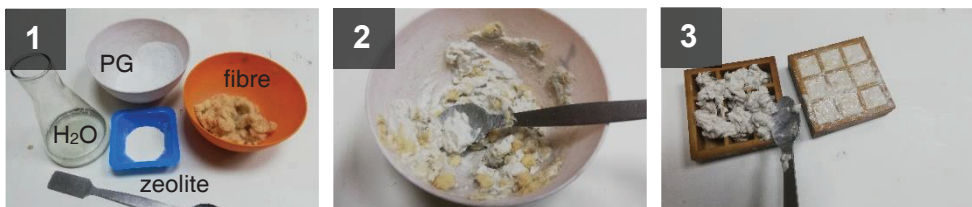


Fig. 55. Images of steps for the paste preparation: preparing separate components in the required amounts (1), blending (2) and casting (3)

Some additional specimens with standard prismatic geometries (40x40x160 mm) were produced for the FS standard test (see Section 2.1.6). Besides, other specimens were produced with panel geometries of 300x300x50 mm

and of 250x250x18 mm for the measurements of thermal and acoustic insulation properties (respectively) which were performed according to the methodologies explained in Section 2.1.5. These prismatic and panel specimens were manufactured with 4 different pastes: control paste 1 and several pastes of group 2 with different amounts of fibre: with 0.5, 3 and 5 wt% of WF. The curing and drying processes of these specimens were performed in the same way as the small cubic specimens. Fig. 56 presents some images of the different manufactured specimens.



Fig. 56. Images of the manufactured specimens for different tests: 2 cm-sided cubes for CS test (a), the 4x4x16 cm prisms for FS test (already tested) (b) and 30x30x5 cm panels for measurements of λ (c)

Finally, the microstructure and the crystal phase of some representative specimens were analysed by conducting SEM and XRD analyses (respectively). A schematic view of the experimental processes is given in Fig. 57.

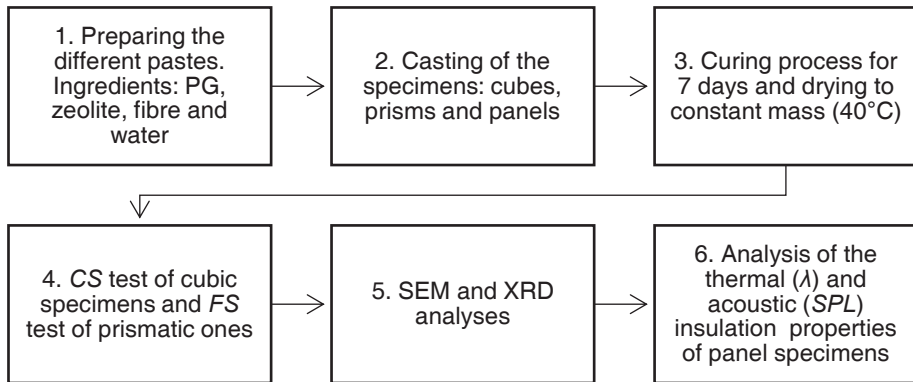


Fig. 57. Flowchart of experimental processes of the 5th stage of the study

3.5.2. Experimental results

The main goal of the current stage of the experiment involves assessing the effect of the wood fibre on the thermal and acoustic insulation properties of the load-bearing PG specimens produced through casting. Moreover, the influence of the fibre (either WF or NF) and of the presence of the ZW additive on the hydration and mechanical properties of the specimens was also evaluated. The purpose of the ZW additive is to reduce the presence of harmful acidic-soluble P_2O_5 compounds in PG, as extensively described in the 3rd stage of the experiment (see Section 3.3.2).

Evaluation of the influence of wood fibre on the hydration degree and mechanical properties of PG specimens

First, the effect of the fibre and ZW presence on the hydration degree of the specimens was evaluated. To do so, in this case, the *LOI* analysis is not a suitable method, since relatively high amounts of additives are included in the mixtures, hence, their presence would alter the *LOI* results, which refer only to the gypsum crystals. Being so, the hydration degree was investigated by analysing the crystal phase of the specimens by applying the XRD method.

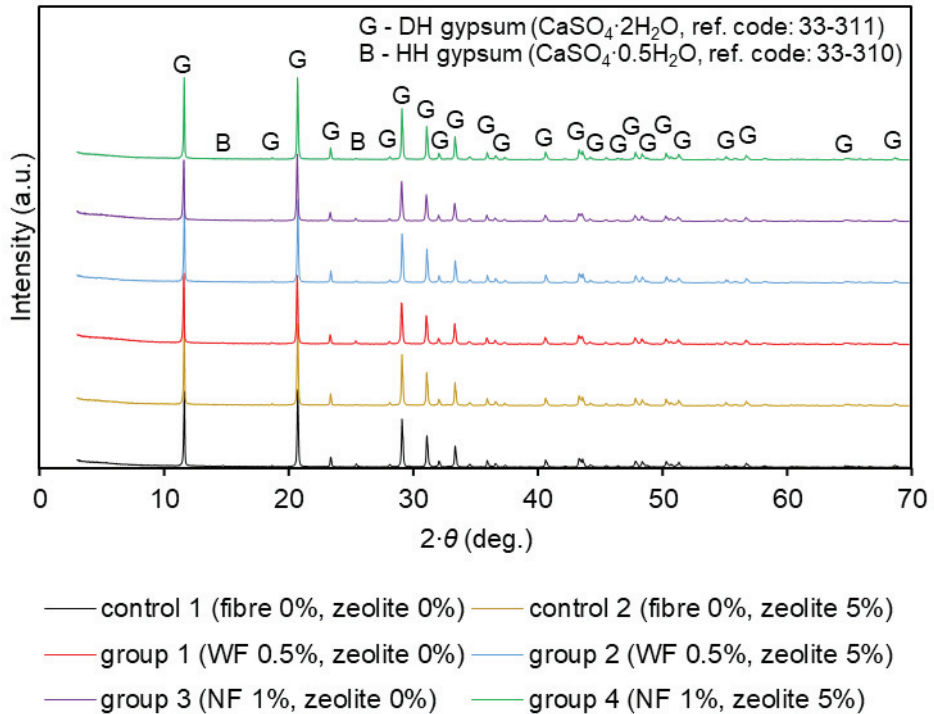


Fig. 58. XRD patterns of PG specimens with different fibre contents and types

The XRD patterns given in Fig. 58 correspond to representative specimens produced with each paste group, including the control ones (see Table 13). The representative specimens were selected for XRD analysis regarding the optimal mechanical properties of each group (see Fig. 59). Being so, the specimens with 0.5 wt% of WF were selected as representative for groups 1 and 2, while the specimens with 1 wt% of NF were selected for groups 3 and 4. All the XRD patterns of Fig. 58 are essentially identical. In all the patterns, the majority of the peaks belong to DH crystals, while only two small HH peaks are observed. Hence, the hydration degree of all the specimens seems to be excellent in all cases, and they are independent from the type and amount of fibre and from the presence of the ZW additive.

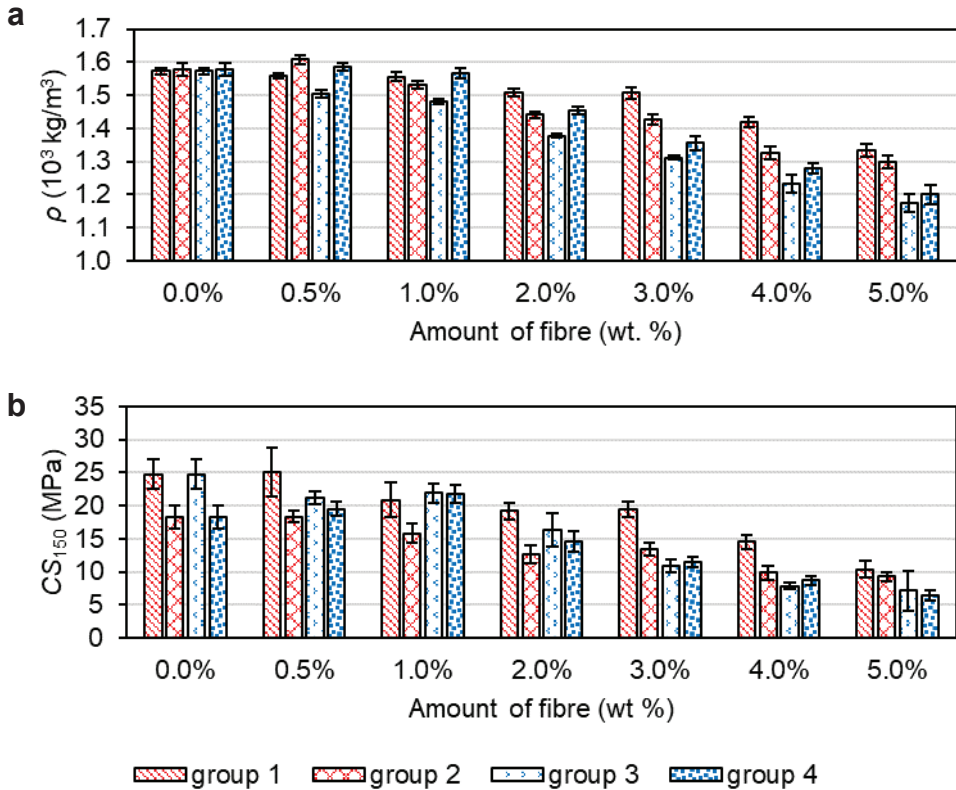


Fig. 59. Dependence of ρ (a) and CS_{150} (b) values of specimens on their content and type of fibre, and on their content of ZW additive

The dependences of the ρ and the CS_{150} values of PG specimens on the type and amount of fibre and on the presence or absence of the ZW additive (according to the groups of specimens, see Table 13) are given in Fig. 59. It must be considered that the results given in this figure correspond to 20 cm-sided cubic specimens, so that the corresponding standard CS_{150} values given in Fig. 59b are obtained by applying the factor $ScF = 0.56$ (see Table 8) to the values measured during the CS test. In general terms, in Fig. 59, it is observed that the higher fibre content reduces the ρ value and, subsequently, the CS_{150} value of the specimens. Meanwhile, the dependence on the type of the fibre is more complex. When low contents of the fibre are included (from 0 to 1%), the values of ρ and CS_{150} do not depend clearly on the type of the fibre: with 0.5 wt% of fibre, the CS_{150} of the specimens with WF (without ZW) are higher than those of the NF specimens, while when the fibre content is 1 wt%, the opposite happens. However, with the higher fibre contents (from 2 wt% to 5 wt%), the dependence on the type of the fibre becomes clearer: the specimens with WF are denoted by higher ρ and CS_{150} than those with NF. Moreover, the influence of ZW also depends on the type of the employed fibre. The specimens produced with WF feature, in general, lower ρ and CS_{150} values when ZW is included. On the other hand, the specimens produced with NF present higher ρ values

when ZW is included, and their CS_{150} values are not clearly altered by the presence or absence of the ZW additive. Hence, it can be stated that, from the ‘mechanical properties’ point of view, WF and ZW are not good teammates, in contrast to the positive joint effect of NF and ZW. Moreover, the best mechanical properties are exhibited by those specimens produced with WF and without the ZW additive; a maximum value of $CS_{150} = 25.1\text{MPa}$ is reached when 0.5 wt% WF is included, which is even slightly higher than the CS_{150} value of the control specimens. On the other hand, when higher amounts of WF are included (4 or 5 wt%), very soft specimens are manufactured ($CS_{150} < 10\text{MPa}$) which are not suitable for load-bearing purposes.

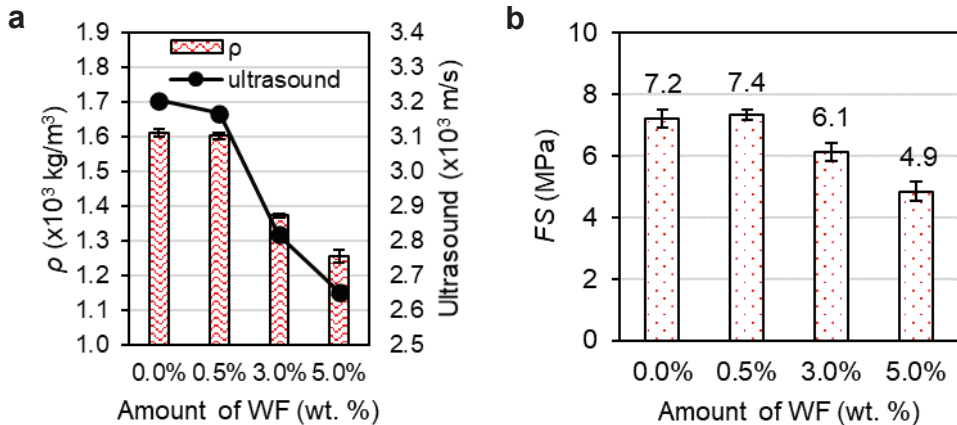


Fig. 60. Results of ρ (a) and the mechanical properties (b) of PG specimens with different amounts of WF

Once the hydration and CS_{150} dependences on the type and amount of fibre and on the presence of the ZW additive had been investigated (see Fig. 58 and Fig. 59), further analyses focus on the specimens produced with WF and with ZW (with the pastes of group 2). Hence, the standard prisms of 40x40x160 mm geometry, manufactured with 5% ZW and various amounts of the WF additive were investigated by the FS test, and the ρ and strength results are presented in Fig. 60a and b, respectively. The observed tendencies are similar to those observed in Fig. 59: the FS value reaches its maximum with 0.5 wt% WF. Somehow, 0.5 wt% WF is the optimal amount, which produces suitable reinforcement for PG, thereby increasing its mechanical properties. Eventually, with higher WF contents, the FS of the specimens gradually decreases, and this tendency is clearly determined by the ρ value.

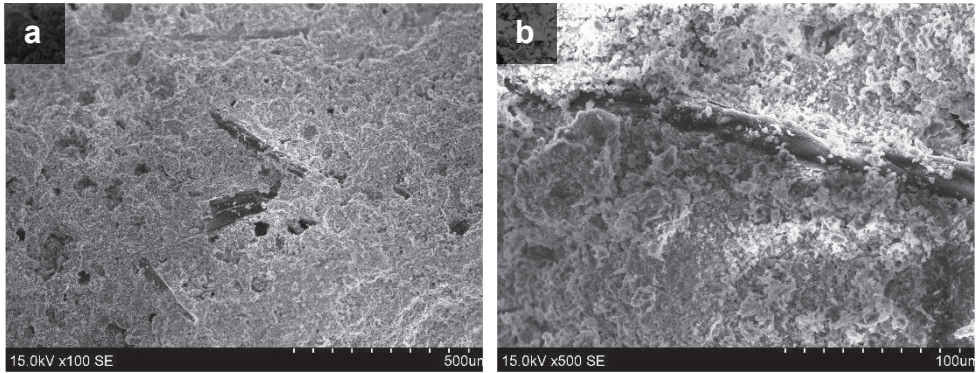


Fig. 61. Microscopic images of PG specimens with wood fibre, enhanced by x100 (a) and x500 (b)

The microstructural analysis of the specimens can help to understand the tendencies of the mechanical properties. In the SEM images of Fig. 61, at different scales, the good bond between the fibres and the PG crystal matrix can be noticed. This ‘reinforcing effect’ may explain that, when the optimal small amount of the fibre is included (0.5% of WF or 1 wt% of NF), the specimens exhibit high strength values (see the results of Fig. 59 and Fig. 60b). However, when higher amounts of the fibre are included, the decrease of the specimens’ ρ value produces a corresponding decrease of CS and FS , so that the ‘reinforcing’ of the fibre effect stops to be positive.

Influence of waste wood fibre (WF) on the thermal and acoustic insulation properties of PG specimens

As previously explained, the main goal of this experiment involves studying the influence of the wood fibre additive on the thermal and acoustic insulation properties of PG specimens in order to make them more suitable to be employed as load-bearing building products for walls.

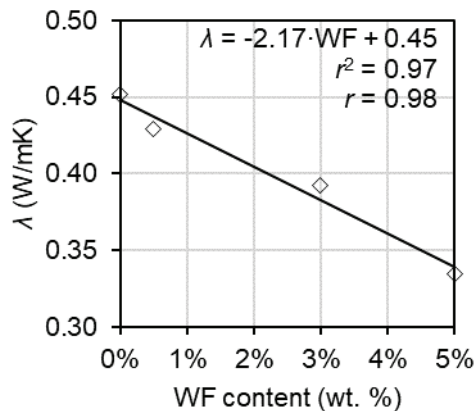


Fig. 62. Dependence of λ on the content of WF in PG specimens

Analysis of the dependence of the thermal conductivity of the specimens on the amount of WF is given in Fig. 62. The results clearly show that the increase of the amount of WF produces a corresponding decrease of the λ value from 0.45 W/mK (of the control specimens) to 0.33 W/mK (of the specimens with 5 wt% WF), i.e., the λ value is reduced by 27%. The λ dependence on the WF content fits accurately with the linear equation given in Fig. 62, with a very strong correlation of $r = 0.98$ [149]. It must be pointed out that the λ values of the manufactured specimens remain much higher than those of the insulation materials, such as rock wool or polystyrene (whose λ is typically in the range of 0.02–0.05 W/mK), but still it is a remarkable improvement when the values are compared with those of the control specimens.

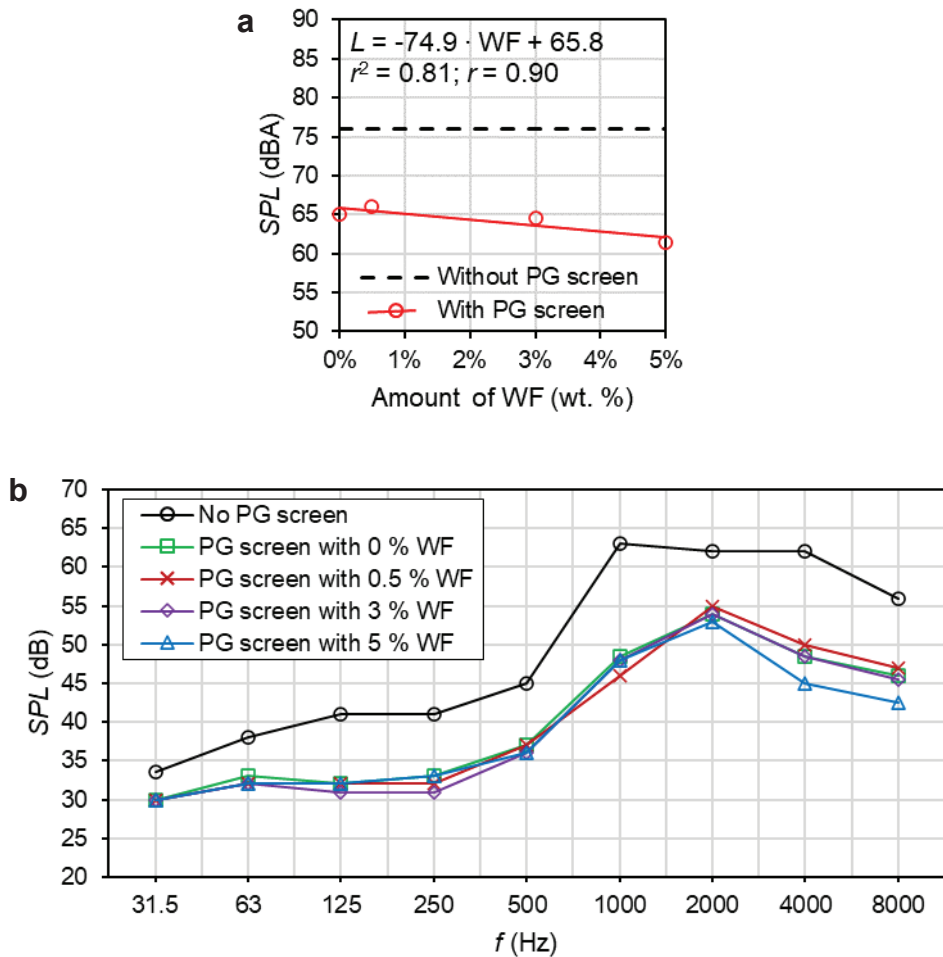


Fig. 63. Dependence of the sound pressure level (*SPL*) of natural noise on the amount of WF in PG screen (a) and the *SPL* frequency spectrum (noise filtered with standard frequency octaves) of PG screens with different WF contents (b)

The results of the investigation of acoustic insulation properties of the PG panels with different amounts of PG are given in Fig. 63, when constant noise emission is applied. The first graph, Fig. 63a, represents the dependence of A-weighted natural sound pressure levels (*SPL*) on the WF content of PG panels. It can be observed that the depicted *SPL* without the PG screen was 75 dBA. When the emitted noise was screened with the PG panel without WF content, the *SPL* value was reduced to 65 dBA. The panels with the fibre further reduced the *SPL* slightly, ultimately reaching 61.5 dBA when the maximum WF content was included (5 wt%). Besides, the measured *SPL* values for the sound filtered with the standard frequency (*f*) octaves are given in Fig. 63b. The results show that the different PG panels reduced the *SPL* levels in a similar way for all the *f* ranges. Since the human hearing is more sensitive to the sounds of mid or higher *f* (from 1500 to 8000 Hz), it can be stated that the panels with 5 wt% of WF showed the best noise insulation performance. Yet, it must be said that the acoustic insulation effect of WF in the specimens is not very significant since WF only reduced the *SPL* levels by 5% more than the control PG panels (without WF).

The specimens produced with the highest WF content (5 wt%), although exhibiting the best thermal and acoustic insulation properties, also suffered from poor mechanical strength ($CS_{150} = 9.3$ MPa). Hence, the author rather recommends a composition with a lower WF content, 3 wt%, which produced stronger specimens ($CS_{150} = 13.5$ MPa) and still improved the thermal insulation properties ($\lambda = 0.33$ W/mK) with respect to those of the control specimens. This composition, with the improved thermal insulation properties and still satisfactory mechanical strength, is suitable to be employed in load-bearing walls. The acoustic insulation properties of PG panels are not significantly improved by the WF content in any case.

Table 14. Mechanical, thermal and acoustic properties of the recommended composition of specimens with WF additive

Recommended composition	Parameter	Value of the recommended specimen, n_{rec}	Value of the control specimen, n_0	n_{rec} / n_0
93 wt% PG 5 wt% ZW 3 wt% WF	CS_{150}	13.5 MPa	18.2 MPa	0.74
	FS	7.1 MPa	7.2 MPa	1.03
	λ	0.39 W/mK	0.45 W/mK	0.87
	<i>SPL</i>	64.5 dB(A)	65 dB(A)	0.99

The properties of the recommended specimens n_{rec} are given in Table 14, where they are also compared with those of the control specimens (n_0).

3.5.3. Partial conclusions

The addition of WF improved the thermal and acoustic properties of the PG specimens and also influenced their physical-mechanical properties. The main conclusions are further summarised.

1. **Mechanical strength.** WF improved the mechanical strength of the specimens more effectively than NF did. The optimal strength value was determined when

a certain small content of the fibre was included (0.5 wt% of WF or 1 wt% of NF) due to the ‘reinforcement’ effect. A further increase of the fibre content produced a decrease of the ρ value and a corresponding weakening of the specimens. The ZW additive, employed to adsorb the soluble-acidic impurities, reduced the CS_{150} value of the specimens when used together with WF, but did not affect it when used with NF.

2. **Thermal and acoustic insulation.** The addition of WF gradually reduced the λ value of the PG specimens. A very strong linear inverse correlation between the content of WF and the λ value was determined. Hence, the λ value was reduced even by 27% when the maximum amount of WF (5 wt%) was included. Meanwhile, the acoustic insulation properties of PG panels were not significantly altered by the WF additive content.
3. **Recommended composition.** The WF additive in higher amounts (4 or 5 wt%) reduced the λ value in an important way. However, at the same time, the CS_{150} value was also reduced ($< 10\text{MPa}$), thus making those specimens unsuitable for load-bearing purposes. Therefore, a ‘compromise’ must be achieved. An amount of 3 wt% of WF seems to be the solution, since the λ value is reduced by 13% (in comparison to the specimens without WF), and the CS_{150} value still remains relatively high (13.5 MPa). Therefore, the WF content of 3 wt% is recommended as a ‘compromise’ solution.

4. MAIN RESULTS AND CONCLUSIONS

The goal of the performed research focused on evaluating the suitability of PG to be utilised as a binding material of structural building products. If the suitability is proved, the global ecological problem of phosphate fertilisers could be palliated, and, at the same time, a more economical and environmentally-friendly alternative to PC-based binding materials would appear in the building sector of the industry. Therefore, during the investigation, the influences of the nature of HH-PG, of the processing method and of the included additives (hydrated lime, ZW, MS, WF) on the radiological protectivity, the neutralisation of acidic-soluble impurities, the hydration degree and the physical-mechanical properties (such as ρ , CS , FS , SF after immersion and λ) have been systematically investigated and assessed. The main general conclusions are further presented; they indicate that, if a suitable HH-PG is employed, an effective processing method is applied, and the right additives are included in the mixture, the above mentioned properties of the manufactured specimens satisfy the requirements of getting employed in structural building products, such as bricks or blocks.

1. **Radiological assessment.** The radionuclide activity concentration of PG was found to be strongly dependent on the nature of the original phosphate rock from which it was manufactured. The PG of types I and III (mostly of igneous origin), presented values of $I=0.93$ and $I=0.8$ (respectively), i.e., below the recommended safety limit for building materials ($I \leq 1.0$) by the European Council. On the other hand, the II type PG, of sedimentary origin, exhibited $I=2.74$, thus strongly surpassing the safety levels, which indicates that this type of PG can only be employed in restricted applications.
2. **Neutralisation of soluble-acidic F⁻ and P₂O₅ impurities.** Both Ca(OH)₂ and MS additives effectively reduced the content of harmful soluble impurities in PG specimens by binding them into non-soluble compounds. In the case of the ZW additive, acid-soluble impurities were reduced by an adsorption mechanism based on ion exchange and chemical sorption processes. Considering the ratio between the times by which the P₂O₅ content was lowered and the corresponding amount of the included additive, MS presented the most effective performance with a value of 30.0 times/wt%, for 26.6 and 1.0 times/wt% presented by Ca(OH)₂ and ZW, respectively.
3. **Factors determining the hydration degree of PG specimens**
 - a) **The microstructure of HH-PG crystals.** The crystals of the I-type PG which presented flat and sharp geometries exhibited a slow hydration process reaching full hydration after 14 days of curing (at 100% humidity conditions). Most likely, the flat geometries of the crystals hindered the approaching of water to the crystal surfaces during the curing period. Meanwhile, the more volumetric crystal shapes of the HH-PG of types II and III allowed better approaching of water to the crystal surfaces, and

therefore the specimens could hydrate faster. These specimens reached full hydration in 7 days of curing.

- b) **Method of processing.** The specimens produced through casting presented much higher *LOI* values than those produced by press-forming whose *LOI* values were fairly poor. Even though, by means of immersing the specimens in water for a certain time during the curing period, the hydration ‘shortage’ was efficaciously corrected, and the *LOI* values of the press-formed specimens became independent from the *w/s* ratio.
- c) **Additives.** The $\text{Ca}(\text{OH})_2$ additive hindered the hydration of the specimens by virtue of strongly acting as a retarder of the DH crystallisation reaction. Meanwhile, the addition of ZW remarkably improved the ‘poor’ hydration of the press-formed specimens, thus enhancing their DH crystal phase content from 78.1 to 95% when the ZW content was enhanced from 0 to 10 wt%. This improvement occurred due to a mechanism of ‘giving back’ to the PG crystals an amount of water which had been absorbed by the ZW additive during the blending of the mixture, thereby producing additional late hydration of the crystal lattice.

4. Factors determining the mechanical strength of PG specimens

- a) **The nature of HH-PG.** The flat and sharp crystals of the I-type PG produced hardened specimens with loose and porous consistency and a weak mechanical strength ($CS_{150} = 8 \text{ MPa}$). Meanwhile, the prismatic and massive shapes of the III-type HH-PG crystals determined a much more compact and less-porous DH crystal matrix of the hardened specimens, which, correspondingly, exhibited the highest *CS* values reaching $CS_{150} = 29 \text{ MPa}$ for the specimens produced through casting, surpassing even by 2.5 times the *CS* value of the specimens produced with the natural gypsum. Considering the low radionuclide concentration level, the low content of soluble-acidic impurities and the high *CS* values, the HH-PG of type III proved to be the best performing binding material among the investigated PG types.
- b) **The processing method.** In all the cases, except for the I-type PG, the press-forming improved by 1.6–2.1 times the CS_{150} values of the specimens with respect to the specimens produced through casting. The optimal parameters of the press-forming processing were identified. Although the highest strength value of $CS_{150} = 46.5 \text{ MPa}$ was obtained from specimens processed with $PPF = 25 \text{ MPa}$, $w/s = 0.15$ and curing without immersion, these specimens were not recommended due to their poor hydration degree ($LOI = 15.1\%$). Hence, in the author’s opinion, the optimal specimens were found to be produced with $w/s = 0.19$, $PPF = 20 \text{ MPa}$ and curing with immersion, by virtue of exhibiting good hydration ($LOI = 19.1\%$) and a satisfactory strength ($CS_{150} = 35.3 \text{ MPa}$). The *CS* values of these press-formed specimens remained high and are even comparable to those of the typical concrete.

5. **Improvement of water-resistance.** When MS was included in amounts of 0.1–0.3 wt%, SF was enhanced by 2 times. With a further increase of the MS content (0.4 and 0.5 wt%), the SF decreased. The mechanism of the increasing of water-resistance was found to be based on the formation of a non-soluble amorphous phase of C-S-H compounds (encouraged by MS particles) which protect PG crystals from dissolving in water. The improvement of the waterproofing properties of PG specimens by adding a small amount of MS is recommended as a simple, economical and ecological technological process in comparison to the other applied methods.
6. **Thermal and acoustic insulation properties.** An inverse lineal correlation between the amount of the WF additive and the λ value was detected. Being so, when the WF content was included in amounts of 5 wt%, the specimens presented a value of $\lambda = 0.33$ W/mK (26% lower than that of the specimens without the fibre). However, this amount of WF resulted so high that ended up weakening the strength of the specimens, reaching CS_{150} values lower than 10 MPa. Hence, a lower amount of WF should be included. The author recommends the usage of WF in amounts of 3 wt%, with which, the λ value was satisfactory ($\lambda = 0.39$ W/mK, 13% lower than that of the specimens without the fibre), and CS_{150} remained over 10 MPa. The reduction of coefficient λ is an important step to encourage the utilisation of PG in such products as bricks or blocks for building walls.

SANTRAUKA

Įvadas

Fosfogipsas (PG) – pagrindinis šalutinis produktas, gaunamas fosfatinių trąšų gamybos metu. Visame pasaulyje šios trąšos yra esminės bei nepakeičiamos žemdirbystės veikloje [1, 2].

Kaip šalutinis efektas susidaro didžiuliai PG kiekiai. Prognozuojama, jog einamuoju dešimtmečiu globali PG gamyba pasieks 200–250 milijonų tonų per metus [1]. Tačiau didžioji dalis šios atliekos nėra perdirbama, o tik sandėliuojama didžiuliuose kalnuose arba pilama į gėlo vandens telkinius ir į jūrą, taip sukeliant nemenką neigiamą poveikį aplinkinėms ekosistemoms. Problema yra ta, kad PG sudėtyje pasitaiko nepageidaujamų priemaišų, tokių kaip ^{226}Ra ir kiti radionuklidai, tirpūs bei rūgštūs P_2O_5 bei F^- junginiai ir potencialiai pavojingi sunkieji metalai.

Vienintelis tinkamas sprendimas glūdi PG perdirbime. Dėl to yra nemažai mokslinių tyrimų, kuriuose yra nagrinėjamas PG pritaikomumas – ypač žemdirbystės, grunto stabilizavimo, kelio pagrindo stiprinimo bei statybinių medžiagų srityse [1]. Kadangi PG pasižymi puikiais rišamosiomis savybėmis, jis yra patrauklus sprendimas statybinių medžiagų pramonei. Be to, PG kaip rišamosios medžiagos panaudojimas turi ir kitą svarbų privalumą. Pagrindinė rišamoji medžiaga statybinėse medžiagose jau ilgą laiką buvo ir yra portlandcementis (PC). Tačiau PC gamybos metu į atmosferą išmetama nemažai šiltnamio efektą sukeliančių dujų CO_2 . Dėl šios priežasties ekologiškų rišamųjų medžiagų ieškojimas, kaip alternatyva nedraugiškam aplinkai portlandcemenčiui, yra viena iš prioritetinių tyrimų sričių medžiagų moksle. Šis kontekstas sukuria geras galimybes gipsinėms rišamosioms medžiagoms. Dėl to PG rišamosios medžiagos statybinuose produktuose panaudojimas gali turėti du esminius ekologinius privalumus: sumažinti PG sandėliavimo sukeltas aplinkosaugines problemas ir būti efektyvi ekologiška rišamoji medžiaga.

Tačiau PG panaudojimą statybinėse medžiagose riboja įvairūs veiksniai. Visų pirma, minėtos kenksmingos PG sudėties priemaišos (ypač radionuklidai) sukelia neigiamų padarinių aplinkai bei žmogaus sveikatai, todėl šis pritaikymas susidūrė su svarbiais teisiniais apribojimais ir netgi draudimais. Antra, reikia atsižvelgti į tai, kad gipsas yra orinė, o PC – hidraulinė rišamoji medžiaga. Skirtingai nuo PC, gipsas (ir PG) suminkštėja veikiamas drėgnos aplinkos, todėl negali būti naudojamas pastato išorinėms reikmėms, pritaikomas tik vidiniams pastato elementams. Mokslininkai bando surasti būdų, kaip sumažinti šituos PG rišamosios medžiagos trūkumus: ne tik kenksmingų priemaišų kiekis turi būti ženkliai neutralizuojamas, bet ir PG produktų fizikinės-mechaninės savybės turi būti pageriamos ir didinamas atsparumas vandeniui. Tik tokiu būdu PG rišamoji medžiaga gali tapti konkurencingu sprendimu statybinių medžiagų sektoriuje.

Tačiau, nepaisant gausių šios tematikos tyrimų, perdirbamas PG kiekis išlieka nereikšmingas, lyginant su visa produkcija, ir kenksmingos atliekos kalnai sparčiai auga. Didelė problemos dalis ta, kad atliekami moksliniai PG rišamosios medžiagos panaudojimo srityje tyrimai labiau fokusuojasi į siaurus aspektus (tobulinti vieną ar kitą PG savybę, nagrinėti tirpių rūgščių priemaišų neutralizavimą, įvertinti

radioaktyvumo riziką ir panašiai), bet labai retai atsižvelgia į problemą visapusiškai. Norint įvertinti PG naudojimo statybinėse medžiagose tinkamumą, reikia plačiau įvertinti kluūtis bei galimybes, ištiriant PG kilmę, mikrostruktūrą, cheminę bei mineralinę sudėtį, priemaišų kiekį, radioaktyvumą, apdirbimo būdą bei priedų panaudojimą, kartu ir šių savybių įtaką fizikinėms-mechaninėms savybėms bei atsparumą vandeniui. Dėl minėtų priežasčių šio mokslinio darbo tikslas yra pateikti visapusišką analizę, kurios metu PG rišamosios medžiagos panaudojimo galimybės būtų plačiai iširtos.

Pagrindinis šio mokslinio darbo tikslas pagerinti pagrindines PG savybes, sudarančias sąlygas jo, kaip rišamosios medžiagos, pritaikomumui konstrukciniuose elementuose, naudojant liejimo bei presavimo formavimo būdus bei įterpiant įvairius pramonės atliekų priedus.

Darbo uždaviniai

1. Iširti skirtingos kilmės (magminės arba nuosėdinės) PG radioaktyvumo lygį ir įvertinti kiekvieno PG tipo tinkamumą statybinėse medžiagose.
2. Sumažinti kenksmingų tirpių ir rūgščių P_2O_5 ir F^- junginių kiekį PG sudėtyje, įterpiant tinkamus priedus, kurie išplės PG panaudojimą įvairiose srityse.
3. Padidinti PG bandinių mechaninių savybių vertes, taikant presavimo metodą ir taip pat įvertinant pradinio pushidračio PG (HH-PG) mikrostruktūrą bei naudotus priedus.
4. Pagerinti PG gaminių atsparumą vandeniui, tinkamai modifikuojant pradinio mišinio sudėtį.
5. Pagaminti PG produktus su pagerintomis šilumos bei triukšmo izoliacinėmis savybėmis.

Mokslinis naujumas

- Nustatyta PG kilmės, mikrostruktūros, sudėties bei formavimo įtaka fizikinėms-mechaninėms savybėms, atsparumo vandens poveikiui bei radioaktyvumo lygiui.
- Pasiūlytas PG gaminių formavimo presuojant metodas, lemiantis ženklų PG bandinių mechaninių savybių pagerinimą.
- Nustatyta hidratuotų kalkių, ceolito atliekos (ZW), atliekinio metalurgijos šlamo (MS) bei atliekinio medžio plaušo (WF) priedų įtaka PG rišamosios medžiagos fizikinėms, mechaninėms bei cheminėms savybėms.

Praktinė vertė

1. PG bandiniai, pasižymintys dideliu mechaniniu stiprumu, pakankamu hidratacijos laipsniu bei padidintomis termoizoliacinėmis savybėmis, suteikia naujų galimybių PG panaudoti statybinių medžiagų srityje kaip konstrukcinius elementus (plytos, blokeliai ir pan.).
2. Padidintas atsparumas vandeniui praplečia PG gaminių panaudojimo galimybes.
3. Radioaktyvumo tyrimų rezultatai bei tirpių rūgščių junginių mažinimo metodai suteikia vertingos informacijos apie PG panaudojimo statybinėse medžiagose saugumą bei rizikas.

4. PG panaudojimas statybiniuose produktuose sumažins šios medžiagos sankaupų sukeltas ekologines problemas.

Ginamieji disertacijos teiginiai

1. HH-PG kristalų mikrostruktūra lemia bandinių hidratacijos laipsnį bei stiprumą.
2. PG bandiniai, pagaminti presavimo būdu, pasižymi 1,6–2,1 didesniu stiprumu nei bandiniai, pagaminti liejimo būdu.
3. Nedidelis kiekis ZW priedo iki 7,5 kartų mažina nepageidaujamas tirpaus P₂O₅ priemaišas.
4. MS priedas 2 kartus padidina PG bandinių atsparumą vandeniui.

Darbo aprobavimas ir publikavimas

Šio mokslinio darbo atliktų tyrimų rezultatai buvo pateikti 3-uose moksliniuose straipsniuose, publikuotuose moksliniuose žurnaluose, kurie yra *Clarivate Analytics Web of Science* duomenų bazėje, su cituojamumo rodikliu, ir priklauso Q1 bei Q2 kvartilams. Kai kurie iš tyrimų buvo taip pat pristatyti trijose tarptautinėse mokslinėse konferencijose: *GreenChem-18* (Madridas, Ispanija), 19th *ICMB* (Brno, Čekija) ir 2nd *Vitrogeowastes* (Baeza, Ispanija).

1. Medžiagos ir tyrimo metodai

Šiame tyrime buvo naudojamos skirtingos pradinės medžiagos bei priedai, kurie turėjo būti ištirti tinkamais metodais. Sukietėję bandiniai taip pat buvo testuojami įvairiais reikalingais būdais. Eksperimentiniai tyrimų metodai bei pradinės medžiagos yra aprašytos šiame skyriuje.

1.1. Eksperimentinių tyrimų metodai

Visų pirma, pradinės medžiagos yra ištirtos bei charakterizuojamos atliekant tinkamus analizės metodus. PG bei priedų mikrostruktūra buvo ištirta skenuojamosios elektroninės mikroskopijos (SEM) metodu, naudojant elektroninį mikroskopą *Hitachi S-3400N Type II* [132]. Pačiame mikroskope yra įstatytas rentgeno spindulių energijos dispersijos spektrometrijos (EDS) detektorius *Bruker Quad 5040*, kuriuo buvo nustatytas cheminių elementų pasiskirstymas tiriamosiose medžiagose. Pradinių medžiagų elementinė sudėtis buvo ištirta rentgeno spindulių fluorescencinės analizės (XRF) būdu naudojant *Bruker X-ray S8 Tiger WD* spektrometrą. Be to, pradinių medžiagų (bei sukietėjusių bandinių) kristaliniai junginiai buvo ištirti rentgeno spindulių difrakcinės analizės (XRD) metodu, naudojant *DRON-6* difraktometrą su *Bragg-Bretano* geometrija. XRD rezultatų individualios fazės buvo identifikuojamos naudojant *Oxford Cryosystems Crystallographica Search-Match* programinę įrangą, besiremiančią PDF-2 duomenų bazės duomenimis [133]. Tam tikrais atvejais programinė įranga *Panalytical HighScore+ 3* buvo taip pat naudojama. XRD tyrimų rezultatų kiekybinė analizė buvo atliekama *Rietveld* metodu, naudojant *General Structure Analysis System* programinę įrangą [134]. PG radionuklidų veiklos koncentracija yra nustatoma gama spinduliuotės spektroskopiniu būdu, naudojant *BEGe, broad-energy* puslaidininkinį detektorių su *Canberra-Packard GENIE 2K v.3.4* programine įranga. Dalelių dydžio

pasiskirstymo analizė buvo atliekama lazerinio pagrindo prietaisu *Cilas 1090* [138], dirbančiu sausos dispersijos režimu.

Kitame etape PG mišinių bei sukietėjusių bandinių savybės yra nustatomos tinkamais metodais. Hidratacijos temperatūra yra nustatyta su 8 kanalų *USB TC-08 Data Logger* prietaisu ir *K* tipo termoporomis [140]. Bandinių hidratacijos kokybė buvo nustatyta remiantis kaitinimo nuostolių (*LOI*) nustatymo metodu, kaitinant medžiagą ≥ 400 °C temperatūroje ir skaičiuojant santykinį skirtumą tarp galutinės bei pradinės bandinio masės. Sukietėjusių bandinių mechaninės savybės yra nustatomos atliekant stiprumų gniuždant (*CS*) bei lenkiant (*FS*) testavimo metodus pagal Europoje galiojančio standarto EN 13279-2 [3] nurodymus, naudojant kompiuterizuotą presą *ToniTechnik 2020.0600/132/02* [143]. PG bandinių atsparumas vandeniui yra įvertinamas nustatant suminkštėjimo koeficientą (*SF*) po 30 arba 90 parų mirkimo vandenyje periodo. Mechaninių savybių bei atsparumo vandeniui rezultatai buvo pagrindžiami bandinių mikrostruktūros SEM mikroskopijos būdu. Tirpių bei rūgščių P_2O_5 bei F^- junginių mažinimas yra įvertinamas dviem vienas kitą papildančiais būdais: atliekant pH tyrimus su *AD8000 Professional Multi-Parameter pH-ORP-Conductivity-TDS-TEMP Bench Meter* prietaisu [139] ir matuojant šių junginių kiekį vandeniniame tirpale su *Hanna HI713 Checker HC® - Phosphate LR* [135] bei *Hanna HI729 Checker HC® - Fluoride LR* [136] kolorimetrais. Galiausiai, PG bandinių termoizoliacinės savybės buvo nagrinėjamos matuojant šilumos laidumą (λ) su šilumos sklidimo matavimo prietaisu ir taikant parengtos būsenos karštosios dėžės priartėjimą bei paruošiant bandinius pagal Europoje galiojančio standarto EN 12667 [142] nurodymus.

1.2. Pradinės medžiagos

Šiam tyrimui atlikti buvo naudojami trys skirtingi HH-PG, vienas natūralus HH gipsas bei keletas priedų. Jų aprašymas pateikiamas toliau.

Skirtingos kilmės pushidratis fosfogipsas

PG atlieka susidaro fosforo rūgšties gamybos metu, apdorojant fosfatines uolienas vadinamojo „šlapio proceso“ metu. Šiame tyrime buvo nagrinėjami trys skirtingos kilmės PG tipai, pagaminti Lietuvoje, fosfatinių trąšų gamykloje. PG susidaro naudojant tokias žaliavas: fosforitą iš Pietų Afrikos Respublikos (PAR) arba Maroko kasyklų ir apatitą iš Rusijos Kirovo bei Kovdoro kasyklų. Fosforitas priskiriamas nuosėdinėms fosfatinėms uolienoms, o apatitas – magminėms fosfatinėms uolienoms. Kiekvienas nagrinėjamas PG buvo gaminamas iš vienos žaliavos arba dozuojant skirtingas minėtas žaliavas. Gamykloje, „šlapio proceso“ metu, PG yra gaunamas HH kristalinės fazės ir, iškart po gamybos, turi šiltų drėgnų miltų konsistenciją. Šių HH-PG kilmė, prigimtis bei savybės (paties gamintojo pamatuotos gamybos linijose, dar medžiagai esant šiltai) yra pateiktos 1 lentelėje.

1 lentelė. Drėgno HH-PG savybės gamybos linijose

PG žymėjimas	I tipas	II tipas	III tipas
Fosfatinių uolienu kasyklų kilmės	Kirovas–Marokas	PAR–Marokas	Kovdoras
Fosfatinių uolienu dozavimas	81 % Kirovas 19 % Marokas	50 % PAR 50 % Marokas	100 % Kovdoras
Fosfatinių uolienu prigimtis	Apatitas (Kirovas) Fosforitas (Marokas)	Fosforitas	Apatitas
PG drėgnis (nesurišto vandens kiekis)	31,8 %	22,0 %	18,5 %
PG suminis (tirpus ir netirpus) P ₂ O ₅ kiekis	0,86 %	0,86 %	1,13 %
PG tirpus P ₂ O ₅ kiekis	0,40 %	0,43 %	0,29 %

1 lentelėje pateikiami duomenys suteikia vertingos informacijos apie kiekvieno HH-PG prigimtį bei esamą P₂O₅ junginių kiekį. Nors III tipo PG pasižymi didžiausiu suminiu P₂O₅ junginių kiekiu, tačiau tuo pačiu metu jame tirpių P₂O₅ junginių kiekis du kartus yra mažesnis nei kituose HH-PG tipuose. Kadangi problemiškesni yra tirpieji junginiai, šiuo požiūriu III tipo HH-PG turi mažiausiai minėtų priemaišų. Be to, reikia paminėti, jog 1 lentelėje pateikiama „drėgno“ vertės nurodo šlapių HH-PG miltų laisvo (nesurišto) vandens kiekį. Todėl šio drėgno nereikia painioti su chemiškai surišto vandens kiekiu, esančiu HH kristaluose. Taigi, kaip matoma 1 lentelėje, laisvo vandens kiekis medžiagoje yra ženklus ir, esant drėgnoms sąlygoms, HH kristalinė fazė nėra stabili, greitai besihidratuodama ir virsdama dihidračiu gipsu (DH), kuris nėra rišamoji medžiaga. Norint gauti rišamąją medžiagą (HH-PG), iš gamybos paimtas šlapias HH-PG iš karto buvo išdžiovinamas 100 °C temperatūroje, kol drėgnis buvo pašalinamas. Taip paruošti tyrimams sausi HH-PG milteliai buvo sandėliuojami sandariose talpose.

Kartu su aptartais HH-PG buvo tiriamas ir vienas komercinis natūralus HH gipsas kaip kontrolinė medžiaga. Visų šių HH medžiagų XRF cheminės sudėtys yra pateikiamos 2 lentelėje.

2 lentelė. Natūralaus (komercinio) HH gipso bei trijų HH-PG XRF cheminės sudėtys (sv %)

Jung.	Natūr.	I-PG	II-PG	III-PG	Jung.	Natūr.	I-PG	II-PG	III-PG
SO ₃	44,30	47,77	48,49	49,50	K ₂ O	0,77	0,07	0,05	0,04
CaO	38,23	38,42	39,32	38,78	ZrO ₂	0,003	-	-	0,005
SiO ₂	5,26	0,83	2,14	2,94	ZnO	-	-	-	0,004
P ₂ O ₅	0,29	1,15	1,08	1,30	TiO ₂	0,07	0,06	0,02	-
SrO	0,18	1,88	0,27	0,41	Y ₂ O ₃	-	0,03	0,03	-
CeO ₂	-	0,35	0,21	0,19	CuO	-	0,008	-	-
Al ₂ O ₃	1,77	0,20	0,09	0,16	Nb ₂ O ₅	-	0,002	0,002	-
MgO	3,17	0,11	0,11	0,15	MnO	0,008	-	-	-
Nd ₂ O ₃	-	0,08	0,10	0,07	F*	-	1,85	1,42	-
Fe ₂ O ₃	0,52	0,08	0,01	0,06	H ₂ O**	6,2	6,9	6,7	6,4
La ₂ O ₃	-	0,21	-	0,05	Sum.	100	100	100	100

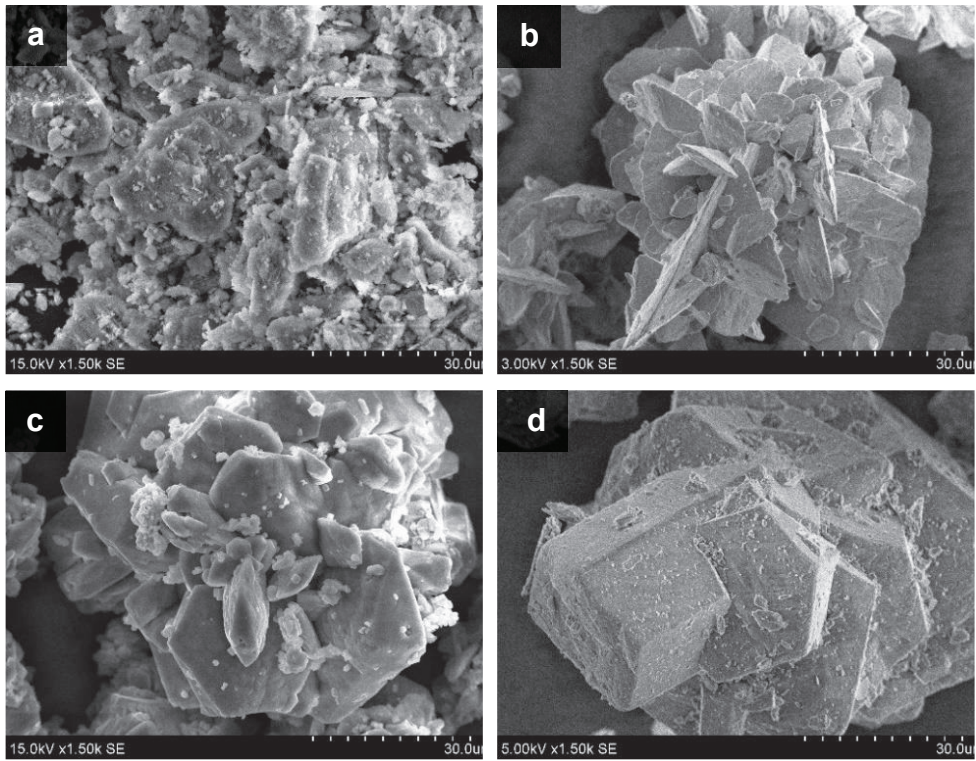
***Pastaba:** F kiekis buvo nustatytas EDS metodu.

****Pastaba:** H₂O kiekis buvo nustatytas *LOI* metodu.

Analizuojamų medžiagų XRF cheminės sudėtys (2 lentelė) atskleidė, kad, neskaitant CaSO₄ specifinių cheminių elementų (SO₃ bei CaO), pagrindiniai aptikti junginiai yra SiO₂, P₂O₅, SrO ir F. Verta paminėti, kad SiO₂ kiekis natūraliame HH gipse yra ženkliai didesnis nei visuose HH-PG tipuose, kita vertus, P₂O₅ kiekiai rodo priešingą tendenciją. Fluoras buvo aptinkamas nedideliais kiekiais I bei II tipų HH-PG, o natūraliame gipse bei III tipo PG jo iš viso nėra. Taip pat verta atkreipti dėmesį į tai, kad Al₂O₃, MgO, Fe₂O₃ bei K₂O nustatyti kiekiai yra daug didesni natūraliame gipse nei visuose PG tipuose. Be to, visuose PG tipuose buvo aptikti nedideli kiekiai kai kurių retųjų žemės elementų (REE): Ce, Nd, La bei Y. Natūraliame gipse šitų elementų nebuvo aptikta. Galiausiai, nė vienoje medžiagoje nebuvo aptikta sunkiųjų metalų, JAV aplinkosaugos agentūros (US EPA) klasifikuojamų kaip potencialiai pavojingi (As, Ba, Cd, Cr, Pb, Hg, Se, Ag), kurie dažnai būna aptinkami PG sudėtyje.

2 lentelėje pateikiamos visų HH medžiagų surišto H₂O kiekiai (*LOI*), kurių vertės yra 6,2–6,9 intervale. Tai patvirtina pushidratinė (HH) visų medžiagų prigimtis, turint omenyje, kad teorinė HH gipso *LOI* vertė yra 6,2 %, o DH gipso – 21,85 % [137]

Rūgščių tirpių P₂O₅ bei F⁻ junginių kiekis, esantis PG sudėtyje, lemia visų I, II bei III tipų mažas pH vertes: 2,88, 2,87 bei 3,63 atitinkamai. Iš tikrųjų, III tipo HH-PG pasižymi mažiausiai rūgščiu pH (lyginant su kitais PG), nes, kaip matoma iš 1 bei 2 lentelių, jame yra mažiausiai tirpių P₂O₅ bei F⁻ junginių. Tuo tarpu natūralaus gipso atveju pH yra beveik neutralus (pH = 6,16), nes jame šių junginių kiekis nereikšmingas.



1 pav. Skirtingų HH medžiagų dalelių SEM mikroskopiniai vaizdai: natūralaus gipso (a), I tipo PG (b), II tipo PG (c), III tipo PG (d). Didinimas: 1500 kartų

Natūralaus HH medžiagų miltelių mikroskopiniai vaizdai yra pateikiami 1 paveiksle. Juose pastebimi reikšmingi skirtumai tarp skirtingų medžiagų kristalų. Visų pirma, 1a paveiksle matoma, kad natūralaus gipso kristalai pasižymi skirtingais dydžiais bei netaisyklingomis formomis dėl to, kad šie milteliai buvo gaunami HH gipsą sumalant. Be to, HH natūralaus gipso kristalai yra atskiri vienas nuo kito, tuo išsiskirdami nuo HH-PG kristalų, kurie yra susijungę didesniais konglomeratais. I tipo HH-PH kristalai (žr. 1b pav.) yra plokšti bei aštrūs ir jų storis bei ilgis gali pasiekti, atitinkamai, 5 bei 15 μm . II tipo HH-PG kristalai (žr. 1c pav.) yra panašūs į I tipo, bet storesni (iki 10 μm) ir su apvalesniais kontūrais. Tuo tarpu III tipo HH PG kristalai (žr. 1d pav.) yra daug masyvesni ir pasižymi taisyklingesne šešiakampio skerspjuvio prizmės geometrija, su 10–30 μm ilgiais ir 2/1 ilgio/diametro santykiu.

Natūralaus HH gipso ir I, II bei III HH-PG santykiniai tankiai yra atitinkamai 2,47, 2,70, 2,74 ir 2,67, dalelių vidutinis diametras yra 50,23 μm , 49,32 μm , 65,75 μm bei 85,14 μm . Kaip anksčiau minėta, natūralaus gipso dalelės yra suformuotos iš atskirų kristalų, o HH-PG dalelės – iš kristalų konglomeratų, dėl to jų dydžių negalima lyginti.

PG priedai – gamybos atliekos: ceolito atlieka (ZW), metalurgijos šlamas (MS) bei medžio atliekos plaušas (WF)

Šiame tyrime buvo naudoti tam tikri PG mišinių priedai, kurių tikslas – pagerinti bandinių aplinkosauginės, fizikinės, mechaninės bei atsparumo vandeniui savybės: ceolito atlieka (ZW), metalurgijos šlamas (MS) bei medžio plaušo atlieka (WF). Kai kuriais atvejais taip pat buvo naudotas $\text{Ca}(\text{OH})_2$ priedas tirpiems F^- bei P_2O_5 junginiams neutralizuoti.

Ceolitai yra alumosilikatinės prigimties porėtos medžiagos, dažnai naudojamos kaip katalizatoriai bei sorbentai pramoniniuose procesuose. Jie gali būti natūralūs arba sintetiniai. Šiam tyrime naudojamas sintetinis ceolitas ZW, kuris buvo gautas iš naftos perdirbimo įmonės. Jis naudojamas kaip sorbentas tokiojo katalizinio krekingo procese, kurio metu šis ceolitas užsiteršė naftos produktais, mechaniškai degradavo ir tapo atlieka. Ši medžiaga sudaryta iš balkšvos spalvos miltelių ir jos cheminė sudėtis yra pateikiama 3 lentelėje. Joje vyrauja alumosilikatinis junginys ir didelė įvairovė kitų elementų oksidų junginiuose: retieji žemės elementai (La, Ce), nemetalai (S, P), pereinamieji metalai (Ti, Fe, V), šarminiai bei šarminiai žemės metalai (Na, K, Mg, Ca) ir kiti. Naudojama vandeninė WZ suspensija yra rūgšti ($\text{pH} = 4,35$). ZW mikrostruktūroje vyrauja dalelės su sferine geometrija bei mikroporėtais paviršiais, jos pateiktos 2a paveiksle. Dalelių santykinis tankis – 2,33, o vidutinis diametras yra 23,3 μm .

3 lentelė. ZW atliekos cheminė sudėtis pagal XRF (sv %)

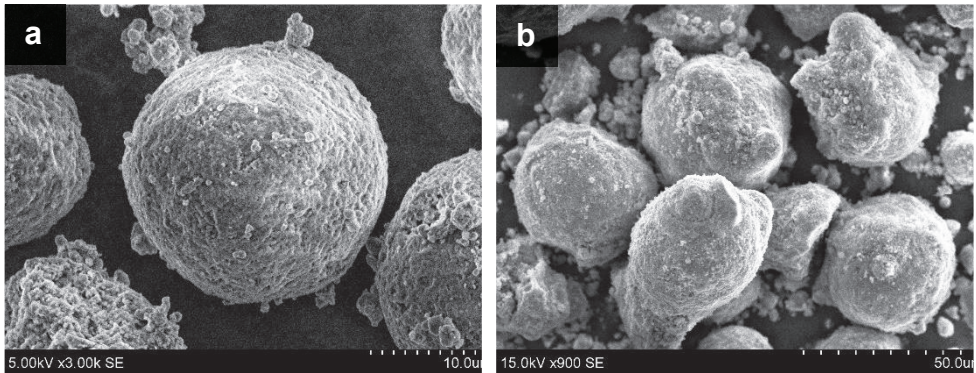
Al_2O_3	SiO_2	La_2O_3	SO_3	TiO_2	Fe_2O_3	MgO	Na_2O	CeO_2	V_2O_5	CaO	P_2O_5
50,7	36,4	1,67	1,14	0,932	0,647	0,634	0,332	0,268	0,117	0,077	0,075
K_2O	WO_3	ZrO_2	NiO	Ga_2O_3	PbO	CuO	ZnO	SrO	Nb_2O_5	CoO	
0,042	0,017	0,013	0,011	0,005	0,005	0,004	0,004	0,003	0,002	0,002	

Metalurgijos šlamo atlieka (MS) yra gaunama iš laivų pjovimo cecho UAB *Metalgama*, esančio Klaipėdos mieste. Joje laivų metalinės dalys (kurios įprastai priklauso S355 konstrukcinio plieno klasei) yra pjaunamos CNC plazmos technologija specialiose vandens voniose. Pjovimo metu išlydytas metalas nusėda vonių dugne ir, pakankamam jo kieki susikaupus, vežamas perdirbti į metalo laužą. Minėtame ceche kiekvienais metais susikaupia 25 tonos šios atliekos. Po džiovinimo šis MS įgauna juodos spalvos miltelių konsistenciją.

4 lentelė. MS atliekos elementinė sudėtis pagal XRF (sv %)

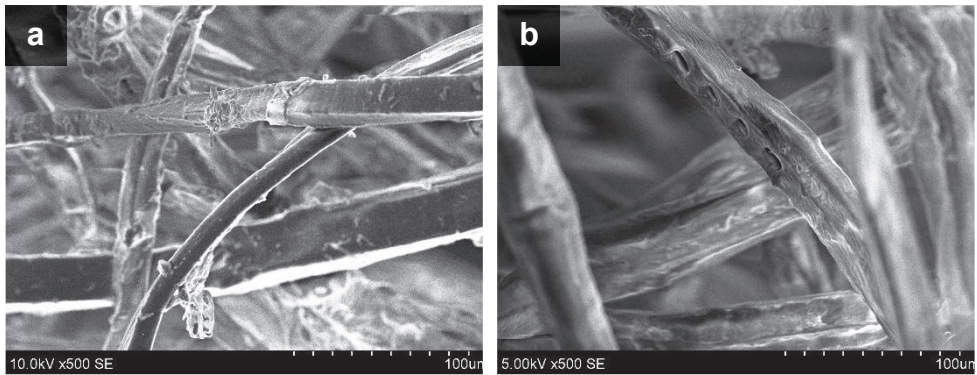
Fe	Mn	Si	Zn	Ca	P	Gd	Al	Cr	Eu	Cu	Ni
95,1	2,65	0,87	0,49	0,24	0,17	0,10	0,08	0,08	0,08	0,04	0,02
Nb	V	S									
0,02	0,02	0,02									

MS atliekos cheminė sudėtis pateikta 4 lentelėje ir yra panaši į S355 plieno sudėtį, kuris yra priskiriamas anglies-mangano plieno tipui. Joje pastebima, kad Fe yra pagrindinis vyraujantis cheminis elementas. Be to, taip pat rasta pereinamųjų metalų (Mn, Zn), nemetalų (Si, P) ir šarminių žemės metalų (Ca). Kiti elementai sudaro mažus kiekius: kai kurių pereinamųjų bei kitų metalų (Al, Cr, Cu, Ni, Nb, V) ir kai kurių retųjų žemių (Gd, Eu). Minėtina tai, kad C kiekis nebuvo nustatytas, nes XRF analizės metodas tam yra netinkamas. Tačiau, pagal tipinę S355 plieno sudėtį, tikimas 0,16–0,18 sv % anglies kiekio. MS dalelių mikrostruktūra yra pateikta 2b paveikslo SEM nuotraukoje, kurioje pastebimos šių dalelių ovalios arba sferinės formos. MS dalelių santykinis tankis yra 7,04 (tris kartus sunkesnės už HH-PG daleles), o vidutinis diametras – 23 μm .



2 pav. ZW (a) bei MS (b) atliekų SEM mikroskopiniai vaizdai. Didinimas: 3000 ir 900 kartų (atitinkamai)

Taip pat buvo naudojamas atliekinis medžio plaušas (WF), gaunamas iš naudotų medžio drožlių plokščių. Palyginimui buvo naudojamas natūralios medienos plaušas (NF). Šių plaušų (arba fibrų) pridėjimo prie PG pagrindinis tikslas – pagerinti PG bandinių šilumos bei garso izoliacines savybes. WF bei NF mikroskopiniai vaizdai yra pateikti 3 paveiksle. Remiantis šiomis mikroskopinėmis nuotraukomis, nepastebima esminių morfologinių skirtumų tarp vieno ir kito tipų fibrų, t. y. jos yra panašios.



3 pav. Medžio plaušų NF (a) bei WF (b) SEM mikroskopiniai vaizdai. Didinimas: 500 kartų

Fibrų dalelių dydžio analizė buvo atliekama siojimo būdu. Reikia paminėti, jog šis metodas yra tinkamesnis miltelių konsistencijos medžiagoms nei fibroms, nes pastarųjų atveju gauti rezultatai nėra nei fibrų diametras, nei ilgis, o tik bendras fibrų dydžio parametras. Tačiau ši analizė leidžia palyginti tarpusavyje abi WF bei NF medžiagas. Abiem atvejais daugumos fibrų dydis yra tarp 2 bei 4 mm (> 40 %). Tačiau, apibendrinant, NF fibros yra neženkliai didesnės už WF.

Visų aprašytų medžiagų pagrindinės savybės yra pateikiamos suvestinėje 5 lentelėje.

5 lentelė. Pradinių medžiagų pagrindinių savybių suvestinė

Medžiaga	pH	Dalelių vid. diametras (μm)	Santykinis tankis	Mikrostruktūra	Spalva
Natūralus HH	6,16	50,23	2,47	Atskiri netaisyklingų formų kristalai	Pilka
I tipo HH-PG	2,88	49,32	2,70	Plokščių bei aštrių kristalų konglomeratai	Pilka
II tipo HH-PG	2,87	65,75	2,74	Sąlyginiai plokščių bei aptakių kraštų kristalų konglomeratai	Balkšva
III tipo HH-PG	3,63	85,14	2,67	Masyvių šešiakampės prizmės geometrijos kristalų konglomeratai	Balta
ZW	4,35	23,26	2,33	Apvalios formos kristalai	Balkšva
MS	6,05	47,9	7,04	Apvalios bei ovalios formos kristalai	Juoda
Ca(OH) ₂	12,79	5,57*	1,97	-	Balta
WF	-	2000 – 4000**	-	Ilgos fibros	Tamsiai ruda
NF	-	2000 – 4000**	-	Ilgos fibros	Šviesiai ruda

***Pastaba:** Ca(OH)₂ dalelių diametras nebuvo tiesiogiai matuojamas, bet interpoliuojamas iš *Bleino* savitojo paviršiaus vertės, lyginant ją su kitų ištirtų medžiagų savitojo paviršiaus vertėmis.

****Pastaba:** medžio plaušo (WF bei NF) „diametro“ pozicijoje pateikiamas apibendrintas šių fibrų dydis (nebūtinai tai yra diametras), gautas sietų analizės būdu.

2. Tyrimo rezultatai ir jų aptarimas

Šioje dalyje apie PG kaip konstrukcinių elementų rišamosios medžiagos tinkamumą buvo vykdomi 5 tyrimo etapai, kurių pagrindiniai rezultatai yra toliau pristatomi.

2.1. Skirtingos kilmės PG rišamosios medžiagos naudojimo konstrukciniuose produktuose tinkamumo vertinimas

Šiame tyrimo etape, visapusiškai buvo ištirti bei palyginti 3 skirtingos kilmės PG. Kaip kontrolinė medžiaga į tyrimą taip pat buvo įtrauktas vienas natūralus HH gipsas. Buvo ištirta kristalų mikrostruktūra, tirpių-rūgščių priemaišų kiekiai, bandinių apdorojimo metodai ir jų įtaka hidratacijos procesui, radioaktyvumo lygiui bei sukietėjusių bandinių fizikinėms-mechaninėms savybėms.

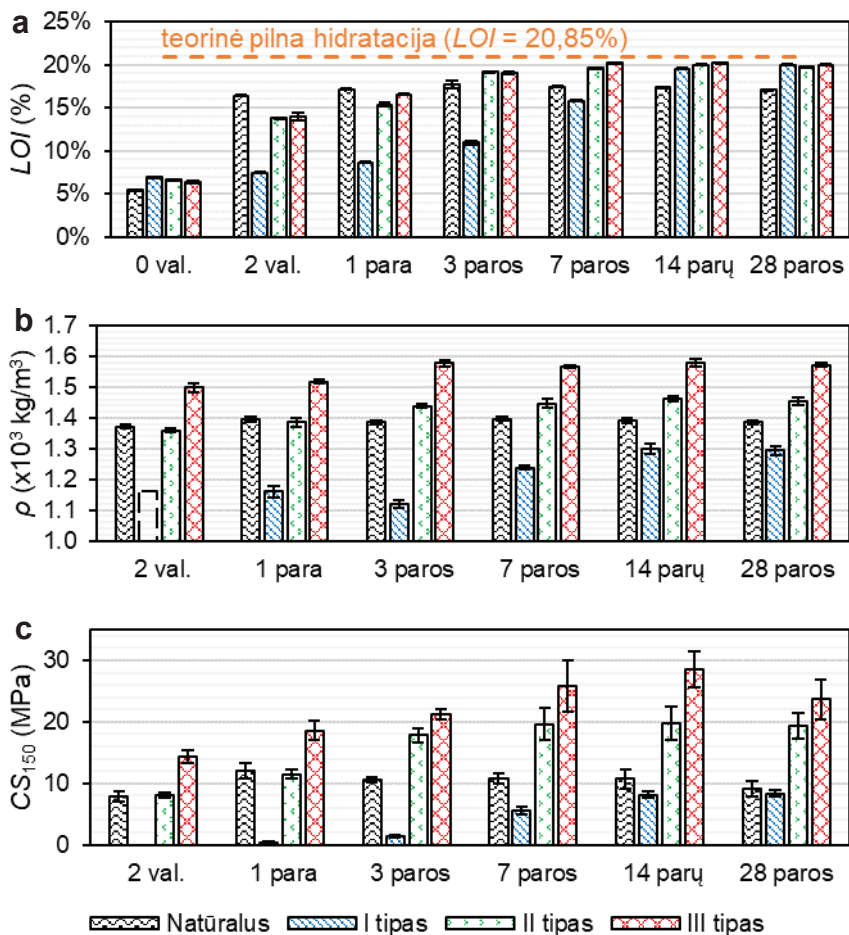
Visų pirma, buvo nustatyta bandinių dydžio įtaka *CS* vertėms. Liejimo būdu buvo suformuoti 20 mm, 70 mm bei 100 mm kraštinių kubiniai bandiniai. Presavimo būdu buvo suformuoti 26,8x26,8 mm, 80x80 mm bei 100x100 mm cilindriniai bandiniai pagal turimas preso formas. Pagal Europos standartą EN 206-1 [148], standartiniai bandiniai betono *CS* testavimui yra 150 mm kraštinių kubai arba 150x150 mm cilindrai. Standartinių bandinių stiprumas gniuždant bus toliau

žymimas tekste trumpiniu CS_{150} . Norint testuoti mažesnius bandinius, skalės koeficientas ScF turi būti taikomas gautai eksperimentinei CS vertei, kad būtų skaičiuojama atitinkama CS_{150} vertė ($CS_{150} = ScF \cdot CS$). Bandant 100 mm kraštinių kubelius arba 100x100 mm cilindrus, Lietuvos standartas LST 1974 [147] nurodo $ScF = 1,00$ bei $ScF = 0,93$ atitinkamas vertes. Turint šią informaciją, visų tirtų dydžių bandiniams buvo nustatyti atitinkami ScF koeficientai, kurie yra pateikti 6 lentelėje.

6 lentelė. Skirtingo dydžio bandinių koeficiento ScF vertės. Paryškintuoju šriftu pateiktos vertės, paimtos iš Lietuvos standarto LST 1974 [147]

Bandinio tipas	Kubinių/cilindrinų bandinių dydis (mm)		
	20 / 26,8	70 / 80	100 / 100
Liejimo būdu pagaminti kubiniai bandiniai	0,56	0,92	1,00
Presavimo būdu pagaminti cilindriniai bandiniai	0,80	0,93	0,93

Paskui PG 2 cm kraštinių kubeliai buvo suformuoti liejimo būdu, naudojant kiekvieną HH-PG tipą bei natūralų HH gipsą ir pakankamą vandens kiekį normalaus tirštumo tešlai gauti. Suformuoti bandiniai buvo kietinti 100 % drėgmės aplinkoje, taikant skirtingas kietėjimo trukmes: nuo 2 val. iki 28 parų. Praėjus atitinkamam kietinimo laikotarpiui, buvo išmatuoti visų bandinių LOI , ρ bei CS .



4 pav. Liejimo būdu suformuotų bandinių LOI (a), ρ (b) bei CS_{150} (c) rezultatai, esant skirtingoms kietėjimo trukmėms. Pastaba: I tipo PG bandinio ρ stulpelis po 2 val. kietėjimo yra pažymėtas punktyriniais kontūrais dėl bandinio minkštumo ir labai mažo stiprumo

4 paveiksle pateikta bandinių LOI , ρ bei CS_{150} priklausomybė nuo HH medžiagos tipo bei nuo kietėjimo 100 % drėgmės aplinkoje trukmės. Nustatyta, jog visų parametų tendencijos yra glaudžiai susijusios tarpusavyje. Bandinių hidratacijos laipsnio (LOI) vertės (4a pav.) didėja kartu su kietėjimo trukme. Natūralaus gipso bandinių kietėjimas vyksta greitai, pasiekiant beveik pilną hidrataciją vos per 2 val. kietėjimo. Tuo tarpu I tipo bandinių hidratacija vyksta lėčiausiai, pasiekiant maksimalią LOI vertę po 14 parų kietėjimo. II bei III tipo PG bandiniai kietėja greičiau, pasiekdami maksimalias LOI vertes per 7 paras. Hidratacijos greičių skirtumai tarp visų medžiagų gali būti paaiškunami HH kristaline mikrostruktūra (žr. 1 pav.). Natūralus HH gipsas yra sudarytas iš atskirų kristalų (žr. 1a pav.), prie kurių paviršių H_2O molekulės gali lengvai prisijungti reaguodamos su HH molekulėmis nei PG atveju, kur HH kristalai yra sulipę į konglomeratus

(žr. 1b, c, d pav.), taip kliudant vandeniui priartėti prie kristalų paviršių. Be to, I-tipo HH-PG kristalai yra plokšti ir prisiglaudę vienas prie kito (žr. 1b pav.), o tai dar labiau trukdo H₂O molekulėms prieiti prie jų paviršių, ir dėl to hidratacija vyksta gana lėtai. Tuo tarpu, II bei III tipų HH-PG kristalai yra masyvesni, ir palieka didesnių ertmių tarp jų, kurie palengvina hidratacijos procesą, kuris vyksta dvigubai greičiau nei I tipo atveju.

Medžiagų tankio rezultatai (žr. 4b pav.) yra iki tam tikro lygio susiję su *LOI* vertėmis – kuo pilnesnė hidratacija, tuo didesnis ρ . Tačiau akivaizdu, kad ρ taip pat priklauso nuo pačios medžiagos prigimties, nes nepaisant to, kad skirtingų PG bandinių *LOI* vertės yra panašios (pvz., po 14 kietėjimo parų), vis tiek I tipo PG bandiniai yra daug lengvesni ($\rho = 1300 \text{ kg/m}^3$) nei II bei III PG bandiniai ($\rho = 1463$ bei 1578 kg/m^3 , atitinkamai). Be to, pastebima, jog *CS*₁₅₀ tendencijos (žr. 4c pav.) koreliuoja su bandinių ρ vertėmis. Kuo tankesnis, tuo stipresnis bandinys. Didžiausia stiprumo verte *CS*₁₅₀ = 29 MPa pasižymėjo bandiniai, pagaminti naudojant III tipo PG, kietinti per 14 parų. Šis stiprumas yra net 2,6 kartus didesnis nei atitinkamų natūralaus gipso bandinių. Mažiausiu stiprumu *CS*₁₅₀ = 8 MPa pasižymėjo I tipo PG bandiniai.

Iš 4 paveikslo rezultatų galima daryti išvadą, jog bandinių *CS* stipriai priklauso nuo jų ρ . Tuo pačiu metu bandinių ρ priklauso nuo *LOI* bei nuo HH-PG prigimties.

Norint pilnai įvertinti PG naudojimo statybinėse medžiagose tinkamumą, reikia ne tik atsižvelgti į hidratacijos bei mechaninio stiprumo savybes, bet ir į radioaktyvumą. PG įprastai pasižymi reikšmingu radioaktyvumu lygiu, dėl to yra priskiriamas NORM (gamtoje pasitaikanti radioaktyvi medžiaga) kategorijai, o tai riboja jo naudojimo galimybes. Norint identifikuoti radioaktyvumo požįrius saugias medžiagas, Europos Sąjungoje yra nustatytas rekomendacinis radionuklidų aktyvumo koncentracijos rodiklis $I \leq 1,0$ statybinėms medžiagoms [63]. Šio rodiklio viršijimas parodo, kad medžiaga turi radiologinių rizikų ir jos naudojimas turi būti apribojamas arba net uždraustas. Rodiklis *I* yra apskaičiuojamas įvertinant ²²⁶Ra, ²³²Th bei ⁴⁰K radionuklidų aktyvumo koncentracijas. Radionuklido ²³²Th aktyvumo koncentracija yra atitinkamai apskaičiuota iš ²²⁸Ra bei ²²⁸Th koncentracijų.

7 lentelė. Kiekvienoje HH medžiagoje esančių pagrindinių radionuklidų aktyvumo koncentracijos (Bq/kg) bei rodiklių *I* vertės

HH medžiaga	²²⁶ Ra	²²⁸ Ra	²²⁸ Th	⁴⁰ K	²¹⁰ Pb	<i>I</i>
Natūralus gipsas	3,8 ± 0,3	3,2 ± 0,4	2,7 ± 0,6	128 ± 10	3,7 ± 1	0,07
I PG	200 ± 10	50,9 ± 2,6	47,4 ± 3,1	23,1 ± 6,3	237 ± 16	0,93
II PG	532 ± 50	191 ± 10	155 ± 10	25,3 ± 4,9	623 ± 22	2,74
III PG	49,1 ± 2,3	125 ± 10	116 ± 10	19,2 ± 3,5	38,4 ± 6,1	0,80

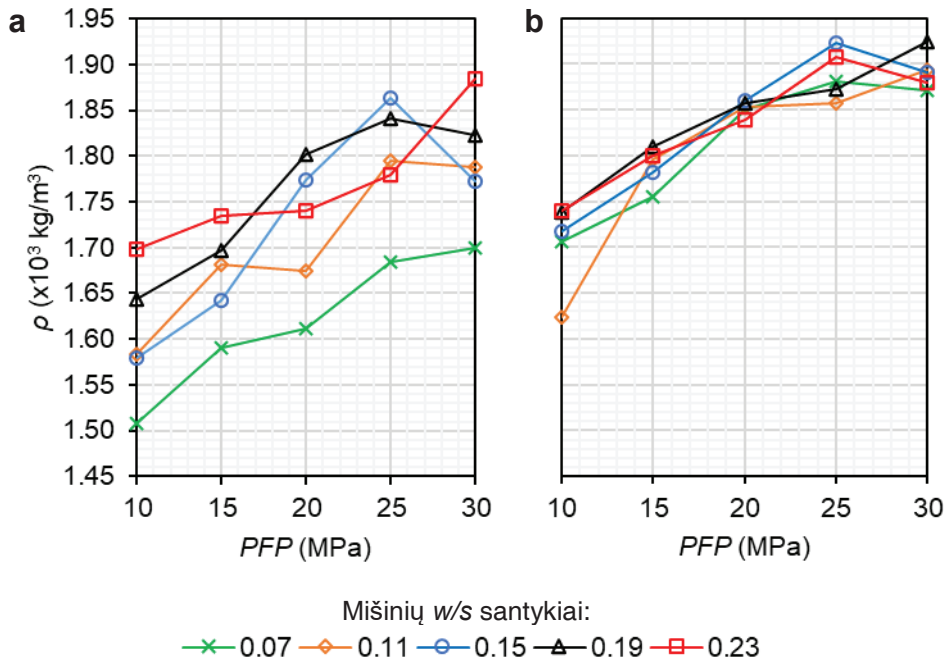
Nagrinėjamų HH medžiagų radionuklidų aktyvumo koncentracijos bei rodiklio *I* vertės yra pateiktos 7 lentelėje. Matoma, kad visi PG pasižymi daug aukštesniu radioaktyvumu nei natūralus gipsas. Pastebima aiški priklausomybė tarp skirtingų PG radioaktyvumo lygio ir jų kilmės (žr. 1 lentelę). Magminės kilmės PG (t. y. III tipo) pasižymi žemesniu radioaktyvumu nei nuosėdinės kilmės PG (t. y. II tipo). O I tipo PG sudarytas iš abiejų tipų uolienu, ir jo rodiklio *I* vertė yra tarp

abiejų anksčiau minėtų verčių. Taigi, II tipo PG daugiau nei 2 kartais viršija ribą, todėl gali būti naudojamas statybinėse medžiagose su apribojimais. Tuo tarpu I bei III tipų PG tenkina ribą ir gali būti naudojami be apribojimų.

Atsižvelgiant į hidratacijos laipsnį, mechanines savybes bei radioaktyvumo lygį, galima teigti, kad tarp visų ištirtų HH-PG magminės kilmės III tipo yra tinkamiausia medžiaga naudojimui statybiniuose produktuose kaip rišamoji medžiaga.

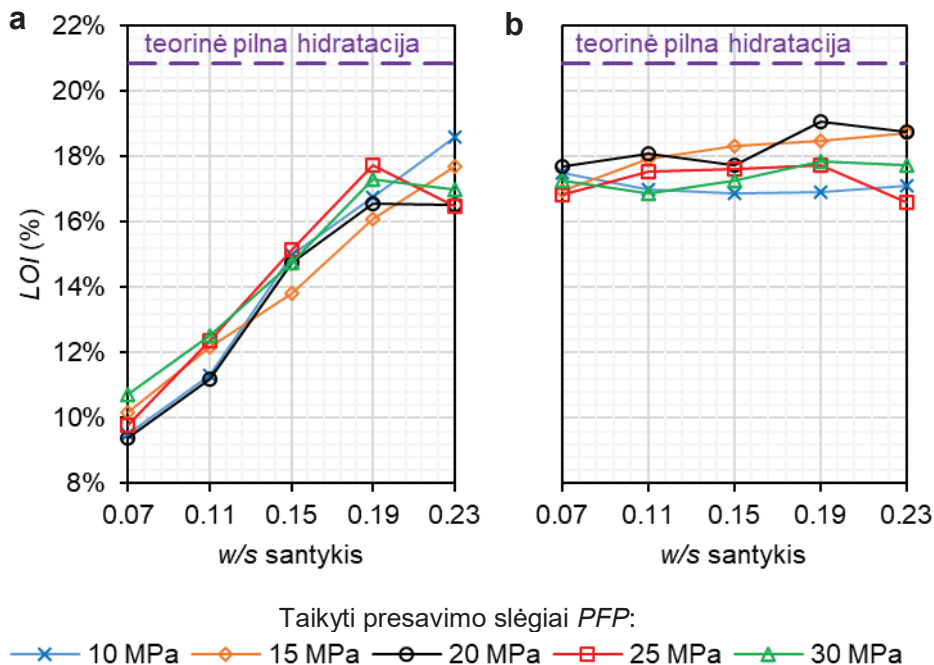
2.2. PG bandinių mechaninių savybių gerinimas taikant presavimo formavimo metodą

Antruoju tyrimo etapu buvo analizuojamas PG mišinio presavimas, kaip būdas pagaminti tankesnius ir tuo pačiu metu stipresnius bandinius. Tačiau presavimo procesas turi vieną svarbų trūkumą: tam, kad vanduo nepasišalintų dėl slėgio veikimo formuojant bandinius, vandens bei HH-PG santykis (w/s) turi būti daug mažesnis nei mišiniuose, skirtuose formuoti liejimo būdu. Jeigu formavimo mišinyje pasitaikytų per didelis vandens kiekis, presavimo slėgis išstumtų tam tikrą vandens kiekį iš medžiagos, ir taip susiformuotų mikrokanalai bei poros, kurie turi įtakos bandinio porėtesnei mikrostruktūrai bei kenkia jo mechaninėms savybėms. Dėl to, dažniausiai, presuotų bandinių hidratacijos laipsnis būna neaukštas, ir papildomas sąlytis su vandeniu arba drėgme gali sukelti nepageidaujamų tūrio pasikeitimų. Tam, kad būtų pašalintas šis trūkumas, kai kuriais atvejais buvo taikomas Zhou et al. [94] pasiūlytas metodas, t. y., supresuoti bei po 1 paros kietinami pusfabrikačiai buvo mirkyti 45 minutes, o paskui kietinimas buvo tęsiamas iki 7 parų laikotarpio. Bandinių savybių palyginimui, kiti bandiniai buvo kietinami tokiu pat būdu, bet neatliekant merkimo. Taigi, presavimo metodas buvo išsamiai ištirtas, analizuojant svarbiausių parametru, tokių kaip presavimo slėgio (PPF), mišinių w/s santykio bei pusfabrikačių kietinimo būdo (be merkimo arba su merkimu) įtaką bandinių savybėms: LOI , ρ bei CS . Šio eksperimento metu presavimo būdu buvo pagaminti 80 x 80 mm cilindriniai bandiniai, ir dėl to standartinės CS_{150} vertės buvo gaunamos taikant koeficientą $ScF = 0,93$ eksperimentiniams CS rezultatams (žr. 6 lentelę). Naudotas HH-PG buvo panašus į II tipo PG. Nepaisant to, kad 1-ame tyrimo etape buvo nustatyta, jog šio tipo gipsas yra netinkamas naudoti statybinėse medžiagose (dėl aukšto radioaktyvumo), gaunami rezultatai apie presavimą gali būti taikomi ir tinkamesniam III tipo PG.



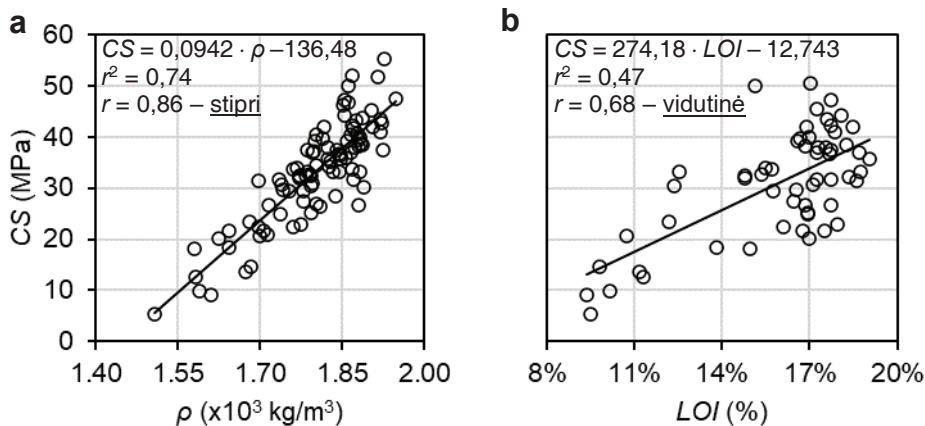
5 pav. Sukietėjusių bandinių, apdorotų taikant kietinimą be merkimo (a) arba su merkimu (b), slėgio *PFP* bei santykio *w/s* įtaka bandinių tankiui ρ

Kaip matėme 1-ame tyrimo etape, bandinių ρ daugiausiai lemia mechanines savybes. Dėl to 5 paveiksle pateikiama ρ priklausomybė nuo taikyto *PFP*, esant skirtingiems *w/s* santykiams bei taikant kietinimą be merkimo arba su juo. Visais atvejais pastebima tiesioginė priklausomybė tarp *PFP* bei ρ : didinant *PFP*, ryškiai didėja ir ρ vertės. Tačiau, pasiekus *PFP* =25 MPa, rezultatai stabilizuojasi, ir padidinant toliau *PFP* iki 30 MPa, ρ vertės nedidėja arba netgi mažėja. Tai rodo, kad bandinių mikrostruktūra gali būti žalojama taikant per didelius *PFP*. Mišinio *w/s* santykis taip pat daro įtaką bandinių ρ vertėms, kai taikomas kietinimas be merkimo (žr. 5a pav.). Šiuo atveju ρ vertės didėja, kai *w/s* kyla nuo 0,07 iki 0,19, o paskui tendencijos tampa neaiškios. Kitą vertus, kai bandinių kietinimas su merkimu yra taikomas (žr. 5b pav.), bandinių ρ nebesipriklauso nuo pritaikyto *w/s* santykio. Tai rodo, kad merkimo procesas „pataiso“ vandens trūkumą hidratacijos procese, sukeltiant nehidratuotų HH-PG kristalų antrinę kristalizavimą.



6 pav. Sukietėjusių bandinių, apdorotų taikant kietinimą be merkimo (**a**) arba su merkimu (**b**), w/s santykio bei presavimo slėgio PFP įtaka bandinių LOI

Bandinių w/s santykio, PFP kietinimo rūšies įtakos hidratacijos (be arba su merkimu) lygiui (LOI) yra pateikiamos 6 paveiksle. Visais atvejais galima pastebėti, jog LOI vertės nepriklauso (arba nereikšmingai priklauso) nuo naudoto PFP. Kitą vertus, kai merkimas nebuvo taikomas (žr. 6a pav.), bandinių LOI vertės stipriai priklausė nuo w/s santykio: kuo didesnis mišinio w/s santykis, tuo aukštesnis hidratacijos lygis. Tačiau, kai merkimas buvo taikomas (žr. 6b pav.), bandinių LOI tapo nebe priklausomi nuo w/s santykio. Galima daryti išvadą, kad merkimo procesas leidžia sumažinti w/s santykį mišinyje, išlaikant tinkamas LOI vertes.



7 pav. Tiesinės koreliacijos analizės tarp ρ bei CS (a) ir tarp LOI bei CS (b) su atitinkamais koreliacijos koeficientais r bei jų interpretacija

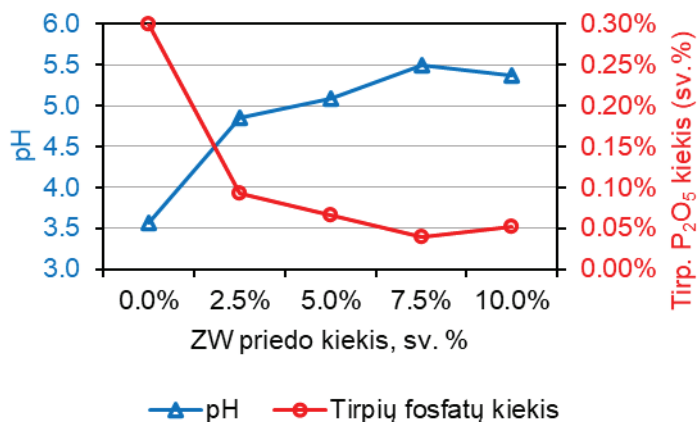
Bandinių CS verčių priklausomybė nuo ρ bei nuo LOI yra pateikiama, atitinkamai, 7a bei 7b paveiksluose. Tiesinės koreliacijos yra analizuojamos bei interpretuojamos pagal gautas atitinkamas koreliacijos koeficiento (r) vertes [149]. Priklausomybė $\rho - CS$ pasižymi „stipria“ koreliacija, o $LOI - CS$ priklausomybė – vidutinė. Kitaip tariant, abu faktoriai: bandinių ρ bei LOI turi įtakos CS vertėms, nors didesnę įtaką daro ρ .

Didžiausias bandinių stiprumas buvo $CS_{150} = 46,5$ MPa, kai bandiniai buvo formuojami taikant $w/s = 0,15$, $PPF = 25$ MPa ir kietinimą be merkimo. Tačiau šis variantas yra nerekomenduotinas, nes bandiniai tuo pačiu ir pasižymi žemu hidratacijos lygiu ($LOI = 15,1$ %). Todėl autoriaus rekomenduojamas formavimo variantas yra $w/s = 0,19$, $PPF = 20$ MPa bei kietinimas su merkimu, nes bandiniai pasižymi dideliu (nors ne didžiausiu) stiprumu, $CS_{150} = 35,3$ MPa, bei geriausia iš visų hidratacija, $LOI = 19,1$ %.

2.3. PG tirpių bei rūgščių P_2O_5 bei F^- junginių mažinimas, naudojant ceolito atliekos (ZW) priedą

Ceolitas yra mikroporėta medžiaga (žr. 2a paveikslą), kuri, pagal Sabadash et al. tyrimų rezultatus [152], efektyviai suriša tirpius fosfatus adsorbcijos būdu, pagrįstu jonų mainų bei cheminės sorbcijos procesais. Todėl trečiame tyrimo etape yra nagrinėjama ZW priedo įtaka PG bandinių tirpių fosfatų junginių mažinimui. Be to, buvo analizuojamas ZW priedo poveikis bandinių hidratacijos laipsniui bei CS vertėms.

Tam tikslui presavimo būdu buvo suformuoti 26,8x26,8 mm cilindriniai bandiniai, naudojant III tipo HH-PG (tinkamiausias iš visų). ZW priedas buvo įdėtas į mišinį skirtingais kiekiais. Supresuoti pusfabrikačiai buvo kietinami 100 % drėgmės aplinkoje kambario temperatūroje, vėliau po 1 paros kietinimo taikant merkimą (kaip aprašyta 2-ame tyrimo etape). Standartinės CS_{150} vertės buvo gaunamos taikant bandinių dydžio koeficientą $ScF = 0,80$ eksperimentiniams CS rezultatams (žr. 6 lentelę).



8 pav. pH bei tirpus P₂O₅ kiekio priklausomybė nuo ZW priedo kiekio PG bandinyje

Tirpių rūgščių junginių kiekio priklausomybė nuo ZW priedo kiekio PG bandiniuose buvo nagrinėta pH matavimais bei tirpių P₂O₅ junginių kiekio kolorimetrine analize, kurių rezultatai yra pateikti 8 paveiksle. Tirpių F⁻ junginių kiekio matavimai nebuvo atlikti, nes III tipo HH-PG medžiagoje fluoro nebuvo aptikta (žr. 2 lentelę). Analizių rezultatai parodo, kad didinant ZW kiekį PG bandiniuose nuo 0 iki 7,5 sv %, bandinių pH didėja nuo 3,56 iki 5,49, ir, atitinkamai, tirpių P₂O₅ kiekis mažėja nuo 0,30 sv % iki 0,04 sv %. Tai reiškia, kad kai 7,5 sv % ZW buvo įterpta į PG bandinius, tirpių junginių kiekis sumažėjo netgi 7,5 kartais. Tolesnis ZW kiekio didinimas neturėjo įtakos nei pH vertėms, nei tirpių fosfatų kiekiui, kurių vertės išliko stabilios.

8 lentelė. PG bandinių kristalinės fazės kiekybinė analizė, atlikta XRD *Rietveld* metodu

Junginys	PG bandinių kristalinė sudėtis su skirtingais ZW kiekiais		
	0 sv % ZW	2,5 sv % ZW	10 sv % ZW
DH gipsas	78,1 %	83,6 %	95,0 %
HH gipsas	19,6 %	14,2 %	2,8 %
Anhidritas	2,3 %	2,2 %	1,4 %
Kiti junginiai	-	-	0,8 %

Bandinių su skirtingais ZW priedo kiekiais hidratacijos lygis buvo vertinamas atliekant CaSO₄ kristalinių fazių kiekybinę analizę, apdorojant XRD matavimus *Rietveld* metodu. Šios analizės rezultatai yra pateikti 8 lentelėje. Aiškiai pastebima, jog ZW priedas skatina DH susiformavimą, didinant jų kiekį nuo 78,1 % iki 95,0 %, kai ZW kiekis yra, atitinkamai, 0 ir 10 sv %. ZW priedas ženkliai prisideda prie didesnės PG bandinių hidratacijos. Atrodo, kad šis reiškinys įvyksta dėl ZW priedo „H₂O grąžinimo“ mechanizmo. Kai mišinys yra paruošiamas, porėtos ZW dalelės sugeria tam tikrą vandens kiekį. Kietėjimo metu, kai supresuotų PG bandinių kristalams reikia daugiau vandens hidratacijos procesui, ZW dalelės „grąžina“ absorbuotą vandens kiekį PG dalelėms, taip skatindamos papildomą hidrataciją. Šis

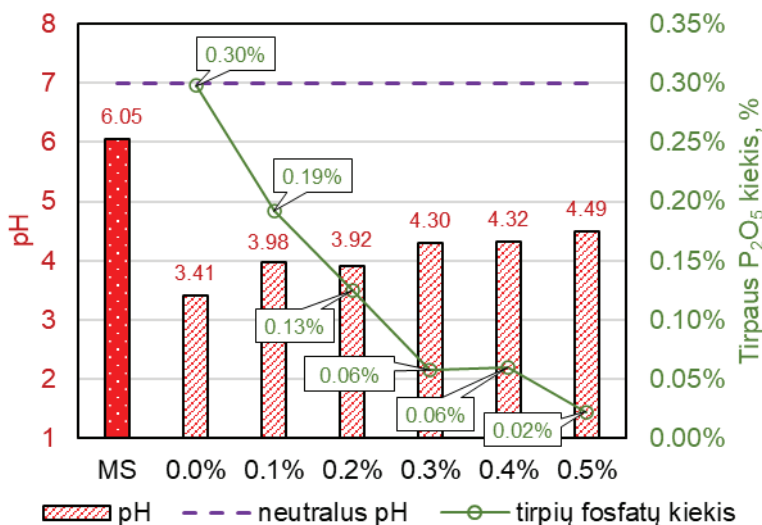
mechanizmas buvo aptiktas Zhou ir Chen [153], kurie panaudojo ceolitą patalpų drėgmės mikroklimatui palaikyti.

Supresuotų PG bandinių CS priklausomybė nuo ZW kiekio taip pat buvo nagrinėta. Bendrai atsižvelgiant į PG bandinių rūgščių bei tirpių junginių mažinimą, į hidratacijos pagerinimą bei į mechanines savybes, autoriaus rekomenduojami pradinio mišinio apdorojimo parametrai yra tokie: ZW priedo kiekis: 7,5 sv %; $PPF = 25$ MPa. Buvo gautos tokios bandinių optimalios savybės: 7,5 kartais mažesnis P_2O_5 kiekis nei kontrolinių bandinių, aukštas hidratacijos laipsnis bei $CS_{150} = 45$ MPa.

2.4. PG bandinių vandens atsparumo padidinimas pridedant metalurgijos šlamo atliekos (MS) priedą

Kaip jau buvo minėta, gipsiniai rišikliai yra ekologiška alternatyva populiariausiam PC naudojimui konstrukciniuose statybinuose elementuose. Tačiau gipsas yra orinė rišamoji medžiaga, t. y. kietėja ir yra eksploatuojama sausoje aplinkoje. Dėl to drėgnose aplinkose gipsiniai produktai tirpsta ir suminkštėja. Tuo tarpu PC yra hidraulinė rišamoji medžiaga ir kietėja vandenyje. Todėl gipsas įprastai yra naudojamas kaip statybinė medžiaga pastatų vidaus darbuose: vidaus paviršių apdailai bei gipskartonio plokštėms, pertvarkų blokeliams ir panašiai. Norint sumažinti šių gipsinių produktų trūkumą ir plėsti jų pritaikymo galimybes lauko sąlygomis, jų atsparumas vandeniui turi būti padidintas. Įprastai tai yra daroma įmaišant polimerus arba kitus organinius junginius, arba naudojant pucolanines medžiagas. Pucolaninė aktyvacija vyksta, kai tam tikri pucolaniniai priedai, tokie kaip pelenai (FA), aukštakrosnių šlakas (BFS), silicio dulkės arba ceolitai, yra aktyvuojami tam tikru PC kiekiu gipso mišinyje. Tačiau šitie sprendimai yra brangūs arba sudėtingi. Dėl to šiame 4-ame tyrimo etape PG bandinių atsparumas vandeniui buvo padidintas įterpiant mažą kiekį MS dulkių, panašiai kaip siūlo Pervyshin et al. [121].

Eksperimentas buvo atliekamas formuojant liejimo būdu 20 mm kraštinių kubelius, kurie paskui buvo kietinami 100 % drėgmės aplinkoje, kambario temperatūroje ir galiausiai išdžiovinti iki pastovios masės. Standartinės CS_{150} vertės buvo gaunamos taikant koeficientą $ScF = 0,56$ eksperimentiškai gautiems CS rezultatams (žr. 6 lentelę).



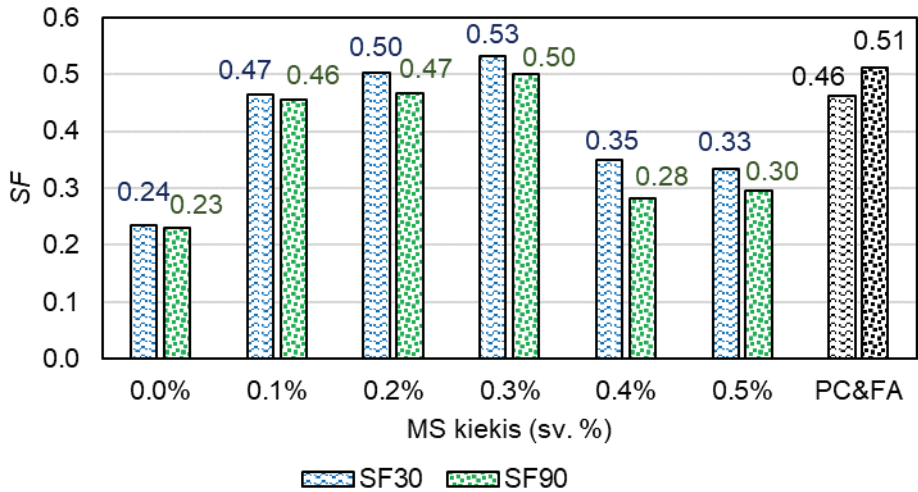
9 pav. pH bei tirpus P₂O₅ kiekio priklausomybės nuo MS kiekio PG bandiniuose

Visų pirma, tirpių bei rūgščių junginių neutralizavimas MS priedu buvo nustatytas pH bei tirpių P₂O₅ junginių matavimais. Šių analizių rezultatai pateikti 9 paveiksle. MS priedas, kuriame vyrauja geležies oksidas, teoriškai suriša tirpų P₂O₅ į netirpius junginius, pagal reakcijas (1) bei (2), kurias pateikia Vaičiukynienė et al. [7] ir Sviklas et al. [157].



9 paveiksle pastebimos ryškios priklausomybės tarp bandinių pH bei tirpus P₂O₅ turinio ir MS kiekio. Didinant MS priedo kiekį nuo 0 iki 0,5 sv %, bandinių pH neženkliai didėja nuo 3,41 iki 4,49, o tirpus P₂O₅ kiekis labai stipriai mažėja nuo 0,30 % iki 0,02 %. Galima pasakyti, jog MS efektas mažinant tirpus P₂O₅ kiekį yra labai ženklaus, turint omenyje, kad su beveik nereikšmingu MS priedo kiekiu (0,5 sv %) šių junginių kiekis sumažėjo apie 15 kartų.

MS priedo efektyvumą mažinant tirpus P₂O₅ kiekį galima lyginti su kitais, panaudotais priedais šiame tyrime: Ca(OH)₂ bei ZW. Suskaičiavus santykį tarp tirpių P₂O₅ junginių kiekio mažinimo (kartais) bei naudotų priedo kiekio (sv %), galima teigti, kad efektyviausiai pasirodė MS (30 kart. / sv %), o paskui Ca(OH)₂ (26,6 kart. / sv %). Mažiausiai efektyvus pasirodė ZW priedas (1,0 kart. / sv %).



10 pav. Mirkėtų PG bandinių minkštėjimo koeficiento SF priklausomybė nuo MS kiekio, esant 30 parų (SF_{30}) arba 90 parų (SF_{90}) mirkymo periodui. Papildomai pateikiami su pucolaniniu priedu pagamintų bandinių atitinkami rezultatai (stulpeliai „PC&FA“)

Vandens atsparumo matavimams bandiniai su MS priedu buvo atskiriami į tris grupes. Pirmajai grupei buvo atliktas CS testas iš karto po džiovinimo. Antra grupė po džiovinimo buvo įmirkyta į vandenį ir palaikyta jame 30 parų. Praėjus šiam laikotarpiui, šlapiems bandiniams buvo atliekamas CS testas. Trečiajai bandinių grupei procedūros tokios pačios kaip antrai grupei, bet su ilgesne merkimo trukme – 90 parų. Bandinių stiprumo mažėjimas dėl sąlyčio su vandeniu yra išreiškiamas minkštėjimo koeficientu (SF), kuris skaičiuojamas kaip atitinkamos sudėties šlapių bei sausų bandinių stiprumų santykis. Bandinių su skirtingais MS priedo kiekiais SF rezultatai yra pateikti 10 paveiksle. Priklausomai nuo bandinių merkimo periodo trukmės (30 arba 90 parų) minkštėjimo koeficientai pažymėti, atitinkamai, SF_{30} bei SF_{90} . Gauti rezultatai parodė, jog lyginant su kontroliniais bandiniais (be priedo), MS priedas ženklai pagerina SF vertes, ypač kai MS kiekis yra nuo 0,1 iki 0,3 sv %, kuomet SF vertės padidėja dvigubai. Didžiausios SF vertės yra pasiektos su 0,3 sv % MS. Toliau didinant MS kiekį, SF koeficientai vėl mažėja. Grafike taip pat galima pastebėti, kad visais bandinių su MS priedu atvejais $SF_{30} > SF_{90}$. Kitaip tariant, ilgesnis merkimas papildomai minkština bandinius.

Palyginimui buvo suformuoti bei išbandyti kai kurie bandiniai su pucolaniniu priedu, naudojant 20 sv % PC ir 5 sv % FA į PG mišinį. Šių bandinių rezultatai pateikti 10 paveiksle „PC&FA“ žymėjimu. Šiuo atveju, gautos SF vertės yra labai panašios į bandinių su MS priedu geriausias SF vertes. Tačiau pagrindinis skirtumas yra tai, jog „PC&FA“ bandiniuose $SF_{30} < SF_{90}$. Tai reiškia, kad pucolanų aktyvacijos mechanizmas „kietina“ bandinius ilgesnio merkimo laikotarpio eigoje.

Pastebėta, jog atsparumo vandeniui pagerinimas naudojant MS priedą vyksta dėl to, kad MS dalelės skatina C-S-H amorfinių junginių susiformavimą aplink PG kristalus, kurie apsaugo juos nuo tirpimo vandens aplinkoje.

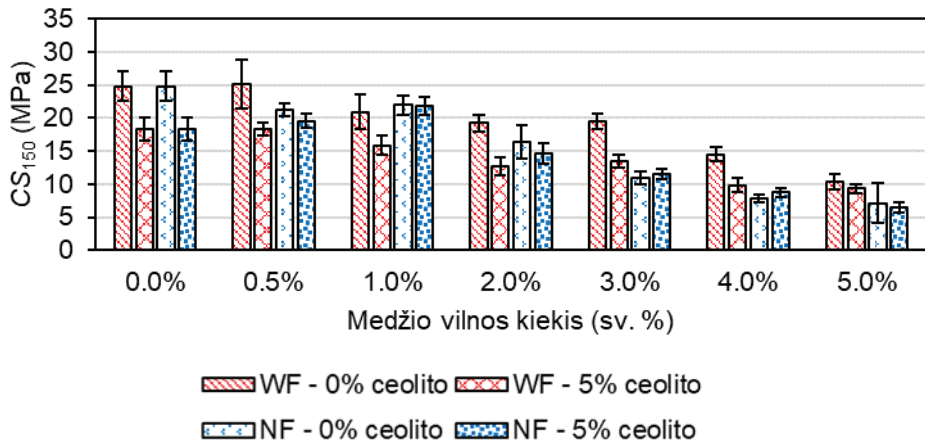
Apibendrinant šio, 4-ojo tyrimo etapo, rezultatus, galima teigti, jog mažas MS priedo kiekio naudojimas yra efektyvus būdas mažinti tirpių rūgščių junginių kiekį PG bandiniuose ir, tuo pačiu, padidinti jų atsparumą vandeniui net du kartus, palyginti su bandiniais, neturinčiais MS priedo. Be to, MS priedo naudojimas yra daug paprastesnis bei reikalauja mažesnių priedo kiekių nei įprastai taikomas pucolaninės aktyvacijos mechanizmas.

2.5. PG gaminių termoizoliacinių savybių gerinimas naudojant medžio atliekas (WF) priedą

Norint pritaikyti PG statybiniuose produktuose, ne tik reikia pagerinti jų mechanines arba hidratacijos savybes, arba mažinti kenksmingų junginių (tirpių fosfatų bei fluoridų) kiekį. Kai statybinė medžiaga yra naudojama pastato pertvarose (pvz., konstrukciniuose blokeliuose arba plytose), taip pat yra svarbūs jų fizikiniai ypatumai, tokie kaip šilumos bei triukšmo izoliaciniai parametrai. Dėl to 5-ame tyrimo etape, 0–5 sv % atliekinio WF plaušo priedas buvo naudotas bandiniuose tam, kad pagerintų šias fizikines PG bandinių charakteristikas. Kartu su šituo priedu buvo naudota ir 5 wt % ZW priedo, tam kad būtų surišti kenksmingi tirpūs junginiai, kaip tirta 3-ame tyrimo etape. Rezultatų palyginimui, kai kuriuose bandiniuose NF plaušas buvo įterptas vietoj WF plaušo.

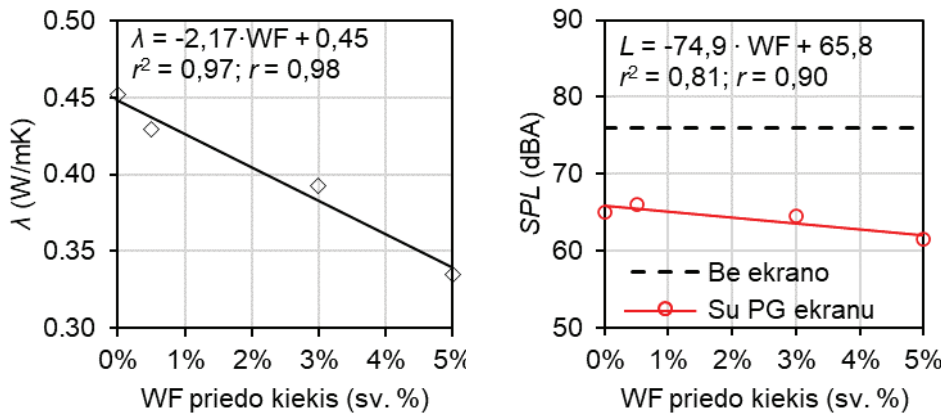
Minėtos savybės buvo tiriamos liejimo būdu formuojant skirtingo dydžio bandinius. *CS* buvo nustatytas su 2 cm kraštinių kubeliais, šilumos laidumo koeficientas (λ) buvo matuojamas naudojant 300x300x50 mm PG plokštes, o garso slėgio lygis (*SPL*) buvo nustatytas slopinant skleistą garsą 245x245x18 mm PG ekranais. Visais atvejais buvo naudotas III tipo HH-PG.

Paminėtina tai, kad *CS* testams (rezultatų palyginimui) buvo formuojami keturių serijų bandiniai, besiskiriantys naudotais priedais (WF arba NF) ir ZW priedo buvimu arba nebuvimu: bandinių serija Nr. 1 – naudojamas WF priedas, be ZW priedo; bandinių serija Nr. 2 – naudojamas WF priedas bei 5 sv % ZW priedo; bandinių serija Nr. 3 – naudojamas NF priedas, be ZW priedo; bandinių serija Nr. 4 – naudojamas NF priedas bei 5 sv % ZW priedo. Kiti tyrimai (šiluminių bei akustinių savybių testai) buvo atlikti su serijos Nr. 2 bandiniais.



11 pav. PG bandinių CS_{150} priklausomybė nuo medžio plaušo priedo kiekio bei rūšies (WF arba NF) ir nuo ZW priedo buvimo arba nebuvimo

Visų keturių bandinių serijų CS rezultatai yra pateikti 11 paveiksle. Pastebima ryški CS priklausomybė nuo plaušo kiekio – kuo didesnis WF arba NF kiekis, tuo silpnesni bandiniai. ZW priedas pablogina bandinių stiprumą, kai naudojamas kartu su WF priedu, tačiau nedaro reikšmingos įtakos jį naudojant kartu su NF priedu. Nepaisant to, bandiniai su WF CS_{150} vertės dauguma atvejų yra didesni nei bandinių su NF vertės.



12 pav. PG bandinių šilumos laidumo λ (a) bei garso slėgio lygio SPL (b) priklausomybė nuo WF priedo kiekio

Serijos Nr. 1 fizikinių bandinių savybės, λ bei SPL , yra pateiktos 12a bei 12b paveiksluose, atitinkamai. Matoma, kad bandinių termoizoliacinės savybės pagerėja (λ vertės mažėja) didinant WF kiekį. Palyginus su kontroliniais bandiniais, λ mažėja 13 %, naudojant 3 sv % WF, ir net 27 %, kai WF kiekis buvo padidintas iki 5 sv %. Atsižvelgiant į triukšmo izoliacijos efektą (žr. 12b paveikslą), galima pastebėti panašias, nors mažiau ryškias tendencijas: didinant WF kiekį PG

bandiniuose, mažėja skleidžiamas triukšmo lygis *SPL*. Lyginant su kontroliniais bandiniais (be WF priedo), kai WF priedo kiekis bandiniuose yra 3 wt %, *SPL* mažėja 0,8 %, o kai WF kiekis yra 5 wt %, *SPL* mažėja net 5,4 %. Todėl galima daryti išvadą, kad WF priedo naudojimas šiek tiek pagerina šilumos bei triukšmo izoliacines savybes, ypač kai priedo kiekis yra didesnis.

9 lentelė. Rekomenduojamos sudėties bandinių mechaninės, šiluminės bei akustinės savybės

Rekomenduojama bandinių sudėtis	Parametras	Rekomenduojamo bandinio parametro vertės, n_{rec}	Kontrolinio bandinio parametrų vertės, n_0	n_{rec} / n_0
93 sv % PG	CS_{150}	13,5 MPa	18,2 MPa	0,74
5 sv % ZW	λ	0,39 W/mK	0,45 W/mK	0,87
3 sv % WF	<i>SPL</i>	64,5 dBA	65,0 dBA	0,99

Šilumos laidumo analizė parodė, jog esant didžiausiam (5 sv %) WF priedo kiekiui, bandiniai pasižymi geriausiomis termoizoliacinėmis savybėmis (žr. 12a pav.). Tačiau 11 paveiksle matoma, jog šių bandinių CS vertės yra mažos ($CS_{150} < 10$ MPa). Todėl, autoriaus manymu, rekomenduojama bandinių sudėtis yra su 3 sv % WF priedo, kuomet termoizoliacinis pagerinimas yra dar reikšmingas ($\lambda = 0,39$ W/mK, t. y. 13 % mažesnis už kontrolinių bandinių), o CS vertės yra didesnės ($CS_{150} < 10$ MPa). Šios rekomenduojamos sudėties bandinių savybės n_{rec} bei (palyginimui) kontrolinių bandinių savybės n_0 yra pateiktos 9 lentelėje.

3. Pagrindiniai rezultatai bei išvados

Šio mokslinio tyrimo metu pagrindinis tikslas buvo įvertinti PG rišamosios medžiagos naudojimo statybiniuose gaminiuose tinkamumą. Jeigu tai pasitvirtintų, PG sandėliavimo kalnų sukeltos aplinkosauginės problemos, lydinės fosfatinių trąšų gamybos procesą, galėtų būti reikšmingai sumažintos. Be to, PG rišamoji medžiaga galėtų būti pigesnė bei ekologiška alternatyva dažniau naudojamam PC. Dėl šių priežasčių darbe buvo išsamiai išnagrinėta HH-PG prigimties, apdorojimo metodo, įterptų priedų (hidratuotų kalkių, ZW, MS bei WF) įtaka radioaktyvumo lygiui, tirpių rūgščių P_2O_5 bei F^- mažinimui, hidratacijos laipsniui ir fizikinėms-mechaninėms savybėms (tokioms kaip ρ , CS , FS , SF po merkimo ir λ). Pagrindinės darbo išvados, kurios yra toliau pateikiamos, leidžia pagrįstai teigti, jog naudojant tinkamą HH-PG tipą, efektyvų apdorojimo metodą bei parenkant tinkamus priedus, PG bandinių parametrai tenkina konstrukcinių elementų reikalavimus ir PG gali būti naudojamas laikančių sienų plytoms arba blokeliams gaminti.

- 1. Radiologinis vertinimas.** Radionuklidų aktyvumo koncentracija stipriai priklausė nuo žaliavinės fosfatinės uolienos, iš kurios PG buvo gautas. Iš magminių uolienu pagamintas PG (I bei III PG tipai) pasižymėjo nedideliu radioaktyvumu ($I = 0,93$ bei 0,8, atitinkamai) bei tenkino Europos Sąjungoje rekomenduojamas radioaktyvumo ribas ($I \leq 1,0$). Tuo tarpu II tipo PG, gautas iš

nuosėdinių uolienu ($I = 2,74$), stipriai viršijo ribinę vertę ir jo naudojimas statybinėse medžiagose turi būti ribojamas.

2. **Rūgščių tirpių P_2O_5 bei F^- junginių neutralizavimas.** $Ca(OH)_2$ arba MS priedų įterpimas PG mišinyje veiksmingai sumažino tirpių P_2O_5 bei F^- kiekius, surišant juos į netirpius junginius. ZW atveju, tirpių junginių mažinimas vyko adsorbcijos būdu, kuris grindžiamas jonų mainų bei cheminės adsorbcijos mechanizmais. Tirpių fosfatų junginių turinį PG bandiniuose efektyviausiai mažino MS priedas (30 kart./sv %), o paskui $Ca(OH)_2$ priedas (26,6 kart./sv %). Mažiausiai efektyvus pasirodė ZW priedas (1,0 kart./sv %).

3. **PG bandinių hidratacijos laipsniui įtaką darantys veiksniai.**

a) **HH-PG kristalų formos bei geometrijos.** I tipo HH-PG, kurio kristalai buvo plokšti bei aštriabriauniai, pasižymėjo lėtu hidratacijos procesu, pasiekiant maksimalią vertę tik po 14 kietėjimo parų 100 % drėgmės aplinkoje. Tikėtina, kad plokščios kristalų formos apsunkino vandens patekimą prie jų paviršių. Tuo tarpu II bei III HH-PG tipai pasižymėjo apvalesniais bei masyvesniais kristalais, ir dėl to vandeniui nebuvo kliudoma patekti prie jų paviršių. Šie bandiniai visiškai hidratavosi per 7 paras.

b) **Bandinių formavimo metodai (liejimas arba presavimas).** Lietų bandinių hidratacijos laipsnis (LOI vertės) buvo didesnis nei presuotų bandinių, kurie be „papildomo apdoravimo“ pasižymėjo žema hidratacija. Tačiau buvo nustatyta, kad trumpai įmerkiant presuotus pusfabrikačius į vandenį praėjus parai nuo presavimo, sukietėjusių bandinių LOI vertės tapo pakankamos ir nebeprisklausančios nuo pradinio vandens kiekio.

c) **Priedai.** $Ca(OH)_2$ priedas stipriai lėtino PG hidratacijos procesą. Tuo tarpu ZW reikšmingai paskatino presuotų bandinių hidrataciją: DH kristalinė fazė padidėjo nuo 78,1 % iki 95 % (didinant ZW priedo kiekį nuo 0 iki 10 sv %, atitinkamai). Šis teigiamas efektas buvo priskiriamas ZW adsorbuoto vandens kiekio grąžinimo PG kristalams mechanizmui.

4. **PG bandinių mechaninėms savybėms įtaką darantys veiksniai.**

a) **HH-PG prigimtis.** I tipo HH-PG plokščios geometrijos kristalai lėmė bandinių porėtą mikrostruktūrą ir mažiausias iš visų stiprumo vertes ($CS_{150} = 8$ MPa). Kita vertus, masyvūs šešiakampių prizmių geometrija pasižymintys III tipo HH-PG kristalai lėmė tai, kad sukietėjusių bandinių mikrostruktūra buvo daug tankesnė (beveik be tuštumų) ir kad šių bandinių stiprumas būtų didžiausias iš visų tirtų ($CS_{150} = 29$ MPa) viršijant net 2,5 kartais natūralaus gipso bandinių stiprumo vertes. Lyginant su kitais PG tipais, III tipo PG pasižymėjo mažiausiu tirpių P_2O_5 bei F^- junginių kiekiu bei radioaktyvumu, greičiausia hidratacija bei didžiausia CS verte. Todėl visais atžvilgiais III tipo PG yra tinkamiausia rišamoji medžiaga iš visų tirtų tipų.

- b) **Presavimo formavimo metodas.** Visų PG tipų (išskyrus I tipo) presavimo būdu formuoti bandiniai pasižymėjo 1,6–2,1 kartų didesniais stiprumais nei atitinkami liejimo būdu suformuoti bandiniai. Stipriausi bandiniai pasiekė net $CS_{150} = 46,5$ MPa (apdorojimo parametrai: $PFPP = 25$ MPa, $w/s = 0,15$ bei netaikant merkimo kietėjimo metu). Tačiau šie bandiniai nerekomenduojami dėl mažo hidratacijos laipsnio ($LOI = 15,1\%$). Autoriaus požiūriu, optimalūs bandiniai pasižymėjo mažesniu stiprumu $CS_{150} = 35,3$ MPa ir pakankamu hidratacijos laipsniu $LOI = 19,1\%$ (apdorojimo parametrai: $w/s = 0,19$, $PFPP = 20$ MPa bei kietėjimas taikant bandinių papildomą merkimą į vandenį). Šių bandinių stiprumas yra tos pačios eilės kaip įprasto betono.
5. **Atsparumas vandeniui.** Įterpant 0,1–0,3 sv % MS į PG bandinių sudėtį, atsparumas vandeniui (įvertintas minkštėjimo koeficientu SF) buvo padidintas 2 kartus, palyginus su kontroliniais bandiniais. Naudojant didesnius MS kiekius (0,4 arba 0,5 sv %), koeficientas SF mažėjo. Be to, buvo nustatyta, kad atsparumo vandeniui didinimo mechanizmas yra pagrįstas netirpių amorfinių C-S-H junginių susiformavimu (dėl MS priedo įtakos), kurie apsaugojo PG kristalus nuo tirpimo vandenyje. Galima teigti, kad PG bandinių vandens atsparumo didinimas įterpant atliekinį MS yra paprastas, ekonomiškasis bei ekologiškasis technologinis procesas, lyginant su kitais taikomais metodais.
6. **Šilumos bei garso izoliacinės savybės.** Nustatyta atvirkštinė tiesinė koreliacija tarp įterpto WF kiekio PG bandinių sudėtyje bei šilumos laidumo koeficiento λ . Esant didžiausiam WF kiekiui (5 sv %), bandiniai atitinkamai turėjo mažiausią vertę, $\lambda = 0,33$ W/mK, t. y., 26 % mažesnę už kontrolinių bandinių (be WF). Tačiau šis variantas buvo nerekomenduojamas dėl mažo bandinių stiprumo ($CS_{150} < 10$ MPa). Dėl šios priežasties, autorius rekomendavo naudoti kompromisinį variantą tarp stiprumo bei šilumos izoliacijos savybių: rekomenduojamas WF kiekis yra 3 sv %, su kuriuo $\lambda = 0,39$ W/mK (13 % mažesnis už kontrolinių bandinių), o stiprumas $CS_{150} > 10$ MPa. Koeficiento λ mažinimas, kartu su dar tenkinančiu stiprumu, suteikia PG gaminiams geresnius parametrus naudoti kaip plytas arba blokelius pertvarose.

REFERENCES

1. IAEA. *Radiation Protection and Management of NORM Residues in the Phosphate Industry, Safety Reports Series no. 78*. Vienna: International Atomic Energy Agency (IAEA), 2013. ISBN 978-92-0135810-3.
2. *Mineral Commodity Summaries 2020*. Reston, VA: U.S. Geological Survey, 2020. Available from: <http://pubs.er.usgs.gov/publication/mcs2020>. USGS Publications Warehouse. DOI: <https://doi.org/10.3133/mcs2020>.
3. EN 13279-2:2014. *Gypsum Binders and Gypsum Plasters - Part 2: Test Methods*. Brussels: European Committee for Standardization, 2014.
4. *Phosphate Deposits of the World: Volume 2, Phosphate Rock Resources*. A. NOTHOLT, R.P. SHELDON and D.F. DAVIDSON eds., Cambridge University Press, 2005. ISBN 052167333X.
5. SAADAOU, E., N. GHAZEL, C. BEN ROMDHANE and N. MASSOUDI. Phosphogypsum: Potential Uses and Problems - a Review. *International Journal of Environmental Studies*. 2017, **74**(4), 558-567. ISSN 0020-7233. DOI: 10.1080/00207233.2017.1330582.
6. TAYIBI, H., et al. Environmental Impact and Management of Phosphogypsum. *Journal of Environmental Management*. 2009, **90**(8), 2377-2386. Available from: <http://www.sciencedirect.com/science/article/pii/S0301479709000784>. ISSN 0301-4797. DOI: <https://doi.org/10.1016/j.jenvman.2009.03.007>.
7. VAIČIUKYNIENĖ, D., D. NIZEVIČIENĖ and L. ŠEDUIKYTĖ. Sustainable Approach of the Utilization of Production Waste: The use of Phosphogypsum and AlF₃ Production Waste in Building Materials. In: *Energy efficient, sustainable building materials and products*. H. IZABELA ed., Krakow: Politechnika Krakowska, 2017, 183-197. ISBN 9788372429667.
8. RASHAD, A.M. Phosphogypsum as a Construction Material. *Journal of Cleaner Production*. 2017, **166**(Supplement C), 732-743. Available from: <http://www.sciencedirect.com/science/article/pii/S0959652617317699>. ISSN 0959-6526. DOI: <https://doi.org/10.1016/j.jclepro.2017.08.049>.
9. KOVLER, K. and M. SOMIN. Producing Environment-Conscious Building Materials from Contaminated Phosphogypsum. *Proceedings of the RILEM International Symposium on Environment-Conscious Materials and Systems for Sustainable Development (ECM 2004), Koriyama, Japan*. 2004, , 241-250.
10. MAZZILLI, B., V. PALMIRO, C. SAUEIA and M.B. NISTI. Radiochemical Characterization of Brazilian Phosphogypsum. *Journal of Environmental Radioactivity*. 2000, **49**(1), 113-122. Available from: <http://www.sciencedirect.com/science/article/pii/S0265931X99000971>. ISSN 0265-931X. DOI: [https://doi.org/10.1016/S0265-931X\(99\)00097-1](https://doi.org/10.1016/S0265-931X(99)00097-1).
11. SZAJERSKI, P. Distribution of Uranium and Thorium Chains Radionuclides in Different Fractions of Phosphogypsum Grains. *Environmental Science and Pollution Research International*. Germany: 2020, **27**(13), 15856-15868. Available from:

<https://www.ncbi.nlm.nih.gov/pubmed/32095961>. PubMed. ISSN 0944-1344. DOI: <https://doi.org/10.1007/s11356-020-08090-y>.

12. BOLIVAR, J.P., R. GARCIA-TENORIO and J. MAS. Radioactivity of Phosphogypsum in South-West of Spain. *Radiation Protection Dosimetry*. 1998, **76**(3), 185-189. [viewed 8/27/2020]. Available from:

<https://academic.oup.com/rpd/article/76/3/185/1631678>. ISSN 0144-8420. DOI: <https://doi.org/10.1093/oxfordjournals.rpd.a032263>.

13. CAMPOS, M.P., L.J.P. COSTA, M.B. NISTI and B.P. MAZZILLI. Phosphogypsum Recycling in the Building Materials Industry: Assessment of the Radon Exhalation Rate. *Journal of Environmental Radioactivity*. 2017, **172**, 232-236. Available from: <http://www.sciencedirect.com/science/article/pii/S0265931X16305392>. ISSN 0265-931X. DOI: <https://doi.org/10.1016/j.jenvrad.2017.04.002>.

14. NIZEVIČIENĖ, D., et al. The Treatment of Phosphogypsum with Zeolite to use it in Binding Material. *Construction and Building Materials*. 2018, **180**, 134-142. Available from: <http://www.sciencedirect.com/science/article/pii/S0950061818312923>. ISSN 0950-0618. DOI: <https://doi.org/10.1016/j.conbuildmat.2018.05.208>.

15. ENNACIRI, Y., I. ZDAH, H. EL ALAOUI-BELGHITI and M. BETTACH. Characterization and Purification of Waste Phosphogypsum to make it Suitable for use in the Plaster and the Cement Industry. *Chemical Engineering Communications*. Philadelphia: 2020, **207**(3), 382-392. Available from: <https://www.tandfonline.com/doi/full/10.1080/00986445.2019.1599865>. ISSN 0098-6445. DOI: <https://doi.org/10.1080/00986445.2019.1599865>.

16. KAZILIUNAS, A., V. LESKEVICIENE, B. VEKTARIS and Z. VALANCIUS. The Study of Neutralization of the Dihydrate Phosphogypsum Impurities. *Ceramics Silikaty*. 2006, **50**(3), 178-184.

17. SINGH, M. Effect of Phosphatic and Fluoride Impurities of Phosphogypsum on the Properties of Selenite Plaster. *Cement and Concrete Research*. 2003, **33**(9), 1363-1369. Available from: <http://www.sciencedirect.com/science/article/pii/S0008884603000681>. ISSN 0008-8846. DOI: [https://doi.org/10.1016/S0008-8846\(03\)00068-1](https://doi.org/10.1016/S0008-8846(03)00068-1).

18. SINGH, M. Treating Waste Phosphogypsum for Cement and Plaster Manufacture. *Cement and Concrete Research*. 2002, **32**(7), 1033-1038. Available from: <http://www.sciencedirect.com/science/article/pii/S0008884602007238>. ISSN 0008-8846. DOI: [https://doi.org/10.1016/S0008-8846\(02\)00723-8](https://doi.org/10.1016/S0008-8846(02)00723-8).

19. ALIEDEH, M.A. and N.A. JARRAH. Application of Full Factorial Design to Optimize Phosphogypsum Beneficiation Process (P₂O₅ Reduction) by using Sulfuric and Nitric Acid Solutions. *Sixth Jordanian International Chemical Engineering Conference, Amman, Jordan*. 2012, , 1-10. Available from: <http://jeaconf.org/UploadedFiles/Document/31365fa2-c30a-442c-ae60-bea341617140.pdf>.

20. World Health Organization. *Guidelines for Drinking-Water Quality*. 4th ed. Geneva: World Health Organization, 2017. ISBN 9789241549950.

21. TORRES-SÁNCHEZ, R., D. SÁNCHEZ-RODAS, Sánchez de la Campa, A. M. and de la Rosa, J. D. Hydrogen Fluoride Concentrations in Ambient Air of an Urban Area Based on the Emissions of a Major Phosphogypsum Deposit (SW, Europe). *Science of the Total Environment*. 2020, **714**, 136891. Available from:

<http://www.sciencedirect.com/science/article/pii/S0048969720304010>. ISSN 0048-9697.
DOI: <https://doi.org/10.1016/j.scitotenv.2020.136891>.

22. PÉREZ-LÓPEZ, R., et al. Dynamics of Contaminants in Phosphogypsum of the Fertilizer Industry of Huelva (SW Spain): From Phosphate Rock Ore to the Environment. *Applied Geochemistry*. 2010, **25**(5), 705-715. Available from: <http://www.sciencedirect.com/science/article/pii/S0883292710000521>. ISSN 0883-2927. DOI: <https://doi.org/10.1016/j.apgeochem.2010.02.003>.

23. MACÍAS, F., et al. Environmental Assessment and Management of Phosphogypsum According to European and United States of America Regulations. *Procedia Earth and Planetary Science*. 2017, **17**, 666-669. Available from: <http://www.sciencedirect.com/science/article/pii/S1878522016302120>. ISSN 1878-5220. DOI: <https://doi.org/10.1016/j.proeps.2016.12.178>.

24. RAFATI RAHIMZADEH, M., M. RAFATI RAHIMZADEH, S. KAZEMI and A. MOGHADAMNIA. Cadmium Toxicity and Treatment: An Update. *Caspian Journal of Internal Medicine*. 2017, **8**(3), 135-145. Available from: <https://pubmed.ncbi.nlm.nih.gov/28932363>
<https://www.ncbi.nlm.nih.gov/pmc/articles/PMC5596182/>. PubMed. ISSN 2008-6164. DOI: 10.22088/cjim.8.3.135.

25. XIE, F., T.A. ZHANG, D. DREISINGER and F. DOYLE. A Critical Review on Solvent Extraction of Rare Earths from Aqueous Solutions. *Minerals Engineering*. 2014, **56**, 10-28. Available from: <http://www.sciencedirect.com/science/article/pii/S0892687513003452>. ISSN 0892-6875. DOI: <https://doi.org/10.1016/j.mineng.2013.10.021>.

26. BINNEMANS, K., et al. Recycling of Rare Earths: A Critical Review. *Journal of Cleaner Production*. 2013, **51**, 1-22. Available from: <http://www.sciencedirect.com/science/article/pii/S0959652612006932>. ISSN 0959-6526. DOI: <https://doi.org/10.1016/j.jclepro.2012.12.037>.

27. SUN, M., et al. On the Production of mg-Nd Master Alloy from NdFeB Magnet Scraps. *Journal of Materials Processing Technology*. 2015, **218**, 57-61. Available from: <http://www.sciencedirect.com/science/article/pii/S0924013614004609>. ISSN 0924-0136. DOI: <https://doi.org/10.1016/j.jmatprotec.2014.11.036>.

28. European Commission–Enterprise and Industry. On the Review of the List of Critical Raw Materials for the EU and the Implementation of the Raw Materials Initiative. *Commission of European Communities Communication no 297*. 2014, .

29. KULCZYCKA, J., Z. KOWALSKI, M. SMOL and H. WIRTH. Evaluation of the Recovery of Rare Earth Elements (REE) from Phosphogypsum Waste – Case Study of the WIZÓW Chemical Plant (Poland). *Journal of Cleaner Production*. 2016, **113**, 345-354. Available from: <http://www.sciencedirect.com/science/article/pii/S0959652615016790>. ISSN 0959-6526. DOI: <https://doi.org/10.1016/j.jclepro.2015.11.039>.

30. RYCHKOV, V.N., et al. Recovery of Rare Earth Elements from Phosphogypsum. *Journal of Cleaner Production*. 2018, **196**, 674-681. Available from: <http://www.sciencedirect.com/science/article/pii/S0959652618317645>. ISSN 0959-6526. DOI: <https://doi.org/10.1016/j.jclepro.2018.06.114>.

31. RUTHERFORD, P.M., M.J. DUDAS and R.A. SAMEK. Environmental Impacts of Phosphogypsum. *Science of the Total Environment*. 1994, **149**(1), 1-38. Available from: <http://www.sciencedirect.com/science/article/pii/0048969794900027>. ISSN 0048-9697. DOI: [https://doi.org/10.1016/0048-9697\(94\)90002-7](https://doi.org/10.1016/0048-9697(94)90002-7).
32. AL ATTAR, L., et al. Radiological Impacts of Phosphogypsum. *Journal of Environmental Management*. 2011, **92**(9), 2151-2158. Available from: <http://www.sciencedirect.com/science/article/pii/S0301479711001071>. ISSN 0301-4797. DOI: <https://doi.org/10.1016/j.jenvman.2011.03.041>.
33. DUEÑAS, C., M.C. FERNÁNDEZ, S. CAÑETE and M. PÉREZ. Radiological Impacts of Natural Radioactivity from Phosphogypsum Piles in Huelva (Spain). *Radiation Measurements*. 2010, **45**(2), 242-246. Available from: <http://www.sciencedirect.com/science/article/pii/S1350448710000089>. ISSN 1350-4487. DOI: <https://doi.org/10.1016/j.radmeas.2010.01.007>.
34. International Commission of Radiological Protection. *ICRP Publication 60: 1990 Recommendations of the International Commission on Radiological Protection: Annals of the ICRP*. 1st ed. Oxford, New York, Seoul, Tokyo, Sydney, Frankfurt: Pergamon Press, 1991. Available from: <http://www.icrp.org/publication.asp?id=ICRP%20Publication%2060>. DOI: [https://doi.org/10.1016/0306-4549\(92\)90053-E](https://doi.org/10.1016/0306-4549(92)90053-E).
35. CÁNOVAS, C.R., F. MACÍAS, R. PÉREZ LÓPEZ and J.M. NIETO. Mobility of Rare Earth Elements, Yttrium and Scandium from a Phosphogypsum Stack: Environmental and Economic Implications. *Science of the Total Environment*. 2018, **618**, 847-857. Available from: <http://www.sciencedirect.com/science/article/pii/S0048969717322192>. ISSN 0048-9697. DOI: <https://doi.org/10.1016/j.scitotenv.2017.08.220>.
36. US Environmental Protection Agency (EPA). *40 CFR Subpart R. National Emission Standards for Radon Emissions from Phosphogypsum Stacks*. 1992. Available from: https://www.law.cornell.edu/rio/citation/57_FR_23317. Federal Register, 57 FR 23317.
37. The Fertilizer Institute. *Revised Request for Approval of Additional Uses of Phosphogypsum Pursuant to 40 C.F.R. § 61.206: Use in Road Construction Projects Authorized by Federal, State and Local Departments of Transportation Or Public Works*. 2020. Available from: <https://www.epa.gov/radiation/approval-other-uses-phosphogypsum-supporting-documents>.
38. US Environmental Protection Agency (EPA). *Approval of the Request for Other use of Phosphogypsum by the Fertilizer Institute*. 2020. Available from: <https://www.federalregister.gov/documents/2020/10/20/2020-23154/approval-of-the-request-for-other-use-of-phosphogypsum-by-the-fertilizer-institute>. Federal Register, 85 FR 66550.
39. *Science Direct. Find Articles with these Terms: "Phosphogypsum"*. 2020. [viewed July 28, 2020]. Available from: <https://www.sciencedirect.com/search?qs=phosphogypsum>.
40. DE FREITAS, B.J. and P.C.W. ALBUQUERQUE. Alternatives to Industrial Recycling of Phosphogypsum in Brazil. *Water Science and Technology*. London: 1991,

24(12), 245-254. Available from: <https://search.proquest.com/docview/1943175153>. CrossRef. ISSN 0273-1223. DOI: 10.2166/wst.1991.0391.

41. GUO, T., R.K. SEALS, R.F. MALONE and K.A. RUSCH. The Effects of Seawater on the Dissolution Potential of Phosphogypsum:Cement Composites. *Environmental Engineering Science*. 1999, **16**(2), 147-156. Available from: <https://www.liebertpub.com/doi/abs/10.1089/ees.1999.16.147>. DOI: <https://doi.org/10.1089/ees.1999.16.147>.

42. NIELAND, D.L., et al. Preliminary Evaluation of the use of Phosphogypsum for Reef Substrate. I. A Laboratory Study of Bioaccumulation of Radium and Six Heavy Metals in an Aquatic Food Chain. *Chemistry and Ecology*. 1998, **14**(3-4), 305-319. Available from: <https://www.tandfonline.com/doi/abs/10.1080/02757549808037611>. ISSN 0275-7540. DOI: <https://doi.org/10.1080/02757549808037611>.

43. WILSON, C.A., et al. Preliminary Evaluation of the use of Phosphogypsum for Reef Substrate. II. A Study of the Effects of Phosphogypsum Exposure on Diversity and Biomass of Aquatic Organisms. *Chemistry and Ecology*. 1998, **14**(3-4), 321-340. Available from: <https://www.tandfonline.com/doi/abs/10.1080/02757549808037612>. ISSN 0275-7540. DOI: <https://doi.org/10.1080/02757549808037612>.

44. JETT, M.E., B.K. MURPHY and M. CADWALLADER. Inverted Composite Liner for Gypsum Stack Expansion. *Geotechnical Fabrics Report*. 1996, **14**, 30-42.

45. ALCORDO, I.S. and J.E. RECHCIGL. Phosphogypsum in Agriculture: A Review. *Advances in Agronomy*. 1993, **49**, 55-118. Available from: <http://www.sciencedirect.com/science/article/pii/S0065211308607932>. ISSN 0065-2113. DOI: [https://doi.org/10.1016/S0065-2113\(08\)60793-2](https://doi.org/10.1016/S0065-2113(08)60793-2).

46. PAPASTEFANO, C., S. STOULOS, A. IOANNIDOU and M. MANOLOPOULOU. The Application of Phosphogypsum in Agriculture and the Radiological Impact. *Journal of Environmental Radioactivity*. 2006, **89**(2), 188-198. Available from: <http://www.sciencedirect.com/science/article/pii/S0265931X06000786>. ISSN 0265-931X. DOI: <https://doi.org/10.1016/j.jenvrad.2006.05.005>.

47. ABRIL, J., et al. The Cumulative Effect of Three Decades of Phosphogypsum Amendments in Reclaimed Marsh Soils from SW Spain: 226Ra, 238U and Cd Contents in Soils and Tomato Fruit. *Science of the Total Environment*. 2008, **403**(1), 80-88. Available from: <http://www.sciencedirect.com/science/article/pii/S0048969708005202>. ISSN 0048-9697. DOI: <https://doi.org/10.1016/j.scitotenv.2008.05.013>.

48. CHANG, W.F., D.A. CHIN and R. HO. *Phosphogypsum for Secondary Road Construction*. Bartow, Florida: Florida Institute of Phosphate Research, 1989.

49. FIGUEROA, J.L., L. ZHOU and W.F. CHANG. Use of Phosphate Mining Waste in Secondary Road Construction. *Transportation Research Record*. 1987, (1106), 59-64. ISSN 0361-1981.

50. GREGORY, C.A., D. SAYLAK and W.B. LEDBETTER. The use of by-Product Phosphogypsum for Road Bases and Subbases. *Transportation Research Board*. 1984, (998), 47-52. ISSN 0361-1981.

51. TAHA, R., et al. Use of by-Product Phosphogypsum in Road Construction. *Transportation Research Record*. 1992, (1345), 28-35. ISSN 0361-1981.

52. PAIGE-GREEN, P. and S. GERBER. An Evaluation of the use of by-Product Phosphogypsum as a Pavement Material for Roads. *South Africa Transport Conference "Action in Transport for the New Millennium"*. 2000, Available from: <https://repository.up.ac.za/dspace/bitstream/handle/2263/8295/73%20PaigeGreen.pdf?sequence=1>. UPSpace Institutional Repository.

53. DEGIRMENCI, N., A. OKUCU and A. TURABI. Application of Phosphogypsum in Soil Stabilization. *Building and Environment*. 2007, **42**(9), 3393-3398. Available from: <http://www.sciencedirect.com/science/article/pii/S0360132306002265>. ISSN 0360-1323. DOI: <https://doi.org/10.1016/j.buildenv.2006.08.010>.

54. FOLEK, S., B. WALAWSKA, B. WILCZEK and J. MIŚKIEWICZ. Use of Phosphogypsum in Road Construction. *Polish Journal of Chemical Technology*. Szczecin: 2011, **13**(2), 18-22. Available from: <https://content.sciendo.com/view/journals/pjct/13/2/article-p18.xml>. ISSN 1899-4741. DOI: <https://doi.org/10.2478/v10026-011-0018-5>.

55. SARKKA, A. Disposal Management System for Utilisation of Industrial Phosphogypsum and Fly Ash. In: *Life Environment in Action: 56 New Success Stories for Europe's Environment*. Luxembourg: Office for Official Publications of the European Communities, 2001, 98-99. ISBN 92-894-0272-5.

56. ANDERSON, N.R. Gypsum Aggregate-a Viable Commercial Venture. *Proceedings of the Second International Symposium on Phosphogypsum, Florida Institute of Phosphate Research, Bartow, Florida*. 1988, , 329-352.

57. CLASTRES, P. Environmental Management of the Phosphogypsum of Sfax. *Proceedings of COVAPHOS III, Marrakech*. 2009, .

58. DVORKIN, L., N. LUSHNIKOVA and M. SONEBI. Application Areas of Phosphogypsum in Production of Mineral Binders and Composites Based on them: A Review of Research Results. *MATEC Web of Conferences*. 2018, **149**(01012)DOI: <https://doi.org/10.1051/mateconf/201814901012>.

59. BANDGAR, G.S., M.B. KUMTHEKAR and A.B. LANDAGE. A Review of Effective Utilization of Waste Phosphogypsum as a Building Material. *International Journal of Engineering Research*. 2016, **5**(1), 277-280. ISSN 2347-5013.

60. KOVLER, K. Radiological Constraints of using Building Materials and Industrial by-Products in Construction. *Construction and Building Materials*. 2009, **23**(1), 246-253. Available from: <http://www.sciencedirect.com/science/article/pii/S0950061808000020>. ISSN 0950-0618. DOI: <https://doi.org/10.1016/j.conbuildmat.2007.12.010>.

61. CÁNOVAS, C.R., et al. Valorization of Wastes from the Fertilizer Industry: Current Status and Future Trends. *Journal of Cleaner Production*. 2018, **174**, 678-690. Available from: <http://www.sciencedirect.com/science/article/pii/S0959652617325982>. ISSN 0959-6526. DOI: <https://doi.org/10.1016/j.jclepro.2017.10.293>.

62. World Health Organization. *WHO Handbook on Indoor Radon: A Public Health Perspective*. H. ZEEB, and F. SHANNOUN eds., Geneva, Switzerland: World Health Organization, 2009. CABDirect. ISBN 9789241547673.

63. The Council of the European Union. Council Directive 2013/59/Euratom of 5 December 2013 Laying Down Basic Safety Standards for Protection Against the Dangers

Arising from Exposure to Ionising Radiation, and Repealing Directives 89/618/Euratom, 90/641/Euratom, 96/29/Euratom, 97/43/Euratom and 2003/122/Euratom. *Official Journal of the European Union*. 2014, **L13**, 1-73. Available from: <http://data.europa.eu/eli/dir/2013/59/oj>.

64. European Commission. *Radiological Protection Principles Concerning the Natural Radioactivity of Building Materials*. Luxembourg: OPOCE, 1999. Available from: <http://bookshop.europa.eu/uri?target=EUB:NOTICE:CR2699126:EN:HTML>. ISBN 9282883760.

65. KOVACS, T., et al. 6 - from Raw Materials to NORM by-Products. In: *Naturally Occurring Radioactive Materials in Construction*. W. SCHROEYERS ed., Woodhead Publishing, 2017, 135-182. ISBN 9780081020098.

66. TREVISI, R., et al. Natural Radioactivity in Building Materials in the European Union: A Database and an Estimate of Radiological Significance. *Journal of Environmental Radioactivity*. 2012, **105**, 11-20. Available from: <http://www.sciencedirect.com/science/article/pii/S0265931X11002402>. ISSN 0265-931X. DOI: <https://doi.org/10.1016/j.jenvrad.2011.10.001>.

67. CAMPOS, M.P., et al. Radiological Assessment of using Phosphogypsum as Building Material. In: *Naturally Occurring Radioactive Material (Norm IV), Proceedings of an International Symposium Marrakesh, Morocco, 22–26 March 2010*. Vienna: IAEA, 2011, 421-432. Available from: http://www-pub.iaea.org/MTCD/publications/PDF/Pub1497_web.pdf http://inis.iaea.org/search/search.aspx?orig_q=RN:42105038. ISBN 0074-1884.

68. KANNO, W.M., et al. High Strength Phosphogypsum and its use as a Building Material. *AIP Conference Proceedings*. 2008, **1034**(1), 307-310. Available from: <http://aip.scitation.org/doi/abs/10.1063/1.2991234>. DOI: <https://doi.org/10.1063/1.2991234>.

69. MÁDUAR, M.F., M.P. DE CAMPOS, E.W. MARTINS and B.P. MAZZILLI. External Dose Assessment and Radon Monitoring in an Experimental House Built with Phosphogypsum-Based Materials. In: *Radioecology and Environmental Radioactivity (Proc. Int. Conf. Bergen, Norway, 2008)*. Norwegian Radiation Protection Authority, Østerås, Norway and Institut de Radioprotection et de Sûreté Nucléaire, Fontenay-aux-Roses, France, 2009, Available from: <http://repositorio.ipen.br/bitstream/handle/123456789/16010/13454.pdf?sequence=1>.

70. KOVLER, K. Inter-Industrial Ecologically Friendly Technologies in Mining Engineering, Chemistry and Construction. *Proceedings of the 11th National Congress on Civil Engineering*. 1997, , 228.

71. KOVLER, K. and M. SOMIN. Inter-Disciplinary Ecologically Friendly Technologies. *Proceedings of the 30th Annual National Conference of Israeli Association of Ecology and Environmental Sciences, Haifa, Israel*. 2000, , 151.

72. KOVLER, K. and M. SOMIN. Direct Production of Sodium Ortho- and/Or Pyrophosphates and Gypsum Binders from Phosphate Rock. *Abstracts of Papers of the American Chemical Society*. 1997, **214**, 5-FERT, Part 1.

73. KOVLER, K. and M. SOMIN. Producing of the Ecologically Friendly (1) Enriched Phosphate Ore and (2) Slaked Lime in One Installation. *Abstracts of Papers of the American Chemical Society*. 1997, **214**, 4-FERT, part 1.

74. KOVLER, K. and M. SOMIN. Inter-Industrial Ecologically Friendly Technologies. *Proceedings of the National Conference "Effective Methods for Advanced Construction in Israel"*, Maalot, Israel. 1997, , 18.

75. SOMIN, M. and K. KOVLER. Ecologically Friendly Technology of Triple Superphosphate and Lime. *Proceedings of the Dahlia Greidinger International Symposium on Fertilization and the Environment*, Haifa, Israel. 1997, , 36.

76. ROMERO-HERMIDA, M.I., et al. Environmental Impact of Phosphogypsum-Derived Building Materials. *International Journal of Environmental Research and Public Health*. Basel: 2020, **17**(12), 4248. Available from: <https://search.proquest.com/docview/2414789401>. CrossRef. ISSN 1660-4601. DOI: <https://doi.org/10.3390/ijerph17124248>.

77. GASCÓ, C., et al. Advantages and Disadvantages of using Phosphogypsum as Building Material Radiological Aspects. *Proceedings of the 1st National Spanish Conference on Advances in Materials Recycling and Eco-Energy (RECIMAT'09)*, Madrid, Spain. 2009, , 83-86. [viewed January 3, 2018]. Available from: https://s3.amazonaws.com/academia.edu.documents/40604204/ADVANTAGES_AND_DISADVANTAGES_OF_USING_PH20151203-16020-1xj4hhc.pdf?AWSAccessKeyId=AKIAIWOWYYGZ2Y53UL3A&Expires=1514974462&Signature=d04C511J%2FXUBs0bv7fKqk3qrHQ%3D&response-content-disposition=inline%3B%20filename%3DADVANTAGES_AND_DISADVANTAGES_OF_USING_PH.pdf. Amazon S3. ISSN 9788-4729239800.

78. CÁRDENAS-ESCUADERO, C., et al. Procedure to use Phosphogypsum Industrial Waste for Mineral CO₂ Sequestration. *Journal of Hazardous Materials*. 2011, **196**, 431-435. Available from: <http://www.sciencedirect.com/science/article/pii/S0304389411011393>. ISSN 0304-3894. DOI: <https://doi.org/10.1016/j.jhazmat.2011.09.039>.

79. ROMERO-HERMIDA, M.I., et al. Phosphogypsum Waste Lime as a Promising Substitute of Commercial Limes: A Rheological Approach. *Cement and Concrete Composites*. 2019, **95**, 205-216. Available from: <http://www.sciencedirect.com/science/article/pii/S0958946518306449>. ISSN 0958-9465. DOI: <https://doi.org/10.1016/j.cemconcomp.2018.11.007>.

80. LEŠKEVIČIENĖ, V., D. NIZEVIČIENĖ and Z. VALANČIUS. The Effect of the Processing Way of Technogenic Raw Materials on the Properties of Gypsum Binding Materials. *Journal of Civil Engineering and Management*. 2003, **9**(1), 76-81. [viewed January 19, 2021]. Available from: <https://www.tandfonline.com/doi/abs/10.1080/13923730.2003.10531304>. ISSN 1392-3730. DOI: <https://doi.org/10.1080/13923730.2003.10531304>.

81. NIZEVIČIENĖ, D., D. VAIČIUKYNIENĖ, V. VAITKEVIČIUS and Ž. RUDŽIONIS. Effects of Waste Fluid Catalytic Cracking on the Properties of Semi-Hydrate Phosphogypsum. *Journal of Cleaner Production*. 2016, **137**(Supplement C), 150-156. Available from: <http://www.sciencedirect.com/science/article/pii/S0959652616309258>. ISSN 0959-6526. DOI: <https://doi.org/10.1016/j.jclepro.2016.07.037>.

82. LI, Z., et al. Investigation of Phosphate Adsorption from an Aqueous Solution using Spent Fluid Catalytic Cracking Catalyst Containing Lanthanum. *Frontiers of Environmental Science & Engineering*. 2018, **12**(6), 15. Available from:

<https://link.springer.com/article/10.1007%2Fs11783-018-1082-3>. ISSN 2095-221X. DOI: <https://doi.org/10.1007/s11783-018-1082-3>.

83. ISLAM, G.M.S., et al. Effect of Phosphogypsum on the Properties of Portland Cement. *Procedia Engineering*. 2017, **171**, 744-751. Available from: <https://www.sciencedirect.com/science/article/pii/S1877705817304502>. ISSN 1877-7058. DOI: <https://doi.org/10.1016/j.proeng.2017.01.440>.

84. AKIN, A.İ and Y. SERT. Utilization of Weathered Phosphogypsum as Set Retarder in Portland Cement. *Cement and Concrete Research*. 2004, **34**(4), 677-680. Available from: <https://www.sciencedirect.com/science/article/pii/S0008884603003740>. ISSN 0008-8846. DOI: <https://doi.org/10.1016/j.cemconres.2003.10.017>.

85. LEŠKEVIČIENĖ, V., N. KYBARTIENĖ, D. NIZEVIČIENĖ and Z. VALANČIUS. The Influence of Mineralogical Composition and Crystal Structure of Phosphogypsum on its Physical-Mechanical Properties. *IBAUSIL: 16. Internationale Baustofftagung, September 20-23, Weimar, Germany*. 2006, , 883-889. ISSN 3000-182632.

86. VALANČIUS, Z., D. NIZEVIČIENĖ, V. LEŠKEVIČIENĖ and N. KYBARTIENĖ. Influence of the Technological Parameters on the Structure and Properties of Hemi-Hydrate Phosphogypsum. *Ceramics-Silikaty*. Prague: 2005, **49**(2), 120-125. [viewed January 19, 2021]. ISSN 0862-5468.

87. DUAN, Z., et al. Influence of Crystal Modifier on the Preparation of A-Hemihydrate Gypsum from Phosphogypsum. *Construction and Building Materials*. 2017, **133**, 323-329. Available from: <http://www.sciencedirect.com/science/article/pii/S0950061816319791>. ISSN 0950-0618. DOI: <https://doi.org/10.1016/j.conbuildmat.2016.12.060>.

88. KYBARTIENE, N., V. LESKEVICIENE, D. NIZEVICIENE and Z. VALANCIUS. The Investigation of the Hydratation of Semi-Hydrate Phosphogypsum by Thermal Analysis Methods. *Materials Science*. 2004, **10**(3), 259-263. ISSN 1392-1320.

89. ZIELIŃSKI, M. Influence of Constant Magnetic Field on the Properties of Waste Phosphogypsum and Fly Ash Composites. *Construction and Building Materials*. 2015, **89**(Supplement C), 13-24. Available from: <http://www.sciencedirect.com/science/article/pii/S0950061815004729>. ISSN 0950-0618. DOI: <https://doi.org/10.1016/j.conbuildmat.2015.04.029>.

90. DEĞIRMENCI, N. Utilization of Phosphogypsum as Raw and Calcined Material in Manufacturing of Building Products. *Construction and Building Materials*. 2008, **22**(8), 1857-1862. Available from: <http://www.sciencedirect.com/science/article/pii/S0950061807001274>. ISSN 0950-0618. DOI: <https://doi.org/10.1016/j.conbuildmat.2007.04.024>.

91. HUA, S., et al. Effects of Fibers on Mechanical Properties and Freeze-Thaw Resistance of Phosphogypsum-Slag Based Cementitious Materials. *Construction and Building Materials*. 2016, **121**(Supplement C), 290-299. Available from: <http://www.sciencedirect.com/science/article/pii/S0950061816309308>. ISSN 0950-0618. DOI: <https://doi.org/10.1016/j.conbuildmat.2016.06.003>.

92. YANG, J., W. LIU, L. ZHANG and B. XIAO. Preparation of Load-Bearing Building Materials from Autoclaved Phosphogypsum. *Construction and Building*

Materials. 2009, **23**(2), 687-693. Available from:
<http://www.sciencedirect.com/science/article/pii/S0950061808000627>. ISSN 0950-0618.
DOI: <https://doi.org/10.1016/j.conbuildmat.2008.02.011>.

93. ZHOU, J., et al. Utilization of Waste Phosphogypsum to Prepare Non-Fired Bricks by a Novel Hydration–Recrystallization Process. *Construction and Building Materials*. 2012, **34**(Supplement C), 114-119. Available from:
<http://www.sciencedirect.com/science/article/pii/S0950061812001225>. ISSN 0950-0618.
DOI: <https://doi.org/10.1016/j.conbuildmat.2012.02.045>.

94. ZHOU, J., et al. A Novel Two-Step Hydration Process of Preparing Cement-Free Non-Fired Bricks from Waste Phosphogypsum. *Construction and Building Materials*. 2014, **73**(Supplement C), 222-228. Available from:
<http://www.sciencedirect.com/science/article/pii/S0950061814010915>. ISSN 0950-0618.
DOI: <https://doi.org/10.1016/j.conbuildmat.2014.09.075>.

95. ZHOU, J., et al. Preparation of Hardened Tiles from Waste Phosphogypsum by a New Intermittent Pressing Hydration. *Ceramics International*. 2016, **42**(6), 7237-7245. Available from: <http://www.sciencedirect.com/science/article/pii/S0272884216001486>. ISSN 0272-8842. DOI: <https://doi.org/10.1016/j.ceramint.2016.01.117>.

96. CHI, J.H. and X.J. LIN. The Method of Producing the Non-Fired Bricks of the Industrial by-Production Phosphogypsum. *State Intellectual Property Office of the People's Republic of China*. 2009, .

97. ZHANG, T.B. and J.H. CHI. The Method of Producing the Non-Fired Bricks of Phosphogypsum. *State Intellectual Property Office of the People's Republic of China*. 2000, , CN00109901.

98. YANG, J.P. The Method of Manufacturing the High-Strength Building Bricks of Phosphogypsum. *State Intellectual Property Office of the People's Republic of China*. 2007, , CN200610054521.

99. LI, Z.J., T. SHEN and Q. XIE. The Method of Manufacturing the Environmental and High-Pressure Non-Fired Bricks of Phosphogypsum. *State Intellectual Property Office of the People's Republic of China*. 2005, , CN200510020444.

100. CHEN, Z.W. The Method of Manufacturing the Non-Fired Bricks of Phosphogypsum. *State Intellectual Property Office of the People's Republic of China*. 2008, , CN20071005382.

101. GARG, M., A.K. MINOCHA and N. JAIN. Environment Hazard Mitigation of Waste Gypsum and Chalk: Use in Construction Materials. *Construction and Building Materials*. 2011, **25**(2), 944-949. Available from:
<http://www.sciencedirect.com/science/article/pii/S0950061810003375>. ISSN 0950-0618.
DOI: <https://doi.org/10.1016/j.conbuildmat.2010.06.088>.

102. LI, J., G. LI and Y. YU. The Influences of Gypsum Water-Proofing Additive on Gypsum Crystal Growth. *Materials Letters*. 2007, **61**(3), 872-876. Available from:
<http://www.sciencedirect.com/science/article/pii/S0167577X06006938>. ISSN 0167-577X.
DOI: <https://doi.org/10.1016/j.matlet.2006.06.005>.

103. SINGH, M. and M. GARG. Study on Anhydrite Plaster from Waste Phosphogypsum for use in Polymerised Flooring Composition. *Construction and Building*

Materials. 2005, **19**(1), 25-29. Available from:
<http://www.sciencedirect.com/science/article/pii/S0950061804000868>. ISSN 0950-0618.
DOI: <https://doi.org/10.1016/j.conbuildmat.2004.04.038>.

104. ZHANG, M., M. CHEN, T. FAN and F. ZHAO. Improving Waterproof Property of Gypsum Block with Organic-Inorganic Compound Materials. *DEStech Transactions on Materials Science and Engineering*. 2015, (icmea) Available from:
<http://dpi-proceedings.com/index.php/dtmse/article/view/7369>. DOI:
10.12783/dtmse/icmea2015/7369.

105. GREVE, D.R. and O'NEILL, E.D. *Water-Resistant Gypsum Products*. L. GEORGIA PACIFIC ed., U.S. patent no. 3,935,021. January 27, 1976 Google Patents.

106. TERADA, I., et al. *Water Repellent Gypsum Composition*. Yoshino Gypsum Co Ltd Mitsubishi Kasei Corp ed., United States: U.S. Patent No. 4,042,409. August 16, 1977 Google Patents. ISBN 4,042,409.

107. LONG, W.J. *Water-Resistant Gypsum Composition and Products, and Process of Making Same*. United States Gypsum Co. ed., U.S. Patent No. 4,094,694. June 13, 1978 Google Patents.

108. SELLERS, D.G., ALTMAN, F.A. and RICHARDS, T.W. *Method of Manufacturing a Water-Resistant Gypsum Composition*. L. GEORGIA-PACIFIC GYPSUM ed., U.S. patent no. 5,135,805. August 4, 1992 Google Patents.

109. VEERAMASUNENI, S. and CAPACASA, K. *Method of Making Water-Resistant Gypsum-Based Article*. United States Gypsum Co. ed., U.S. Patent No. 7,892,472. February 22, 2011 Google Patents.

110. BORENSTEIN, L. *Water-Resistant Gypsum Compositions and Emulsion for Making Same*. HENRY Co CANADA Inc. ed., U.S. Patent No 5,437,722. August 1, 1995 Google Patents.

111. MAGALLANES-RIVERA, R.X., C.A. JUAREZ-ALVARADO, P. VALDEZ and J.M. MENDOZA-RANGEL. Modified Gypsum Compounds: An Ecological–economical Choice to Improve Traditional Plasters. *Construction and Building Materials*. 2012, **37**, 591-596. Available from:
<http://www.sciencedirect.com/science/article/pii/S0950061812005247>. ISSN 0950-0618.
DOI: <https://doi.org/10.1016/j.conbuildmat.2012.07.054>.

112. SINGH, M. and M. GARG. Phosphogypsum Based Composite Binders. *Journal of Scientific & Industrial Research*. 2001, **60**, 812-817. ISSN 0975-1084.

113. HUANG, X., X. ZHAO, S. BIE and C. YANG. Hardening Performance of Phosphogypsum-Slag-Based Material. *Procedia Environmental Sciences*. 2016, **31**, 970-976. Available from:
<http://www.sciencedirect.com/science/article/pii/S1878029616001286>. ISSN 1878-0296.
DOI: <https://doi.org/10.1016/j.proenv.2016.03.002>.

114. CAMARINI, G. and J.A. DE MILITO. Gypsum Hemihydrate–cement Blends to Improve Renderings Durability. *Construction and Building Materials*. 2011, **25**(11), 4121-4125. [viewed January 19, 2021]. Available from:
<http://www.sciencedirect.com/science/article/pii/S0950061811001887>. ISSN 0950-0618.
DOI: <https://doi.org/10.1016/j.conbuildmat.2011.04.048>.

115. PANG, M., Z. SUN and H. HUANG. Compressive Strength and Durability of FGD Gypsum-Based Mortars Blended with Ground Granulated Blast Furnace Slag. *Materials*. 2020, **13**(15), 3383. [viewed January 19, 2021]. Available from: <https://www.mdpi.com/1996-1944/13/15/3383>. DOI: <https://doi.org/10.3390/ma13153383>.

116. KURYATNYK, T., C. ANGULSKI DA LUZ, J. AMBROISE and J. PERA. Valorization of Phosphogypsum as Hydraulic Binder. *Journal of Hazardous Materials*. 2008, **160**(2), 681-687. Available from: <http://www.sciencedirect.com/science/article/pii/S0304389408003634>. ISSN 0304-3894. DOI: <https://doi.org/10.1016/j.jhazmat.2008.03.014>.

117. ALONSO, M.C., J.L. GARCÍA CALVO, A. HIDALGO and L. FERNÁNDEZ LUCO. 10 - Development and Application of Low-pH Concretes for Structural Purposes in Geological Repository Systems. In: *Geological Repository Systems for Safe Disposal of Spent Nuclear Fuels and Radioactive Waste*. J. AHN and M.J. APTED eds., Woodhead Publishing, 2010, 286-322. ISBN 9781845695422.

118. TOKAREV, Y. and G. YAKOVLEV. Activation of Hardening Anhydrite Compositions with Superdispersed Agents. *Modern Building Materials, Structures and Techniques. Proceedings of the International Conference*. 2010, **10**, 295.

119. SOKOLOVA, Y.A. and I.V. MOREVA. Using Domestic Modifiers for Regulating the Properties of Low-Grade Plaster. *Dry Building Mixtures*. 2011, **3**, 16-17.

120. YAKOVLEV, G., et al. Anhydrite and Gypsum Compositions Modified with Ultrafine Man-made Admixtures. *Procedia Engineering*. 2015, **108**, 13-21. [viewed January 19, 2021]. Available from: <http://www.sciencedirect.com/science/article/pii/S1877705815011492>. ISSN 1877-7058. DOI: <https://doi.org/10.1016/j.proeng.2015.06.195>.

121. PERVYSHIN, G.N., et al. Water-Resistant Gypsum Compositions with Man-made Modifiers. *Procedia Engineering*. 2017, **172**, 867-874. Available from: <http://www.sciencedirect.com/science/article/pii/S1877705817305933>. ISSN 1877-7058. DOI: <https://doi.org/10.1016/j.proeng.2017.02.087>.

122. ARROYO, F.N., et al. Development of Plaster Foam for Thermal and Acoustic Applications. *Construction and Building Materials*. 2020, **262**, 120800. Available from: <https://www.sciencedirect.com/science/article/pii/S0950061820328051>. ISSN 0950-0618. DOI: <https://doi.org/10.1016/j.conbuildmat.2020.120800>.

123. YONG, C., W. QIANG and X. JUNFENG. Novel Foam Insulation Material Produced by Calcined Phosphogypsum and H₂O₂. *Journal of Materials in Civil Engineering*. 2020, **32**(12), 04020379. Available from: [https://doi.org/10.1061/\(ASCE\)MT.1943-5533.0003473](https://doi.org/10.1061/(ASCE)MT.1943-5533.0003473). DOI: 10.1061/(ASCE)MT.1943-5533.0003473.

124. VIMMROVÁ, A., M. KEPPERT, L. SVOBODA and R. ČERNÝ. Lightweight Gypsum Composites: Design Strategies for Multi-Functionality. *Cement and Concrete Composites*. 2011, **33**(1), 84-89. Available from: <https://www.sciencedirect.com/science/article/pii/S0958946510001411>. ISSN 0958-9465. DOI: <https://doi.org/10.1016/j.cemconcomp.2010.09.011>.

125. BINICI, H., O. AKSOGAN and C. DEMIRHAN. Mechanical, Thermal and Acoustical Characterizations of an Insulation Composite made of Bio-Based Materials.

Sustainable Cities and Society. 2016, **20**, 17-26. Available from:
<https://www.sciencedirect.com/science/article/pii/S2210670715300305>. ISSN 2210-6707.
DOI: <https://doi.org/10.1016/j.scs.2015.09.004>.

126. CHERKI, A., et al. Experimental Thermal Properties Characterization of Insulating Cork–gypsum Composite. *Construction and Building Materials*. 2014, **54**, 202-209. Available from:
<https://www.sciencedirect.com/science/article/pii/S0950061813012336>. ISSN 0950-0618.
DOI: <https://doi.org/10.1016/j.conbuildmat.2013.12.076>.

127. GUNA, V., et al. Wool and Coir Fiber Reinforced Gypsum Ceiling Tiles with Enhanced Stability and Acoustic and Thermal Resistance. *Journal of Building Engineering*. 2021, **41**, 102433. Available from:
<https://www.sciencedirect.com/science/article/pii/S2352710221002904>. ISSN 2352-7102.
DOI: <https://doi.org/10.1016/j.jobe.2021.102433>.

128. SAIR, S., B. MANDILI, M. TAQI and A. EL BOUARI. Development of a New Eco-Friendly Composite Material Based on Gypsum Reinforced with a Mixture of Cork Fibre and Cardboard Waste for Building Thermal Insulation. *Composites Communications*. 2019, **16**, 20-24. Available from:
<https://www.sciencedirect.com/science/article/pii/S2452213919300853>. ISSN 2452-2139.
DOI: <https://doi.org/10.1016/j.coco.2019.08.010>.

129. CAO, W., et al. A Novel Low-Density Thermal Insulation Gypsum Reinforced with Superplasticizers. *Construction and Building Materials*. 2021, **278**, 122421. Available from:
<https://www.sciencedirect.com/science/article/pii/S0950061821001811>. ISSN 0950-0618. DOI: <https://doi.org/10.1016/j.conbuildmat.2021.122421>.

130. GENCEL, O., et al. A Novel Lightweight Gypsum Composite with Diatomite and Polypropylene Fibers. *Construction and Building Materials*. 2016, **113**, 732-740. Available from:
<https://www.sciencedirect.com/science/article/pii/S0950061816304299>. ISSN 0950-0618. DOI: <https://doi.org/10.1016/j.conbuildmat.2016.03.125>.

131. LI, Y., et al. Preparation and Thermal Insulation Performance of Cast-in-Situ Phosphogypsum Wall. *Journal of Applied Biomaterials & Functional Materials*. 2018, **16**(1), 81-92. Available from:
<https://journals.sagepub.com/doi/full/10.1177/2280800017751487>. ISSN 2280-8000. DOI: <https://doi.org/10.1177/2280800017751487>.

132. *Hitachi Scanning Electron Microscope S3400N*. High-Tech Instruments. December 12, 2018. [viewed January 28, 2020]. Available from:
<http://htiweb.com/Products/Advanced%20Microscopy/EM/SEM/SEMS3400N.html>.

133. International Centre for Diffraction Data, (ICDD). *PDF-2: Powder Diffraction File*. 12 Campus Blvd, Newtown Square, PA 19073, USA: International Centre for Diffraction Data. 2019. [viewed February 24, 2020]. Available from:
<http://www.icdd.com/pdf-2/>.

134. LARSON, A.C. and R. DREELE. General Structure Analysis System (GSAS). *Report LAUR*. Los Alamos National Laboratory ed. 2004, , 86-748.

135. *Phosphate Low Range Checker HC® Colorimeter: Range 0.00 to 2.50 Ppm (mg/L)*. Hanna Instruments. 2017. [viewed March 5, 2021]. Available

from:<https://hannainst.lt/en/produktas/delniniai-fotometrai-checker-hc/hi713-checker-hc-fosfatams-mazose-koncentracijose/>.

136. *Fluoride LR Checker HC®*, 0.00 to 2.00 Ppm. Hanna Instruments. 2017. [viewed March 5, 2021]. Available from:<https://hannainst.lt/en/produktas/delniniai-fotometrai-checker-hc/hi729-checker-hc-fluoridui-mazose-koncentracijose/>.

137. BALANDIS, A., R. KAMINSKAS and G. VAICKELIONIS. *Statybinių Medžiagų Chemija: Mokojoji Knyga*. Kaunas: Technologija, 2004. ISBN 9955097280.

138. Cilas. *Particle Size Analyzer Cilas 1090*. Cilas S.A. [viewed March 5, 2021]. Available from:<http://www.bruben.com.ar/pdf/cilas/IL.pdf>.

139. *AD8000 Professional Multi-Parameter pH-ORP-Conductivity-TDS-TEMP Bench Meter*. Adwa Instruments Inc. 2016. [viewed January 28, 2020]. Available from:<https://www.adwainstruments.com/bench-meters/95-professional-multi-parameter-ph-orp-ec-tds-temp-bench-meter/33-ad8000>.

140. *8 Channel Thermocouple Data Logger*. Pico Technology. [viewed March 5, 2021]. Available from:<https://www.picotech.com/data-logger/tc-08/thermocouple-data-logger>.

141. ASADI, I., P. SHAFIGH, Abu Hassan, Zahiruddin Fitri Bin and N.B. MAHYUDDIN. Thermal Conductivity of Concrete – A Review. *Journal of Building Engineering*. 2018, **20**, 81-93. Available from:
<https://www.sciencedirect.com/science/article/pii/S2352710218304650>. ISSN 2352-7102.
DOI: <https://doi.org/10.1016/j.jobe.2018.07.002>.

142. EN 12667:2001. *Thermal Performance of Building Materials and Products - Determination of Thermal Resistance by Means of Guarded Hot Plate and Heat Flow Meter Methods - Products of High and Medium Thermal Resistance*. Brussels: European Comitee for Standartisation (CEN), 2001. Available from: <https://www.en-standard.eu/bs-en-12667-2001-thermal-performance-of-building-materials-and-products.-determination-of-thermal-resistance-by-means-of-guarded-hot-plate-and-heat-flow-meter-methods.-products-of-high-and-medium-thermal-resistance/>.

143. *Compressive Strength Testing Machines*. Toni Technic. 2019. [viewed January 28, 2020]. Available from:<https://tonitechnik.com/en/products/machines/compressive-strength-testing-machines/>.

144. BONCZYK, M. Determination of 210Pb Concentration in NORM Waste – an Application of the Transmission Method for Self-Attenuation Corrections for Gamma-Ray Spectrometry. *Radiation Physics and Chemistry*. 2018, **148**, 1-4. Available from:
<https://www.sciencedirect.com/science/article/pii/S0969806X17303985>. ISSN 0969-806X.
DOI: <https://doi.org/10.1016/j.radphyschem.2018.02.011>.

145. PACEWSKA, B., I. WILIŃSKA and M. BUKOWSKA. Hydration of Cement Slurry in the Presence of Spent Cracking Catalyst. *Journal of Thermal Analysis and Calorimetry*. Dordrecht: 2000, **60**(1), 71-78. Available from:
<https://akjournals.com/view/journals/10973/60/1/article-p71.xml>. ISSN 1388-6150. DOI:
<https://doi.org/10.1023/a:1010120518062>.

146. WU, J., W. WU and K. HSU. The Effect of Waste Oil-Cracking Catalyst on the Compressive Strength of Cement Pastes and Mortars. *Cement and Concrete Research*.

2003, **33**(2), 245-253. Available from:
<http://www.sciencedirect.com/science/article/pii/S0008884602010062>. ISSN 0008-8846.
DOI: [https://doi.org/10.1016/S0008-8846\(02\)01006-2](https://doi.org/10.1016/S0008-8846(02)01006-2).

147. LST 1974:2012. *LST EN 206-1 Taikymo Taisyklės Ir Papildomieji Nacionaliniai Reikalavimai = Rules for the Application of LST EN 206-1 and Additional National Requirements*. Vilnius: Lietuvos standartizacijos departamentas, 2012.

148. EN 206-1:2013. *Concrete - Specification, Performance, Production and Conformity. European Standard*. Brussels: European Comitee for Standartisation (CEN), 2013.

149. TAYLOR, R. Interpretation of the Correlation Coefficient: A Basic Review. *Journal of Diagnostic Medical Sonography*. 1990, **6**(1), 35-39. ISSN 8756-4793. DOI: 10.1177/875647939000600106.

150. MICHALIK, B., G. DE WITH and W. SCHROEYERS. Measurement of Radioactivity in Building Materials – Problems Encountered Caused by Possible Disequilibrium in Natural Decay Series. *Construction and Building Materials*. 2018, **168**, 995-1002. Available from:
<https://www.sciencedirect.com/science/article/pii/S0950061818302770>. ISSN 0950-0618.
DOI: <https://doi.org/10.1016/j.conbuildmat.2018.02.044>.

151. DE WITH, G., B. MICHALIK, B. HOFFMANN and M. DÖSE. Development of a European Harmonised Standard to Determine the Natural Radioactivity Concentrations in Building Materials. *Construction and Building Materials*. 2018, **171**, 913-918. Available from: <https://www.sciencedirect.com/science/article/pii/S0950061818306524>. ISSN 0950-0618. DOI: <https://doi.org/10.1016/j.conbuildmat.2018.03.153>.

152. SABADASH, V., J. GUMNITSKY and A. HYVLYUD. Mechanism of Phosphates Sorption by Zeolites Depending on Degree of their Substitution for Potassium Ions. *Chemistry & Chemical Technology*. 2016, **10**(2), 235-240. CrossRef. ISSN 1996-4196. DOI: <https://doi.org/10.23939/chcht10.02.235>.

153. ZHOU, B. and Z. CHEN. Experimental Study on the Hygrothermal Performance of Zeolite-Based Humidity Control Building Materials. *Heat and Technology*. 2016, **34**(3), 407-414. [viewed September 7, 2020]. Available from: <http://www.iicta.org/journals/ijht/paper/10.18280/ijht.340309>. CrossRef. ISSN 0392-8764. DOI: <https://doi.org/10.18280/ijht.340309>.

154. GRINYS, A., et al. The using of Aggressive Waste, Generated from the Marine Repair Production, to the Concrete Technology. *Sardinia 2015 : Proceedings of the 15th International Waste Management and Landfill Symposium, Cagliari, Sardinia, Italy, 5-9 October 2015 [Elektroninis Išteklius]*. Cagliari: 2015, , 1-11. ISSN 9788-862650212.

155. DE CARVALHO GOMES, S., J.L. ZHOU, W. LI and F. QU. Recycling of Raw Water Treatment Sludge in Cementitious Composites: Effects on Heat Evolution, Compressive Strength and Microstructure. *Resources, Conservation and Recycling*. 2020, **161**, 104970. Available from:
<https://www.sciencedirect.com/science/article/pii/S0921344920302883>. ISSN 0921-3449.
DOI: <https://doi.org/10.1016/j.resconrec.2020.104970>.

156. DE CARVALHO GOMES, S., J.L. ZHOU, W. LI and G. LONG. Progress in Manufacture and Properties of Construction Materials Incorporating Water Treatment

Sludge: A Review. *Resources, Conservation and Recycling*. 2019, **145**, 148-159. Available from: <https://www.sciencedirect.com/science/article/pii/S0921344919300953>. ISSN 0921-3449. DOI: <https://doi.org/10.1016/j.resconrec.2019.02.032>.

157. SVIKLAS, A.M., R. PALECKIENĖ and R. ŠLINKŠIENĖ. *Fosforo Trąšos: Vadovėlis (En.: Phosphorus Fertilizers: The Handbook)*. Kaunas: Technologija, 2014. ISBN 9955250364.

CURRICULUM VITAE

Personal information

Name, surname Ignacio, Villalon Fornes
Date of birth June 13, 1992
Place of birth Madrid, Spain
Nationality Spain
Phone +370 675 79085
email ignacio.villalon@ktu.lt, naxo.villalon@gmail.com

Education

2017–2021 Kaunas University of Technology – PhD studies, Civil Engineering
2015–2017 Kaunas University of Technology – Master of Civil Engineering, programme of Civil Engineering
2011–2015 Kaunas University of Technology – Bachelor of Civil Engineering, programme of Civil Engineering
1998–2010 Colegio Retamar, Madrid – primary and secondary school

Work experience

2019–present Kaunas University of Technology – lecturer
2015–2018 JSC “Smailusis Skliautas” – structural engineer

Languages

Spanish – mother tongue; Lithuanian (B2); English.

Scientific work

2017-present Scientific research and published articles with the team of prof. dr. Danutė Vaičiukynienė on the topic of the doctoral dissertation.
2015-2017 Investigations with prof. dr. Viktoras Doroševas on the topic of the master’s thesis. Aim of the work: to analyse the behaviour of a cantilever beam loaded under impact force.
2015-2016 Scientific research and a published article with the team of dr. Šarūnas Kelpša. Aim of the work: to evaluate the influence of the ground stiffness on the structures of buildings
2014 Scientific research and published extended abstract with the team of prof. dr. Mindaugas Daukšys and dr. Albertas Klovas on the topic: Aim of the work: to investigate the quality of the surface of concrete by using the open-source software *ImageJ*

LIST OF PUBLICATIONS ON THE TOPIC OF THE DISSERTATION

Publications in journals indexed in the Web of Science with Impact Factor

1. **Villalón Fornés, Ignacio**; Dorosevas, Viktoras; Vaiciukyniene, Danute; Nizevicene, Dalia. The investigation of phosphogypsum specimens processed by press-forming method // Waste and biomass valorization. Dordrecht : Springer. ISSN 1877-2641. eISSN 1877-265X. 2021, vol. 12, iss. 3, p. 1539-1551. DOI: 10.1007/s12649-020-01067-5. [Science Citation Index Expanded (Web of Science); Scopus] [IF: 3.703; AIF: 5.201; IF/AIF: 0.711; Q2 (2020, InCites JCR SCIE)] [CiteScore: 4.20; SNIP: 1.145; SJR: 0.615; Q2 (2020, Scopus Sources)].
2. **Villalón Fornés, Ignacio**; Vaičiukynienė, Danutė; Nizevičienė, Dalia; Dorošėvas, Viktoras; Dvořák, Karel. A method to prepare a high-strength building material from press-formed phosphogypsum purified with waste zeolite // Journal of building engineering. Amsterdam : Elsevier. eISSN 2352-7102. 2021, vol. 34, art. no. 101919, p. 1-10. DOI: 10.1016/j.job.2020.101919. [Science Citation Index Expanded (Web of Science); Scopus] [IF: 5.318; AIF: 4.252; IF/AIF: 1.250; Q1 (2020, InCites JCR SCIE)] [CiteScore: 5.50; SNIP: 2.290; SJR: 0.974; Q1 (2020, Scopus Sources)].
3. **Villalón Fornés, Ignacio**; Vaičiukynienė, Danutė; Nizevičienė, Dalia; Dorošėvas, Viktoras. The improvement of the water-resistance of the phosphogypsum by adding waste metallurgical sludge // Journal of building engineering. Oxford : Elsevier. ISSN 2352-7102. 2021, vol. 43, art. no. 102861, p. 1-11. DOI: 10.1016/j.job.2021.102861. [Science Citation Index Expanded (Web of Science); Scopus] [IF: 5.318; AIF: 4.252; IF/AIF: 1.250; Q1 (2020, InCites JCR SCIE)] [CiteScore: 5.50; SNIP: 2.290; SJR: 0.974; Q1 (2020, Scopus Sources)].
4. **Villalón Fornés, Ignacio**; Vaičiukynienė, Danutė; Nizevičienė, Dalia; Dorošėvas, Viktoras; Michalik, Bogusław. A comparative assessment of the suitability of phosphogypsum from different origins to be utilised as the binding material of construction products // Journal of building engineering. Amsterdam : Elsevier. ISSN 2352-7102. 2021, vol. 44, art. no. 102995, p. 1-16. DOI: 10.1016/j.job.2021.102995. [Science Citation Index Expanded (Web of Science); Scopus] [IF: 5.318; AIF: 4.252; IF/AIF: 1.250; Q1 (2020, InCites JCR SCIE)] [CiteScore: 5.50; SNIP: 2.290; SJR: 0.974; Q1 (2020, Scopus Sources)].

Presentations in conferences

1. July 23-25, 2018 – Conference “Green chemistry and sustainable engineering: 4th international conference”, Madrid, Spain. Oral presentation “Initial investigation on press-formed phosphogypsum products”.
2. December 3, 2020 – Conference “19th ICBM: International Conference Binders and Materials”, Brno, Czech Republic. Oral presentation “The influence of phosphogypsum microstructure on the main properties of press-formed samples”.
3. May 23-26, 2021 – Conference “2nd Vitrogeowastes”, Baeza, Spain. Oral presentation “The influence of waste wood fibre on the physical-mechanical properties of phosphogypsum specimens”

ACKNOWLEDGEMENTS

First, I want to thank my supervisor dr. Danutė Vaičiukynienė for her patience, encouragement with the investigations and kind help in achieving the goals of the dissertation. I am also very grateful to my scientific consultant dr. Viktoras Doroševas who came up with the topic of the dissertation, and whose friendly advice, interesting conversations and essential support with cold *Coca-Cola* (while performing experiments during the hot summer) were very important for me during the PhD studies. Of course, I also want to thank dr. Dalia Nizevičienė for her expertise and kind advice on the field of phosphogypsum, and for her help while carrying the material for the tests to the respective laboratories.

I also want to express my gratitude to the staff of the laboratories of the Faculty of Civil Engineering, to Romualdas Jokubauskas, Kastytis Štrimas, Rimas Morkūnas and Ignas Šiškauskas for their help, encouragement and, especially, good humour.

I want also to express my warm thanks to the fellow PhD students who made easier and kinder the work in the laboratories, especially to Deividas Martinavičius, Vadimas Kitovas, Suman Adhikary, Andrius Kielė, dr. Vytautas Bocullo, Gintautas Tamošaitis and all the others. Besides, I am profoundly grateful to dr. Šarūnas Kelpša, dr. Albertas Klovas and dr. Titas Braukyla for the inspiration and encouragement to end up choosing the PhD path.

I also want to express my gratitude to some persons who have collaborated with the investigations in various manners: to Valdas Rudelis for providing the materials; to dr. Darius Pupeikis (from the Centre for Smart Cities and Infrastructure), for the thermal conductivity investigations, to dr. Simona Tučkutė and dr. Martynas Lelis (from Lietuvos Energetikos Institutas) for their professional SEM-EDS and XRD investigations; to Juozas Bražėnas for the manufacturing of the metallic press-forms; to dr. Karel Dvořák (from Brno University of Technology) for his collaboration with XRD quantitative analysis; to dr. Boguslaw Michalik (from the GIG Central Mining Institute of Poland) for the detailed radionuclide acidity concentration analysis.

Of course, I lack words to express my thankfulness for the help and motivation provided by the people of Aukštakalnis centre who have given and still continue giving important information to face the good things and problems in life: Fernando Antúnez, Raul Barranco, dr. Rev. Paulius Gil, dr. Rev. Petras Pich and Tomas Liukaitis.

Finally, but not less important, my most profound gratitude goes to my parents and to my brothers and sisters who ‘remotely’ have been always a support for my projects and decisions. A special mention goes to my grandfather Juan Fornés, who was the best example as a Civil Engineer and, what is more, as a person.

UDK 661.634+666.913](043.3)

SL344. 2021-11-22, 22 leidyb. apsk. I. Tiražas 16 egz. Užsakymas 278.
Išleido Kauno technologijos universitetas, K. Donelaičio g. 73, 44249 Kaunas
Spausdino leidyklos „Technologija“ spaustuvė, Studentų g. 54, 51424 Kaunas

